Université de Montréal

The Impact of Ischemic Injury on Behavioral Outcomes and Cortical Interactions in Rats.

Par

Boris Touvykine

Département de Neurosciences, Faculté de Médecine

Thèse présentée en vue de l'obtention du grade de Philosophiae Doctor en Neurosciences

Mars 2022

Université de Montréal

Unité académique : Département de Neurosciences, Faculté de Médecine

---

Cette thèse intitulée

The impact of ischemic injury on behavioral outcomes and cortical interactions in rats.

Présenté par

Boris Touvykine

Sera évalué(e) par un jury composé des personnes suivantes

Dr. Roberto Araya

Président-rapporteur

Dr. Numa Dancause

Directeur de recherche

Dr. Matthieu Vanni

Membre du jury

Dre. Marie-Hélène Boudrias

Examinateur externe (pour une thèse)

ACKNOWLEDGEMENTS

I would like to thank my supervisor Numa Dancause for his mentorship throughout these years. It was a long journey for me and he offered support and advice that helped me best navigate and succeed in my Ph.D.

I would also like to thank laboratory members who have helped me with my experiments, support, and scientific discussions: Stephan Quessy, Ian Moreau-Debord, Eleonore Serrano, Charles Labbé, and Babak Mansoori. I would also like to thank our main collaborators Dale Corbett and Matthew Jeffers who were great to work with and even though not all of our projects worked out, it was a pleasure to share a part of my scientific journey with you guys.

In addition, I would like to thank Serge Rossignol and Dorothy Barthelemy who were on my comité de parrainage, for keeping track of my progress and making sure I was making progress towards my goal.

Last, but not least, I would like to thank my family, especially you Janine, without patient support I would not have graduated.

RÉSUMÉ

L’accident vasculaire cérébral (AVC) est une maladie débilitante qui a rendu des centaines de milliers de personnes handicapées. Les lésions du cortex moteur entraînent des déficiences motrices dont certaines sont permanentes. Le rat est le modèle animal le plus populaire dans la recherche sur les AVC. Il est capable de mouvements adroits d'atteinte et de préhension malgré un système moteur cortical beaucoup plus simple qui se compose de deux régions motrices des membres antérieurs, une plus grande région, l’aire caudale de la patte antérieure (CFA), considérée comme un équivalent du M1; et une plus petite, l’aire rostrale de la patte antérieure (RFA), considérée comme prémoteur. Leur contribution exacte à la production de mouvement, et leurs effets modulateurs sur le cortex moteur controlatéral ne sont pas clairs. L'effet des AVC sur les différentes modalités de mouvement et sur la réorganisation ipsi- et contralésionnelle n'a pas non plus été quantifié chez le rat.

L'ensemble actuel d'expériences vise à établir l'impact de l'AVC ischémique sur les résultats comportementaux et les interactions corticales chez le rat. Dans le chapitre 1, le contexte scientifique et les connaissances actuelles de l’AVC comme trouble moteur du système nerveux central sont revus. Dans le chapitre 2, une relation entre les accidents vasculaires cérébraux de différentes tailles et les troubles du comportement et la récupération sur différentes modalités comportementales a été établie. Dans le chapitre 3, nous avons caractérisé les différences de retour moteur de deux régions corticales du membre antérieur et quantifié les effets modulateurs du cortex moteur du membre antérieur controlatéral sur ledit retour moteur. Enfin, nous avons quantifié la réorganisation du retour moteur et la modulation controlatérale suite à un accident vasculaire cérébral dans le cortex moteur des membres antérieurs au chapitre

4. Le chapitre 5 conclue la thèse avec une discussion générale et des orientations futures pour la recherche.

Les résultats présentés ici établissent un lien clair entre les dommages aux sous-régions corticales et l'altération de domaines moteurs spécifiques. La caractérisation des différences dans les retours moteurs du CFA et du RFA ainsi que leurs interactions interhémisphériques ont confirmé leurs rôles distincts dans le contrôle moteur et établit une base pour des comparaisons avec les primates. Enfin, des preuves nouvelles et surprenantes de réorganisation bilatérale après un AVC ont été définies et caractérisées.

Mots clés : rat, cortex moteur, accident vasculaire cérébral (AVC), neuroplasticité, réorganisation bilatérale, étendue lésionnelle

ABSTRACT

Stroke is a debilitating condition that has left hundreds of thousands of people disabled. Injury to the motor cortex leads to motor impairments, some of which are permanent. The rat is the most popular animal model in stroke research. It is capable of dexterous reach and grasp movements, despite having a much simpler cortical motor system, which consists of two forelimb motor regions; the larger area is the caudal forelimb area (CFA), thought to be an M1 equivalent, and the smaller one is rostral forelimb area (RFA), considered to be premotor. Neither their exact contribution to movement production nor modulatory effects on the contralateral motor cortex are clear. The effect of strokes on different movement modalities and the ipsi- and contralesional reorganization has not been quantified in the rat either.

The current set of experiments set out to establish the impact of ischemic stroke on behavioral outcomes and cortical interactions in the rat. Chapter 1 introduces the scientific background and the present understanding of stroke as a motor disorder of the central nervous system. In Chapter 2, a relationship between strokes of various sizes and behavioral impairment and recovery on different behavioral modalities was established. In Chapter 3, we characterized the differences in motor outputs from two cortical forelimb regions and quantified the modulatory effects of the contralateral forelimb motor cortex on said motor outputs. Lastly, we quantified the reorganization of motor outputs and contralateral modulation following a stroke in the forelimb motor cortex in Chapter 4. Chapter 5 concludes the thesis with the general discussion and future directions.

The results presented here establish a clear link between damage to cortical subregions and impairment to specific motor domains. Characterization of differences in motor outputs of

the CFA and RFA as well as their interhemispheric interactions confirmed their distinct roles in motor control and lay the groundwork for comparisons to primates. Lastly, novel and surprising evidence of bilateral reorganization after stroke was defined and characterized.

Keywords: rat, motor cortex, stroke, neuroplasticity, bilateral reorganization, lesion extent

TABLE OF CONTENTS

TABLE OF FIGURES

TABLE OF TABLES

LIST OF ABBREVIATIONS

AGl - agranular lateral cortex

AGm - agranular medial cortex

AP - anteriorposterior

cCFA - contralateral caudal forelimb area

CFA - caudal forelimb area

CFA_{lesion} - ipsilesional/perilesional caudal forelimb area

CFA_{naive} - caudal forelimb area in naive animals

CMA - cingulate motor area

CMAr - rostral cingulate motor area

CMAd - dorsal cingulate motor area

CMAv - ventral cingulate motor area

CNS - central nervous system

CPG - Central pattern generator

cRFA - contralateral rostral forelimb area

C_{stim} - Conditioning stimulus

CST - corticospinal tract

DNA - deoxyribonucleic acid

EF - elbow flexor

EMG - electromyographic

ET-1 - endothelin-1

EXCITE - Extremity Constraint Induced Therapy Evaluation

FMA - Fugl-Meyer Assessment

fMRI - functional magnetic resonance imaging

h - hour

HL - hindlimb

Hz - hertz

ICMS - intracortical microstimulation

ISI - interstimulus intervals

kg - kilogram

kHz - kilohertz

M1 - primary motor area

µA - microampere

MEP - motor evoked potential

mg - milligrams

min - minute

ml - millilitre

ML - mediolateral

mm - millimetres

MRI - magnetic resonance imaging

ms - milliseconds

µV - microVolt

NHP - non-human primates

nm - nanometer

PMd - premotor dorsal cortex

PMv - premotor ventral cortex

PREP - predicting recovery potential

RAS - right- anterior-superior

RFA - rostral forelimb area

$RFA_{ipsilesional}$ - ipsilesional rostral forelimb area

RFA_{naive} - rostral forelimb area in naive animals

RNA - ribonucleic acid

rTMS - repeated transcranial magnetic stimulation

S1 - primary somatosensory cortex

SMA - supplementary motor area

sMRI - structural magnetic resonance imaging

TIAs - transient ischemic attacks

TMS - transcranial magnetic stimulation

T_{stim} - Test stimulus

WE - wrist extensor

WF - wrist flexor

CHAPTER 1 GENERAL INTRODUCTION

1.1 Discovery of the motor cortex, its definition and early studies.

The study of stroke, specifically motor impairments caused by stroke is inextricably linked to the study of the motor system, and more specifically the motor cortex in mammals. Its modern history begins with two German physicians: Gustav Fritsch and Edvard Hitzig in 1870 (Gross, 2007). They demonstrated that in the dog there is a cortical region that can evoke movements when stimulated electrically. By doing so they were the first to discover and characterize the motor cortex. Around the same time, an English physician by the name of John Huglings Jackson proposed the idea that epileptic seizures are caused by neural discharge and proposed the cortex as the likely origin (Jackson, 1870). Influenced by his ideas, as well as Fritsch and Hitzig's findings, Jackson's friend, Scottish physician David Ferrier conducted a more methodical study. Using longer stimulation trains, he managed to evoke localized contralateral and trunk movements (Ferrier, 1874). To further demonstrate that the cortex was responsible for the evoked movements, he proceeded to lesion the previously stimulated regions, which led to the inability to evoke further movements with electrical stimulation. Ferrier had also performed lesions experiments and described resulting deficits (Ferrier, 1883). Both Jackson and Ferrier made further contributions to neurology and neuroscience and co-founded the journal "Brain" in 1878. Particularly notable was Jackson's seminal publication in 1884, in which following his own observations on epilepsy in patients as well as Ferrier's animal experiments, led him to propose a hierarchical organization of the nervous system. Early in the 20th century, Ferrier's findings in primates were further corroborated and expanded by Leyton and Sherrington (Leyton & Sherrington, 1917). Part of the precentral gyrus (where the primary motor cortex is located) was

ablated in the chimpanzee, which was then allowed to recover under observation. Following recovery, further experiments were conducted on the animals with galvanic stimulation of the cortex and the lesion. Furthermore, the animals received secondary lesions to evaluate either new or returning deficits. Leyton and Sherrington were the first to characterize motor deficits in meticulous detail and provide detailed observations of the recovery of the animal. The clinical pathogenesis of ablation lesions is very different from stroke, however, both result in the focal neuronal death in the motor cortex and cause subsequent reorganization of the central nervous system (CNS). Their seminal experiments effectively made Leyton and Sherrington the founding fathers of the field of stroke recovery. The next significant leap in our understanding of the motor system was a series of stimulation experiments conducted by Wilder Penfield. He applied surface electrodes to the cortex of awake epileptic patients under local anesthesia, and along with Edwin Boldrey, they developed the famous homunculus in 1937 (Penfield & Boldrey, 1937). It presented a structured relationship between different body parts and motor regions in the cerebral cortex. For example, leg movements were evoked medially to the arm region, and the mouth movements - lateral to the arm region. This spacial organization was confirmed in multiple human patients. Penfield also noted that the relative size of the representation of each body part in the motor cortex did not correlate with the actual size of the body part. The size of the hand and the mouth were disproportionally greater compared to the cortical area dedicated to arm and leg movements. The disproportional size of hands and lips correlates with the complexity of movements we can perform with these body parts, as we are the most dexterous animals with our hands, as well as having intricate control of our mouths and vocal cords which is necessary to

produce language. Consequent research into stroke recovery and the motor system was based on findings of these pioneers.

1.2 General definition of the motor cortex.

Most of the important early work on the motor cortex was conducted in primates. While, the motor cortex was discovered in dogs by Fritsch and Hitzig in 1870, just four years later Ferrier reported his findings on dogs and monkeys. In the late 19th and early 20th century almost all neurophysiologists and neuroanatomists studying the motor system had a medical background, and consequently one of their main motivations was the hope to discover ways to help their patients. The phylogenic proximity of non-human primates (NHPs) to humans makes discoveries in these animals easily transposable to humans. Early in the 20th century, the motor cortex was understood to be located in the frontal cortex and consisted of Brodmann area 4 and 6, both defined cytoarchitectonically as agranular, i.e. lacking in layer IV (Brodmann, 1999). In 1935, Fulton proposed the naming convention where the anterior part of the excitable cortex was designated "premotor" (Brodmann area 6), and the posterior portion was "motor" (Brodmann area 4), and eventually "primary motor area" (M1) (Fulton, 1935). Today, the motor cortex is generally defined as the regions of telencephalon located in the frontal cortex, which send descending projections to the spinal cord; and when stimulated electrically can evoke movements (Randolph J. Nudo & Frost, 2007). Pyramidal cells located in layer V of the cerebral cortex send their axons all the way to different segments of the spinal cord forming the corticospinal tract (CST). The majority of CST axons originating in one hemisphere descend to the brainstem, where they cross to the contralateral side from their hemisphere of origin. They continue to

descend in the spinal cord on the side opposite to their hemisphere of origin, where they connect to effectors by forming synapses with spinal interneurons, which in turn connect to motoneurons. Unilateral stimulation of the motor cortex typically results in evoking muscle twitches and movements on the contralateral side. The "premotor" cortex was also further refined and separated into dorsal premotor (PMd) and ventral premotor (PMv) areas, as well as the supplementary motor area (SMA) located in the medial wall of area 6 (Dum & Strick, 1991; He, Dum, & Strick, 1995; Mitz & Wise, 1987). Further down in the medial wall, three cingulate motor areas (rostral, dorsal, and ventral) have been identified, and are located in Brodmann areas 23 and 24 (Dum & Strick, 1991; He et al., 1995).

1.3 Anatomy of M1.

In primates, M1 is located in Brodmann area 4 in the posterior part of the frontal lobe, and anterior to the central sulcus. It is characterized cytoarchitecturally by the absence of layer IV, defined in the cerebral cortex by the presence of granular cells. It contains somatotopic representation of the body, with the leg representation located medially, the face laterally, and the arm between them. Compared to any other cortical region, it is the greatest contributor to the CST, which originates in cortical layer V (He et al., 1995; Randolph J. Nudo & Frost, 2007). The M1 sends projections throughout the whole spinal cord, including both cervical and lumbar enlargements in the spinal cord. A unique feature of M1 is the presence of Betz cells, which are large pyramidal neurons found in layer V (Randolph J. Nudo & Frost, 2007). They are among the largest neurons in the central nervous system, and can form direct corticomotor synapses. These synapses are between CST axons and motoneurons enervating typically distal forelimb muscles

(Dancause, Touvykine, & Mansoori, 2015). Corticomotor projections are present in higher order primates such as humans, great apes, macaques, and ceebus and are thought to be the underlying substrate of high manual dexterity of the hand movements in these species (Bortoff & Strick, 1993). In contrast, the vast majority of CST forms indirect connections with motoneurons, typically through spinal interneurons acting as a relay. Another interesting aspect of descending projections in the spinal cord is their ability to have numerous collaterals. These collaterals are typically limited to their target member e.g. CST projections from the arm regions in M1 have axonal terminals localized within the cervical enlargement. However, within the cervical enlargement, they can form multiple synapses at different spinal segments and innervate different muscles (Shinoda, Yokota, & Futami, 1981). Furthermore, M1 is interconnected with the ventral lateral posterior nucleus of the thalamus and sends mostly unilateral projections to the striatum (Rouiller et al., 1998). In addition, corticofugal projections originating in M1 descend to subcortical structures such as the red nucleus, and pontoreticular formation. Two independent descending spinal tracts originate from these structures (rubrospinal and reticulospinal respectively). Lastly, M1 has numerous reciprocal connections to premotor areas and S1 (Dea, Hamadjida, Elgbeili, Quessy, & Dancause, 2016; Hamadjida, Dea, Deffeyes, Quessy, & Dancause, 2016).

1.4 Physiology and function of M1.

Importance of M1 to motor control cannot be overstated. Even partial inactivation of M1 causes loss of individual finger movements (Marc H. Schieber & Poliakov, 1998). Lesions of M1 result in flaccid paralysis of the contralateral limb, and can cause permanent loss of individual finger

movements (Leyton & Sherrington, 1917; Travis, 1955), whereas inactivations of premotor areas result in much more subtle deficits. Heavy deficits resulting from loss of M1 functionality are not surprising considering that it is the major contributor to CST, and while it is clearly the most important node in control of voluntary movement generation, the exact functions of M1 are still being examined.

Hiroshi Asanuma hypothesized that the motor cortex had columnar organization, similar to primary somatosensory area (Asanuma, 1975; Asanuma & Sakata, 1967; Stoney, Thompson, & Asanuma, 1968). He drew these conclusions following experiments using a novel stimulation technique he developed. Unlike topical electrodes, which are applied to the top of the cortex; he utilized metal electrodes insulated along their length except for the very tip. Asanuma would lower these fine needle-like electrodes into the motor cortex, passing current through them. Because the origin of the electrical field was the tip of the electrode typically lowered to be within layer V, it allowed for much more focal and precise stimulation compared to aforementioned surface electrodes. The resulting electrical field depolarized a relatively small number of corticospinal neurons (CSNs), and at threshold stimulation intensity typically evoked twitches in a single muscle (Asanuma & Rosén, 1972). In contrast with topical stimulation that produced more general movements; Asanuma's intracortical microstimulation (ICMS) technique evoked very localized muscle twitches at stimulation threshold. The ability to evoke single muscle twitches led Asanuma to conclude that he must have been stimulating the motor equivalent of the cortical column found in the sensory cortex. While this powerful stimulation technique is still in use today, Asanuma's interpretation of his ICMS results did not turn out to be correct.

As discussed in the previous section, CST originating from M1 has a divergent pattern of descending corticospinal projections. The physiological significance of this divergent pattern of collaterals was investigated using a technique called spike triggered averaging. It consists of recording action potentials of a single neuron and correlating it to EMG activity in forelimb muscles. Multiple muscles have been found to correlate with spiking of individual pyramidal neurons in M1, whereas stimulation in M1 resulted in greater facilitation in distal compared to proximal musculature (Cheney & Fetz, 1985; Park, Belhaj-Saïf, & Cheney, 2004). Furthermore, activity of a single corticospinal neuron in M1 has been found to be active during movements of different fingers without any kind of fine somatotopy (M. H. Schieber & Hibbard, 1993). Gross somatotopy first identified by Penfield is present and large representations of body parts are still consistently located within M1 (hand representations will be located within the arm representation, while the leg representation will be located laterally to the arm). However, nothing resembling columnar organization of the sensory systems, where a cortical column would be responsible for a specific muscle, has been found in M1. CST neurons in smaller subdivisions of M1 (such as hand area) appear to lack specific spatial organization. Rather, motor control is achieved through coordinated and synchronized firing of locally distributed pyramidal neurons, which send converging signals to target effectors (Georgopoulos, Kalaska, Caminiti, & Massey, 1982; M. H. Schieber & Hibbard, 1993). The exact parameters controlled by M1 remain to be determined, nonetheless Georgopoulos has found correlations between neural activity in M1 with acceleration and velocity of movement, as well as position of reaching target in 2D space (Ashe & Georgopoulos, 1994). However, the most pronounced feature encoded by M1 neurons was the direction of movement (Ashe & Georgopoulos, 1994; Georgopoulos, 1986;

Georgopoulos et al., 1982; Georgopoulos, Schwartz, & Kettner, 1986; Lukashin & Georgopoulos, 1993).

1.5 Definition premotor areas.

After some debate as to what constitutes a premotor area (Dum & Strick, 1991; Picard & Strick, 1996), a general anatomical definition should be the following: cortical regions located in the frontal or cingulate cortex, which send descending projections to the spinal cord as well as corticocortical projections to the ipsilateral M1; and when electrically stimulated evoke movements or muscle twitches (Dum & Strick, 2002; Randolph J. Nudo & Frost, 2007). In this section, anatomical and physiological features, as well as theorized functions of six premotor areas, will be covered.

1.6 Premotor areas of the cingulate cortex.

The three premotor areas located in the limbic lobe are the rostral, dorsal, and ventral cingulate motor areas (CMAr, CMAd, and CMAv, respectively). They are located in Brodmann areas 23, 6, and 24 respectively. Cingulate motor areas send projections to the spinal cord through the CST, both to the cervical and lumbar enlargements; as well as numerous corticocortical projections to M1 (Dum & Strick, 1991; Muakkassa & Strick, 1979). ICMS can evoke movements of the contralateral leg and arm, but output to upper limb muscles are much weaker compared to the M1 (M.-H. Boudrias, Lee, Svojanovsky, & Cheney, 2010). A possible role of CMAs is to participate in reward processing for motor action selection (Shima & Tanji, 1998b). Lesions of these areas in two patients seem to have caused deficits in bimanual coordination,

without affecting unimanual dexterity of either limb (Stephan et al., 1999). The same study found activation of cingulate motor areas during bimanual task performance in healthy subjects. Overall, the three cingulate motor areas are the newest motor regions to be identified and are the least studied to date.

1.7 Anatomy of the supplementary motor area.

Supplementary motor area (SMA) is located in the medial most part of the Brodmann area 6, which is characterized by its agranular cytoarchitecture i.e. the absence of granular cells and therefore of cortical layer IV. It was first defined in 1952, when a supplementary motor representation rostral to the medial most part of M1 was found after completion of somatotopic map in M1 (Woolsey et al., 1952). The corticospinal projections originating in the SMA descend to both cervical and lumbar enlargements (Dum & Strick, 1996). SMA is heavily interconnected with cingulate motor areas, PMd, PMv, and M1 (Luppino, Matelli, Camarda, & Rizzolatti, 1993). Furthermore, it sends and receives numerous projections to the distal forelimb portion of M1. SMA projects heavily to the nucleus medialis dorsalis of the ipsilateral thalamus, as well as nuclei ventralis anterior and ventralis lateralis (Rouiller et al., 1998). Furthermore, it projects bilaterally to the putamen, the caudate nucleus, and claustrium (Jurgens, 1984). Corticorubral projections are predominantly unilateral with heavy labelling of projections from SMA in the ipsilateral red nucleus; and non-existent to sparse labelling in the contralateral red nucleus. Corticoreticular projections from SMA are not particularly dense, but do appear to be bilateral (Jurgens, 1984).

1.8 Physiology and function of the supplementary motor area.

SMA has been shown to be implicated in the sequencing of complex movements (Shima & Tanji, 1998a, 2000). SMA neurons have also been found to be preferentially active during bimanual tasks (~48% of recorded neurons), compared to unimanual contralateral movements (~9%) or ipsilateral movements (~3%) (Kermadi, Liu, Tempini, Calciati, & Rouiller, 1998). Furthermore, unilateral lesions of macaques SMA result in deficits of bimanual movement coordination, which the animal did not recover from until experimenters performed a callosotomy (Brinkman, 1984). Brinkman's interpretation of this result was the following: unilateral lesion of SMA disrupts the inhibition of "mirror movements" which are fed into the bilateral motor system through callosal projections by the intact SMA in the contralateral hemisphere. Following callosotomy, this aberrant input is no longer present, and the animal recovers the use of its bimanual coordination. Furthermore, unilateral SMA lesions did not cause deficits in simple unilateral movements of the hand (Brinkman, 1984). Stimulation in awake monkeys resulted in weaker output and no preference for distal or proximal musculature compared to M1 (M. H. Boudrias, Belhaj-Saïf, Park, & Cheney, 2006). In addition, neural activity in the SMA was found to play an important role in action selection, instructed by behavioural sensory clues (Kurata & Tanji, 1985; Tanji, 1985; Tanji & Kurata, 1985). Overall, these studies suggest that SMA does not play a big role in the execution of simple unilateral movements, but implicate SMA as an important node in bimanual coordination, as well as the sequential organization of complex movement execution.

1.9 Anatomy of the dorsal premotor area.

Dorsal premotor cortex is located in Broadmann area 6, lateral to SMA and medial to the arcuate sulcus. Similar to SMA, PMd lacks cortical granular layer IV and its corticospinal projections descend to both cervical and lumbar enlargement in the spinal cord (Barbas & Pandya, 1987; He et al., 1995). PMd has almost complete somatotopy, with ICMS evoking movements of the contralateral hindlimb, arm, and trunk (Godschalk, Mitz, van Duin, & van der Burg, 1995). In contrast with the cingulate areas, SMA, M1, and ventral premotor cortex (which will be discussed below), no orofacial representation has been found in the PMd. PMd was further subdivided into rostral and caudal parts, and PMd rostral actually has a very thin layer of granular cells, making it disgranular, whereas in PMd caudal there was a complete absence of layer IV (Barbas & Pandya, 1987; Wu, Bichot, & Kaas, 2000). The rostral part of PMd sends numerous reciprocal projections to the prefrontal cortex, SMA, and cingulate motor areas, in addition to a small number of projections to the ventral premotor cortex (PMv). The caudal part of PMd projects to M1 and back to rostral PMd. The connection pattern suggests that the caudal part of PMd is the motor component, whereas the rostral part is more involved in preprocessing information it receives from other premotor areas and prefrontal cortex, before feeding it into caudal PMd. The majority of corticothalamic projections originating from PMd target the ipsilateral mediodorsal thalamic nucleus (Rouiller et al., 1998). Its corticostriatal projections are bilateral and predominantly target the caudate putamen (Künzle, 1975, 1978; Takada, Tokuno, Nambu, & Inase, 1998).

1.10 Physiology and function of the dorsal premotor area.

In terms of output properties, stimulation of PMd produced weaker muscle responses with with a preference for proximal musculature (M.-H. Boudrias, McPherson, Frost, & Cheney, 2010). Functionally, inactivation of PMd results in deficits in conditional motor behavior i.e. behavior that is cued by a specific condition, such as a color cue instructing the monkey to reach to the right and not the left target (Kurata & Hoffman, 1994). Furthermore, disruption of PMd activity in humans results in mild deficits during reach and grasp movements (Davare, Andres, Cosnard, Thonnard, & Olivier, 2006). Specifically, decoupling between lifting the arm and grasping the object movement phases. Neural activity in the PMd begins to ramp up after cue presentation and prior to movement initiation, and continues during movement execution (Churchland, Santhanam, & Shenoy, 2006). Furthermore, microstimulation in PMd disrupts preparatory activity, which causes a delay in movement initiation (Churchland & Shenoy, 2007). Multiple studies have found that neural activity in PMd encodes for movement parameters, such as direction, amplitude, and speed of movement (Churchland et al., 2006; di Pellegrino & Wise, 1993; Fu, Flament, Coltz, & Ebner, 1995; Kurata, 1993; Messier & Kalaska, 2000). Further experiments revealed that neurons in the PMd encode for the relative position of the target, hand, and eye; suggesting their role in computing a motor plan for the hand to reach the target (Pesaran, Nelson, & Andersen, 2006). During actual movement execution neural activity in PMd and M1 closely resembles each other. Moreover, just like in M1, neural activity in PMd is influenced by hand trajectory and arm orientation (Scott, Sergio, & Kalaska, 1997). Hoshi and Tanji proposed that PMd is an important node where an action plan is selected and a motor plan of a planned movement is formulated (Hoshi & Tanji, 2007).

1.11 Anatomy of the ventral premotor area.

Premotor ventral area is located in the ventral most part of Brodmann area 6. As was already discussed area 6 is characterized by the absence of cortical layer IV, however as early as 1919 Vogt and Vogt, questioned this cytoarchitectural result (Nieuwenhuys, 2013). In 1987, Barbas and Pandya (Barbas & Pandya, 1987) found an emergent layer IV in the ventral part of area 6, lateral to the arcuate sulcus, where PMv is located. PMv has incomplete somatotopy, where stimulation evokes face and specifically mouth movements in its most lateral part, and movements of the contralateral arm can be evoked medial to the face representation. PMv has reciprocal connections with the prefrontal cortex, cingulate motor areas, and the rostral part of PMd, and is heavily interconnected with M1 (Dea et al., 2016; Hamadjida et al., 2016; Stepniewska, Preuss, & Kaas, 2006). Corticospinal projections from PMv are unique amongst premotor areas, because they project predominantly to the upper cervical segments, whence motoneurons enervating neck and shoulder muscles originate. Corticospinal projections descending to lower cervical segments have been found, but they are very sparse (Elena Borra, Abdelouahed Belmalih, Marzio Gerbella, Stefano Rozzi, & Giuseppe Luppino, 2010; He, Dum, & Strick, 1993). Given the absence of projections to lower cervical segments; it is that within the arm representation, movements of distal forelimb can be evoked. It has been hypothesized that the distal movements in PMv are mediated by its strong connections with the distal area of M1 (Dea et al., 2016; Hamadjida et al., 2016). In fact, inactivation of distal forelimb region in M1 of macaques results in significant decrease of EMG activity in distal musculature evoked with PMv stimulation (Schmidlin, Brochier, Maier, Kirkwood, & Lemon, 2008). Corticothalamic projections from PMv preferentially target ipsilateral mediodorsal and ventral posterior medial

thalamic nuclei (M. Rouiller, 2003). Corticostriatal projections are bilateral and preferentially target the ipsilateral caudate nucleus (Künzle, 1975, 1978; Takada et al., 1998)

1.12 Physiology and function of the ventral premotor area.

Output properties of PMv shared a number of similarities with PMd, specifically smaller effect in the muscles and a preference for proximal musculature compared to M1 (M.-H. Boudrias, McPherson, et al., 2010). Lesions of PMv result in deficits in attention to peripersonal space, as well as biasing and orienting on the contralateral side (Rizzolatti, Matelli, & Pavesi, 1983; M. H. Schieber, 2000). Furthermore, the inactivation of PMv caused deficits in the adaptation of visuomotor transformation when viewing goal objects through prisms (Kurata & Hoshi, 1999). Another very interesting consequence of PMv inactivation were deficits in reshaping of the hand prior to grasp, which results in difficulties grasping objects (Fogassi et al., 2001). This deficit was not due to paralysis or weakness of digits as was the case with M1 inactivation. In fact, to grasp an object with the affected hand following PMv inactivation; the monkey had to initially touch it, presumably using tactile feedback to correct for deficits of visuomotor transformation. Furthermore, almost complete unilateral inactivation of PMv caused bilateral deficits, although they were more pronounced in the arm contralateral to inactivation (Fogassi et al., 2001). In addition, PMv inactivation biased the laterality choice on which arm to use for the task (Fogassi et al., 2001; M. H. Schieber, 2000). Experiments that examined neural activity in the PMv are in line with lesion and inactivation studies. Activity in PMv is involved in movement preparation as it commences before movement initiation and goes on until object is grasped (Kakei, Hoffman, & Strick, 2001; Moreau-Debord, Serrano, Quessy, & Dancause, 2021). Furthermore, 94% of

neurons in PMv have been found to be selective for movement direction in space, regardless of posture. PMv neurons also appear to encode the start and end positions of a forelimb movement and its trajectory in visual space (Ochiai, Mushiake, & Tanji, 2005; Schwartz, Moran, & Reina, 2004). These results have led to the proposal that PMv matches the visual space to motor space by transforming visual information of target shape and location into a set of motor coordinates that are used for reaching (Kurata & Hoshi, 2002). PMv works in conjunction with PMd, but is not involved in action selection. Instead, it receives information on the target object and transforms visual information to a set of outputs that match the target location and properties (Hoshi & Tanji, 2007).

1.13 Interhemispheric connections between motor cortices.

Corpus callosum is the largest bundle of white matter connecting two hemispheres of the cerebrum. The vast majority of signalling takes place through this structure. A brief summary of projections and their possible function will be given below.

M1 is preferentially connected to its homologue in the other hemisphere (Rouiller et al., 1994). In fact, it appears to be a general pattern where cortical motor regions preferentially project to their contralateral counterpart in the other hemisphere. This is true for SMA, PMd, and PMv (Rouiller et al., 1994; Marconi et al., 2003; Boussaoud et al., 2005; Dancause et al., 2007). All of these areas are interconnected forming a bilateral network.

As was previously discussed stimulation of these regions evokes contralateral movements, which is expected considering the majority of CST crosses over from its hemisphere of origin. However, that majority of neurons recorded in the motor cortex were found to

modulate their activity as monkeys performed movements with either contralateral or ipsilateral hand. This includes SMA, PMd, PMv, and M1 (Kermadi, Liu, & Rouiller, 2000; Kermadi et al., 1998). A more rigorous comparison of neural activity in PMd and M1 found that the activity in bilateral M1 neurons was more robust for contralateral movements (Cisek, Crammond, & Kalaska, 2003). Furthermore, during the preparatory stages of movement, a greater number of neurons modulated their activity with the contralateral rather than ipsilateral arm. In contrast, activity in the PMd appeared bilateral without a strong preference for either arm. Lack of lateral preference, along with the ramp up of activity in PMd during movement preparation suggests that the premotor area is "effector independent" (i.e. not dependent on which arm is used to achieve the task) and more concerned with task demands. Therefore, motor regions form a constantly communicating, distributed network spanning across both hemispheres (Badoud et al., 2017). PMd and likely other premotor areas are less dependent on what side the effector (forelimb) is, as their role is more abstract. M1, despite being part of this bihemispheric motor system does seem to have a strong preference for the contralateral effector. This does not come as a surprise, considering that neural activity in M1 is not preparatory and is most robust during movement execution. Furthermore, M1 lesions have very pronounced, and very lateralized motor deficits. In conclusion, the motor system consists of multiple nodes in both hemispheres in constant communication, with M1 being the most lateralized i.e. having the strongest influence/ input to the contralateral limb.

1.14 Motor system of the rat.

The motor system of the rat is much simpler compared to the motor system of primates. In terms of cytoarchitecture two distinct agranular cortical regions have been identified: agranular lateral (AGl) and agranular medial (AGm) (Neafsey et al., 1986). Corticospinal neurons originating from the AGl descend to both cervical and lumbar enlargements of the rat spinal cord (Li, Florence, & Kaas, 1990). Complete somatotopy has been found in AGl with the hindlimb representation located most mediocaudally, forelimb - medially, trunk - mediorostrally, and orofacial – laterorostrally (Neafsey et al., 1986). Cortical stimulation studies have found that somatotopic representations of motor regions in AGl partially extend into the adjacent primary somatosensory cortex (parietal granular cortex) (Halley, Baldwin, Cooke, Englund, & Krubitzer, 2020; Neafsey et al., 1986). Defined with intracortical microstimulation, the forelimb representation located primarily in AGl is known as the caudal forelimb area (CFA) and the hindlimb – simply as hindlimb motor area (HL). Numerous descending projections to the contralateral cervical enlargement also originate from the AGm (Akintunde & Buxton, 1992). Using ICMS, this area was defined as a second forelimb motor region, aptly named the rostral forelimb area (RFA) (Neafsey & Sievert, 1982). RFA and CFA are separated by a strip of cortex, where stimulation typically evokes vibrissae and trunk responses. While Neafsey succeeded in evoking hindlimb movements from AGm, after a literature review no other study replicated this result. Nonetheless, projections to the lumbar enlargements originating from the AGm have been found (Starkey et al., 2012a). The significance of these projections remains to be elicited. Mediorostral to the RFA, stimulation can evoke eye movements, and even more medially vibrissae twitches can be evoked (Neafsey et al., 1986). Therefore, AGl, and likely AGm contain partial somatotopic representations of the body with forelimb and hindlimb regions present in

both. Movements of eyes appear to be exclusive to the AGm, whereas movements of the mouth and tongue are in the AGl (Kosinski, Neafsey, & Castro, 1986). Most corticospinal projections to the cervical enlargement originate in the CFA, with a smaller number coming from the RFA, whereas almost all CST projections to the lumbar enlargement originate in what is HL motor area (Starkey et al., 2012a). The corticospinal tract in the rat appears even more lateralized compared to primates with 95% of fibers crossing over at the pyramids (Brösamle & Schwab, 1997, 2000).

1.15 Connection pattern of CFA and RFA.

An extensive study characterizing and comparing connectivity of RFA and CFA was conducted by Rouiller and colleagues in 1993. A brief summary of their findings follows below and is summarized in Figure I1. Ipsilaterally the biggest proportion of corticocortical connections from CFA go to RFA, and from RFA to the CFA. Other regions interconnected with CFA are somatosensory areas, anterior cingulate cortex, and perirhinal cortex. In addition to being interconnected with the same cortical areas as CFA; RFA also sends and receives projections from the insular cortex.

Significant differences have been identified in the subcortical connection pattern between RFA and CFA. CFA receives projections from the ventral nucleus, nucleus basalis, the posterior nucleus, ventromedial nucleus, central medial, and paracentral nuclei of the thalamus. RFA receives projections from all these areas except the ventrolateral thalamic nucleus and nucleus basalis. Ipsilateral corticothalamic projections tend to be reciprocal with thalamocortical ones. Specifically, CFA sends projections primarily to the ipsilateral ventrolateral nucleus, nucleus basalis, and posterior nucleus of the thalamus. RFA sends projections to the posterior and

ventromedial nucleus of the thalamus. In contrast with CFA, the corticothalamic projections from RFA are bilateral and also project to posterior and ventromedial nucleus of the contralateral thalamus (Rouiller, Moret, & Liang, 1993). Corticostriatal projections are also ipsilateral from the CFA, and bilateral from the RFA.

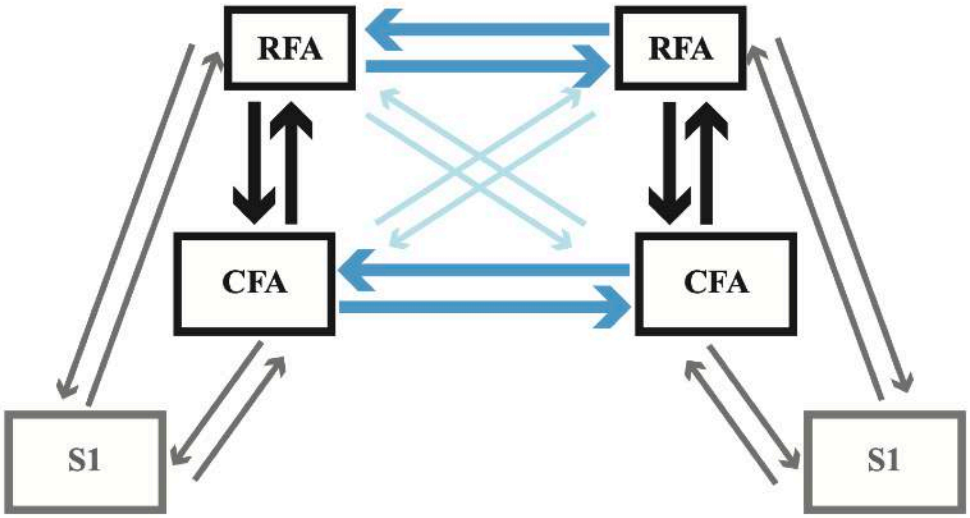

Figure I1. Summary of incoming and outgoing projections to and from forelimb cortical motor areas (CFA and RFA). Thick black arrows represent the largest proportions of ipsilateral corticocortical projections to and from CFA and RFA. Thin grey arrows represent the second biggest proportion for ipsilateral projections. Thick and thin blue lines do the same for transcallosal projections. Adapted from Rouiller et al. 1993.

In the other hemisphere, CFA preferentially projects to its contralateral homologue, with the second most numerous projections going to contralateral RFA. In similar fashion, RFA's principal contralateral projects target its homologue, with the secondary target being the contralateral CFA.

Both RFA and CFA appear to send corticorubral projections, however they predominantly target the red nucleus ipsilaterally. Similarly, corticoreticular projections are also present, and appear more bilateral. It should also be noted that unlike primates where collaterals from the corticospinal tract project to the red nucleus and the reticular formation, rats appear to have

relatively segregated populations of neurons forming corticorubral, corticoreticular, and corticospinal tract (Akintunde & Buxton, 1992).

1.16 Physiology and function of the motor system of the rat.

Lesions of the forelimb motor cortex of the rat result in persistent deficits in reach and grasp movements, spontaneous limb use, as well as precision placement of forelimb during locomotion (Schaar, Brenneman, & Savitz, 2010; Schallert, Fleming, Leasure, Tillerson, & Bland, 2000; I. Q. Whishaw, Pellis, Gorny, & Pellis, 1991). Interestingly, lesion of the hindlimb motor region results in deficits in precision placement of hindlimb, but only results in transient deficits in overground, and no impairment during treadmill locomotion (manuscript in preparation Delcourt, Touvykine et al.). This is similar to results reported in the cat, which are also capable of treadmill and overground locomotion even after inactivation/removal of the motor cortex (Drew, Jiang, Kably, & Lavoie, 1996). CNS in the motor cortex of the cat was not strongly involved in overground locomotion until the cat had to either navigate an obstacle or precisely place its paws. Drew and colleagues conclude that the motor cortex is involved in correcting and adjusting parameters of locomotion to navigate challenges (gait modification), but is not essential for overground locomotion, which is dependent on subcortical circuits and non-corticospinal descending pathways, such as reticulospinal and rubrospinal pathways, as well as intraspinal circuitry such as central pattern generators (CPG) (Grillner, 1985). Thus, it is not surprising that lesions of the HL region in the rat did not result in significant or lasting deficits in locomotion.

As quadrupeds, rodents are among few mammalian species capable of grasping objects with their forelimb digits. This dual function of their forelimbs is reflected in the patterns of activity in the motor cortex. Kinetically similar components of reaching movements and locomotion coincide with very different patterns of neural activity in the forelimb motor cortex (Hermer-Vazquez et al., 2004). Furthermore, it turns out that the motor cortex is not essential for the execution of extremely well learned movement patterns (stereotyped movements). Complete ablation of the motor cortex after the movement was learned to the point of stereotypy did not impede rats from executing previously learned movements in order to obtain a reward (Kawai et al.). However, ablation of the motor cortex prior to learning abolished animals' capacity to learn a new motor task and thus achieve any kind of stereotypy. Together these results indicated that the rat forelimb motor cortex is positioned at the hierarchical top of the motor system, i.e. it is essential for motor learning to develop new movement patterns, which can be used to manipulate the animals' environment more effectively. Furthermore, the two forelimb motor areas have distinct contributions to motor behaviour. Long-train ICMS stimulation in the RFA and CFA with acute cooling of either region has revealed that RFA appears to be more involved in the grasp phase of reach and grasp movements, whereas the CFA was more involved in the reach component (Brown & Teskey, 2014). Furthermore, an imaging study in awake rodents confirmed these findings, with the corticospinal neurons in the CFA more active during a reach and post-grasp phase, and the CSN in the RFA more active during the grasping (X. Wang et al., 2017). Lastly, the pattern of corticocortical connections between RFA and CFA is uneven, with RFA receiving projections from the CFA layer II/III and Va, and the CFA receiving projections from the RFA layer Vb (Hira et al., 2013b; Rouiller et al., 1993). This pattern of connections suggests

that the RFA likely occupies a higher hierarchical position than the CFA in the organization of the motor system in the rat.

1.17 Stroke.

Stroke is neuronal death caused by the interruption of blood flow to a specific area of the brain, which results in lesions of the central nervous system (Phac, 2011). There are two main types of stroke, that is to say, two main ways blood flow to the brain is interrupted. Hemorrhagic stroke is caused by a burst blood vessel in the brain and the resulting hemorrhage. Ischemic stroke is caused by a blocked or severely constricted blood vessel preventing nutrients and oxygen from reaching specific areas of the brain, and resulting in neuronal death. Approximately, 90% of strokes are ischemic in nature (Andersen, Olsen, Dehlendorff, & Kammersgaard, 2009). The largest blood vessel supplying blood to the brain is the middle cerebral artery. This blood vessel and many of its branches irrigate cortical and subcortical elements of the sensorimotor system in primates, and thus strokes resulting from interruption of blood flow to this artery or to one of its branches are the most frequent, representing 80% of all strokes (Harrison, 1994). Such damage to the motor system is typically unilateral and can result in significant and highly variable motor deficits, such as hemiparesis, muscle weakness, loss of individualized finger movements, and spasticity. These deficits typically present themselves in the forelimb contralateral to stroke, i.e. the paretic arm, and are particularly persistent in the hand. A loss of ability to use one hand significantly decreases stroke survivors' quality of life because a large majority of our daily motor manipulations are bimanual and require both hands to execute effectively. Something as simple as opening a can of soda, or unscrewing the top of a bottle, becomes an insurmountable

obstacle if the patient is restricted to the use of only one hand. There are over 300,000 stroke survivors in Canada, many of whom live with permanent deficits that significantly decrease their quality of life, and would greatly benefit from further recovery of motor function (Hakim, Silver, & Hodgson, 1998; Phac, 2011).

There is a degree of spontaneous recovery in stroke patients, even without any therapeutic interventions. Three major post-stroke recovery stages have been identified in humans. Acute is defined as the first two weeks following stroke, followed by the subacute stage which lasts from 2 weeks to 3 months, when patients enter the chronic recovery stage (Cramer, 2008; Rehme, Eickhoff, Rottschy, Fink, & Grefkes, 2012). Most recovery happens within the first 3 months post-stroke (Duncan, Goldstein, Matchar, Divine, & Feussner, 1992; Kwakkel, 2006). Stroke survivors will typically recover a proportion of the lost motor control (~70%), hence the name - proportional recovery rule (Prabhakaran et al., 2008). I.e. if the maximum value of a sensorimotor test, such as Fugl-Meyer Assessment (FMA) scale is 66 (for healthy individuals and 0 for complete lack of sensorimotor function), and the score of a patient at 2 weeks post-stroke is 46; then the proportional recovery score at 3 months should be (66-46)*0.7+46 = 60. However, whereas this rule is reliable for patients with moderate to mild deficits, it has limited application to those with severe deficits (below FMA of 20), as only a fraction of the people demonstrates proportional recovery in this subpopulation (Prabhakaran et al., 2008; Winters, van Wegen, Daffertshofer, & Kwakkel, 2015). The authors subdivided their patient cohort into subjects whose recovery followed the proportional rule (“fitters”) and those who didn’t (“nonfitters”). The nonfitters are the most affected individuals and at present, we lack the understanding of the biological processes which lead some patients with severe deficits to

recover some motor control whereas others do not. It should be stated that a recent publication has identified problems with the calculation of Proportional recovery, and which might lead to its re-evaluation in the future (Hawe, Scott, & Dukelow, 2018).

At present, our understanding of the exact processes of neuroplasticity underlying recovery of function (or lack of) is not sufficient to design an intervention that would be universally effective. Two approaches in rehabilitation are thought to be efficient in improving motor control during recovery from stroke: training to use the paretic hand and constraint-induced therapy (Kwakkel, Veerbeek, van Wegen, & Wolf, 2015; McCabe, Monkiewicz, Holcomb, Pundik, & Daly, 2015). Post-stroke rehabilitative training involves training patients to use their paretic limb, under the supervision and assistance of a therapist. Unfortunately, there is a surprising lack of consistency in the parameters of rehabilitative training. Furthermore, it seems that the amount of therapy most patients receive is insufficient for the treatment to be effective (Bernhardt, Dewey, Thrift, & Donnan, 2004; Lang et al., 2009). The study by McCabe and colleagues (2015) demonstrates that an intensive rehabilitation regimen is effective in improving motor function following stroke. Unfortunately, to date, high-intensity rehabilitation training is not standard practice. The other approach is constraint-induced movement therapy. It consists of limiting the use of the non-paretic limb, to force the patient to attempt to use the paretic limb (Ince, 1980). This treatment was inspired by observations that deafferented monkeys quickly learn not to use the affected hand, using instead the non-affected hand for unimanual tasks (Taub, 1976). Even after animals recovered enough to use the paretic hand they did not use it, having learned early in recovery that this limb is dysfunctional. Taub dubbed it “learned non-use” as even though the animals could effectively manipulate objects with the paretic hand, since it

learned not to use it, the monkey continued to ignore it. Constraint-induced movement therapy was designed to overcome this phenomenon by binding the non-paretic limb and forcing the animal to use its paretic hand. The EXCITE clinical trials evaluated the efficacy of constraint-induced movement therapy and found that after two weeks patients who received the treatment had improved motor performance scores (Wolf et al., 2010). Unfortunately, it appears that the beneficial effect was largely due to the development of compensatory strategies by patients and not due to the restitution or recovery of motor control of the paretic limb (Kitago et al., 2013). Thus, while rehabilitative training of the paretic hand and constraint-induced movement therapy can be effective in improving motor control in stroke patients; it is dependent on certain conditions. The intensity of training is the most significant limiting factor for rehabilitation. To benefit from constraint-induced movement therapy patients most likely need at least some functionality in the paretic hand to develop compensatory strategies.

The ability to give a patient an accurate prognosis would permit clinicians to prescribe more effective treatment regimens, as well as allow for better allocation of healthcare resources. In turn, better allocation of resources should lead to increased time and attention allocated to an individual patient to maximize their recovery. Overall, we need a better understanding of neuroplasticity post stroke to be able to effectively harness the processes to improve the quality of life of stroke survivors living with permanent deficits.

1.18 Plasticity in the motor cortex.

Whereas plasticity in adults is no longer disputed, neuroplasticity in the motor cortex of healthy specimens as a result of behavioural experience was first discovered and confirmed in adult

primates in M1 (R. J. Nudo, Milliken, Jenkins, & Merzenich, 1996). In this seminal paper, Nudo and colleagues characterized changes in ICMS maps in M1 following different forelimb training regimens. Training to retrieve a pellet by precision pinch resulted in the expansion of the digits and thumb representation, whereas training an animal to rotate a lever to a specific degree (eyebolt turning task), caused the expansion of the forelimb representation. Another finding of note was that when the task was a simple retrieval that did not require learning of a new motor strategy, no significant changes were found in the M1. The expansion of M1 representations relevant to motor skill acquisition was a beautiful demonstration of inherent neuroplasticity in M1. These results were later confirmed in the rat when the skilled pellet retrieval task caused the expansion of the distal representation in the CFA, whereas a precise lever pulling task, resulted in the increase of the proximal forelimb area in the CFA (Kleim, Barbay, & Nudo, 1998). Lastly, using a different methodology, neuroplasticity in M1 as the result of behavioural experience has also been found in humans, where motor training changed the direction of a movement evoked from the same spot on the brain with transcranial magnetic stimulation (TMS) pulses (Classen, Liepert, Wise, Hallett, & Cohen, 1998).

Specific neuroanatomical changes are thought to underlie the aforementioned changes in M1 discerned with stimulation. Using TMS, researchers found increased excitability in the motor cortex of humans engaged in motor learning (Rioult-Pedotti, Friedman, Hess, & Donoghue, 1998). High-frequency (10 Hz) or excitatory intermittent theta-burst repeated transcranial magnetic stimulation (rTMS) hyper-excited M1, and was found to improve the rate of motor learning (Y.-H. Kim, Park, Ko, Jang, & Lee, 2004; Thomas Platz, Adler-Wiebe, Roschka, & Lotze, 2018). In contrast, inhibition of M1 with inhibitory rTMS (continuous theta-burst)

resulted in decreased motor performance (T. Platz et al., 2012). Further changes in excitability are supported by findings that there is a temporary decrease in inhibition during motor learning in both humans and rodents, which is mediated by GABAergic neurons in the cortex (Dayan & Cohen, 2011; Hess, 2004; S. Kim, Stephenson, Morris, & Jackson, 2014).

We have previously discussed how the CST projections from M1 are highly divergent and have multiple collaterals, some of them spanning different spinal segments (Shinoda et al., 1981). Consequently, movements are generated through coordinated convergence and synchronization of signal mediated by intra M1 projections as well afferent projections coming primarily from premotor regions. This synchronization is necessary to execute voluntary movements. During motor learning, new movements strategies have to be developed, and an essential part of motor learning is decreasing the errors committed in training. In the early stage of motor learning acquisition, there is increased co-contraction, which presumably is due to increased control of movement components required for a new movement strategy (Osu et al., 2002). This co-contraction decreases with increased precision of movement (i.e. decrease in error), signifying motor learning. This process of discovering new ways of moving the effector (arm) is the likely "raison d'être" for the increased excitability of the motor cortex because previously inhibited and inactive synapses become functional when the overall state of excitability in the system is increased (Jacobs & Donoghue, 1991). Further investigation into this phenomenon revealed that there was a temporary decrease in axonal boutons of GABAergic interneurons during motor learning, causing the temporary disinhibition in the motor cortex of mice (S. X. Chen, Kim, Peters, & Komiyama, 2015). This local disinhibition results in the unmasking of previous existing but not functional connections in the cortex (Jacobs &

Donoghue, 1991). If these unmasked connections and synapses result in increased success of the new motor strategy, they are reinforced and eventually consolidated when motor learning attains a sufficient level. This interpretation is supported by a recent study, which found that the weakest coupling of CSN activity and movement parameters were in early and late motor learning, whereas the tightest coupling was in the middle, at the height of motor learning (Peters, Lee, Hedrick, O'Neil, & Komiyama, 2017). These results suggest that early in motor learning, the CSN activity can not produce "sufficiently good" movements to satisfy the demands of the animal. As the animal keeps attempting to perform a "satisfactory" movement, it improves and thus the CSN activity becomes more tightly coupled with movement parameters. At this point, the animal has discovered a "satisfactory" way to fulfill the behavioural requirements of the task and moves on to stabilize this performance. One possible interpretation is that the motor cortex "passes along" the parameters of the newly learned movement, and its consolidation takes place elsewhere in subcortical structures. Such a process would explain the decreased correlation between CSNs' activity and movement parameters at the end of motor learning, as the motor performance improves and stabilizes. Furthermore, it would also explain the expansion of ICSM maps during motor learning, and subsequent contraction once motor learning has been complete, as well as the rats' ability to execute previously learned movements in the absence of motor cortex (Kawai et al.; Molina-Luna, Hertler, Buitrago, & Luft, 2008; R. J. Nudo et al., 1996).

Overall, rebalancing of synaptic strength seems to be the main mechanism for motor learning in healthy adults. Furthermore, this neuroplasticity, where synaptic strength is rebalanced to subserve motor learning, likely happens not just in the cortex, but along the whole motor axis. Professional dancers were found to have spinal reflexes of smaller amplitudes

compared to professional athletes (Nielsen, Crone, & Hultborn, 1993). Even more interesting is that operant conditioning was found to modify the strength of spinal reflexes in both humans and rodents (Angulo-Kinzler, Mynark, & Koceja, 1998; X. Y. Chen, Chen, Chen, & Wolpaw, 2006; Wolpaw, 2007). Investigations in rodents found decrease in the number of GABAergic terminals in the spinal cord following successful training to decrease the strength of spinal reflex (Y. Wang, Pillai, Wolpaw, & Chen, 2006). Therefore, motor learning takes place through selective synaptogenesis, and likely happens all along the motor axis. At present, it is important to underline that plasticity due to motor learning is not thought to cause neurogenesis or axonal sprouting of any kind, but only rebalancing of synaptic strength and synaptogenesis.

1.19 Ipsilesional plasticity in the acute stroke period.

Immediately after stroke, the cortex is disinhibited by what is likely a global downregulation of GABA bindings in the cortex (Qü et al., 1998; Schiene et al., 1996). This step of post-stroke reorganization likely shares some similarities to regular motor learning, because any initial decrease in motor control and the resulting inability to perform motor tasks will be treated as gross errors in movement, therefore requiring motor learning to improve motor performance. Here, it should be pointed out that there exists a subtype of small strokes that do not present gross deficits or otherwise extremely obvious symptoms. Lesions caused by these small strokes can be hard to detect on MRI scans and are called Transient Ischemic Attacks (TIAs). Each individual TIA does not cause enough damage to present obvious deficits or symptoms, which highlights the high level of redundancy in the motor system. Of course, repeated TIAs eventually do result in deficits, but it appears that a minimum amount of damage must accumulate before

the symptoms manifest themselves. Furthermore, some people recover exceptionally well after stroke, with clinicians scoring them as completely recovered (Fujii & Nakada, 2003). If such recovery takes place within a few weeks post stroke it is likely that the damage to the motor cortex and the corticospinal tract was not significant enough to require axonal sprouting, and neuroplasticity similar to motor learning in healthy subjects was sufficient to "relearn" normal movement patterns. I.e. if recovery from small lesions is too rapid for axonal sprouting and growth to take place, it is likely mediated by the rebalancing of synaptic strength. However, while it is important for us to understand what is happening there, these strokes are not the reason millions of stroke survivors live with permanent motor deficits.

Whereas this type of neuroplasticity can be largely attributed to endogenous mechanisms of synaptic rebalancing already present in healthy motor systems and discussed in the section on motor learning, one should be careful as the two are not interchangeable. The pattern of neural activity induced in a distant cortical region by small strokes in the motor cortex differed from the neural activity induced in the same region by inactivation of the motor cortex (Mohajerani, Aminoltejari, & Murphy, 2011). Whatever cellular signalling takes place as the result of stroke, its immediate effects (< 2 hours) are not reproduced by a simple inactivation in the same location. The mechanistic difference between reversible inactivation and stroke remains to be elicited. One possibility is that inflammation associated with damage to neurons and their apoptosis results in cellular cascades and changes in network dynamics, which are not reproduced by reversible inactivation. These processes are thought to open a window on neuroplasticity usually absent from healthy adults. From this point on, the CNS either proceeds with synaptic rebalancing if enough motor cortex has remained intact for its inherent redundancy

to be sufficient to restore function, or it commits to a demanding process of axonal sprouting, rerouting, and forming new connections in place of lost ones in an attempt to regain motor functionality.

1.20 Ipsilesional plasticity in the sub-acute stroke period.

Stroke patients who take over a month to recover from stroke and end up seeing significant recovery of function, likely do so through significant anatomical reorganization (Fujii & Nakada, 2003). To the best of our knowledge neurogenesis has not been shown to contribute to functional recovery (Rahman, Amruta, Pinteaux, & Bix, 2021). This is despite experiments attempting to boost/harness neurogenesis in the subventricular zone, or even directly implant stem cells into the lesioned area in hope that functional circuitry will eventually develop (Rahman et al., 2021). Two main reasons have been identified for the lack of success (or "sucksess") of such treatments: first, glial scar forming around the lesion in the days and weeks following stroke prevents axons from growing through it and neuronal precursor cells from migrating to the lesioned region; second, development of the six cortical layers with functional projections to their targets requires a complex interplay of signalling molecules only present during development (Harel & Strittmatter, 2006; Yiu & He, 2006). Whereas there have been some promising results concerning the first problem, the second problem presents a much greater challenge and no advances have been made in identifying possible solutions. Therefore, significant anatomical reorganization following stroke does not depend on neurogenesis and will be limited to sprouting of new axons or collaterals from surviving neurons to reorganize the remaining CNS circuitry.

From multiple animal studies that have explored this subject, we know that the remaining motor cortex reorganizes to function vicariously to compensate for the loss of neurons in the M1. Inactivation of ipsilesional PMd and PMv following recovery from M1 lesion results in the return of deficits in primates; strongly suggesting that premotor areas reorganize to support the motor function of the impaired limb and compensate for the lesion in M1 (Liu & Rouiller, 1999). Similarly, secondary lesion in the ipsilesional RFA following recovery from stroke in the CFA led to the reinstatement of motor defects in the paretic forelimb (Zeiler et al., 2013). One aspect of such reorganization that has been identified is axonal sprouting from remaining motor regions and has been found to occur in both primates and rodents (Dancause, 2006; Dancause et al., 2005; Wahl et al., 2017; Wahl et al., 2014). In non-human primates, Dancause and colleagues found that following recovery from the M1 lesion, S1 and PMv became much more highly connected through corticocortical projections, absent in healthy controls. Instead axons originating from the S1 and PMv project towards the distal forelimb area in M1. Since the distal forelimb area in M1 was lesioned in the experimental group, the authors hypothesized that this is an attempt by the CNS to reestablish connections between S1 and the closest functionally relevant motor area (ipsilateral PMv), which reorganized to vicariously act as the lesioned part of M1. It should be underlined that these changes likely take place all across the motor axis. Recovery of motor function following a stroke in the forelimb motor cortex was better in rats in which some corticospinal neurons in the untouched hindlimb motor region developed axonal collaterals projecting to the cervical enlargement (Starkey et al., 2012b). Furthermore, it is important to note that reorganization to reestablish vicarious function takes place in areas that are already fulfilling a similar function to at least some extent. Ipsilesional premotor and hindlimb

regions have corticospinal projections and are already involved in movement generation, thus there is likely a degree of similarity in the microcircuitry of these regions. Therefore, the extent of reorganization other motor regions need to undergo to completely or partially fulfill the function of lesioned M1 would be smaller compared to the reorganization necessary for a non-motor region. For example, the visual cortex, the organization of which serves sensory processing, not movement generation, would have to completely reorganize to vicariously function as a motor region, which according to our current understanding it impossible.

1.21 Contralesional reorganization.

As was discussed previously the motor cortex is heavily interconnected across the two hemispheres and the role of the contralesional cortex is not entirely clear in the recovery process. fMRI studies found abnormal activity in the contralesional cortex with the movement of the paretic limb (Calautti, Leroy, Guincestre, Marié, & Baron, 2001). A decrease in said contralesional activation has been found to correlate with improved recovery of function of the paretic limb (Calautti et al., 2001; Jaillard, Martin, Garambois, Lebas, & Hommel, 2005; Ward, Brown, Thompson, & Frackowiak, 2003). Furthermore, reversible inactivation using non-invasive methods results in better recovery in some patients but makes paretic deficits greater in others (Bradnam, Stinear, Barber, & Byblow, 2012). Such conflicting findings require further investigation into factors that could account for the discrepancy in results.

1.22 Contralesional plasticity in the acute stroke period.

Unilateral inactivation studies have found very rapid changes in the contralateral hemisphere. For example, disinhibition in the contralateral sensorimotor cortex of monkeys takes place minutes after inactivation (Clarey, Tweedale, & Calford, 1996). Similarly, changes in neural activity in the contralateral PMv were found within minutes after inactivation (Moreau-Debord et al., 2021). Furthermore, mini-strokes in rodents have been found to cause enhancement of cortical responses, suggesting disinhibition within 30-50 minutes (Mohajerani et al., 2011). Considering that the two hemispheres are heavily interconnected and function bilaterally, the increased facilitation and activity is likely part of the "plasticity window/window of opportunity" opened by stroke. This plasticity is not limited to the ipsilesional hemisphere, but likely spans the whole CNS. A study corroborated that generalisability of this enhanced plasticity, whereby the motor performance of the non-paretic hand was improved beyond that of healthy animals by training said forelimb following unilateral stroke (Luke, Allred, & Jones, 2004). What is even more fascinating is that increased synaptogenesis was found in the contralesional hemisphere of stroke rats, whether they received motor training or not, indicating that the stroke itself causes increased plasticity, however specifically what functional goal this plasticity will serve likely depends on the behavioural experience post-stroke. In fact, training the non-paretic forelimb in rats seems to result in interference with the recovery of the paretic hand, a phenomenon which is prevented by training both paretic and non-paretic forelimbs (Allred & Jones, 2008; Kerr, Wolke, Bell, & Jones, 2013). The results of these studies strongly suggest that immediately after unilateral stroke, a window of opportunity opens up along and across the motor axis allowing for increased neuroplasticity that is normally not possible in adults.

1.23 Contralesional plasticity in the subacute stroke period.

As we discussed previously the ipsilesional motor cortex has been shown to reorganize with intact premotor regions functioning vicariously to support the reinstatement of function of the paretic limb, due to disinhibition and increased plasticity caused by stroke. Furthermore, these processes are not limited to the ipsilesional motor system and are also present contralesionally. The functional outcome in terms of recovery of function can be highly variable. While we previously discussed the importance of behavioural experience, studies in patients tend to control for overall levels of activity in patients and nonetheless findings are conflicting (Saunders, Greig, & Mead, 2014). A clue regarding a likely important factor came from a rodent study (Biernaskie, Szymanska, Windle, & Corbett, 2005). Following a period of recovery from stroke, the inactivation of the contralesional motor cortex resulted in much greater deficits of the paretic hand in rats with large lesions. The authors proposed that when the damage to the motor cortex is significant enough, the ipsilesional motor regions cannot compensate for lost functionality, the contralesional hemisphere reorganizes to support the function of the paretic hand. This hypothesis is a logical continuation of the idea that functionally and structurally similar areas are more likely to assume the function of a lesioned area when the damage in the said area is too great for the redundancy to compensate for the injury. With particular extensive strokes remaining, the ipsilesional motor cortex might not be sufficient to reorganize and assume the functions of the destroyed neural circuits. If the behavioral experience prioritizes the use of the paretic limb (such as with forced use or constrained induced therapy), the system likely engages the contralesional motor cortex to reorganize in an effort to assume part of the functions of the lesioned cortex and support the motor recovery of the paretic hand. Results from patients

corroborate the importance of the extent of unilateral damage, where inhibition of the contralesional M1 in patients with mild deficits and moderate damage to CST resulted in improved motor control of the paretic limb (Bradnam et al., 2012). In contrast, inhibition of the contralesional M1 in patients with extensive damage to the corticospinal tract and severe motor deficits of the paretic limb worsened motor control of the paretic limb. Therefore, the extent of unilateral damage to the motor cortex coupled with behavioral experience likely determines whether the contralesional motor cortex will support or be detrimental to recovery. In cases of extensive damage and severe deficits, the CNS likely reorganizes to support the recovery of the paretic hand to some extent; whereas with moderate damage and deficits, plasticity permitted by the lesion and subsequent reorganization is likely detrimental to the recovery of the paretic limb.

1.24 Rationale for the present set of experiments.

Using the rat model of stroke, this thesis sets out to fulfill the following general objective: following recovery from an ischemic lesion in the motor cortex, characterize the extent of damage to different cortical regions on behavioral outcomes and motor recovery, as well as changes to ipsilesional motor output and the effect of the contralesional hemisphere on it. The general hypothesis is that recovery from stroke depends on the extent of damage to various cortical regions and will cause substantial changes in output properties of the spared motor cortex, as well as bilateral interactions. The general objective will be fulfilled in three chapters.

The specific goal of chapter 2 was to quantify the impact of the extent of damage to different cortical regions on resulting motor deficits, and the extent of functional recovery. Specific hypothesis 1a is that the extent of damage to motor regions results in task-specific

deficits. Specific hypothesis 1b is that the extent of damage to adjacent motor regions capable of compensatory reorganization and vicarious function can predict the extent of the final recovery.

The specific goal of chapter 3 was to characterize and quantify the motor output of cortical forelimb regions (CFA and RFA) and modulation of said motor output by the forelimb motor regions of the opposite hemisphere (CFA and RFA), in healthy rats. This is an explorative study and the specific hypothesis 2 was simply to see how different the modulation was from previously published results in non-human primates.

The specific goal of chapter 4a was to characterize and quantify the change of motor outputs of two forelimb motor regions following recovery from stroke. Specific hypothesis 3a is that reorganization following lesion will alter output properties of ipsilesional cortical motor regions (perilesional CFA and RFA).

The specific goal of chapter 4b was to characterize and quantify the change the modulatory effect of contralesional forelimb motor regions on ipsilesional motor output following recovery from stroke. Specific hypothesis 3b is that following recovery from ischemic lesion the modulatory drive of the contralesional hemisphere on ipsilesional output will change compared to healthy controls.

Chapter 2.

Post-stroke impairment and recovery are predicted by task-specific regionalization of injury.

Matthew S. Jeffers, Boris Touvykine, Allyson Ripley, Gillian Lahey, Anthony Carter, Numa Dancause, Dale Corbett

Published in the Journal of Neuroscience, 40(31), 6082-6097, 2020.

Abstract

Lesion size and location affect the magnitude of impairment and recovery following stroke, but the precise relationship between these variables and functional outcome is unknown. Herein, we systematically varied the size of strokes in motor cortex and surrounding regions to assess effects on impairment and recovery of function. Female Sprague Dawley rats (N=64) were evaluated for skilled reaching, spontaneous limb use, and limb placement over a 7-week period post-stroke. Exploration and reaching were also tested in a free ranging, more naturalistic, environment. MRI voxel-based analysis of injury volume and its likelihood of including the caudal forelimb area (CFA), rostral forelimb area (RFA), hindlimb (HL) cortex (based on intracranial microstimulation), or their bordering regions was related to both impairment and recovery. Severity of impairment on each task was best predicted by injury in unique regions: impaired reaching – by damage in voxels encompassing CFA/RFA, hindlimb placement – by damage in HL, and spontaneous forelimb use – by damage in CFA. An entirely different set of voxels predicted recovery of function: damage lateral to RFA reduced recovery of reaching, damage medial to HL reduced recovery of hindlimb placing, and damage lateral to CFA reduced recovery of spontaneous limb use. Precise lesion location is an important, but heretofore relatively neglected, prognostic factor in both preclinical and clinical stroke studies, especially those employing region-specific therapies such as transcranial magnetic stimulation.

Introduction

The ability to predict patients' potential for post-stroke recovery is of utmost importance for developing more effective, individualized therapies (Boyd et al., 2017; Stinear et al., 2017). Research in this area suggests that post-stroke "biomarkers" could reveal an individual patient's propensity for recovery. For example, early motor impairment (Prabhakaran et al., 2008; Krakauer and Marshall, 2015; Winters et al., 2015), structural and neurophysiological biomarkers, such as integrity of the corticospinal tract (CST), and presence of motor evoked potentials (MEPs), have been used successfully to predict outcome in subpopulations of stroke patients (Byblow et al., 2015; Feng et al., 2015). However, no single outcome measure reliably predicts recovery in all patients (Kim and Winstein, 2016). Instead, combining different biomarkers better predicts recovery across a larger spectrum of stroke patients. Accordingly, Stinear and colleagues (Stinear et al., 2012) first developed the Predict Recovery Potential (PREP) algorithm based on clinical and neurological outcomes. More recently, the PREP2 algorithm, has shown improved accuracy, predicting 3-month recovery in approximately 75% of patients (Stinear et al., 2017). However, clinical studies have several shortcomings including an inability to directly gauge the influence of rehabilitation on recovery (Stinear et al., 2020). For example, while some meta-analyses have hinted at a dose response effect of rehabilitation on recovery (Lohse et al., 2014; Lang et al., 2015), the evidence is not compelling (Winstein et al., 2016; Krakauer and Carmichael, 2017; Bernhardt et al., 2019; Dalton et al., 2019; Stinear et al., 2020). Furthermore, previous biomarker studies include relatively few severely impaired patients (Winters et al., 2015; Stinear et al., 2017) potentially limiting generalization of the findings to this important population. We previously addressed

these issues in a large cohort of rats with strokes in different brain regions that included many animals with severe impairments on a skilled reaching task (Jeffers et al., 2018a, 2018b). As in human studies, the initial skilled reaching impairments predicted the final level of recovery, but only in a subpopulation of animals. We then developed an algorithm based on animals' initial impairment, infarct size, and whether they received an effective dose of rehabilitation.

This combination of biomarkers more accurately predicted final outcome than initial impairment alone, including animals with profound impairments (Jeffers et al., 2018b). In a subsequent rodent study, the extent of post-stroke impairment and recovery varied in relation to both cortical versus subcortical lesion location and the functional domain assessed (Karthikeyan et al., 2019) suggesting that lesion location may influence the level of recovery. In humans, both lesion location and volume have been shown to affect recovery (Chen et al., 2000) but volume, without consideration for location, is a relatively poor predictor of recovery (Chen et al., 2000; Page et al., 2013). In contrast, others have reported that location of stroke is not related to long term outcome (Dromerick and Reding, 1995; Hayward et al., 2017). Such inconsistency is not surprising given most clinical studies classify lesion location without regard to important functional subdivisions within brain regions (Dromerick and Reding, 1995; Edwardson et al., 2017; Hayward et al., 2017; Harvey et al., 2018). In a recent international consensus paper (Boyd et al., 2017), the authors recommended that investigating lesion location as a potential biomarker of stroke recovery should be a research priority. In the present study, we systematically varied lesion size, and then precisely mapped lesion location relative to the hindlimb, caudal forelimb, and rostral forelimb motor areas in a rat model of stroke. We examined relationships between lesion location, impairments, and subsequent recovery of different motor domains including

reaching/grasping, spontaneous forelimb use, limb placement and balance, and general activity in a semi-naturalistic environment. As expected, impairments in specific motor domains were linked to the cortical sub-region damaged. However, depending on the specific task, damage to spatially unique regions of peri-infarct cortex reduced the ability to recover. Our results suggest that lesion location, a relatively neglected prognostic biomarker, is an important predictor of post-stroke recovery that should be considered in the design of new therapeutic approaches that target brain plasticity, such as transcranial magnetic stimulation.

Materials and Methods

Experimental Design

Female Sprague-Dawley rats (N=64, Charles River, Montreal, Canada) weighing 200-225g upon arrival were trained and tested on a battery of motor tasks under 12/12-hour reverse day/night conditions and randomly assigned to stroke (n=44) or sham groups (n=20). Females were employed because with the prolonged post-stroke testing period male rats tend to outgrow the size of several behavioral testing chambers. Photothrombosis was used to create lesions of varying size and location around the caudal forelimb (CFA), rostral forelimb (RFA), and hindlimb (HL) motor areas. Lesion size and location was quantified from T2-weighted MRI stacks and motor performance was assessed 1-week pre-stroke and 1, 3, 5, and 7 weeks post-stroke (Figure 1). These measures have previously been shown to strongly correlate with lesion volumes acquired using histological reconstruction (Peeling et al., 2001). Multiple linear

regressions were used to relate the size and location of brain injury to the corresponding behavioral impairments. All experimental procedures were approved by the institutional animal care committee of the University of Ottawa and comply with guidelines set by the Canadian Council of Animal Care.

Stroke Induction

Strokes of varying size were generated using cold-light photothrombosis and a range of aluminum foil illumination apertures with the following dimensions: 2.5x2.5 mm (n=9), 3.0x5.0 mm (n=11), 5.0x7.5 mm (n=12), and a 10.0 mm circular diameter (n=12; no aperture). Briefly, rats were anesthetized using isoflurane (4% induction, 2% maintenance, in 100% O2 given at 1.6 L/min) and received a midline scalp incision. Illumination apertures were aligned to Bregma and the midline of the skull, with the light source placed over the skull at +2.3 mm anterior and ±2.5 mm lateral to Bregma. Individual differences in the vascular topography lead to natural variance in the exact area damaged by the procedure. The hemisphere contralateral to each rat's dominant paw in the staircase task (preferred paw) was selected for stroke induction. Rats were injected with 20 mg/kg Rose Bengal in a 0.9% NaCl solution via the tail vein. Two minutes after Rose Bengal injection the light (Intralux 5100, Harvard Apparatus) was turned on for 10 minutes, illuminating the brain through the intact skull and generating a unilateral focal lesion. Following incision closure, 0.2 ml of Bupivacaine was applied along the sutures as a topical analgesic. The sham group received a control injection of 0.9% NaCl and underwent the same lesion induction procedures as the stroke group.

Infarct Quantification

Forty-eight hours following surgery, MRI scans were used to confirm presence of stroke and quantify infarct volume and location relative to the CFA, RFA, and HL motor representations. Infarct volume measured at this time is strongly correlated with final infarct volume from histological assessment (Biernaskie et al., 2001; Karthikeyan et al., 2019). Rats were anesthetized using isoflurane (4% induction, 2% maintenance, 1.6 L/min O_2) and moved into the MRI bore (7T General Electric/Agilent MR901 small animal scanner). T2-weighted structural images were obtained using the following parameters: 21 coronal slices; slice thickness = 800 m; in-plane resolution = 132.8 m; echo train = 8; echo time = 27 ms; scan time = 5 min. MRI stacks were analyzed using ImageJ (National Institute of Health) to verify that infarcts were present following surgery. No lesion was observable in 3 rats using the 2.5x2.5 mm, and 1 rat using the 3.0x5.0 mm aperture. Additionally, no significant decrease in performance on any behavioral task was observed from the pre- to 1-week post-stroke time points in these rats. Consequently, they were reassigned to the sham group, resulting in the final number of animals per group previously described. An experimenter experienced in infarct volume segmentation and blind to illumination aperture size manually delineated the infarcted tissue in each section based on visual identification of the high-contrast area of the cortex. The workflow for this segmentation was assisted using a custom ImageJ script, but the segmentation itself was manually determined by the experimenter (Figure 2-1). This script was used to determine the voxel-wise location and volume of infarcted tissue within each animal (Figure 2). Briefly, a stack of MRI images for each animal was imported into ImageJ and viewed in the coronal plane. The experimenter used the

midline of the brain as a reference point to rotate each stack into the correct coronal orientation and identified the posterior-most section where the anterior commissure crossed the midline. The voxel in the center of the anterior commissure in this section was manually selected and the stack was transposed so that this voxel was centered in the image space and designated as the origin voxel (0,0,0) for purposes of determining the relative location of all other voxels in right-anterior-superior (RAS) orientation. This anterior commissure coordinate also corresponds to the commonly used Bregma skull landmark in the rat (Papp et al., 2014). The experimenter was then sequentially presented with each image in the stack and instructed to delineate the infarct boundary using the polygon tool in ImageJ (Figure 2A). Voxels in contact and within this boundary were designated as infarcted tissue, and those outside it as non-infarcted tissue. The volume of infarcted voxels and their position relative to the origin voxel provided a three-dimensional, whole brain, representation of infarct size and location in each animal (Figure 2B-C). For alignment of the lesion with the motor maps (see below; Figure 2D), this three-dimensional representation was reduced to a two-dimensional lesion map in the horizontal plane by summing the infarcted voxels along the superior-inferior axis for each given anterior-posterior / right-left coordinate.

Behavior Testing

Staircase

The staircase reaching task was used as a test of fine motor dexterity (Montoya et al., 1991). Each side of the staircase contained 7 wells with 3 food reward pellets each (5TUL, TestDiet).

Rats were food restricted (14 g/rat/day) the day prior to testing to encourage reaching. Each training/testing day consisted of two, 15-minute trials separated by 4 hours. Rats were trained on the staircase for 10 consecutive days, with the last two days used as the pre-stroke data. Post-stroke testing consisted of 3 days of consecutive testing with the final two days of data used to represent each timepoint.

Cylinder

An open transparent Plexiglas cylinder (diameter: 20 cm, height: 30 cm) was placed on a plastic support with a camera to record from below (Schallert et al., 2000). This test detects asymmetries in spontaneous limb use following stroke as the animals rear to explore the environment. As such, it provides a measure of whether the animals actually use the impaired limb in a semi-naturalistic setting or instead compensate by relying upon the unimpaired limb (Corbett et al., 2017; Balkaya et al., 2018). Rats were recorded until they had reared and touched the cylinder wall with a forelimb 20 times. The number of times the subject supported its body weight using the left paw, right paw, or bilaterally was quantified from slow-motion replay of each session. The results were used to calculate the relative impaired paw usage in the cylinder as a ratio using the following equation:

$$Ratio = \frac{contralateral + 1/2bilateral}{total}$$

Where contralateral is the number of times the rat used the impaired paw to contact the cylinder wall, bilateral is the number of times the rat used both paws simultaneously for wall contact, and

total being the total number of times the rat contacted the cylinder wall with a paw during rearing.

Beam

A tapered beam (90 cm length x (5.3 cm – 0.5 cm width)) with 1.0 cm ledge and a black goal box situated at the narrow end of the beam was used to quantify paw placement accuracy during walking (Schallert et al., 2002). This test is sensitive at detecting impairments in limb placement, especially of the hindlimb, and balance (Corbett et al., 2017; Balkaya et al., 2018). Each test period consisted of four trials per rat that were filmed using a wide-angle camera. Each trial was scored from slow-motion replay of recorded videos by counting the number of steps taken and number of foot faults where the rat stepped down to the lower ledge of the beam. The percentage of successful steps for each limb were individually calculated as follows:

$$\%\,Success = \frac{\text{total number of steps} - \text{total number of errors}}{\text{total number of steps}} * 100\,\%$$

Where the total number of errors is the sum of errors across all 4 trials for the timepoint and total number of steps is the sum of steps across all 4 trials for the timepoint.

Quantification of spontaneous activities, socialization, and limb use

General activity, socialization, and spontaneous limb use was measured in a free-ranging environment consisting of a custom-designed series of 4 connected PhenoTyper (Noldus Information Technology) cages (Figure 3). These PhenoTypers were arranged so that pairs of rats were separately able to explore two cages (Cage 1+2, Cage 3+4), while still able to maintain social contact with their cage mate in the “social zone”. Each rat had access to standard rodent

chow, water, 2 infrared-transmitting shelters, and a pellet tray. The pellet tray was placed on the exterior of the cages in which the rat could gain access to pellets by reaching through one of two slits. Each slit only allowed the use of either the right or the left limb, allowing quantification of the spontaneous use of each limb throughout the task period. Each pellet tray had two wells that held 4.0g of pellets each. Cages contained Regular Texture Pelleted PAPERCHIP (Sheppard Specialty Papers) as bedding that also helped to absorb the IR lighting and improve detection of each animal. Cage mates were placed into their respective cages in the PhenoTyper where activities were tracked using EthovisionXT (Noldus Information Technology) for a 1-hour period at each behavioral test point. Pellet consumption with each limb, the proportion of time spent in each zone of interest, and total distance travelled by each animal was quantified using this software. Only the sub-group of rats that received the 10.0 mm circular diameter lesion type were analyzed in this task (sham = 12, stroke = 12).

Euthanasia and Collection

Rats were killed at week 8 post-surgery by intraperitoneal injection of euthanyl (1.0 ml, 65 mg/mL). Euthanasia was confirmed by cardiac perfusion with heparinized saline (20 mL/minute) for 5 minutes followed by 4% paraformaldehyde (20 mL/minute) for 5 minutes. Rats were decapitated using a rodent guillotine and their heads placed in 4% paraformaldehyde. Twenty-four hours following euthanization, brains were removed from skulls and placed 4% paraformaldehyde.

Composite Motor Map of Female Sprague-Dawley Rats

To evaluate the location of the lesions in relation to movement representations in the motor cortex we co- registered the location of voxels affected by the lesion in the MRI data with a 'composite motor map' based on intracortical microstimulation (ICMS) data collected in naïve, age and sex matched, Sprague Dawley rats (N=16). Mapping experiments were conducted, as previously described (Dancause et al., 2008; Deffeyes et al., 2015; Dea et al., 2016) to cumulate 10 motor maps of RFA, CFA, and HL. For each animal, anesthesia was induced with an initial intraperitoneal injection of 80 mg/kg of ketamine hydrochloride (Ketaset; Pfizer) and maintained during the surgical procedures with 2% isoflurane (Furane; Baxter) in 100% oxygen. Animals received injections of dexamethasone (1 mg/kg; intramuscular) to reduce inflammation and saline (5 ml/kg/h; subcutaneous) to maintain hydration over the experimental procedure. Animal body temperature was maintained near 36.5°C throughout the surgery with a homeothermic blanket (Harvard Apparatus). A craniotomy and durectomy were performed to expose the representations of the motor cortex. The opening was covered with mineral oil to protect the cortex. An incision of the cisterna magna was made to drain cerebral spinal fluid to lower intracranial pressure and reopened as needed when cerebral swelling was observed. After the surgical procedures, the anesthesia was turned off and the animals transitioned to ketamine sedation (3-5 mg/kg/10min; intraperitoneal) for the collection of physiological data. A high-resolution digital photograph of the cortex was used to record the locations of electrode penetrations with an image-processing software (Canvas, version 11; ACD Systems). The picture included bregma and a small ruler to allow the alignment of motor maps across animals and ensure consistent scaling. ICMS mapping was conducted using an interpenetration distance of ~333 μm. At each cortical penetration site, a glass insulated tungsten microelectrode (~500

kΩ) was lowered into the cortex to a depth of 1500 to 1600 μm to target layer V neurons. A stimulation train consisted of 13 monophasic square pulses (0.2 ms duration; 3.3 ms interpulse interval), and trains were delivered at 1 Hz from an electrically isolated, constant current stimulator (BAK electronics inc., Umatilla, FL). Stimulation intensity was progressively increased, and the movement evoked at threshold current intensity (the current at which movements were evoked by 50% of the stimulation trains) was identified and used for subsequent analyses. Movements were categorized as forelimb, hindlimb, neck, vibrissae, or mouth (jaw or tongue movements). If no movement was evoked at a maximum current intensity of 100 μA, the site was defined as unresponsive. Custom-made MATLAB codes (MathWorks, MA) were used for ICMS map analyses. First, motor maps of individual control animals were reconstructed using an algorithm that expanded the specific color assigned to the response type (i.e. CFA, RFA, HL, trunk, vibrissae or no response) from each electrode penetration site on the map to neighboring pixels using nearest-neighbor interpolation until all pixels were assigned a color (Touvykine et al., 2016). Pixelated reconstructions were then transformed into vector images and scaled to the calibration ruler placed on the top of brain during ICMS data collection. Using bregma as the origin (0, 0), each vector based ICMS map was rotated so that the midline of the skull was aligned with the X-axis (horizontal axis of the classical Cartesian plane) oriented in the same way as in Figure 2D. Vector-based images were converted back to pixel image (pixel size: 0.1328mm AP by 0.1328mm ML) to match the ML resolution of the MRI scan. Then, to match the AP resolution of MRI scans (pixel size: 0.8mm AP by 0.1328mm ML), the pixelated ICMS maps were downsampled in the AP axis using linear interpolation. Downsampled ICMS maps of all animals were combined and superimposed on top of each other to reveal the cortical

regions from which movements were consistently evoked across multiple rats. The zone with maximal overlap included all 10 rats for the CFA, 8 out of 10 rats for the HL, and 6 out of the 10 rats for RFA. For subsequent analyses, cortical territory consistently evoking movements in 50% or more of the maximal overlap was defined as 'region of coherence' for each motor representation. Accordingly, the region of coherence corresponds to cortical territory that consistently evoked movements in 5 or more animals for CFA (surface area, 4.99 mm^2) and 4 or more animals for HL (3.51 mm^2), and in 3 or more animals for RFA (1.49 mm^2). The cortex was further arbitrarily subdivided into 6 regions of interest around the regions of coherence: medial to RFA (surface area: 9.03 mm^2), lateral to RFA (12.43 mm^2), medial to CFA (8.60 mm^2), lateral to CFA (8.82 mm^2), medial to HL (9.88 mm^2), and lateral to HL (15.93 mm^2). The resulting composite ICMS map and infarct map from the MRI with matching pixel resolutions were aligned using the origin pixels of the MRI lesion in the horizontal plane (posterior point of anterior commissure = 0,0) and the composite ICMS map in the horizontal plane (bregma = 0,0). The infarct volume of each pixel within regions of coherence of CFA, RFA, HL, as well as each adjacent sub-region of interest was calculated from the aligned horizontal plane infarct map (Figure 2D). Infarct volumes of all pixels within a given sub-region were summed to provide a total sub-regional infarct volume that was utilized for regression modeling to relate injury location to impairment and recovery on the motor tasks previously described.

Statistical Analysis

All analyses were conducted for the limb contralateral to the injured hemisphere (i.e. the impaired limb). Analysis of behavioral data used repeated measures ANOVA with time (across weeks for all analyses) and zone (for only the PhenoTyper analysis) as within-subject variables and group (stroke vs. sham) as a between-subject variable. The Greenhouse-Geisser correction was applied when assumptions of sphericity were violated. Sidak-corrected t-tests were used for post-hoc analysis with = 0.05 used to define all statistically significant differences. Multiple linear regressions were used to predict individual animal performance at week 1 (initial impairment) and week 7 (performance with spontaneous recovery) post-stroke based on the size and location of each animal's brain lesion. As described in the previous section, infarct volumes within each sub-region of the composite motor map were entered as predictor variables for linear regressions (total infarct volume and infarct volume in the following sub-regions: medial to HL, lateral to HL, HL, medial to CFA, lateral to CFA, CFA, medial to RFA, lateral to RFA, RFA; entry criterion: $p \leq 0.05$; removal criterion: $p \geq 0.10$). Performance in each of the motor behaviors (staircase, cylinder, beam forelimb, beam hindlimb, pellet retrieval in PhenoTyper) were used as the determinants in the regression model. All analyses were conducted using SPSS Statistics version 25 (IBM). All data is presented as group mean ± standard error.

Results

Infarct Volume and Location

The cold light photothrombosis procedure created a lesion in ~92% of subjects (n = 44/48). The use of multiple light apertures to restrict lesion size resulted in an even distribution of small to large infarcts (5.7 – 155.5 mm^3) with a mean of 70.6 ± 7.03 mm^3 (Figure 2A-B). The maximum range of anterior-posterior injury across all animals was from +7.2 to -3.2 mm relative to Bregma (Figure 2C). Injury volume was primarily centered around RFA, CFA, and HL (Figure 2D). The range of lesion sizes and differential impact on forelimb, hindlimb, and surrounding brain regions across animals provided an excellent sample for relating lesion characteristics to impairment and recovery on a battery of motor outcomes and to make predictions of the behavioral effects of stroke at the individual level (Figures 4 to 11).

Staircase

Photothrombotic stroke resulted in significant group impairments in pellet grasping and retrieval in the staircase task at all post-stroke weeks ($F_{4,248} = 24.213$, $p < 0.001$; Figure 4A-B). The mean difference in pellet retrieval between sham and stroke rats at the post-stroke time points was 5.68 ± 0.99 pellets. Multiple linear regression indicated that the sum of damage in both the CFA and RFA was most predictive of staircase performance at week 1 post-stroke ($R = 0.784$; $R^2_{adj} = 0.595$; $p < 0.001$; Table 1, Table 2, Figure 4C-D; Figure 5A-B). In contrast, at week 7 post-stroke the sum of damage to the CFA and the adjacent region lateral to RFA were the sub-regions most predictive of pellet retrieval ($R = 0.849$; $R^2_{adj} = 0.707$; $p < 0.001$; Figure 4E-F, Figure 5C-D). At both week 1 and 7, infarct volume in the predictive regions was negatively

related to task performance, meaning that greater damage in these sub-regions was associated with reduced task performance.

Cylinder

Spontaneous use of the forelimb for exploration in the cylinder was also significantly reduced by stroke at weeks 1, 3, and 5 post-stroke ($F_{4,248} = 10.819$, $p < 0.001$; Figure 6A-B). Mean use of the impaired limb was reduced by 14.1 ± 3.3% in rats with stroke compared to sham rats at these time points. Infarct volume within the CFA alone was the best predictor of impaired limb usage at week 1 post-stroke ($R = 0.591$; $R^2_{adj} = 0.334$; $p < 0.001$; Figure 6C-D, Figure 7A-B), whereas the infarct volume of the region lateral to the CFA was the best predictor of impaired limb usage at week 7 ($R = 0.562$; $R^2_{adj} = 0.299$; $p < 0.001$; Figure 6E-F, Figure 7C-D).

Beam

Accuracy of paw placement during walking was assessed in both the impaired forelimb and hindlimb using the beam-walking task (Figure 8A). Although impairments could be observed in some individual rats, the overall stroke group did not show a significant reduction in successful steps with the forelimb compared to the sham group at any post-stroke time point ($F_{4,248} = 1.328$, $p = 0.264$; Figure 8B). However, mean reductions in successful hindlimb placements were observed at post-stroke weeks 1, 3, and 7 ($F_{4,248} = 3.457$, $p = 0.009$; Figure 8C). Rats in the stroke group demonstrated a mean reduction of 7.2 ± 2.6% successful steps compared to shams at these time points. Individual performance in successful placement of the forelimb at week 1

was best predicted by the infarct volume in the CFA ($R = 0.393$; $R^2_{adj} = 0.134$; $p = 0.008$; Figure 8D, Figure 9A-B), whereas performance with the hindlimb was best predicted by infarct volume in HL ($R = 0.550$; $R^2_{adj} = 0.286$; $p < 0.001$; Figure 8E, Figure 9E-F). As similarly observed in the staircase and cylinder tasks, regions adjacent to those that predicted performance at week 1 were the best predictors of both forelimb and hindlimb performance in the beam at week 7. In the case of the forelimb, infarct volume in the region lateral to CFA was the best predictor of week 7 performance ($R = 0.488$; $R^2_{adj} = 0.220$; $p = 0.001$; Figure 8F, Figure 9C-D). For the hindlimb, infarct volume in the region medial to HL was the best predictor of successful steps on the beam at week 7 ($R = 0.516$; $R^2_{adj} = 0.249$; $p < 0.001$; Figure 8G, Figure 9G-H).

Spontaneous Activity, Socialization, and Limb Use

The PhenoTyper cage enabled analysis of locomotor activity (distance travelled), socialization, and spontaneous use of the forelimb for reaching and grasping in a semi-naturalistic caging environment over an extended period of time (1 hour/session). This afforded an opportunity to assess how rats engage with their environment and whether they use their impaired limbs spontaneously, rather than in a task where they were trained/forced to use it (i.e. staircase). This is an important complement to the task-based measures (i.e. staircase, cylinder, beam), as it has been previously shown that ability to perform a motor task does not necessarily translate into increased use of the paretic limb during activities of daily living (Rand and Eng, 2012). We

observed no significant difference in total distance travelled within a session between the sham (261.9 ± 12.2 m) and stroke (257.4 ± 11.7 m) groups ($F_{4,84} = 0.718$, $p = 0.582$). We observed a significant group by zone interaction in the proportion of time spent in the PhenoTyper ($F_{7,147} = 3.035$, $p = 0.005$; Figure 10A). Post-hoc analysis of this effect indicated that rats in the stroke group spent a significantly greater proportion of time in the PhenoTyper in the pellet tray zone than rats in the sham group ($t_{(22)} = 4.475$, $p = 0.047$; Figure 10B). Based on this effect, the pellet zone accessible by using only the impaired limb was selected for further analysis. There was no significant difference in the amount of time that stroke and sham groups spent in the pellet zone for the impaired limb ($F_{4,84} = 1.345$, $p = 0.260$; Figure 10C); however, sham rats retrieved significantly more pellets than stroke rats at weeks 5 and 7 post-stroke in the PhenoTyper ($F_{4,84} = 3.662$, $p = 0.028$; Figure 10D). Pellet retrieval in the PhenoTyper at week 1 was best predicted by infarct volume in CFA ($R = 0.712$; $R^2_{adj} = 0.457$; $p = 0.009$; Figure 10E-F, Figure 11A-B), while pellet retrieval at week 7 was best predicted by infarct volume in the adjacent RFA region ($R = 0.764$; $R^2_{adj} = 0.542$; $p = 0.004$; Figure 10G-H, Figure 11C-D).

Discussion

Lesion volume in domain-specific motor sub-regions best predicts post-injury task impairment

Following photothrombotic stroke in the motor cortex, rats exhibited impairments in several motor domains, including skilled reaching, spontaneous forelimb use and limb placement during walking, that were assessed using classic rodent tasks (Corbett et al., 2017; Balkaya et al., 2018). We also assessed unrestricted reaching and spontaneous activity in a free-ranging housing

environment. We observed that the degree of impairment at week 1 post-stroke was best predicted by the volume of damage within domain-specific regions of the motor cortex. In other words, each task had specific motor sub-regions, that when damaged, decreased the performance on that task in a volume-dependent manner. Damage to the CFA and RFA impaired forelimb function on the staircase task, while damage to the CFA and HL impaired forelimb and hindlimb placing responses respectively on the beam task. Furthermore, damage to the CFA impaired spontaneous use of the impaired forelimb in the cylinder task, as well as the spontaneous retrieval of pellets within the PhenoTyper. For each of these domains, impairment was positively correlated with the volume of damage to the corresponding motor sub-region. The hierarchical, region-specific representation of motor functions within the motor cortex is an established principle (Leyton and Sherrington, 1917; Hall and Lindholm, 1974; Barth et al., 1990), and our results are consistent with other preclinical studies demonstrating the importance of specific motor sub-regions to single behavioral tasks (Schallert et al., 2002; Kim and Jones, 2010; Touvykine et al., 2016). These findings emphasize the importance of mapping both the size and specific location of cortical damage when contextualizing behavioral impairments after stroke.

Perilesional regions that are unique to each motor domain influence degree of recovery from brain injury.

Recovery from initial impairment at week 7 post-stroke followed a similar pattern as impairment at week 1, wherein each motor domain corresponded to a unique topographical sub-region of the motor cortex. However, the regions involved in recovery at week 7 were adjacent to those involved in initial impairment at week 1. Damage to the CFA and area lateral to the RFA, which corresponds to mouth (jaw and tongue) motor area (Neafsey et al., 1986) decreased

functional recovery of performance in the staircase task at week 7 post-stroke. Damage to the area lateral to the CFA, corresponding to somatosensory region of the forelimb (Palomero-Gallagher and Zilles, 2015), impaired recovery of forelimb placement during the beam task. Whereas, damage to the area medial to the HL, related to vibrissae and frontal eye fields regions (Neafsey et al., 1986), impaired the functional recovery of hindlimb placement. Increased volume of damage in the area lateral to the CFA resulted in a decrease in recovery of spontaneous usage of the impaired forelimb during the cylinder task, while the volume of damage within RFA impacted recovery of spontaneous retrieval of pellets within the PhenoTyper. In all cases, damage that encroached on areas adjacent to the initial domain-specific regions reduced the ability to recover from lesion-induced impairments. Reorganization of motor representations in adjacent brain regions is thought to contribute to functional recovery (Nudo and Milliken, 1996; Xerri et al., 1998; Jones and Adkins, 2015). However, the present study suggests that each motor domain has specific brain regions that are primarily associated with recovery, and that reorganization of post-stroke motor functions in the undamaged cortex is highly localized. For example, tissue rostral to the stroke may not have the same potential for restoring function of a given motor domain as tissue located lateral or medial to the stroke. This conclusion is congruent with other studies in which two-stage lesions have been performed in attempts to reinstate post-stroke deficits that have recovered over time. For example, simply enlarging the motor cortex lesion and/or lesioning the homologous motor area in the other hemisphere did not reinstate upper limb deficits in non-human primates (Leyton and Sherrington, 1917). In contrast, McNeal et al (McNeal et al., 2010), showed that the recovered upper limb deficits in rhesus monkeys following M1 lesions could be reinstated by secondary injury to the

supplementary motor area (SMA or M2). Similar findings have been reported following photothrombotic stroke to the RFA portion of the mouse motor cortex. Single pellet reaching was disrupted by the lesion, followed by behavioral recovery. A second stroke in the agranular medial cortex (M2 in rodents), a region thought to be analogous to the primate's premotor areas, reinstated the original deficits (Zeiler et al., 2013). These findings have important implications as technologies for region-specific activation/suppression of brain activity become more readily available in clinical practice (Smith and Stinear, 2016). It may be that techniques such as TMS will need to target domain-specific brain regions based on the lesion profile and impairments of each individual patient in order to obtain benefit. Indeed, a failure to individualize treatment based on lesion characteristics could contribute to failure of clinical trials (Stinear et al., 2020).

Spontaneous activity and limb use following stroke

During inpatient hospital stays, a decrease in physical activity is common following stroke (Bernhardt et al., 2004; West and Bernhardt, 2011). We did not observe such a decrease, our rats maintained activity levels similar to their sham counterparts. This disparity may be due to differences between typical clinical and preclinical environments. Rats in our study were exposed to an enriched environment in which they had full autonomy to explore and engage with the objects around them. In a hospital setting, even though patients report boredom they are encouraged to remain in bed and rest, discouraging physical activity (Kenah et al., 2018). Our findings in rats using the PhenoTyper task are similar to those of Rosbergen et al in humans, who found that employing an enriched environment promoted increased levels of physical activity, along with associated benefits, following stroke (Rosbergen et al., 2017). While in the

PhenoTyper, the stroke rats spent more time on average than the sham rats within the pellet reaching zone, despite being relatively unsuccessful at retrieving pellets with their impaired limb. This contrasts with the clinical literature where the ability to use the impaired limb does not necessarily translate into increased use of that limb in daily life (Rand and Eng, 2012). This discrepancy highlights the fact that the rats remained highly motivated to utilize their impaired limb for food rewards, and that impairment does not necessarily lead to limb learned non-use (Taub et al., 2006). The brain regions associated with impaired pellet retrieval in the PhenoTyper were consistent with those of the staircase at both weeks 1 and 7. This finding reinforces the conclusion that CFA and RFA are critical motor regions for skilled reaching tasks, and that the most important areas for recovery appear to be those that are adjacent, in a spatially selective manner (i.e. lateral vs medial), to the initial domain-specific site.

Lesion location and patient-specific interventions for stroke recovery

It is evident from our study that lesion location is a critical determinant of cortical reorganization and subsequent functional recovery following stroke. However, despite the ubiquity of reporting lesion volume within the preclinical literature, precise infarct location is rarely considered as influencing functional outcome (Karthikeyan et al., 2019). Clinical research has placed greater importance on location, but analyses of location tend to be descriptive in nature (e.g. cortical, sub-cortical), with relatively few studies adjusting treatment parameters based on individualized lesion characteristics (Kirton et al., 2008). Here, using imaging methods like those that can be employed clinically, we demonstrate a clear relationship between lesion characteristics and post-stroke impairment and recovery, indicating that detailed lesion assessment should be a routine element of all stroke research. Given that preclinical research often precedes clinical adoption,

attempts should be made to standardize lesion mapping practices across species in order to maximize the likelihood of translational success (Corbett et al., 2017). The term "perilesional" is commonly used to describe the region surrounding the infarct and represents a potential target of localized interventions to maximize recovery (Krakauer and Carmichael, 2017). In preclinical studies, interventions (e.g. application of drugs, optogenetic stimulation) related to perilesional areas are common, but without regard to specific functional sub-regions within this area or the individual functional impairments of each animal (Alia et al., 2017; Coleman et al., 2017). In light of the present study, we propose that this lack of precision may be an important contributing factor to the conflicting results observed in clinical trials where a treatment such as TMS delivered to one specific brain region across patients can differentially interfere with or promote recovery (Nowak et al., 2009; McDonnell and Stinear, 2017). Instead, the targeted area in the perilesional region or contralesional hemisphere should be carefully selected based on the specific lesion profile and impairments, on a subject by subject basis. This approach is beginning to emerge in clinical noninvasive brain stimulation studies (Di Pino et al., 2014; Boddington and Reynolds, 2017). Similarly, delivery of other interventions, including stem cells and rehabilitation, could be adjusted based on knowledge of precise stroke location, level of impairment, and other predictive variables. This more personalized approach would not require that patients be enrolled in clinical trials based on lesion location. Instead, the knowledge of lesion location and the implications for recovery could help explain variability in differential responses to treatment between individuals. It is essential that preclinical research should also move in the same direction as clinical studies (Corbett et al., 2017), incorporating quantification of lesion volume and location when assessing therapies (e.g. optogenetic stimulation, stem cell

transplants) to enhance stroke recovery (Tennant et al., 2017; Wahl et al., 2017; Jeffers et al., 2018b). An important goal of preclinical and clinical research is the development of post-stroke biomarkers that will lead to individualized stroke treatments to optimize post-stroke recovery (Corbett et al., 2015, 2017; Boyd et al., 2017; Stinear et al., 2017). To accomplish this, individual biomarkers, be they functional, structural, or electrophysiological, need to be evaluated for their ability to predict long term functional outcome. The results of the present study suggest that precise lesion location may be one such important prognostic factor for stroke recovery.

References

Alia C, Spalletti C, Lai S, Panarese A, Lamola G, Bertolucci F, Vallone F, Di Garbo A, Chisari C, Micera S, Caleo M (2017) Neuroplastic changes following brain ischemia and their contribution to stroke recovery: Novel approaches in neurorehabilitation. Front Cell Neurosci 11:76.

Balkaya MG, Trueman RC, Boltze J, Corbett D, Jolkkonen J (2018) Behavioral outcome measures to improve experimental stroke research. Behav Brain Res 352:161–171.

Barth TM, Jones TA, Schallert T (1990) Functional subdivisions of the rat somatic sensorimotor cortex. Behav Brain Res 39:73–95.

Bernhardt J, Dewey H, Thrift A, Donnan G (2004) Inactive and alone: Physical activity within the first 14 days of acute stroke unit care. Stroke 35:1005–1009.

Bernhardt J, Hayward KS, Dancause N, Lannin NA, Ward NS, Nudo RJ, Farrin A, Churilov L, Boyd LA, Jones TA, Carmichael ST, Corbett D, Cramer SC (2019) A stroke recovery trial development framework: Consensus-based core recommendations from the Second Stroke Recovery and Rehabilitation Roundtable. Int J Stroke 14:792–802.

Biernaskie J, Corbett D, Peeling J, Wells J, Lei H (2001) A serial MR study of cerebral blood flow changes and lesion development following endothelin-1-induced ischemia in rats. Magn Reson Med 46:827–830.

Boddington LJ, Reynolds JNJ (2017) Targeting interhemispheric inhibition with neuromodulation to enhance stroke rehabilitation. Brain Stimul 10:214–222.

Boyd LA, Hayward KS, Ward NS, Stinear CM, Rosso C, Fisher RJ, Carter AR, Leff AP, Copland DA, Carey LM, Cohen LG, Basso DM, Maguire JM, Cramer SC (2017) Biomarkers of stroke recovery: Consensus-based core recommendations from the Stroke Recovery and Rehabilitation Roundtable. Int J Stroke 12:480–493.

Byblow WD, Stinear CM, Barber PA, Petoe MA, Ackerley SJ (2015) Proportional recovery after stroke depends on corticomotor integrity. Ann Neurol 78:848–859.

Chen CL, Tang FT, Chen HC, Chung CY, Wong MK (2000) Brain lesion size and location: Effects on motor recovery and functional outcome in stroke patients. Arch Phys Med Rehabil 81:447–452.

Coleman ER, Moudgal R, Lang K, Hyacinth HI, Awosika OO, Kissela BM, Feng W (2017) Early rehabilitation after stroke: A narrative review. Curr Atheroscler Rep 19:59.

Corbett D, Carmichael ST, Murphy TH, Jones TA, Schwab ME, Jolkkonen J, Clarkson AN, Dancause N,

Weiloch T, Johansen-Berg H, Nilsson M, McCullough LD, Joy MT (2017) Enhancing the alignment of the preclinical and clinical stroke recovery research pipeline: Consensus-based core recommendations from the Stroke Recovery and Rehabilitation Roundtable translational working group. Int J Stroke 12:462–471.

Corbett D, Jeffers M, Nguemeni C, Gomez-Smith M, Livingston-Thomas J (2015) Lost in translation: Rethinking approaches to stroke recovery. In: Prog Brain Res, pp 413–434.

Dalton E, Churilov L, Lannin NA, Corbett D, Hayward KS (2019) Dose articulation in preclinical and clinical stroke recovery: Refining a discovery research pipeline and presenting a scoping review protocol. Front Neurol 10:1148.

Dancause N, Duric V, Barbay S, Frost SB, Stylianou A, Nudo RJ (2008) An additional motor-related field in the lateral frontal cortex of squirrel monkeys. Cereb Cortex 18:2719–2728.

Dea M, Hamadjida A, Elgbeili G, Quessy S, Dancause N (2016) Different patterns of cortical inputs to subregions of the primary motor cortex hand representation in Cebus apella. Cereb Cortex 26:1747– 1761.

Deffeyes JE, Touvykine B, Quessy S, Dancause N (2015) Interactions between rostral and caudal cortical motor areas in the rat. J Neurophysiol 113:3893–3904.

Di Pino G, Pellegrino G, Assenza G, Capone F, Ferreri F, Formica D, Ranieri F, Tombini M, Ziemann U, Rothwell JC, Di Lazzaro V (2014) Modulation of brain plasticity in stroke: A novel model for neurorehabilitation. Nat Rev Neurol 10:597–608.

Dromerick AW, Reding MJ (1995) Functional outcome for patients with hemiparesis, hemihypesthesia, and hemianopsia: Does lesion location matter? Stroke 26:2023–2026.

Edwardson MA, Wang X, Liu B, Ding L, Lane CJ, Park C, Nelsen MA, Jones TA, Wolf SL, Winstein CJ, 22

Dromerick AW (2017) Stroke lesions in a large upper limb rehabilitation trial cohort rarely match lesions in common preclinical models. Neurorehabil Neural Repair 31:509–520.

Feng W, Wang J, Chhatbar PY, Doughty C, Landsittel D, Lioutas VA, Kautz SA, Schlaug G (2015) Corticospinal tract lesion load: An imaging biomarker for stroke motor outcomes. Ann Neurol 78:860–870.

Hall RD, Lindholm EP (1974) Organization of motor and somatosensory neocortex in the albino rat. Brain Res 66:23–38.

Harvey RL, Edwards D, Dunning K, Fregni F, Stein J, Laine J, Rogers LM, Vox F, Durand-Sanchez A, Bockbrader M, Goldstein LB, Francisco GE, Kinney CL, Liu CY (2018) Randomized sham- controlled trial of navigated repetitive transcranial magnetic stimulation for motor recovery in stroke the NICHE trial. Stroke 49:2138–2146.

Hayward KS, Schmidt J, Lohse KR, Peters S, Bernhardt J, Lannin NA, Boyd LA (2017) Are we armed with the right data? Pooled individual data review of biomarkers in people with severe upper limb impairment after stroke. NeuroImage Clin 13:310–319.

Jeffers MS, Karthikeyan S, Corbett D (2018a) Does stroke rehabilitation really matter? Part A: Proportional stroke recovery in the rat. Neurorehabil Neural Repair 32:3–6.

Jeffers MS, Karthikeyan S, Gomez-Smith M, Gasinzigwa S, Achenbach J, Feiten A, Corbett D (2018b) Does stroke rehabilitation really matter? Part B: An algorithm for prescribing an effective intensity of rehabilitation. Neurorehabil Neural Repair 32:73–83.

Jones TA, Adkins DL (2015) Motor system reorganization after stroke: Stimulating and training toward perfection. Physiology 30:358–370.

Karthikeyan S, Jeffers MS, Carter A, Corbett D (2019) Characterizing spontaneous motor recovery following cortical and subcortical stroke in the rat. Neurorehabil Neural Repair 33:27–37.

Kenah K, Bernhardt J, Cumming T, Spratt N, Luker J, Janssen H (2018) Boredom in patients with acquired brain injuries during inpatient rehabilitation: A scoping review. Disabil Rehabil 40:2713– 2722.

Kim B, Winstein C (2016) Can neurological biomarkers of brain impairment be used to predict poststroke motor recovery? A systematic review. Neurorehabil Neural Repair 31:3–24.

Kim SY, Jones TA (2010) Lesion size-dependent synaptic and astrocytic responses in cortex contralateral to infarcts in middle-aged rats. Synapse 64:659–671.

Kirton A, Chen R, Friefeld S, Gunraj C, Pontigon AM, DeVeber G (2008) Contralesional repetitive transcranial magnetic stimulation for chronic hemiparesis in subcortical paediatric stroke: A randomised trial. Lancet Neurol 7:507–513.

Krakauer JW, Carmichael ST (2017) Broken movement: the neurobiology of motor recovery after stroke. Cambridge, MA: MIT Press.

Krakauer JW, Marshall RS (2015) The proportional recovery rule for stroke revisited. Ann Neurol 78:845–847.

Lang CE, Lohse KR, Birkenmeier RL (2015) Dose and timing in neurorehabilitation: Prescribing motor therapy after stroke. Curr Opin Neurol 28:549–555.

Leyton ASF, Sherrington CS (1917) Observations of the excitable cortex of the chimpanzee, orang-utan, and gorilla. Q J Exp Physiol 11:135–222.

Lohse KR, Lang CE, Boyd LA (2014) Is more better? Using metadata to explore dose-response relationships in stroke rehabilitation. Stroke 45:2053–2058.

McDonnell MN, Stinear CM (2017) TMS measures of motor cortex function after stroke: A meta- analysis. Brain Stimul 10:721–734.

McNeal DW, Darling WG, Ge J, Stilwell-Morecraft KS, Solon KM, Hynes SM, Pizzimenti MA, Rotella DL, Vanadurongvan T, Morecraft RJ (2010) Selective long-term reorganization of the corticospinal projection from the supplementary motor cortex following recovery from lateral motor cortex injury. J Comp Neurol 518:586–621.

Montoya CP, Campbell-Hope LJ, Pemberton KD, Dunnett SB (1991) The “staircase test”: a measure of independent forelimb reaching and grasping abilities in rats. J Neurosci Methods 36:219–228.

Neafsey EJ, Bold EL, Haas G, Hurley-Gius KM, Quirk G, Sievert CF, Terreberry RR (1986) The organization of the rat motor cortex: A microstimulation mapping study. Brain Res Rev 11:77–96.

Nowak DA, Grefkes C, Ameli M, Fink GR (2009) Interhemispheric competition after stroke: Brain stimulation to enhance recovery of function of the affected hand. Neurorehabil Neural Repair 23:641–656.

Nudo RJ, Milliken GW (1996) Reorganization of movement representations in primary motor cortex following focal ischemic infarcts in adult squirrel monkeys. J Neurophysiol 75:2144–2149.

Page SJ, Gauthier L V, White S (2013) Size doesn't matter: Cortical stroke lesion volume is not associated with upper extremity motor impairment and function in mild, chronic hemiparesis. Arch Phys Med Rehabil 94:817–821.

Palomero-Gallagher N, Zilles K (2015) Isocortex. In: The Rat Nervous System: Fourth Edition (Paxinos G, ed), pp 601–625. San Diego, CA: Elsevier Inc.

Papp EA, Leergaard TB, Calabrese E, Johnson GA, Bjaalie JG (2014) Waxholm space atlas of the Sprague Dawley rat brain. Neuroimage 97:374–386.

Peeling J, Corbett D, Del Bigio MR, Hudzik TJ, Campbell TM, Palmer GC (2001) Rat middle cerebral artery occlusion: Correlations between histopathology, T2-weighted magnetic resonance imaging, and behavioral indices. J Stroke Cerebrovasc Dis 10:166–177.

Prabhakaran S, Zarahn E, Riley C, Speizer A, Chong JY, Lazar RM, Marshall RS, Krakauer JW (2008) Inter-individual variability in the capacity for motor recovery after ischemic stroke. Neurorehabil Neural Repair 22:64–71.

Rand D, Eng JJ (2012) Disparity between functional recovery and daily use of the upper and lower extremities during subacute stroke rehabilitation. Neurorehabil Neural Repair 26:76–84.

Rosbergen IC, Grimley RS, Hayward KS, Walker KC, Rowley D, Campbell AM, McGufficke S, Robertson ST, Trinder J, Janssen H, Brauer SG (2017) Embedding an enriched environment in an acute stroke unit increases activity in people with stroke: A controlled before-after pilot study. Clin Rehabil 31:1516–1528.

Schallert T, Fleming SM, Leasure JL, Tillerson JL, Bland ST (2000) CNS plasticity and assessment of forelimb sensorimotor outcome in unilateral rat models of stroke, cortical ablation, parkinsonism and spinal cord injury. Neuropharmacology 39:777–787.

Schallert T, Woodlee MT, Fleming SM (2002) Disentangling multiple types of recovery from brain injury recovery of function. Pharmacol Cereb Ischemia:201–216.

Smith MC, Stinear CM (2016) Transcranial magnetic stimulation (TMS) in stroke: Ready for clinical practice? J Clin Neurosci 31:10–14.

Stinear CM, Barber PA, Petoe M, Anwar S, Byblow WD (2012) The PREP algorithm predicts potential for upper limb recovery after stroke. Brain 135:2527–2535.

Stinear CM, Byblow WD, Ackerley SJ, Smith MC, Borges VM, Barber PA (2017) PREP2: A biomarker-based algorithm for predicting upper limb function after stroke. Ann Clin Transl Neurol 4:811–820.

Stinear CM, Lang CE, Zeiler S, Byblow WD (2020) Advances and challenges in stroke rehabilitation. Lancet Neurol 19:348–360.

Taub E, Uswatte G, Mark VW, Morris DMM (2006) The learned nonuse phenomenon: implications for rehabilitation. Eura Medicophys 42:241–256.

Tennant KA, Taylor SL, White ER, Brown CE (2017) Optogenetic rewiring of thalamocortical circuits to restore function in the stroke injured brain. Nat Commun 8:15879.

Touvykine B, Mansoori BK, Jean-Charles L, Deffeyes J, Quessy S, Dancause N (2016) The effect of lesion size on the organization of the ipsilesional and contralesional motor cortex. Neurorehabil Neural Repair 30:280–292.

Wahl AS, Büchler U, Brändli A, Brattoli B, Musall S, Kasper H, Ineichen B V., Helmchen F, Ommer B, Schwab ME (2017) Optogenetically stimulating intact rat corticospinal tract post-stroke restores motor control through regionalized functional circuit formation. Nat Commun 8:1187. West T, Bernhardt J (2011) Physical activity in hospitalised stroke patients. Stroke Res Treat 2012:813765.

Winstein CJ, Wolf SL, Dromerick AW, Lane CJ, Nelsen MA, Lewthwaite R, Cen SY, Azen SP (2016) Effect of a task-oriented rehabilitation program on upper extremity recovery following motor stroke the ICARE randomized clinical trial. J Am Med Assoc 315:571–581.

Winters C, Van Wegen EEH, Daffertshofer A, Kwakkel G (2015) Generalizability of the proportional recovery model for the upper extremity after an ischemic stroke. Neurorehabil Neural Repair 29:614–622.

Xerri C, Merzenich MM, Peterson BE, Jenkins W (1998) Plasticity of primary somatosensory cortex paralleling sensorimotor skill recovery from stroke in adult monkeys. J Neurophysiol 79:2119–2148.

Zeiler SR, Gibson EM, Hoesch RE, Li MY, Worley PF, O'Brien RJ, Krakauer JW (2013) Medial premotor cortex shows a reduction in inhibitory markers and mediates recovery in a mouse model of focal stroke. Stroke 44:483–489.

Figures

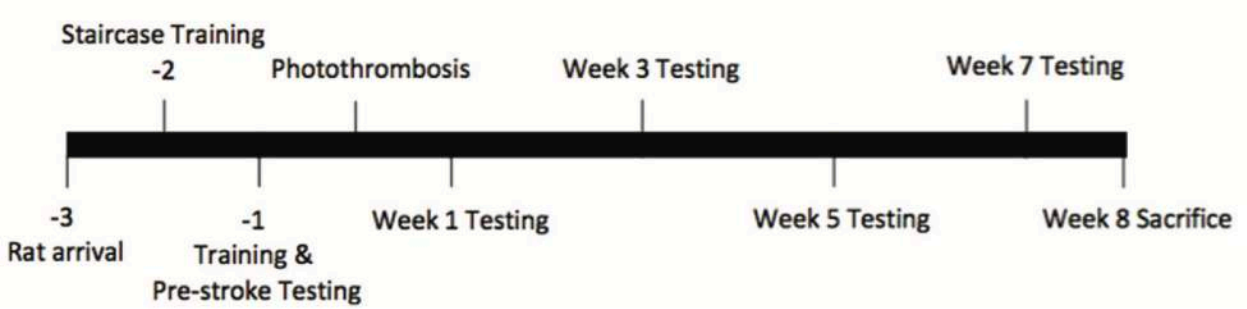

Figure (Ch2)1. Experimental timeline. All timepoints are shown as weeks relative to photothrombosis surgery.

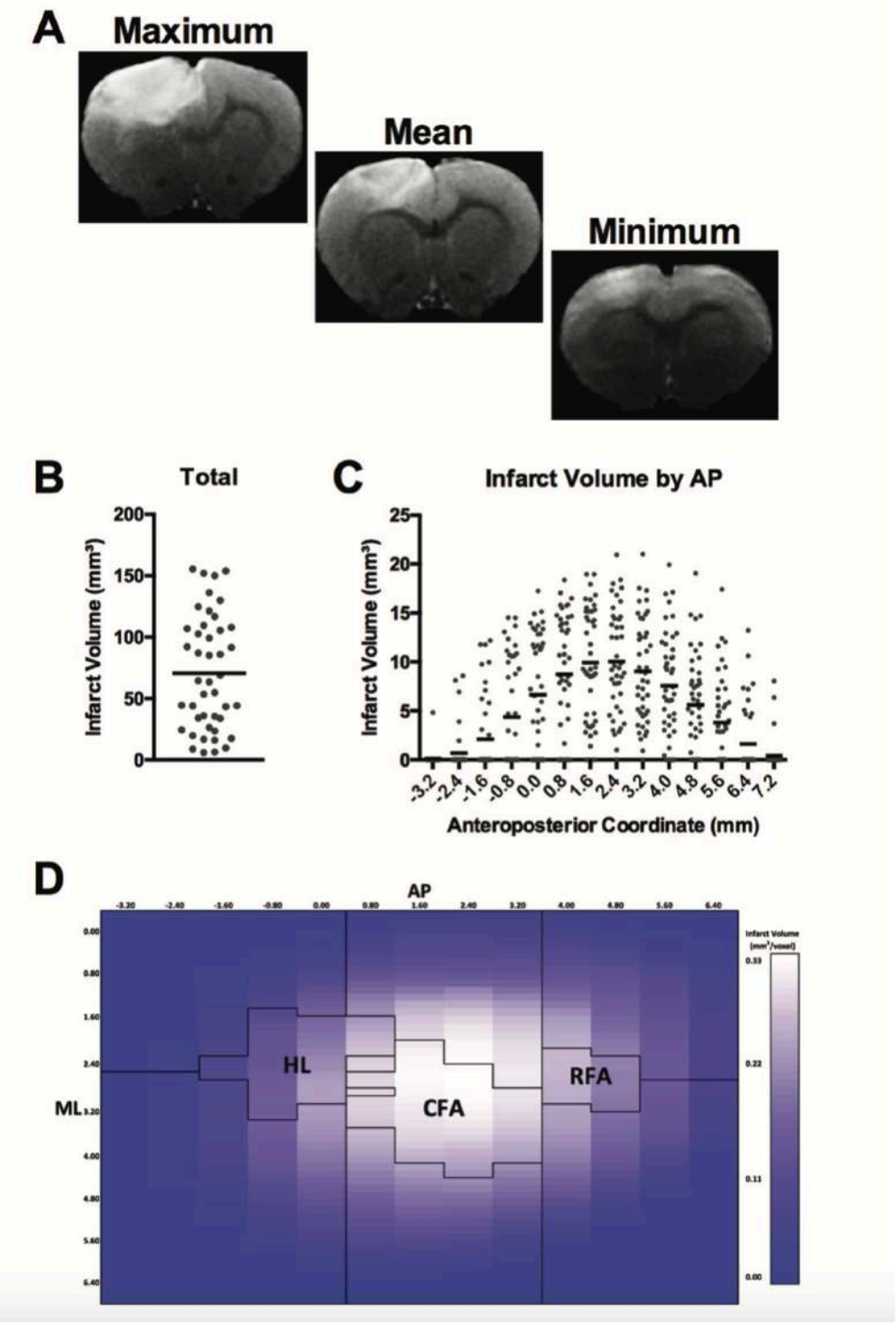

Figure (Ch2)2. (A) Example T2-weighted MRI coronal slice from the slice 2.4 mm anterior to Bregma in animals with the maximum (155.5 mm^3), closest to the mean (68.9 mm^3), and

minimum (5.7 mm^3) infarct volumes respectively. **(B)** Total infarct volumes of all animals that received strokes. Mean infarct volume ± standard deviation was 70.6 ± 46.6 mm^3. **(C)** Anterior-posterior distribution of infarct volume relative to Bregma. The mean infarct volume at a given coordinate is shown with a black line, while the grey dots indicate the infarct volumes of individual animals at a given AP coordinate. **(D)** Longitudinal-plane heat map showing mean distribution of infarct location within the stroke group. The black outlines in the left, center, and right of the image delineate position of the coherence region of the hindlimb, caudal forelimb, and rostral forelimb areas respectively. These boundaries were determined by ICMS mapping in age-, sex-, and strain-matched rats. Infarct location in all animals was centered on these motor regions. The brightness of each square represents the mean infarct volume across all animals with stroke within the dorsal-ventral column of injury at a given AP and ML coordinate. N = 44 in all panels. AP = anteroposterior; ML = mediolateral. ImageJ script for assessing infarct volume and location can be found in Figure 2-1.

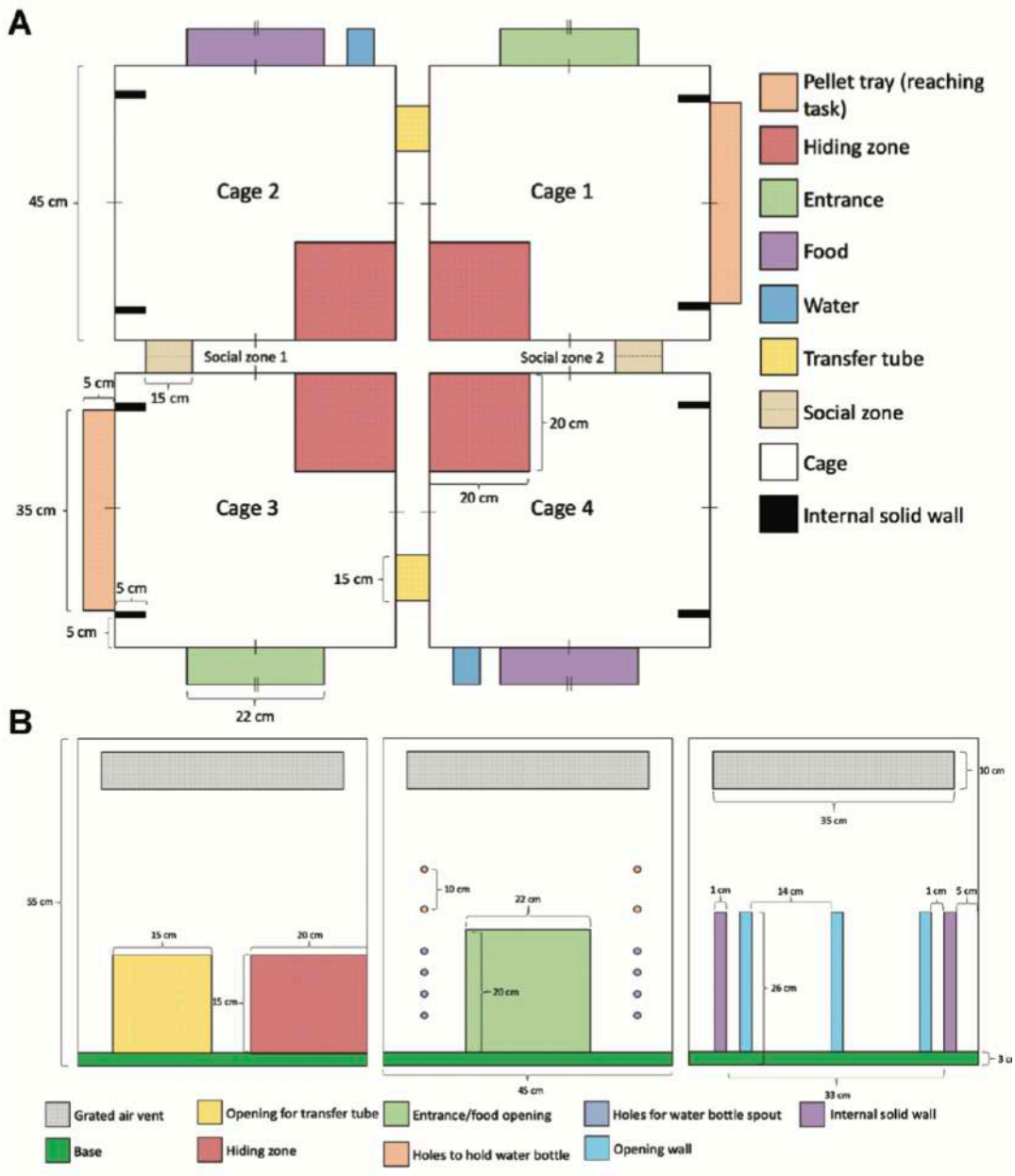

Figure (Ch2)3. (A) Top-down view of the full PhenoTyper arena. Roof-mounted infrared cameras allowed tracking of rat position across the regions of interest shown in the legend. Rats were placed into the PhenoTyper in pairs, with one rat able to access Cage 1 and Cage 2 via the transfer tube, and its cage-mate able to access Cage 3 and Cage 4 via a similar tube. Cage-mates could interact with each other via the tube in Social Zone 1 and 2 but could not cross into each other's cage due to wire bars slotted through the social tube. **(B)** Side-view of each of the

PhenoTyper walls. A recessed tray on the outside of the cage allowed spontaneous limb use to obtain food rewards. Interior walls limited rats to reaching for the right-hand tray with their right paw, and the left-hand tray with their left paw, so that use of the impaired and non-impaired limbs could be determined.

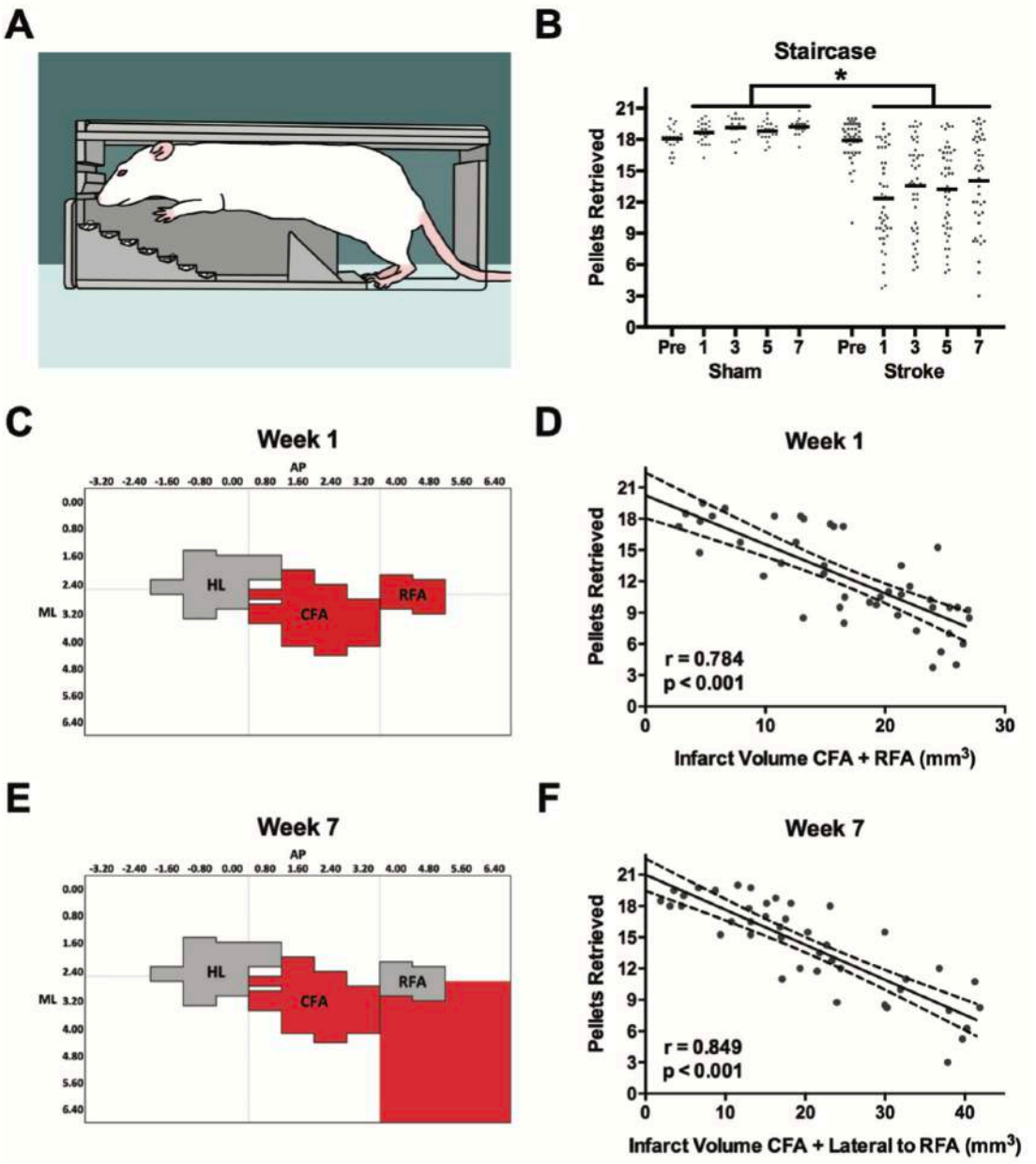

Figure (Ch2)4. (A) Staircase task. The rat must reach downward to grasp and retrieve pellets that are increasingly more distant from the animal as the step decreases. **(B)** Mean performance (black lines) of rats with stroke was significantly worse than shams at all times post-stroke. **(C-D)** Initial post-stroke impairment (pellet retrieval at week 1) was best predicted by the sum of damage to the CFA and RFA (highlighted red). **(E-F)** In contrast, the adjacent region lateral to

RFA was the best predictor of pellet retrieval at week 7. Full regression parameters shown in Table 1. N=64 (sham = 20, stroke = 44). * = $p < 0.05$.

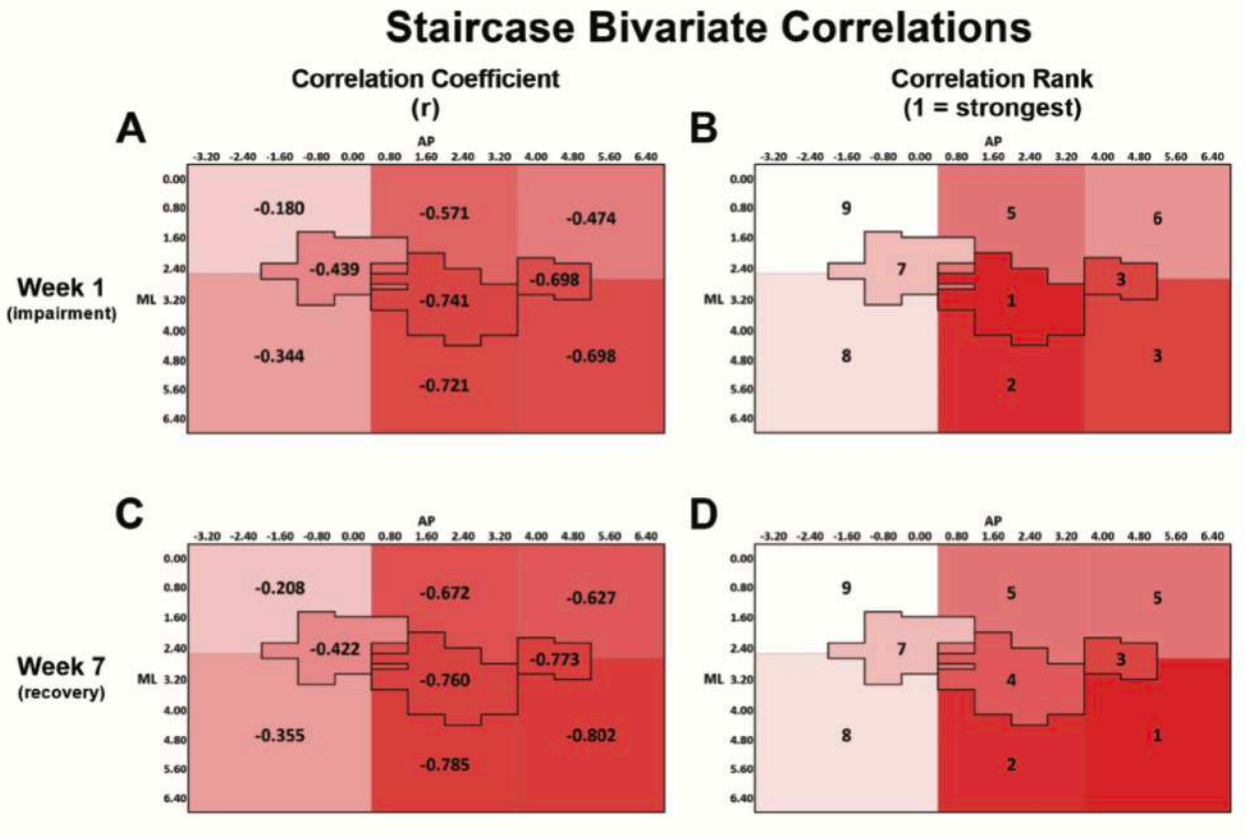

Figure (Ch2)5. (A) Bivariate Pearson correlation coefficients (r) between staircase performance at week 1 and lesion volume within each region of interest. **(B)** Rank-order of correlation coefficients from panel A with "1" indicating the strongest correlation and "9" indicating the weakest correlation. **(C)** Bivariate correlation coefficient between staircase performance at week 7 and lesion volume within each region of interest. **(D)** Rank-order of correlation coefficients from panel C, with the same ranking structure as previously described. Overall, these panels demonstrate the change in spatial relationship *between infarct volume and staircase performance* from week 1 to week 7 with infarct volume in *anterior and lateral* regions more strongly predicting performance at week 7 than at week 1. All correlations were significant at the $p < 0.05$ level except for the region medial to hindlimb at both week 1 and 7 (Table 2). Darker red

coloration indicates stronger correlations between variables in all panels.

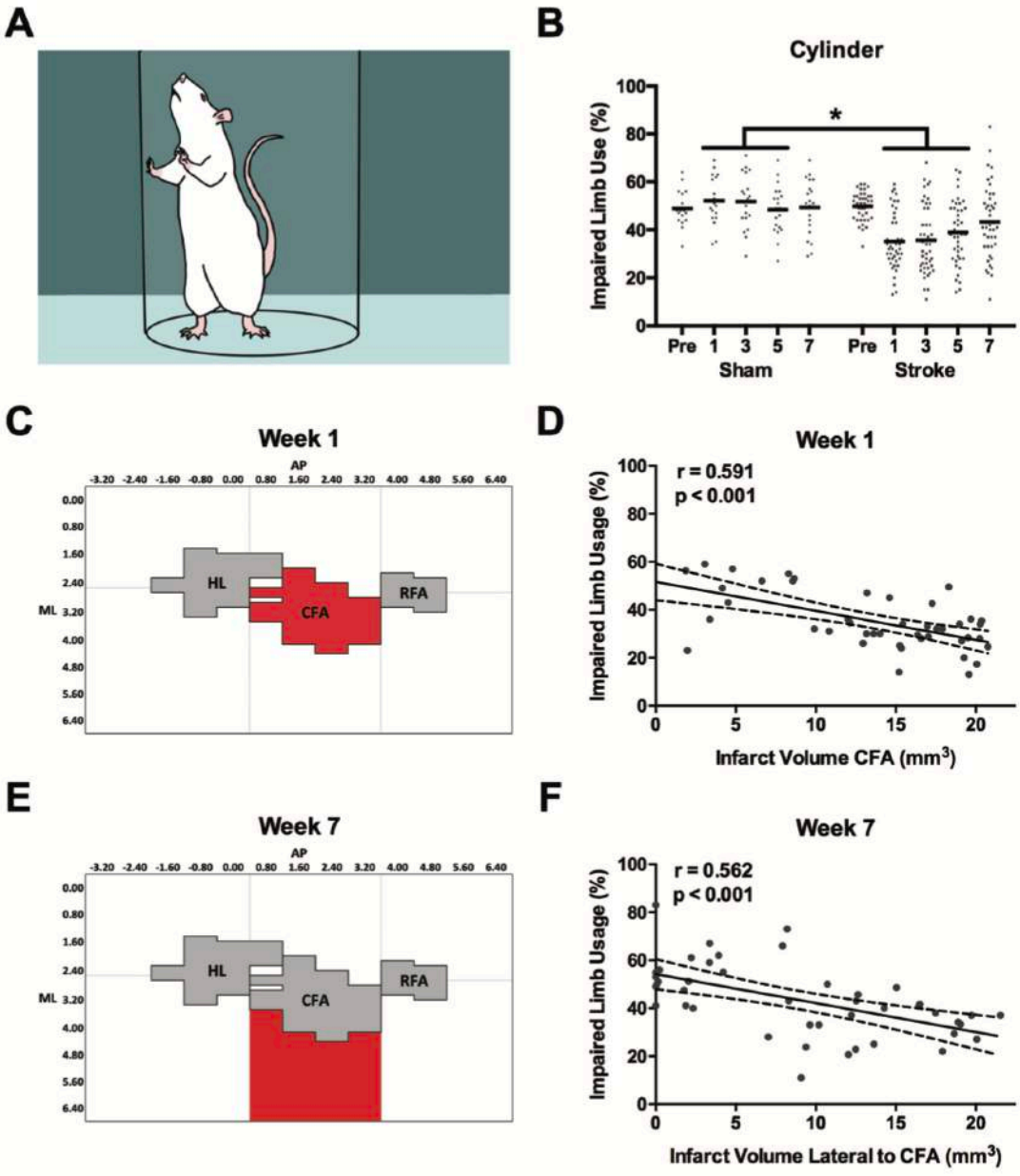

Figure (Ch2)6. (A) Cylinder task. Rats spontaneously rear and support their body weight using their forelimbs against the cylinder as they explore the environment. **(B)** Mean use of the impaired limb in the cylinder task was significantly reduced compared to sham rats at weeks 1, 3, and 5 post-stroke. **(C-D)** Impaired limb use at week 1 was best predicted by infarct volume in the CFA sub-region. **(E-F)** However, limb use at week 7 was best predicted by infarct volume in the

sub-region lateral to CFA. Full regression parameters shown in Table 1. N=64 (sham = 20, stroke = 44). * = $p < 0.05$.

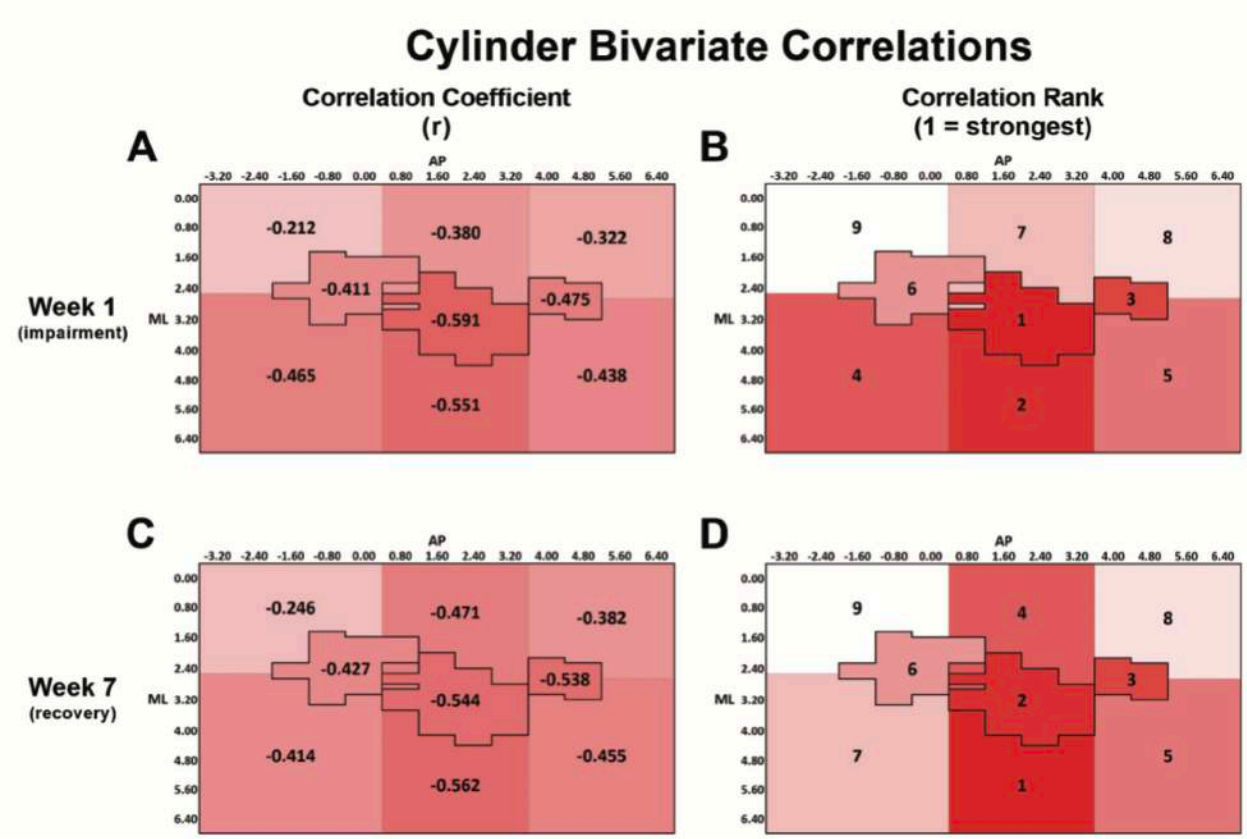

Figure (Ch2)7. (A) Bivariate Pearson correlation coefficients (r) between cylinder performance at week 1 and lesion volume within each region of interest. **(B)** Rank-order of correlation coefficients from panel A with "1" indicating the strongest correlation and "9" indicating the weakest correlation. **(C)** Bivariate correlation coefficient between cylinder performance at week 7 and lesion volume within each region of interest. **(D)** Rank-order of correlation coefficients from panel C, with the same ranking structure as previously described. Overall, these panels demonstrate the change in spatial relationship between *infarct volume and cylinder performance* from week 1 to week 7 with infarct volume in both *medial and lateral* regions surrounding CFA more strongly predicting performance at week 7 than at week 1. All correlations were significant at the $p < 0.05$ level except for the region medial to hindlimb at both week 1 and 7 (Table 2).

Darker red coloration indicates stronger correlations between variables in all panels.

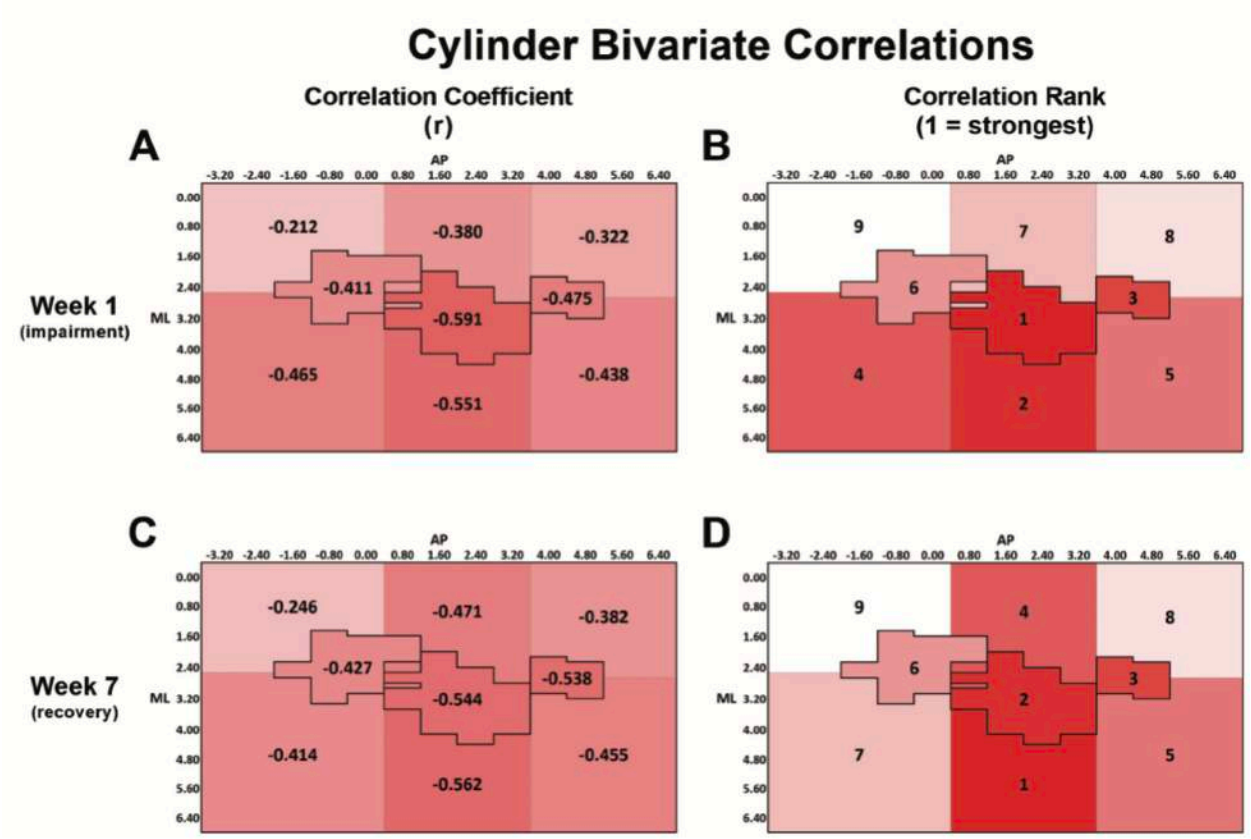

Figure (Ch2)8. (A) Beam task. Rats cross the beam toward the darkened goal box and avoid stepping on the lower ledge. Successful stepping becomes more difficult following stroke as the goal box is approached as width of the beam gradually tapers. **(B)** Overall, the mean forelimb performance on the beam task was not significantly different between stroke and sham groups. However, impairments in this task can still be observed on an individual animal level (grey dots). **(C)** In contrast, hindlimb performance on the beam task was significantly impaired in stroke rats relative to sham at weeks 1, 3, and 7 post-stroke. **(D)** Successful steps with the forelimb at week 1 post-stroke were best predicted by infarct volume in the CFA, **(E)** whereas infarct volume in the HL was the best predictor of hindlimb performance. **(F)** At week 7 post-stroke, successful steps with the forelimb were best predicted by infarct volume in the region lateral to CFA, **(G)**

while successful steps with the hindlimb were predicted by infarct volume medial to the HL. Full regression parameters shown in Table 1. N=64 (sham = 20, stroke = 44). * = $p < 0.05$.

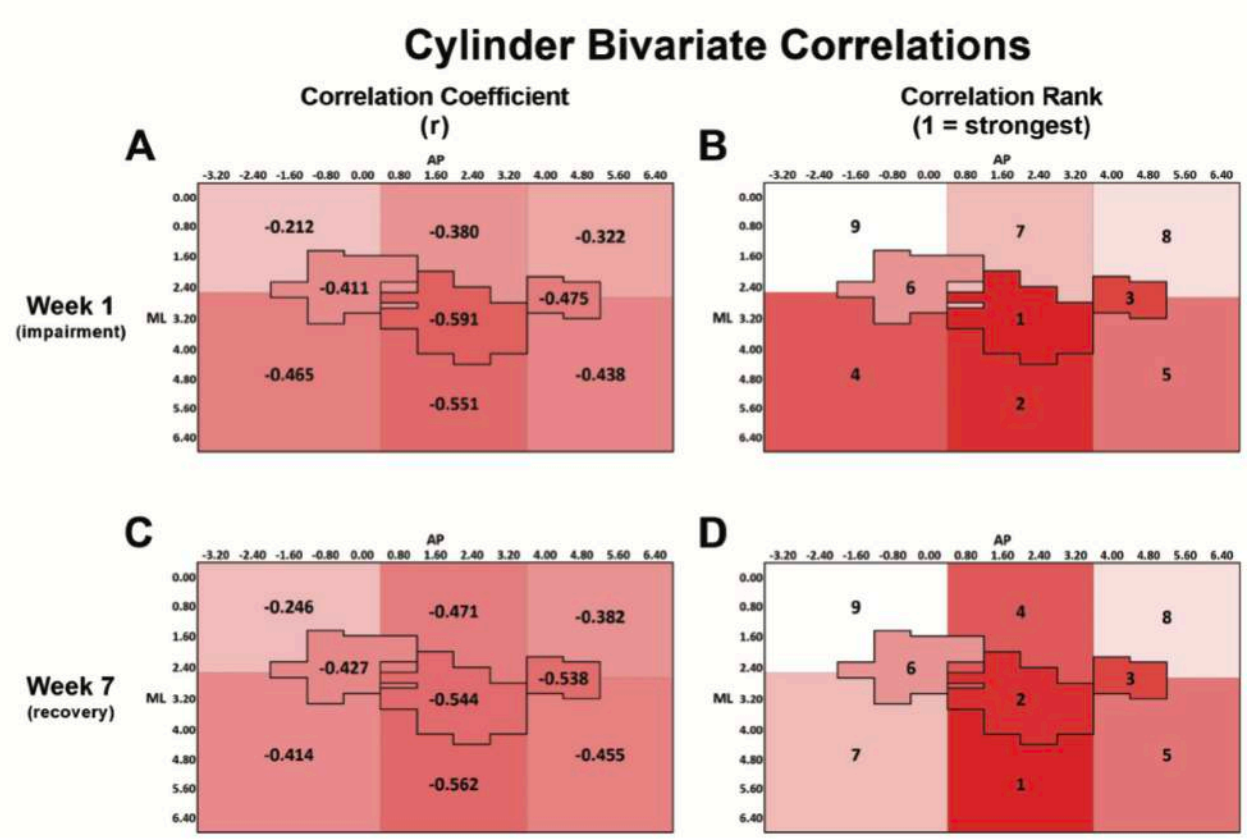

Figure (Ch2)9. (A) Bivariate Pearson correlation coefficients (r) between forelimb beam performance at week 1 and lesion volume within each region of interest. **(B)** Rank-order of correlation coefficients from panel A with "1" indicating the strongest correlation and "9" indicating the weakest correlation. At week 1, the correlations for HL, CFA, RFA, and the regions medial and lateral to CFA were significant at the $p < 0.05$ level (Table 2). **(C)** Bivariate correlation coefficient between forelimb beam performance at week 7 and lesion volume within each region of interest. **(D)** Rank-order of correlation coefficients from panel C, with the same ranking structure as previously described. At week 7, the correlations for CFA, RFA, and the regions lateral to HL, CFA, and RFA were significant at the $p < 0.05$ level (Table 2). Overall, panels A-D demonstrate the change in spatial relationship between *infarct volume and forelimb*

beam performance from week 1 to week 7 with infarct volume in *all the regions lateral to HL, CFA, and RFA* more strongly predicting performance at week 7 than at week 1. **(E)** Correlation between hindlimb beam performance at week 1 and lesion volume within each region of interest. **(F)** At week 1, the correlations for all regions except RFA and the region medial to RFA were significant at the $p < 0.05$ level (Table 2). **(G)** Bivariate correlation coefficient between hindlimb beam performance at week 7 and lesion volume within each region of interest. **(H)** At week 7, only the correlations for HL and the regions both medial and lateral to HL were significant at the $p < 0.05$ level (Table 2). Overall, panels E-H demonstrate the change in spatial relationship between infarct volume and hindlimb beam performance from week 1 to week 7 with infarct volume in the region medial to HL more strongly predicting performance at week 7 *than at week 1*. Darker red coloration indicates stronger correlations between variables in all panels.

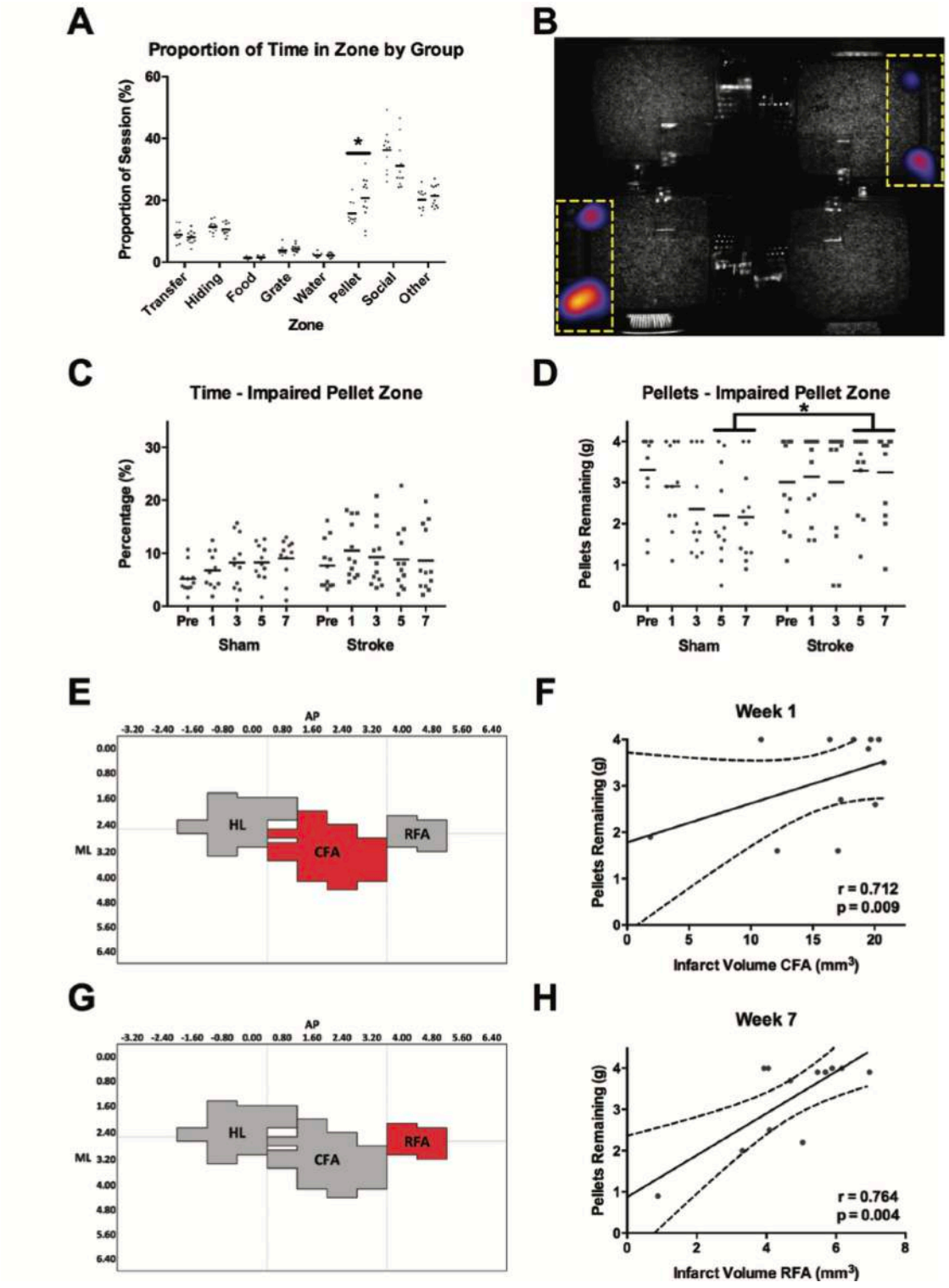

Figure (Ch2)10. (A) Following stroke, rats spent a larger proportion of their time in the pellet reaching zones (non-impaired + impaired) of the PhenoTyper than sham rats. **(B)** Mean group

heat map showing the difference in time spent in the pellet zones (indicated by yellow dashed line) between the sham and stroke groups. Brighter color corresponds to areas where stroke rats spent more time than sham. **(C)** Rats with stroke did not spend significantly less time attempting to reach pellets with their impaired limb than sham rats. **(D)** Despite this, on average rats with stroke had significantly more pellets remaining at the end of a PhenoTyper session than shams at weeks 5 and 7 post-stroke. This indicates that on average shams learned to successfully reach and grasp pellets in the PhenoTyper environment, while rats with stroke did not. **(E-F)** Pellet retrieval in the PhenoTyper at week 1 was best predicted by infarct volume in CFA, **(G-H)** while infarct volume in RFA best predicted pellet retrieval at week 7. Full regression parameters shown in Table 1. N=24 (sham = 12, stroke = 12) * = $p < 0.05$.

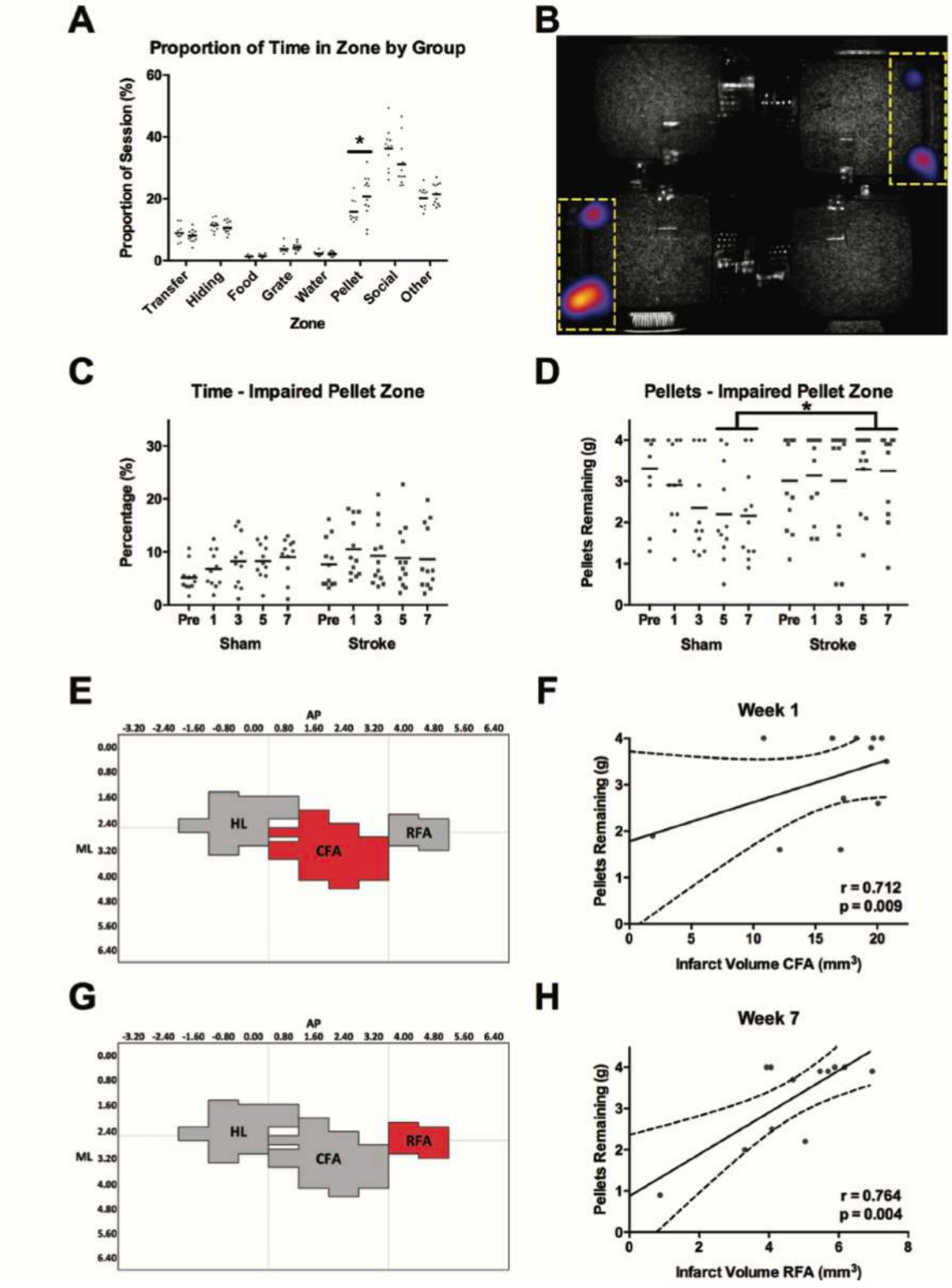

Figure (Ch2)11. (A) Bivariate Pearson correlation coefficients (r) between pellets remaining in the PhenoTyper at week 1 and lesion volume within each region of interest. **(B)** Rank-order of

correlation coefficients from panel A with “1” indicating the strongest correlation and “9” indicating the weakest correlation. At week 1, the correlations for CFA and the regions lateral to both CFA and HL were significant at the $p < 0.05$ level (Table 2). **(C)** Bivariate correlation coefficient between pellets remaining in the PhenoTyper at week 7 and lesion volume within each region of interest. **(D)** Rank-order of correlation coefficients from panel C, with the same ranking structure as previously described. At week 7, all regions except for the region medial to RFA and both the regions medial and lateral to HL were significant at the $p < 0.05$ level (Table 2). Overall, these panels demonstrate the change in spatial relationship between *infarct volume and pellets remaining in the PhenoTyper* from week 1 to week 7 with infarct volume in the *regions* surrounding CFA both medially and laterally, as well as RFA and the region lateral to RFA more strongly predicting performance at week 7 than at week 1. Darker red coloration indicates stronger correlations between variables in all panels.

Table (Ch2)1. Regions of brain injury that most significantly predict performance for all behavioral tasks.[a]

Determinant	Predictors	Unstandardized Coefficients		R	Adjusted R^2	p
		B	*Std. Error*			
Staircase – Impaired Limb Pellets Retrieved (Week 1)	(Constant)	19.972	1.110	0.784	0.595	< 0.001
	CFA	-0.382	0.104			
	RFA	-0.755	0.285			
Staircase – Impaired Limb Pellets Retrieved (Week 7)	(Constant)	20.773	1.003	0.849	0.707	< 0.001
	Lateral to RFA	-0.362	0.079			
	CFA	-0.305	0.091			
Cylinder – Impaired Limb Usage (Week 1)	(Constant)	0.516	0.038	0.591	0.334	< 0.001
	CFA	-0.012	0.003			
Cylinder – Impaired Limb Usage (Week 7)	(Constant)	0.542	0.031	0.562	0.299	< 0.001
	Lateral to CFA	-0.012	0.003			
Beam Forelimb - % of Successful Steps (Week 1)	(Constant)	0.983	0.024	0.393	0.134	0.008
	CFA	-0.005	0.002			
Beam Forelimb - % of Successful Steps (Week 7)	(Constant)	0.977	0.012	0.488	0.220	0.001
	Lateral to CFA	-0.004	0.001			
Beam Hindlimb - % of Successful Steps (Week 1)	(Constant)	0.928	0.023	0.550	0.286	< 0.001
	HL	-0.013	0.003			
Beam Hindlimb - % of Successful Steps (Week 1)	(Constant)	0.905	0.013	0.516	0.249	< 0.001
	Medial to HL	-0.011	0.003			
% Time in Impaired Pellet Zone (Week 1)	(Constant)	16.517	2.268	0.696	0.433	0.012
	CFA	-0.703	0.229			
% Time in Impaired Pellet Zone (Week 7)	(Constant)	20.774	4.397	0.677	0.404	0.016
	RFA	-2.593	0.892			
Pellets Remaining in Impaired Pellet Zone (Week 1)	(Constant)	1.970	0.423	0.712	0.457	0.009
	CFA	0.137	0.043			
Pellets Remaining in Impaired Pellet Zone (Week 7)	(Constant)	0.873	0.667	0.764	0.542	0.004
	RFA	0.507	0.135			

[a]All predictors represent the sum of infarct volume within a specific sub-region. The unit for each determinant is task-specific and shown in its corresponding Figure. See Table 2 for bivariate correlations between each behavior and all regions of interest.

Table (Ch2)2. Bivariate correlations between behavioral tasks and each region of interest.[a]

	Region of Interest								
Behavioral Task	**Medial HL**	**Lateral HL**	**Medial CFA**	**Lateral CFA**	**Medial RFA**	**Lateral RFA**	**HL**	**CFA**	**RFA**
Staircase – Impaired Limb Pellets Retrieved (Week 1)	-.180	-.344	-.571	-.721	-.474	-.698	-.439	-.741	-.698
Staircase – Impaired Limb Pellets Retrieved (Week 7)	-.208	-.355	-.672	-.785	-.627	-.802	-.442	-.760	-.773
Cylinder – Impaired Limb Usage (Week 1)	-.212	-.465	-.380	-.551	-.322	-.438	-.411	-.591	-.475
Cylinder – Impaired Limb Usage (Week 7)	-.246	-.414	-.471	-.562	-.382	-.455	-.427	-.544	-.538
Beam Forelimb - % of Successful Steps (Week 1)	-.270	-.296	-.340	-.350	-.194	-.250	-.351	-.393	-.379
Beam Forelimb - % of Successful Steps (Week 7)	-.080	-.335	-.132	-.488	-.084	-.389	-.218	-.346	-.321
Beam Hindlimb - % of Successful Steps (Week 1)	-.370	-.482	-.357	-.426	-.244	-.312	-.550	-.434	-.260
Beam Hindlimb - % of Successful Steps (Week 1)	-.516	-.392	-.241	-.138	-.072	-.083	-.454	-.178	-.071
Pellets Remaining in Impaired Pellet Zone (Week 1)	.461	.620	.267	.599	.114	.441	.484	.712	.396
Pellets Remaining in Impaired Pellet Zone (Week 7)	.344	.437	.650	.664	.526	.731	.614	.733	.764

[a]Cell values are the Pearson correlation coefficient (r) between the intersecting behavioral task and region of interest. Significant p-values are indicated by the color within each cell: white, $p > 0.05$; light green, $p < 0.05$; yellow, $p < 0.01$; red, $p < 0.001$.

Chapter 3.

Interhemispheric modulations of motor outputs by the rostral and caudal forelimb areas in rats.

Boris Touvykine, Guillaume Elgbeili, Stephan Quessy, Numa Dancause

Published in the Journal of Neurophysiology, 123 (4), 1355-1368, 2020.

Abstract

In rats, forelimb movements are evoked from two cortical regions, the caudal and rostral forelimb areas (CFA and RFA, respectively). These areas are densely interconnected and RFA induces complex and powerful modulations of CFA outputs. CFA and RFA also have interhemispheric connections and these areas from both hemispheres send projections to common targets along the motor axis, providing multiple potential sites of interactions for movement production. Our objective was to characterize how CFA and RFA in one hemisphere can modulate motor outputs of the opposite hemisphere. To do so, we used paired-pulse protocols with intracortical microstimulation techniques (ICMS), while recording electromyographic (EMG) activity of forelimb muscles in sedated rats. A subthreshold conditioning stimulation was applied in either CFA or RFA in one hemisphere simultaneously or prior to a suprathreshold test stimulation in either CFA or RFA in the opposite hemisphere. Both CFA and RFA tended to facilitate motor outputs with short (0-2.5ms) or long (20-35ms) delays between the conditioning and test stimuli. In contrast, they tended to inhibit motor outputs with intermediate delays, in particular 10ms. When comparing the two areas, we found that facilitatory effects from RFA were more frequent and powerful than the ones from CFA. In contrast, inhibitory effects from CFA on its homolog were more frequent and powerful than the ones from RFA. Our results demonstrate that interhemispheric modulations from CFA and RFA share some similarities, but also have clear differences that could sustain specific functions these cortical areas carry for the generation of forelimb movements.

Introduction

In non-human primates (NHPs), the largest proportion of the corticospinal tract originates from the primary motor cortex (M1) (Dum and Strick 1991). In addition, there are 6 premotor cortical areas that send projections to the spinal cord and to M1 (Dum and Strick 2002). Electrical stimulations in M1 and premotor areas can evoke electromyographic (EMG) responses in forelimb muscles (Boudrias et al. 2010a; Boudrias et al. 2010b; Park et al. 2004). In contrast, although rats are capable of dexterous movements (Whishaw 1996), responses in forelimb muscles are evoked from only two cortical areas (Neafsey et al. 1986; Neafsey and Sievert 1982).

The larger of these two motor regions, the caudal forelimb area (CFA), is the origin of the majority of corticospinal neurons and is located predominantly in the lateral agranular cortex (Neafsey et al. 1986; Rouiller et al. 1993). CFA projects to the ventrolateral thalamic nucleus, a pathway shared by M1 in NHPs (Rouiller et al. 1998). Based on these features, CFA is generally considered to be a homolog of M1. The smaller forelimb motor region is rostral to CFA, in the medial agranular cortex and is consequently referred to as the rostral forelimb area (RFA) (Neafsey et al. 1986; Neafsey and Sievert 1982). Like CFA, RFA sends projections to the spinal cord (Neafsey et al. 1986; Rouiller et al. 1993), and most RFA neurons discharge prior and during contralateral reaching and grasping, supporting its role in the preparation and execution of contralateral forelimb movements (Hyland 1998; Zhuravin and Bures 1988; Zhuravin and Bures 1989). However, there are discrepancies between the pattern of anatomical projections of CFA and RFA. First, corticospinal projections from RFA are sparser than from CFA (Neafsey et al.

1986; Starkey et al. 2012). Second, corticothalamic projections from RFA predominantly target the ventromedial thalamic nucleus (Rouiller et al. 1993). Third, unlike CFA, RFA is interconnected with the insular cortex, a pathway present for premotor areas, but not M1 of NHPs (Jurgens 1984; Matelli et al. 1986; Stepniewska et al. 1993). Together, this pattern of connections suggests that RFA could be an homolog of a premotor area in NHPs. Moreover, much like a premotor area, RFA send projections to CFA (Rouiller et al. 1993) and can exert powerful intrahemispheric modulations of CFA outputs (Deffeyes et al. 2015).

Similar to premotor areas and M1 in NHPs (Dancause et al. 2007; Marconi et al. 2003; Rouiller et al. 1994), RFA and CFA are interconnected across the two hemispheres and form a complex bihemispheric network (Rouiller et al. 1993). Moreover, RFA and CFA from both hemispheres send projections to common targets along the motor axis, providing multiple potential sites of interactions for their outputs. This anatomical substrate may allow the involvement of RFA and CFA in the control of the ipsilateral arm and hand. Not surprisingly, some neurons in these regions are modulated during ipsilateral movements (Dolbakyan et al. 1977; Soma et al. 2017) and motor cortex lesions induce deficits in the ipsilateral forelimb (Gonzalez et al. 2004; Price and Fowler 1981). Moreover, inactivation or permanent cortical injuries affecting motor cortex induce changes in the size of CFA and RFA in the opposite hemisphere (Maggiolini et al. 2008; Touvykine et al. 2016), suggesting the presence of reciprocal interhemispheric influences. Yet, the modulatory impact of CFA and RFA on the production of motor outputs from opposite hemisphere have not been investigated. These data would reveal similarities and differences between CFA and RFA and help us understand how these areas can contribute to the production of movements of the ipsilateral arm. Moreover, they would allow us

to compare patterns of interhemispheric modulations of RFA to the ones of premotor areas in NHPs (Cote et al. 2020; Cote et al. 2017; Quessy et al. 2016). Therefore, we sought to characterize output properties of CFA and RFA and then studied how these outputs are modulated by conditioning stimulations delivered in forelimb motor areas of the opposite hemisphere. In the present set of experiments, we focussed on the modulation from CFA and RFA on their respective homolog in the opposite hemisphere. In addition, considering that RFA has been suggested to be on a higher hierarchical level than CFA (Rouiller et al. 1993), we also studied modulatory effects from RFA on motor outputs of CFA. We discuss how these effects compare to the pattern of interhemispheric modulation between premotor areas and M1 in NHPs (Cote et al. 2020; Cote et al. 2017; Quessy et al. 2016).

Materials and Methods

Subjects

Our experimental protocol followed the guidelines of the Canadian Council on Animal Care and was approved by the Comité de Déontologie de l'Expérimentation sur les Animaux of the Université de Montréal. Thirteen single housed adult Sprague Dawley rats weighing between 307g and 480g, with unrestricted but identical enrichment, food and water ad libitum were used in our experiments (mean = 380g). All animals were at least 3 ½ months of age with the oldest animal being 5-month-old at the time of the experiment (mean age ~4 months). Females were chosen to keep in line with our previous work (Deffeyes et al. 2015; Mansoori et al. 2014; Touvykine et al. 2016). To the best of our knowledge, there are no reported differences between male and female rats in regard to the pattern of anatomical projections from either CFA or RFA. Accordingly, modulatory effects should be consistent across sexes, although this will have to be tested experimentally. We collected data to study the modulatory effect of CFA on the outputs of CFA in the opposite hemisphere in 7 out of 13 animals (Table 1). Modulatory effects of RFA on the outputs of CFA in the opposite hemisphere were collected in 5 rats. Finally, the effects of RFA on the outputs of RFA in the opposite hemisphere were studied in 7 out of the 13 rats.

Surgical procedures

All surgical procedures were performed as part of an aseptic, non-sterile, terminal experiment (Deffeyes et al. 2015; Touvykine et al. 2016). Anaesthesia was induced with a single dose of

ketamine hydrochloride via intraperitoneal injection (80mg/kg). The animals were transitioned to ~2% isoflurane general anaesthesia (Furane; Baxter) in 100% oxygen and remained under general anaesthesia for the duration of the surgical procedures. They received a dose of dexamethasone (1mg/kg) intramuscularly and mannitol (~3000mg/kg) intraperitoneally to prevent the inflammation and swelling of the brain, respectively. Sub-cutaneous injections of physiological saline (2ml) were delivered every 2 hours to prevent dehydration. Body temperature was monitored continuously via an anal probe and kept to ~36.0°C with a homeothermic blanket system (Harvard apparatus, Holliston, Massachusetts, USA).

Multistranded microwires (Cooner Wire, Chatsworth, CA, USA) were implanted intramuscularly to record electromyographic (EMG) signals. In the forearm, we implanted the extensor digitorum communis, a wrist extensor (WE) and the palmaris longus, a wrist flexor (WF). In the arm, we implanted the biceps brachii, an elbow flexor (EF) and the tricep brachii. Finally, we implanted the spinodeltoid on the back. However, in offline analyses, few responses were observed in the tricep brachii and spinodeltoid. We therefore focussed our analyses on WE, WF and EF muscles, for which we had sufficient data. For each muscle, the accurate placement of the EMG wires was confirmed using electrical stimulations through the implanted wires and visual inspection of the evoked movements. To ensure the quality of implantation, movements had to be evoked through the EMG wires with stimulation intensities <300μA. Following the implantation of EMG wires, the animal was positioned in a stereotaxic frame and bilateral craniectomies and durectomies were performed to expose forelimb motor areas of the two cerebral hemispheres. Craniectomies exposed the cortex from approximately 5mm to -1.5mm AP and 1.5mm to 6mm ML in relation to bregma. Upon completion of the durectomies, the exposed

cortex was covered in warm neutral mineral oil to prevent dehydration, and was added as needed until the end of the procedure.

Localization of motor representations

At the end of the surgical procedures isoflurane was turned off and deep sedation was maintained with intraperitoneal injections of ketamine hydrochloride (~3-5 mg/kg/10 min) (Touvykine et al. 2016). Prior to collecting electrophysiological data for the paired-pulse experiments, RFA and CFA were located using intracortical microstimulation (ICMS) trains delivered at 1Hz and generated by RZ5 real-time processor (Tucker Davis Technologies (TDT), Alachua, FL, USA). Each train consisted of 13 cathodal 0.2ms duration square pulses with 3.3ms interpulse interval (Touvykine et al. 2016). For each cortical site tested, a glass insulated tungsten microelectrode (~0.5 MΩ impedance; FHC Bowdoin, ME, USA) was lowered 1500-1600µm below the cortical surface with a microdrive (model 2662; David Kopf Instruments, Tujunga, CA) mounted on a micromanipulator (David Kopf Instruments, Tujunga, CA). Trains were delivered with a constant current stimulus isolator (model B51-2; BAK, Mount Airy, MD) and the intensity was gradually increased to a maximum current intensity of 100µA or until a clear movement was evoked. Movements were categorized as forelimb, neck, vibrissae, or mouth (jaw or tongue movements). To delineate RFA from CFA we characterized a strip of cortex between these two areas from which non-forelimb responses (typically neck movements) were evoked (Kleim et al. 1998; Neafsey et al. 1986; Touvykine et al. 2016). To further confirm the location of RFA, we explored the cortical territory laterally to this representation to confirm that mouth motor responses were evoked, as expected (Neafsey et al. 1986) (Figure 1A-B). An average of 9.1± 8.1 (mean±SD)

cortical sites were required to define this border (minimum=3; maximum= 37) (Table 1). Accordingly, cortical sites evoking forelimb movements located rostral to the strip of neck responses and medial to the mouth representation were considered to be in RFA. Forelimb responses caudal to the strip of neck motor responses were considered to be in CFA. After establishing the border between CFA and RFA in both hemispheres, no further mapping was done on the experimental animals, and we proceeded to collect paired-pulse stimulation protocols.

Paired-pulse stimulations and EMG recording

For the paired-pulse experiments, two glass-coated tungsten microelectrodes (~0.5MΩ impedance; FHC Bowdoin, ME, USA) were positioned with two independent micromanipulators. In different protocols, the conditioning stimulation (C_{stim}) electrode was either positioned in CFA or RFA of one hemisphere and the test stimulation (T_{stim}) electrode was positioned in either CFA or RFA of the opposite hemisphere. We have conducted a total of 54 paired pulse protocols in 13 rats. Protocols were separated in 3 different types. First, in some protocols (n=20) the C_{stim} was delivered in CFA and the T_{stim} in the opposite CFA in order to characterize the modulatory effects from CFA on motor outputs of its homolog (i.e. CFA-CFA protocols). In the second type of protocols (n=18) the C_{stim} was delivered in RFA and the T_{stim} in CFA to characterize the modulatory effects from RFA on motor outputs of CFA in the opposite hemisphere (i.e. RFA-CFA protocols). In the third type of protocols (n=16), the C_{stim} was delivered in RFA and the T_{stim} in RFA of the opposite hemisphere in order to characterize the modulatory effects from RFA on motor outputs of its homolog (i.e. RFA-RFA protocols).

For each cortical site included in these protocols, we first confirmed that it evoked clear forelimb movements in the arm contralateral to the electrodes using ICMS trains. Stimulations were then switched to single, 0.2ms cathodal pulses delivered at 2Hz. The current intensity was increased to a maximal intensity of 300μA, while simultaneously looking at the EMG signals of all recorded muscles on a custom-built interface using OpenEx software (TDT, Alachua, FL, USA). Once a motor evoked potential (MEP) was identified in at least one of the muscles in the arm contralateral to the stimulation, the intensity was adjusted to establish the threshold value. This procedure was used for both the electrodes delivering the T_{stim} and C_{stim}. The T_{stim} intensity was then set to 125% of the threshold value and the C_{stim} intensity was set to 75% of threshold. For the T_{stim}, if we found that the MEP was either too big or too small with 125% of the threshold value after the initiation of data collection of the protocol, data collection was interrupted. Stimulation intensity was adjusted to re-establish threshold stimulation intensity and the protocol reinitiated. For example, if we found that the single-pulse T_{stim} evoked twitches on a large proportion of trials, the stimulation was considered 'too big' and the stimulation intensity was decreased to re-establish thresholds current intensity. This however did not occur in the present set of experiments. Alternatively, if after initiation of the protocol we observed that the single-pulse T_{stim} evoked responses in less than 50% of trials with visual inspection on the oscilloscope, the intensity was considered 'too small' and the stimulation intensity was increased. This was necessary for 5.9% (n=3) of T_{stim} sites included in the study. Having a large enough response with the T_{stim} was essential to ensure that the C_{stim} could either increase or decrease this response. If no MEPs were evoked with T_{stim} using the maximal stimulation intensity of 300μA, the cortical site was discarded and the electrode moved to another location. For the C_{stim}, if no

response was observed using single-pulses with the maximum intensity of 300μA, the stimulation intensity was arbitrarily set to 225μA (i.e. 75% of 300μA). This was the case for 37.3% (n=19) of C_{stim} sites included in the study.

Once the cortical sites were identified and stimulation intensities established, a paired-pulse stimulation protocol was initiated. The protocol included 9 stimulation conditions: the T_{stim} delivered alone (T-only trials), the C_{stim} delivered alone (C-only trials), or both the C_{stim} and the T_{stim} delivered (paired stimulation) with one of 7 different interstimulus intervals (ISIs). In the paired stimulation conditions, the C_{stim} and the T_{stim} were either delivered simultaneously (ISI0) or with the C_{stim} preceding the T_{stim} by 2.5ms (ISI2.5), 5ms (ISI5), 10ms (ISI10), 15ms (ISI15), 20ms (ISI20), and 35ms (ISI35).

During a protocol, the stimulation condition was randomized across trials, until a total of 100 trials were collected for each stimulation condition (total number of trials for each protocol = 900). All cortical sites in an animal were only used once. After data collection for a paired pulse protocol was completed, both electrodes were moved to new cortical locations, and all procedures were repeated. The selection of these additional cortical sites was random. We did not attempt to specifically select cortical sites based on corresponding stereotaxic locations or find comparable location within the motor representations (Figure 1C). On average, 3.9±1.6 (mean±standard deviation) paired-pulse protocols were collected per animal (minimum=1; maximum=7; see Table 1). Data collection was stopped after ~5 hours from the moment the cortex was exposed to ensure stable responsiveness of the preparation and avoid any potential effects of overstimulation.

We verified if the order of data collection (i.e. rank at which each site was tested within a given rat) had affected modulatory effects using a mixed linear model. In this model, the dependent variable was the Z-score, the fixed factors were the type of protocol (3 levels), the site rank (7 levels), and ISI (7 levels), and the random factors were site rank nested within rat (13 levels). We found that site rank was not a significant predictor of Z-scores (p-value = 0.79). Based on this analysis, it appears that order in which data was collected across cortical sites within an animal does not affect the pattern of modulation. This finding is in line with the lack of cumulative effects we have previously found when using similar protocols in both rats (Deffeyes et al. 2015) and monkeys (Cote et al. 2020; Cote et al. 2017; Quessy et al. 2016).

The EMG data were recorded with custom OpenEx software running on an RZ5 real-time processor (TDT, Alachua, FL, USA). Each EMG channel was recorded at 4.9kHz, and raw EMG data were stored for offline analysis.

EMG data analyses

EMG analyses were conducted offline using custom written MatLab (version R2013a; Natick, MA, USA) code. The continuous EMG data collected during the experiments were separated into individual trials for each condition and aligned to stimulation time stamps. The signal was full wave rectified and smoothed using five point moving average (window size = 1.02ms), with no additional filtering. For each condition, the baseline was calculated from a 25ms window before the first stimulus (-26ms to -1ms prior to the first stimulus timestamp). The motor evoked potentials (MEPs) were calculated from a window of 3 to 30ms after the end of the last stimulation timestamp. For each channel of recorded EMG, we first averaged all trials in the T-

only condition and compared the average MEP to the average baseline activity for the same trials. MEPs with amplitudes greater than 1 standard deviation (SD) above baseline value were considered large enough to be either facilitated or inhibited by C_{stim} and kept for further analyses. Cases in which the MEP with the T-only condition smaller than 1 SD above baseline were excluded. Second, we verified that the C-only condition did not evoke MEPs in the muscles of the arm contralateral to the C_{stim} electrode. This validates the assumption of linear summation for the calculation of the predictor (see below)(Baker and Lemon 1995). Three protocols were removed due to such undesirable responses. Out of the 54 protocols, 3 had no significant MEP (> 1 SD above baseline) in offline analyses and were rejected from further analyses. From the 51 remaining protocols, a total of 143 significant MEPs with the T-only condition in the arm contralateral to the T_{stim}, and that has satisfied the criterion of being greater than 1 SD, above the baseline were included in the study. These MEPs were used to characterize and compare the output properties of CFA and RFA (see below).

To quantify the modulatory effect of the C_{stim} on each of the 143 significant MEPs in paired-pulse conditions, we first calculated a predictor using a modified bootstrapping procedure to generate a population of predicted responses, if no interaction took place between the outputs from Test and Conditioning cortical sites (Quessy et al. 2016). To this end, we linearly summed all possible combinations of single T-only traces (n=100) with single C-only traces (n=100) to generate a population of 10,000 traces. It should also be noted that since we ensured that the C_{stim} was subthreshold, any resulting MEPs are largely driven by T-only responses. Next, we randomly drew 100 traces from the population of predicted traces and averaged them to create an average predicted MEP. For each of the average predicted MEPs we found the peak voltage by

taking the maximum value between 8ms and 23ms after the T_{stim} and subtracting the voltage value at peak onset. Peak onset was found by performing a backward march that started at 10% of the peak maximum voltage value. The voltage value of each data point was compared to the one of the next point, moving back toward the stimulus onset. If the difference between the two points was smaller than 4% of the value of the first point, then that first point was considered as peak onset. Peak amplitude was calculated by subtracting the voltage value at onset from the maximal value. This process was repeated 10,000 times to create a population of predicted amplitudes based of T-only and C-only traces (Figure 1D-E).

To quantify the modulatory effect of the C_{stim}, the amplitudes of the MEP obtained with paired stimulation conditions were compared to the population of predicted amplitudes. For each of the 7 ISIs, the single trials (n=100) were averaged and the MEP peak amplitude calculated as described above. The conditioned MEP peak amplitude was compared to the population of predicted amplitudes to establish the direction of modulation (facilitation, inhibition, or no modulation) and the normalized strength of modulation (Z-score) using the following formula:

$$Z - score = \frac{\text{Amplitude with ISI(n)} - \text{mean amplitude of the predicted population}}{\text{SD of the mean amplitude of the predicted population}}$$

Where n is the value of the ISI (e.g. ISI0). A negative Z-score indicates a decrease of the MEP amplitude by the C_{stim} in comparison to the predictor, which we refer to as an 'inhibition'. A positive Z-score indicates an increase of the MEP amplitudes by the C_{stim} in comparison to the predictor, which refer to as a 'facilitation'. Modulation was considered significant when the Z-score was $\geq$1.96 (facilitation) or $\leq$-1.96 (inhibition).

For each type of protocol (i.e. CFA-CFA; RFA-CFA and RFA-RFA), we calculated the proportion of MEPs significantly modulated by the conditioning stimulus (i.e. incidence of significant effects) and the strength of the modulations (average Z-score). In addition, to provide a global measure that reflects the potential impact of CFA and RFA on motor outputs of the opposite hemisphere, we combined the incidence and magnitude values of modulatory effects into a single *Impact score*, calculated for facilitatory or inhibitory effects separately. For each type of protocol, using data with all ISIs and all 3 muscles combined, we multiplied incidence of significant effects by the mean magnitude of these significant effects.

Statistical analysis

We first examined the output properties of CFA and RFA using the MEPs with the T-only condition. A one-way ANOVA compared the absolute amplitudes of MEPs from the 3 types of interaction protocols, as well as to compare the latencies of MEPs from CFA across all 3 muscles and onset latencies of MEPs from RFA across all 3 muscles. Bonferroni corrected post-hoc t-tests were used if the main effect of ANOVA was significant. The stimulation intensity used for the T_{stim} in CFA and in RFA protocols and the mean onset latency of MEPs evoked from RFA and CFA were compared using two-sample Student t-tests.

Second, we examined the modulatory effects of the conditioning stimulation on MEPs with the various ISIs. Combining data from the 3 types of protocols, we used an ANOVA to test if the magnitudes of modulation of MEPs (Z-score) was different in the three muscles. Linear regressions were used to test if there was a relation between the magnitude of the modulation and

onset latency of the MEPs with T-only stimulations. One regression was used for each type of protocol and each regression combined data from all 7 ISIs and all 3 muscles. The comparisons of incidence of facilitatory or inhibitory effects were performed with Chi-square tests (X^2), followed by a *post hoc* two-proportion *Z* tests. Similarly, to compare the pattern of modulation across ISIs and the pattern of modulation across muscles evoked with the 3 types of protocols, X^2 followed by a *post hoc* two-proportion *Z* tests were used. Comparisons of the magnitude of effects between the 3 types of protocols were performed with two one-way ANOVAs, one for facilitatory and one for inhibitory effects. Bonferroni post-hoc tests were used if significant main effects were identified between protocols.

For all analyses using X^2 tests, a total of 3 tests were conducted: 1) comparing CFA-CFA protocols with RFA-CFA protocols; 2) comparing CFA-CFA with RFA-RFA protocols and 3) comparing RFA-CFA with RFA-RFA protocols. With the adjustment for multiple comparisons, p values ≤ 0.017 were considered significant. For all other tests including the *post hoc* two-proportion *Z* test, p values ≤ 0.05 were considered significant. Unless otherwise specified, results are expressed as mean ± standard error (SE). All statistical analyses were performed using MATLAB (Version R2014a).

Results

Using the data obtained with the T-only stimulation, we first characterized the output properties of responses from CFA and RFA in the arm contralateral to T_{stim} (Figure 1A). For protocols testing the modulatory effects from CFA on the motor outputs of its homolog (CFA-CFA protocols), we obtained 60 significant MEPs (> 1 SD above baseline; see methods) with T-only stimulation (20 in WE, 20 in WF and 20 in EF). For protocols testing modulatory effects from RFA on motor outputs of CFA in the opposite hemisphere (RFA-CFA protocols), we found 49 significant MEPs with T-only stimulation (17 in WE, 16 in WF and 16 in EF). Finally, in protocols that tested the modulatory effects from RFA on motor outputs of its homolog (RFA-RFA protocols) we found 34 significant MEPs with T-only stimulation (13 in WE, 9 in WF and 12 in EF). Then, we studied the effects of C_{stim} delivered in the opposite hemisphere with different ISIs on these motor outputs (Figure 1D-E).

Comparison of output properties of CFA and RFA

Using the significant MEPs (> 1 SD above baseline) with T-only stimulation condition (mean current intensity±standard deviation=253±7.1μA; max=300μA), we wanted to establish whether the output properties of CFA and RFA were different. We compared the amplitudes (μV) of MEPs with the T-only condition in the 3 types of protocols (Figure 2A) and found significant differences ($F_{(2,140)}$=3.41, p=0.04). The amplitudes of MEPs from RFA (RFA-RFA protocols mean ± SE = 13.6±4.2μV) were significantly smaller than the ones from CFA (CFA-CFA: 38.9±8.0μV p=0.02; RFA-CFA: 37.4±5.7μV, p=0.03). As expected, there was no significant

difference in absolute amplitudes of MEPs evoked from CFA, whether the protocol was designed to test the modulatory effects of CFA or RFA (p=0.9). Then, we compared the mean threshold T_{stim} intensities used in CFA (243.3±7.2μA; data from CFA-CFA and RFA-CFA protocols pooled) and RFA (287.0±6.5μA) and found that values for CFA were significantly lower ($T_{(141)}$=-3.25, p=0.001) (Figure 2B). Thus, MEPs from RFA had smaller peak amplitudes than the ones from CFA, eventhough current intensities used to evoke these responses were greater. These results support that higher stimulation intensities are required to evoke MEPs from RFA in comparison to CFA.

We also verified if MEPs from CFA and RFA had different onset latencies. Once again, there was no difference of onset latencies for MEPs from CFA, whether they were collected during CFA-CFA or RFA-CFA protocols (11.0±0.2ms and 11.0±0.2ms respectively; $T_{(107)}$=-0.18, p=0.9). We thus combined these data to obtain 109 MEPs with T-only stimulation in CFA. Figure 2C shows onset latencies of these 109 MEPs and Figure 2D shows onset latencies value of the 34 MEPs with T-only stimulation in RFA (RFA-RFA protocols). The range of latency values was greater for MEPs from RFA (range=6.7ms) than from CFA (range=5.9ms). For RFA however, short latency responses (<10ms) were less common (RFA=8.8% versus CFA=17.4%) and long latency responses (>13ms) more common (RFA=14.7% versus CFA=2.7%). When comparing the mean onset latency of MEPs from CFA (11.0±0.2ms) to the one from RFA (11.6±0.3ms), we found it was significantly shorter ($T_{(141)}$=-2.56, p<0.01). We found no difference of onset latencies across all 3 muscles (WE, WF, and EF), regardless if the MEPs were from CFA ($F_{(2,106)}$=2.74, p=0.07) or RFA ($F_{(2,31)}$=0.54, p=0.6).

Together our analyses of MEPs amplitudes and latencies support the idea that the output properties of CFA and RFA are different, with RFA evoking smaller and slightly slower EMG responses than CFA.

Modulatory effects of CFA and RFA with each ISI tested

For any given protocol, we obtained the population of predicted amplitudes evoked in the T-only and C-only trials (see Methods). We then compared the MEPs obtained in the paired-pulse conditions with each ISI to the population of predicted amplitudes. Figure 3 shows the complete dataset of modulatory effects across rats with the different ISIs tested. The data are separated according to the 3 types of interaction protocols, respectively testing the modulatory effects from CFA on the outputs of its homolog (CFA-CFA protocols, n=20; Figure 3A), from RFA on the outputs of CFA in the opposite hemisphere (RFA-CFA protocols, n=17; Figure 3B) and from RFA on the outputs of its homolog (RFA-RFA protocols , n=14; Figure 3C). For all 3 types of protocols, modulatory effects were clearly affected by ISIs. There were some common features observed for the 3 types of protocols. While more facilitatory effects were evoked with short (ISI0 and ISI2.5) and long ISIs (ISI20 and ISI35), inhibitory effects were most common with intermediate ISIs, in particular ISI10. There were also some clear differences between the 3 types of protocols. For example, inhibitory effects appeared to be more common and powerful for CFA-CFA protocols then for the others two types of protocols. In contrast, conditioning stimulations in RFA with short or long ISIs seemed to induce more powerful facilitatory effects than conditioning stimulation in CFA. Finally, this figure also showed no obvious differences in the pattern of modulation for the different muscles (i.e. Figure 3A-C). This was confirmed

statistically, as we found no difference in the magnitude of modulations of MEPs in the three muscles, when combining data from the 3 types of protocols ($F_{(2,998)}$=0.34, p=0.7). Finally, combining data from the 3 muscles and 7 ISIs, we found a weak correlation between the onset latency of MEPs with T-only stimulation and the magnitude of the modulation (Z-score) for CFA-CFA (Rho=0.156, p=0.001) and RFA-RFA protocols (Rho=0.166, p=0.01). This suggests that slower MEPs from CFA or RFA tended to be more facilitated when conditioning stimulation was delivered in the homolog cortical region. However, since this relation was weak we did not investigate this possibility further.

For each ISI, we calculated the proportion of significant facilitatory and inhibitory effects induced by the conditioning stimulation (i.e. the numbers of MEPs with a Z-score ≥1.96 and ≤-1.96, respectively; see method) and the average magnitude of modulatory effects (mean Z-scores ± SE). For CFA-CFA protocols, out of the 420 MEPs (60 significant responses with T-only, conditioned with 7 ISIs), we found 179 (42.6%) cases in which CFA conditioning significantly modulated the outputs of its homolog. Out of these significant effects, there was a comparable number of facilitation (n=94, 22.4%) and inhibition (n=85, 20.2%). While both facilitatory and inhibitory effects were observed with every ISI, the proportion of facilitatory and inhibitory effects induced by CFA was highly variable with each ISIs tested (Figure 4A). Significant facilitatory effects were most common when the C_{stim} and T_{stim} were delivered simultaneously (ISI0: n=21, 35.0%) or separated with 35ms (ISI35: n=21, 35.0%). In contrast, significant inhibitory effects were most common with intermediate ISIs (ISI5: n=24, 40.0%; and ISI10: n=26, 43.3%). Figure 4B shows the average magnitude of modulations induced by CFA on the outputs of its homolog with each ISI. Note that to better reflect the general magnitude of

modulations, these data include all MEPs (see Figure 2) and are not restricted to the MEPs that were significantly modulated. In general, the magnitude of modulatory effects from CFA followed a similar pattern with the various ISIs as described for the incidence. The strongest facilitatory effects were observed when the C_{stim} was delivered at the same time or shortly prior to the T_{stim} (i.e. ISI0 and ISI2.5) or with long ISIs (i.e. ISI20 and ISI35). Inhibition was most powerful with intermediate ISIs, in particular with ISI5 and ISI10.

For RFA-CFA protocols, out of the 343 MEPs (49 significant responses with T-only conditioned with 7 ISIs), we found 185 (53.9%) cases in which RFA conditioning significantly modulated the outputs of CFA in the opposite hemisphere. Out of these significant effects, there were many more cases of facilitation (n=157, 45.7%) than cases of inhibition (n=28, 8.2%) (Figure 4C). As described for CFA-CFA protocols, significant facilitatory effects were most common with short (ISI0: n=29, 60.0%; ISI2.5: n=35, 71.4) or long ISIs (ISI20: n=30, 61.2%; and ISI35: n=32, 65.3%) and significant inhibitory effects were most common with intermediate ISIs, in particular ISI10 (n=17, 34.7%). In fact, this was the only ISI with which inhibitory effects were more common than facilitatory effects. Furthermore, conditioning of RFA did not induce any case of inhibition with short ISIs (ISI0 and ISI2.5). For the magnitude of facilitatory effects (Figure 4D), the most powerful facilitatory effects were observed with short (ISI0, ISI2.5) and long ISIs (ISI20 and ISI35). Inhibition was more powerful with ISI10 but also when longer delays were used between the conditioning and test stimuli (ISI20-ISI35).

For RFA-RFA protocols, from the 238 MEPs (34 significant responses with T-only conditioned with 7 ISIs), we found 98 cases in which RFA conditioning significantly modulated the outputs of its homolog (41.2%). Again for this type of protocol, RFA conditioning induced

many more cases of facilitation (n=73, 30.7%) than inhibition (n=25, 10.5%) (Figure 4E). Facilitatory effects were most common with short (ISI0: n=16, 47.1%; ISI2.5: n=17, 50.0%) and long ISIs (ISI20; n=12, 35.3%; ISI35: n=19, 55.9%), and inhibitory effects most common with intermediate ISIs (ISI5: n=5, 14.7%; ISI10: n=13, 38.2%; and ISI15: n=5, 14.7%). As for RFA-CFA protocols, and in contrast to CFA-CFA protocols, conditioning stimulations exclusively induced facilitatory effects with ISI0 and ISI2.5. For both the facilitatory and inhibitory effects, the magnitude of modulation with the different ISIs followed a similar pattern as the one described for incidence (Figure 4F). The strongest facilitatory effects were observed when the C_{stim} was delivered at the same time or shortly prior to the T_{stim} (i.e. ISI0 and ISI2.5) or with long ISIs (i.e. ISI20 and ISI35). Inhibition was most powerful with intermediate ISIs, in particular with ISI5 and ISI10.

In summary, these figures highlight that there are clear similarities in the pattern of modulatory effects evoked with the various ISIs for the 3 interaction protocols studied. Cortical motor areas of the contralateral hemisphere (i.e. both CFA and RFA) induce more frequent and powerful facilitation of motor outputs with short (ISI0 and ISI2.5) and long ISIs (ISI20 and ISI35). In contrast, frequent and powerful inhibitory effects are induced when conditioning is delivered 10ms prior to the T_{stim}. These figures also reveal clear differences between the 3 types of protocols. They show that CFA can induce inhibitory effects with all the ISIs we tested and that inhibitory effects are not only frequent and powerful with ISI10, but also with ISI5. In contrast, RFA exclusively induces facilitatory effects when the C_{stim} is delivered simultaneously (ISI0) or 2.5ms prior (ISI2.5) to the T_{stim}, and that regardless if it is to modulate outputs of CFA or RFA in the opposite hemisphere.

Comparison of the modulatory effects of CFA and RFA with all ISIs combined

To statistically compare the overall incidence of modulatory effects for the 3 types of protocols, we pooled the significant effects evoked with all ISIs (Figure 5A). First, we wanted to know if delivering the C_{stim} in CFA versus RFA induced different proportions of facilitatory and inhibitory effects on the outputs of CFA in the opposite hemisphere (i.e. CFA-CFA versus RFA-CFA protocols) and found it did (X^2=54.6; p<0.001). CFA conditioning induced less facilitation (n=94, 22.4%) than RFA conditioning (n=157, 45.8%; p<0.001) and more inhibition (CFA n=85, 20.2% versus RFA n=28, 8.2%; p<0.001) on the outputs of CFA in the opposite hemisphere. Second, we asked if CFA and RFA induced different proportions of facilitatory and inhibitory effects on the outputs of their homologs (i.e. CFA-CFA versus RFA-RFA protocols). The incidence of significant effects was different (X^2=12.8; p=0.01), with CFA inducing fewer facilitatory effects (n=94, 22.4%) than RFA (n=73, 30.7%; p=0.02) and more inhibitory effects (n=85, 20.2%) than RFA (n=25, 10.5%; p=0.001). Finally, we compared the proportions of facilitatory and inhibitory effects induced by RFA on the outputs of CFA and RFA in the opposite hemisphere (i.e. RFA-CFA versus RFA-RFA protocols) and found it was different (X^2=13.4; p=0.01). The incidence of facilitatory effects induced by RFA was greater on the outputs of CFA (RFA-CFA: n=157, 45.8%) than on the output of RFA (RFA-RFA: n=73, 30.7%; p<0.001), but the incidence of inhibitory effects was comparable (RFA-CFA: n=28, 8.2%; RFA-RFA: n=25, 10.5%, p=0.3).

The magnitude of modulatory effects evoked with the various ISIs were also pooled to compare the 3 types of protocols (Figure 5B). The magnitude of facilitatory effects was different

($F_{(2,594)}$=13.5; p<0.001). Facilitatory effects from CFA on the outputs of its homolog were weaker (CFA-CFA: Z score=2.05±0.11) than the ones from RFA. This was true for both when RFA modulated the outputs of CFA in the opposite hemisphere (RFA-CFA: Z score=3.17±0.18, p<0.001), or of its homolog (RFA-RFA: Z score=3.07±0.26, p<0.001). However, the magnitude of facilitatory effects from RFA on the outputs of its homolog and of CFA in the opposite hemisphere were not significantly different (p=1.0). For the magnitude of inhibitory effects, there were also significant differences for the 3 types of protocols ($F_{(2,401)}$=6.1, p=0.002). CFA induced more powerful inhibition on the outputs of its homolog (CFA-CFA: Z score=-2.05±0.13) than RFA on the outputs of its homolog (RFA-RFA: Z score=-1.40±0.01; p=0.003).

In conclusion, while the conditioning of CFA induced fewer and weaker facilitatory effects, it induced more and generally stronger inhibitory effects than the conditioning of RFA. For RFA conditioning, the magnitude of modulations was similar on both the motor output of CFA or of its homolog in the opposite hemisphere. However, facilitatory effects were more common when RFA modulated the outputs of CFA than the outputs of its homolog in the opposite hemisphere.

Pattern of modulatory effects from CFA and RFA across ISIs

Next, we characterized how individual MEPs were modulated across the 7 ISIs tested and compared the pattern of modulations for the 3 types of protocols. Out of the significant MEPs evoked with the T-only condition (> 1 SD above baseline), we found few that were not modulated with any of the ISIs tested for CFA-CFA (8 out of 60 MEPs; 13.3%; number cortical

sites tested or protocols = 20), RFA-CFA (2 out of 49 MEPs; 4.1%; number of protocols = 17), and RFA-RFA (4 out of 34 MEPs; 11.8%; number of protocols = 14). This supports that the conditioning stimulations in either CFA or RFA were very likely to affect motor outputs of the opposite hemisphere with one or more of the ISIs tested. For these modulated MEPs, we separated the pattern of modulation across ISIs into 3 groups (Deffeyes et al. 2015). First, for a given MEP the conditioning stimulation could be significantly facilitatory with one or more ISIs, and never induce significant inhibition across the ISIs tested (i.e. group pure facilitation). Second, the conditioning stimulation could be significantly inhibitory with one or more ISIs, and never induce significant facilitation across the ISIs tested (i.e. group pure inhibition). Third, the conditioning stimulation could be significantly facilitatory with one or more ISIs and significantly inhibitory one or more ISIs (i.e. group opposite).

For CFA-CFA protocols, out of the 52 MEPs that were significantly modulated with at least one ISI, CFA conditioning induced a comparable number of cases of pure facilitation (n=18; 34.6%), pure inhibition (n=18; 34.6%) and opposite effects (n=16; 30.7%) (Figure 6A). The pattern of modulation of CFA outputs across ISIs was very different when the conditioning stimulation was applied in RFA (RFA-CFA protocols; $X^2=20.71$, $p<0.001$). Out of 47 that were significantly modulated with at least one ISI, most cases were pure facilitation (n=30; 63.8%), some were opposite (n=17; 36.2%) and none were pure inhibition. Thus, all cortical sites tested in RFA that modulated the outputs of CFA induced significant facilitation with at least one of the ISI tested. When comparing the patterns of modulation of these two types of protocols, we found that conditioning stimulation delivered in CFA evoked significantly fewer cases of pure facilitation ($p=0.004$) and more cases of pure inhibition ($p<0.001$) than when the conditioning

stimulations were delivered in RFA. When RFA conditionned the outputs of its homolog (i.e. RFA-RFA protocols), values lied somewhat in between the ones of the other two types of protocols. Out of 30 MEPs significantly modulated with at least one ISI, cases of pure facilitation (n=15; 50.0%) were more common than opposite effects (n=11; 36.7%), and cases of pure inhibition were rarely observed (n=4; 13.3%). These values were not significantly different then the ones of CFA-CFA (X^2=7.6, p=0.03) or RFA-CFA (X^2=5.61, p=0.06) protocols.

Pattern of modulatory effects from CFA and RFA simultaneously induced across muscles

We then studied how a given cortical site in CFA or RFA simultaneously modulated the outputs to various muscles. Once again we separated patterns of modulation into 3 different groups. First, a given cortical site in CFA or RFA could induce a significant facilitation on the MEP of one and up to all 3 muscles simultaneously (i.e. group pure facilitation across muscles). Second, it could induce a significant inhibition on the MEP of one and up to all 3 muscles (i.e. group pure inhibition across muscles). Third, the conditioning stimulation could simultaneously facilitate and inhibit different combinations of muscles (i.e. group simultaneous mixed effects across muscles). For a given protocol, we calculated the proportion of occurrence of these groups of effects across muscles for all 7 ISIs.

For protocols testing the modulatory effects from CFA on the outputs of its homolog (CFA-CFA protocols; 20 cortical sites tested x 7 ISIs = 140 cases), we found 48 cases (34.3%) of pure facilitation and a comparable proportion of pure inhibition across muscles (n=47; 33.6%) (Figure 6B). Out of these cases, 29 (20.7%) involved simultaneous facilitation in more than one muscle and 26 (18.6%) simultaneous inhibition in more than one muscle. We found no case in

which conditioning stimulation in CFA simultaneously facilitated the outputs to one muscle while inhibiting outputs to another muscles (i.e. mixed effects). The pattern of modulation across muscles was very different for protocols testing the modulatory effects from RFA on the outputs of CFA in the opposite hemisphere (RFA-CFA protocols; 17 protocols X 7 ISIs = 119 cases; X^2=24.4; p=0.001). There were many more cases of pure facilitation across muscles (n=73; 61.3%) than pure inhibition (n=15; 12.6%). Out of these cases, 49 (35.0%) involved simultaneous facilitation in more than one muscle and 5 (3.6%) simultaneous inhibition in more than one muscle. In addition, we found a few cases in which RFA simultaneously induced facilitation and inhibition in different muscles (n=5; 4.2%). When comparing the patterns of modulation for the two types of protocols, we found that conditioning stimulation delivered in CFA evoked significantly less pure facilitatory ($p<0.001$) and mixed effects (p=0.01), but significantly more pure inhibitory effects ($p<0.001$). Once again, the pattern of modulatory effects for protocols testing the effects from RFA on the outputs of its homolog was somewhat in between the ones of CFA-CFA (X^2=8,8, p=0.6) and RFA-CFA (X^2=11.2, p=0.2) protocols, with no significant differences. Out of the 98 cases (14 protocols X 7 ISIs), we found many more pure facilitation (n=41; 41.8%) than pure inhibition (n=16; 16.3%) across muscles and no mixed effects. Out of these cases, 22 (15.7%) involved simultaneous facilitation in more than one muscle and 6 (4.3%) simultaneous inhibition in more than one muscle.

Comparison of global modulatory impact of CFA and RFA

In a last series of analyses, we wanted to provide a 'global' measure that reflects the potential impact from CFA and RFA on motor outputs of the opposite hemisphere. To do so, for each type of protocol we combined the incidence of significant modulations and their magnitude values into a single *impact score* for facilitation and one for inhibition (see methods; Figure 7). The greatest facilitatory impact score was from RFA on the outputs of CFA in the opposite hemisphere (2.02). This value was much larger than the facilitatory impact of RFA on its homolog (1.53) and more than twice the facilitatory impact of CFA on its homolog (0.77). In contrast, the greatest inhibitory impact score was from CFA on the output of its homolog (-0.74). This value was more than twice the inhibitory impact of RFA conditioning on either the outputs of its homolog or of CFA (-0.30 and -0.28 respectively). When looking at the pattern of modulation for each type of protocols, it appears that CFA has a balanced pattern of modulation, with a comparable capacity to facilitate or inhibit the outputs of its homolog in the opposite hemisphere. In contrast, RFA has a much greater potential to facilitate motor outputs from the opposite hemisphere, regardless if the output is originating from CFA of the opposite hemisphere or from its homolog.

Discussion

In the present study, we first characterized the output properties of CFA and RFA using single-pulse intracortical microstimulation techniques and found that CFA evokes larger EMG responses with slightly shorter latencies in comparison to RFA. Then, we studied how conditioning stimulation delivered in either CFA or RFA in the opposite hemisphere affected these outputs. Facilitatory effects from both CFA and RFA were always more frequent when the C_{stim} and T_{stim} were delivered with short, or with long ISIs. In contrast, inhibitory effects were more common with intermediate ISIs. There were also differences between the modulatory effects induced by CFA and RFA. When the conditioning stimulation was delivered in CFA, inhibitory effects were more common than when it was in RFA. In contrast, RFA induced many more facilitatory effects and they were stronger than the ones from CFA. These data support that motor areas in rats can exert powerful and complex modulations of motor outputs from the opposite hemisphere. They also suggest that CFA and RFA make distinct contributions for the production of these outputs.

Output properties of CFA and RFA

Output properties of RFA and CFA have been compared in a previous electrophysiological study in albino rats (Liang et al. 1993), although in lighly sedated preparations with active EMG backround. Under these conditions, EMG responses were evoked with much lower stimulation intensities and had shorter onset latencies than in our study. Furthermore, following stimulations in CFA and RFA, MEPs had similar latencies, although CFA was much more likely to evoke

responses than RFA (1.5 to 3 times). The lower efficacy of RFA to evoke reponses in forelimb muscles is thus a consistent finding across studies. With intensities based on threshold current values, we found that smaller currents were required to evoke responses from CFA and yet, that these MEPs were greater than those from RFA. Similarly in macaques, much larger responses are evoked from M1 than from premotor areas (Boudrias et al. 2010a; Boudrias et al. 2010b). Across premotor areas, stimulation in PMv evokes the largest responses, which are nonetheless more than 7 times smaller than the ones from M1. Accordingly, although there is a clear difference in the efficiency of CFA and RFA to evoke responses in contralateral forelimb muscles, this difference is much smaller than the one between M1 and premotor areas in primates. The larger difference of output efficacy in primates may be due to the addition of more direct corticomotoneuronal projections from M1 onto cervical motoneurons (Rathelot and Strick 2006; 2009), a trait that appears to be lacking for CFA in rats (Alstermark et al. 2004; Yang and Lemon 2003).

The lower stimulation intensities and faster responses under light sedation (Liang et al. 1993) could be explained by higher summation probability of outputs from multiple neurons near firing threshold at the time of stimulation and the amplification of potential synchrony effects (Schieber and Rivlis 2005). This increased excitability of neurons in the various structures targeted by the outputs of CFA and RFA could also explain the presence of ipsilateral responses under light sedation (Liang et al. 1993), which we generally failed to find (only 3 out of 58 protocols; see methods). Given our relatively limited data set for RFA (n=34) and the methodological differences between our study and previous work, the potential differences between the average output latency of MEPs from CFA and RFA will need futher investigation.

Similarities of modulatory effects from CFA and RFA

For both CFA and RFA, using very short (0 and 2.5ms) or long delays (20 and 35ms) between the C_{stim} and T_{stim} evoked many more facilitatory than inhibitory effects. With long delays, the potential locus of interactions and pathways involved are numerous. They may favor effects carried by slower conducting fibers, oligosynaptic pathways between the two hemispheres, or give time for outputs from CFA or RFA to induce changes of excitability at downstream sites of convergence with outputs from the opposite motor areas. There are fewer mechanisms that can sustain modulations with very short delays. Considering that callosal conduction takes at least 5ms in adult rats (Seggie and Berry 1972), it is unlikely that these very fast interactions take place at the cortical level. It is more probable that descending outputs from the two hemispheres interact at converging sites along the motor axis, in particular if we assume that conduction velocities of outputs from the two stimulation sites are comparable. Uncrossed corticospinal projections could be involved, although they are not numerous in rats (Brosamle and Schwab 1997; 2000). An alternative pathway is through cortical projections to the red nucleus, on either side of the brain. However, there are also few corticorubral projections that cross midline (Bernays et al. 1988; Naus et al. 1985; Z'Graggen et al. 1998). Rather, short latency interactions may primarily take place in the reticular formation, which does receive numerous projections from the ipsi and contralateral motor cortex (Shammah-Lagnado et al. 1987; Valverde 1962). Corticoreticular projections play a crucial role for the control of hand movements in rats (Alstermark and Pettersson 2014; Whishaw et al. 1998). The powerful short-latency facilitatory

effects could thus favor efficacious integration of outputs from the two hemispheres for the execution of forelimb movements.

With intermediate ISIs (ISI5-ISI15), but particularly ISI10, conditioning stimulations in either CFA or RFA induced many more inhibitory than facilitatory effects. In adult rats, the onset of transcallosal cortical responses occur approximately 5ms and peak 13ms after stimulation (Seggie and Berry 1972). Based on these values, modulatory effects observed with ISI5 could potentially be due to callosal interactions, in particular if the callosal inputs affect the I-waves created by the T_{stim} (Ziemann et al. 1998). However, using 10ms of delay would provide sufficient time for more callosal inputs to reach the opposite cortex at the time when the T_{stim} was delivered and modulate its output. Because the vast majority (95%-97%) of callosal neurons in rats are excitatory (Gonchar et al. 1995), transcallosal inhibition is likely due to intracortical microcircuitry at the post-synaptic site and connections onto GABAergic interneurons (Karayannis et al. 2007). This indirect pattern of connection for pattern, may favor the greater incidence of inhibitory effects observed at ISI10 in comparison to ISI5. In contrast, direct excitatory callosal projections onto pyramidal neurons in deep cortical layers (Karayannis et al. 2007) could be involved in facilitatory effects observed with shorter ISIs (e.g. ISI2.5 and ISI5). Overall, the observed predominance of inhibitory effects at ISI5 and ISI10 aligns with findings in cats, in which callosal projections have also been reported to mainly exert inhibition on motor cortex (Asanuma and Okuda 1962). In rats, the release of callosal inhibition following cortical injury could explain the increased hemodynamic responses in the contralesional hemisphere (Dijkhuizen et al. 2001).

Differences of modulatory effects from CFA and RFA

One main difference between the pattern of modulation of CFA and RFA is that the conditioning stimulation in CFA induced more powerful and a greater proportion of inhibitory effects than RFA. For both CFA and RFA, the primary target of interhemispheric projections is the homolog region in the opposite hemisphere (Rouiller et al. 1993). If inhibitory effects are mainly carried through callosal projections as discussed above, the number of connections could account for the more potent inhibitory effects from CFA on its homolog than from RFA on the outputs of CFA in the opposite hemisphere. This pattern of connectivity however, cannot explain why RFA has weaker inhibitory effects on the outputs of its homolog than CFA on its homolog. We estimate that the radius of current spread with the stimulation intensities we used (i.e. ≤ 225μA; radius ≤ 0.4mm using a k value of 1,292 mA/mm^2) (Stoney et al. 1968) should have been contained within both CFA or RFA, respectively having surface areas of ~5.8mm^2 and ~1.2mm^2 in aged and sex matched Sprague Dawley rats (Touvykine et al. 2016). If the area of cortex directly activated by the C_{stim} was similar in both forelimb regions, one possibility is that the density of callosal neurons in CFA is greater than in RFA. Another possibility is that I-waves evoked by the C_{stim} can propagate further in the larger CFA and eventually activate more callosal neurons that strengthen inhibitory effects observed with longer ISIs (15-35ms).

A second major difference we found is that RFA induced more powerful and a greater proportion of facilitatory effects than CFA. As discussed above, short latency facilitatory effects may be largely carried through corticoreticular pathway and if so, our data suggest that these projections are much more impactful from RFA than from CFA. In NHPs corticoreticular projections from premotor areas are denser than from M1 (Fregosi et al. 2017). If a similar

pattern of projection for RFA and CFA exists in rats, it could explain how RFA can induce stronger short-latency facilitation. Although not as common, facilitatory effects from RFA on the outputs of its homolog were as strong as the ones from RFA on the outputs of CFA, and this was true for both short and long ISIs. It is not clear what is the role of such powerful facilitation between the two RFAs. However, they highlight the possibility that premotor areas in primates could dramatically affect their reciprocal outputs, a question that has received virtually no attention.

To date, studies on interhemispheric interactions in humans or NHPs have focussed on the modulatory effects of premotor areas on M1 outputs (Buch et al. 2010; Cote et al. 2017; Fiori et al. 2017; Koch et al. 2007; Mochizuki et al. 2004a; Mochizuki et al. 2004b; Quessy et al. 2016). In NHPs, we have compared the pattern of modulation from various premotor areas on M1 outputs using very similar techniques as the ones in the present study (Cote et al. 2017; Quessy et al. 2016). Much like RFA in rats, premotor areas induce strong modulations that are affected by the timing of stimulations. However, no single premotor area has a pattern of modulation that is similar to the one induced by RFA on the outputs of CFA in the opposite hemisphere. This suggests that the contribution of RFA to movement production is different to the one carried by the any one of the various premotor areas in primates. This is not particularly surprizing when considering that a common ancestor of rats and primates lived approximately 90-100 million years ago (Murphy et al. 2004; Nei et al. 2001), likely prior to the emergence of a 'premotor' field (Kaas 2013). The development of these additional motor fields in rats and primates may thus be a phylogenetic convergence. They have emerged in parallel due to behavioral pressure to solve more complex motor problems, but in a species-specific manner.

Understanding these interspecies differences between rats and primates is important given the large use of rodent models in motor control and recovery studies. This knowledge can help us to make more accurate predictions of how the findings in rodents motor system can relate to mechanisms present in humans.

References

Alstermark B, Ogawa J, and Isa T. Lack of monosynaptic corticomotoneuronal EPSPs in rats: disynaptic EPSPs mediated via reticulospinal neurons and polysynaptic EPSPs via segmental interneurons. *J Neurophysiol* 91: 1832-1839, 2004.

Alstermark B, and Pettersson LG. Skilled reaching and grasping in the rat: lacking effect of corticospinal lesion. *Frontiers in neurology* 5: 103, 2014.

Asanuma H, and Okuda O. Effects of transcallosal volleys on pyramidal tract cell activity of cat. *J Neurophysiol* 25: 198-208, 1962.

Baker SN, and Lemon RN. Non-linear summation of responses in averages of rectified EMG. *J Neurosci Methods* 59: 175-181, 1995.

Bernays RL, Heeb L, Cuenod M, and Streit P. Afferents to the rat red nucleus studied by means of D-[3H]aspartate, [3H]choline and non-selective tracers. *Neuroscience* 26: 601-619, 1988.

Boudrias M-H, Lee S-P, Svojanovsky S, and Cheney PD. Forelimb Muscle Representations and Output Properties of Motor Areas in the Mesial Wall of Rhesus Macaques. *Cereb Cortex* 20: 704-719, 2010a.

Boudrias M-H, McPherson RL, Frost SB, and Cheney PD. Output Properties and Organization of the Forelimb Representation of Motor Areas on the Lateral Aspect of the Hemisphere in Rhesus Macaques. *Cereb Cortex* 20: 169-186, 2010b.

Brosamle C, and Schwab ME. Cells of origin, course, and termination patterns of the ventral, uncrossed component of the mature rat corticospinal tract. *J Comp Neurol* 386: 293-303, 1997.

Brosamle C, and Schwab ME. Ipsilateral, ventral corticospinal tract of the adult rat: ultrastructure, myelination and synaptic connections. *J Neurocytol* 29: 499-507, 2000.

Buch ER, Mars RB, Boorman ED, and Rushworth MF. A network centered on ventral premotor cortex exerts both facilitatory and inhibitory control over primary motor cortex during action reprogramming. *J Neurosci* 30: 1395-1401, 2010.

Cote SL, Elgbeili G, Quessy S, and Dancause N. Modulatory effects of the supplementary motor area on primary motor cortex outputs. *J Neurophysiol* 123: 407-419, 2020.

Cote SL, Hamadjida A, Quessy S, and Dancause N. Contrasting Modulatory Effects from the Dorsal and Ventral Premotor Cortex on Primary Motor Cortex Outputs. *J Neurosci* 37: 5960-5973, 2017.

Dancause N, Barbay S, Frost SB, Mahnken JD, and Nudo RJ. Interhemispheric connections of the ventral premotor cortex in a new world primate. *J Comp Neurol* 505: 701-715, 2007.

Deffeyes JE, Touvykine B, Quessy S, and Dancause N. Interactions between rostral and caudal cortical motor areas in the rat. *J Neurophysiol* jn.00760.02014, 2015.

Dijkhuizen RM, Ren J, Mandeville JB, Wu O, Ozdag FM, Moskowitz MA, Rosen BR, and Finklestein SP. Functional magnetic resonance imaging of reorganization in rat brain after stroke. *Proc Natl Acad Sci U S A* 98: 12766-12771, 2001.

Dolbakyan E, Hernandez-Mesa N, and Bures J. Skilled forelimb movements and unit activity in motor cortex and caudate nucleus in rats. *Neuroscience* 2: 73-80, 1977.

Dum RP, and Strick PL. Motor areas in the frontal lobe of the primate. *Physiology & behavior* 77: 677-682, 2002.

Dum RP, and Strick PL. The Origin of Corticospinal Projections from the Premotor Areas in the Frontal Lobe. *J Neurosci* 11: 667-689, 1991.

Fiori F, Chiappini E, Candidi M, Romei V, Borgomaneri S, and Avenanti A. Long-latency interhemispheric interactions between motor-related areas and the primary motor cortex: a dual site TMS study. *Sci Rep* 7: 14936, 2017.

Fregosi M, Contestabile A, Hamadjida A, and Rouiller EM. Corticobulbar projections from distinct motor cortical areas to the reticular formation in macaque monkeys. *The European journal of neuroscience* 45: 1379-1395, 2017.

Gonchar YA, Johnson PB, and Weinberg RJ. GABA-immunopositive neurons in rat neocortex with contralateral projections to S-I. *Brain Res* 697: 27-34, 1995.

Gonzalez CL, Gharbawie OA, Williams PT, Kleim JA, Kolb B, and Whishaw IQ. Evidence for bilateral control of skilled movements: ipsilateral skilled forelimb reaching deficits and functional recovery in rats follow motor cortex and lateral frontal cortex lesions. *The European journal of neuroscience* 20: 3442-3452, 2004.

Hyland B. Neural activity related to reaching and grasping in rostral and caudal regions of rat motor cortex. *Behav Brain Res* 94: 255-269, 1998.

Jurgens U. The efferent and afferent connections of the supplementary motor area. *Brain Res* 300: 63-81, 1984.

Kaas JH. The evolution of brains from early mammals to humans. *Wiley Interdiscip Rev Cogn Sci* 4: 33-45, 2013.

Karayannis T, Huerta-Ocampo I, and Capogna M. GABAergic and pyramidal neurons of deep cortical layers directly receive and differently integrate callosal input. *Cereb Cortex* 17: 1213-1226, 2007.

Kleim JA, Barbay S, and Nudo RJ. Functional Reorganization of the Rat Motor Cortex Following Motor Skill Learning. *J Neurophysiol* 80: 3321-3325, 1998.

Koch G, Franca M, Mochizuki H, Marconi B, Caltagirone C, and Rothwell JC. Interactions between pairs of transcranial magnetic stimuli over the human left dorsal premotor cortex differ from those seen in primary motor cortex. *The Journal of physiology* 578: 551-562, 2007.

Liang F, Rouiller EM, and Wiesendanger M. Modulation of sustained electromyographic activity by single intracortical microstimuli: comparison of two forelimb motor cortical areas of the rat. *Somatosens Mot Res* 10: 51-61, 1993.

Maggiolini E, Viaro R, and Franchi G. Suppression of activity in the forelimb motor cortex temporarily enlarges forelimb representation in the homotopic cortex in adult rats. *The European journal of neuroscience* 27: 2733-2746, 2008.

Mansoori BK, Jean-Charles L, Touvykine B, Liu A, Quessy S, and Dancause N. Acute inactivation of the contralesional hemisphere for longer durations improves recovery after cortical injury. *Exp Neurol* 254: 18-28, 2014.

Marconi B, Genovesio A, Giannetti S, Molinari M, and Caminiti R. Callosal connections of dorso-lateral premotor cortex. *The European journal of neuroscience* 18: 775-788, 2003.

Matelli M, Camarda R, Glickstein M, and Rizzolatti G. Afferent and efferent projections of the inferior area 6 in the macaque monkey. *J Comp Neurol* 251: 281-298, 1986.

Mochizuki H, Huang YZ, and Rothwell JC. Interhemispheric interaction between human dorsal premotor and contralateral primary motor cortex. *The Journal of physiology* 561: 331-338, 2004a.

Mochizuki H, Terao Y, Okabe S, Furubayashi T, Arai N, Iwata NK, Hanajima R, Kamakura K, Motoyoshi K, and Ugawa Y. Effects of motor cortical stimulation on the excitability of contralateral motor and sensory cortices. *Experimental brain research* 158: 519-526, 2004b.

Murphy WJ, Pevzner PA, and O'Brien SJ. Mammalian phylogenomics comes of age. *Trends Genet* 20: 631-639, 2004.

Naus CG, Flumerfelt BA, and Hrycyshyn AW. An HRP-TMB ultrastructural study of rubral afferents in the rat. *J Comp Neurol* 239: 453-465, 1985.

Neafsey EJ, Bold EL, Haas G, Hurley-Gius KM, Quirk G, Sievert CF, and Terreberry RR. The organization of the rat motor cortex: a microstimulation mapping study. *Brain Research* 396: 77-96, 1986.

Neafsey EJ, and Sievert C. A second forelimb motor area exists in rat frontal cortex. *Brain Research* 232: 151-156, 1982.

Nei M, Xu P, and Glazko G. Estimation of divergence times from multiprotein sequences for a few mammalian species and several distantly related organisms. *Proc Natl Acad Sci U S A* 98: 2497-2502, 2001.

Park MC, Belhaj-Saif A, and Cheney PD. Properties of primary motor cortex output to forelimb muscles in rhesus macaques. *J Neurophysiol* 92: 2968-2984, 2004.

Price AW, and Fowler SC. Deficits in contralateral and ipsilateral forepaw motor control following unilateral motor cortical ablations in rats. *Brain Res* 205: 81-90, 1981.

Quessy S, Côté SL, Hamadjida A, Deffeyes J, and Dancause N. Modulatory Effects of the Ipsi and Contralateral Ventral Premotor Cortex (PMv) on the Primary Motor Cortex (M1) Outputs to Intrinsic Hand and Forearm Muscles in Cebus apella. *Cereb Cortex* 26: 3905-3920, 2016.

Rathelot JA, and Strick PL. Muscle representation in the macaque motor cortex: an anatomical perspective. *Proc Natl Acad Sci U S A* 103: 8257-8262, 2006.

Rathelot JA, and Strick PL. Subdivisions of primary motor cortex based on cortico-motoneuronal cells. *Proc Natl Acad Sci U S A* 106: 918-923, 2009.

Rouiller EM, Babalian A, Kazennikov O, Moret V, Yu XH, and Wiesendanger M. Transcallosal connections of the distal forelimb representations of the primary and supplementary motor cortical areas in macaque monkeys. *Experimental brain research* 102: 227-243, 1994.

Rouiller EM, Moret V, and Liang F. Comparison of the connectional properties of the two forelimb areas of the rat sensorimotor cortex: support for the presence of a premotor or supplementary motor cortical area. *Somatosens Mot Res* 10: 269-289, 1993.

Rouiller EM, Tanné J, Moret V, Kermadi I, Boussaoud D, and Welker E. Dual morphology and topography of the corticothalamic terminals originating from the primary, supplementary motor, and dorsal premotor cortical areas in macaque monkeys. *J Comp Neurol* 396: 169-185, 1998.

Schieber MH, and Rivlis G. A spectrum from pure post-spike effects to synchrony effects in spike-triggered averages of electromyographic activity during skilled finger movements. *J Neurophysiol* 94: 3325-3341, 2005.

Seggie J, and Berry M. Ontogeny of interhemispheric evoked potentials in the rat: significance of myelination of the corpus callosum. *Exp Neurol* 35: 215-232, 1972.

Shammah-Lagnado SJ, Negrao N, Silva BA, and Ricardo JA. Afferent connections of the nuclei reticularis pontis oralis and caudalis: a horseradish peroxidase study in the rat. *Neuroscience* 20: 961-989, 1987.

Soma S, Saiki A, Yoshida J, Rios A, Kawabata M, Sakai Y, and Isomura Y. Distinct Laterality in Forelimb-Movement Representations of Rat Primary and Secondary Motor Cortical Neurons with Intratelencephalic and Pyramidal Tract Projections. *J Neurosci* 37: 10904-10916, 2017.

Starkey ML, Bleul C, Zörner B, Lindau NT, Mueggler T, Rudin M, and Schwab ME. Back seat driving: hindlimb corticospinal neurons assume forelimb control following ischaemic stroke. *Brain* 135: 3265-3281, 2012.

Stepniewska I, Preuss TM, and Kaas JH. Architectonics, somatotopic organization, and ipsilateral cortical connections of the primary motor area (M1) of owl monkeys. *J Comp Neurol* 330: 238-271, 1993.

Stoney SD, Jr., Thompson WD, and Asanuma H. Excitation of pyramidal tract cells by intracortical microstimulation: effective extent of stimulating current. *J Neurophysiol* 31: 659-669., 1968.

Touvykine B, Mansoori BK, Jean-Charles L, Deffeyes J, Quessy S, and Dancause N. The Effect of Lesion Size on the Organization of the Ipsilesional and Contralesional Motor Cortex. *Neurorehabil Neural Repair* 30: 280-292, 2016.

Valverde F. Reticular formation of the albino rat's brain stem cytoarchitecture and corticofugal connections. *J Comp Neurol* 119: 25-53, 1962.

Whishaw IQ. An endpoint, descriptive, and kinematic comparison of skilled reaching in mice (Mus musculus) with rats (Rattus norvegicus). *Behavioural Brain Research* 78: 101-111, 1996.

Whishaw IQ, Gorny B, and Sarna J. Paw and limb use in skilled and spontaneous reaching after pyramidal tract, red nucleus and combined lesions in the rat: behavioral and anatomical dissociations. *Behav Brain Res* 93: 167-183, 1998.

Yang HW, and Lemon RN. An electron microscopic examination of the corticospinal projection to the cervical spinal cord in the rat: lack of evidence for cortico-motoneuronal synapses. *Experimental brain research* 149: 458-469, 2003.

Z'Graggen WJ, Metz GA, Kartje GL, Thallmair M, and Schwab ME. Functional recovery and enhanced corticofugal plasticity after unilateral pyramidal tract lesion and blockade of myelin-associated neurite growth inhibitors in adult rats. *J Neurosci* 18: 4744-4757, 1998.

Zhuravin IA, and Bures J. Changes of cortical and caudatal unit activity accompanying operant slowing of the extension phase of reaching in rats. *The International journal of neuroscience* 39: 147-152, 1988.

Zhuravin IV, and Bures J. Activity of cortical and caudatal neurons accompanying instrumental prolongation of the extension phase of reaching in rats. *The International journal of neuroscience* 49: 213-220, 1989.

Ziemann U, Tergau F, Wassermann EM, Wischer S, Hildebrandt J, and Paulus W. Demonstration of facilitatory I wave interaction in the human motor cortex by paired transcranial magnetic stimulation. *The Journal of physiology* 511 (Pt 1): 181-190, 1998.

Figures

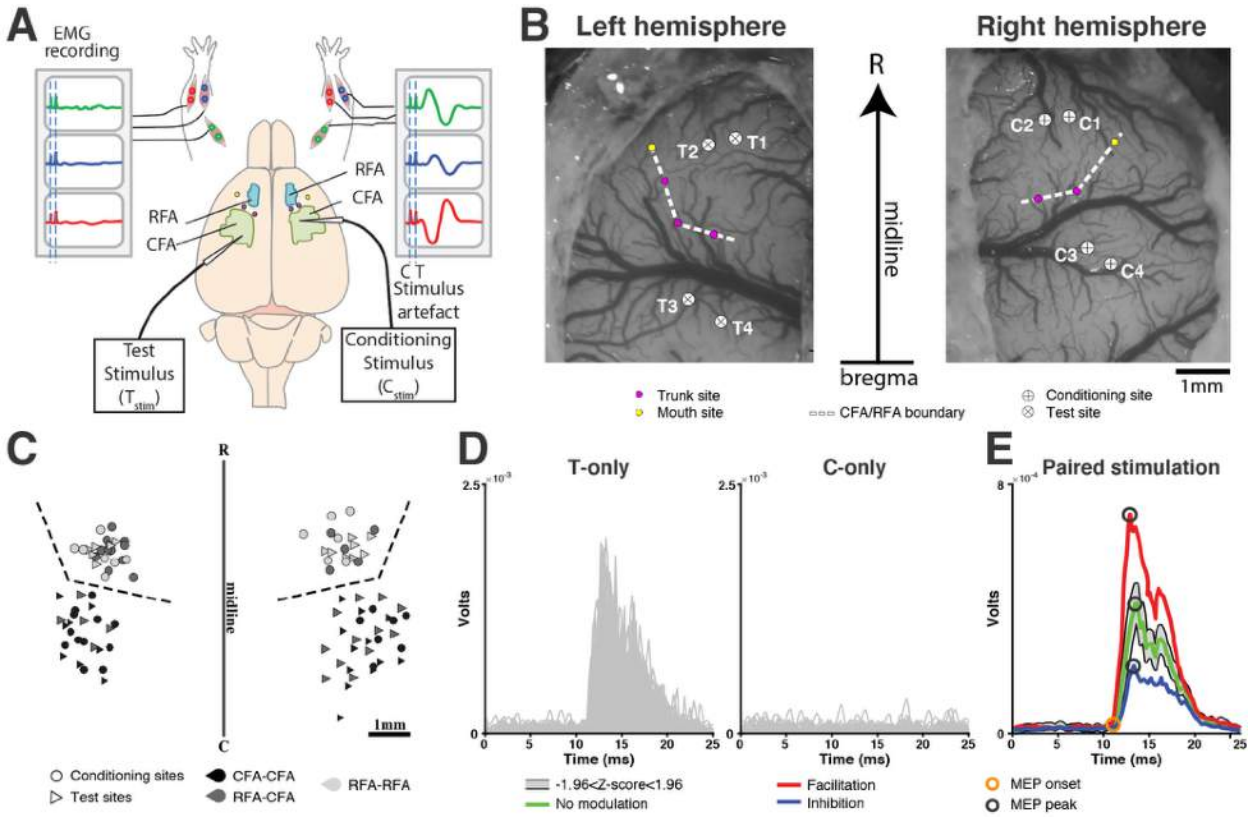

Figure (Ch3)1. Experimental setup and location of cortical stimulation sites. A) Schematic representation of the experimental setup. EMG signals from three forelimb muscles (WE: wrist extensor, WF: wrist flexor, EF: elbow flexor) implanted bilaterally were analyzed. For paired pulse stimulation protocols, the electrode delivering the conditioning stimulus (C_{stim}) was positioned in either CFA or RFA of one hemisphere. The electrode delivering the test stimulus (T_{stim}) was positioned in either CFA or RFA of the opposite hemisphere. The stimulation intensity of the T_{stim} was suprathreshold and evoked EMG responses in the contralateral arm (right arm EMG recording). For the C_{stim}, the intensity was subthreshold and did not evoke MEPs in either arm (left arm EMG recording). B) Example of bilateral craniotomy showing the location of the

C_{stim} and T_{stim} electrodes in a rat. Note that the figure is an exact scaled reproduction of the position and orientation of the two craniotomies in relation to the skull midline (vertical arrow) and Bregma (horizontal line on the arrow). ICMS trains were first used to locate non forelimb responses, in this case neck (purple dots) and mouth (yellow dots) movements, in order to define the border between RFA and CFA (white dashed line). In this animal, a total of four paired pulse protocols were conducted. In the first two protocols, the C_{stim} was delivered in RFA (C1 and C2) of one hemisphere and T_{stim} in RFA of the opposite hemisphere (T1 and T2). In the last two protocols, the C_{stim} was delivered in CFA (C3 and C4) of one hemisphere and T_{stim} in CFA of the opposite hemisphere (T3 and T4). C) Schematic representation of all Test and Conditioning sites. Test (triangles) and Conditioning (circles) sites for CFA-CFA (black), RFA-CFA (dark gray), and RFA-RFA (light gray) protocols are aligned on the border (dashed line) between RFA and CFA. R stands for rostral, and C for caudal.

D) Example of responses evoked in WE contralateral to T_{stim} with single pulses in the T-only (n=100; left panel) and C-only (n=100; right panel) conditions. EMG traces are rectified and smoothed. As expected, the T_{stim} evoked a clear MEP and the C_{stim} did not evoke any clear responses. E) To quantify the modulation of the MEP in the paired stimulation conditions, we first calculated a predictor (shaded gray area) based on the responses obtained in the T-only and C-only conditions shown in (C). Responses evoked in the paired conditions were compared to this predictor. In this example, when the C_{stim} was delivered simultaneously with the T_{stim} (ISI0; red trace), the amplitude of the MEP was significantly greater than the predictors (Z-score $\geq$ 1.96) and the effect was classified as facilitatory. When the C_{stim} was delivered 15ms before the T_{stim} (ISI15; green trace), the amplitude of the MEP fell within the predictors and the effect was

classified non-significant. Finally, when the C_{stim} was delivered 10ms before the T_{stim} (ISI10; blue trace), the amplitude of the MEP was significantly smaller than the predictors (Z-score ≤ 1.96) and the effect was classified as inhibitory. Open circles on the traces show the response peak (black) and onset (orange) time that were used to calculate the amplitude of the responses.

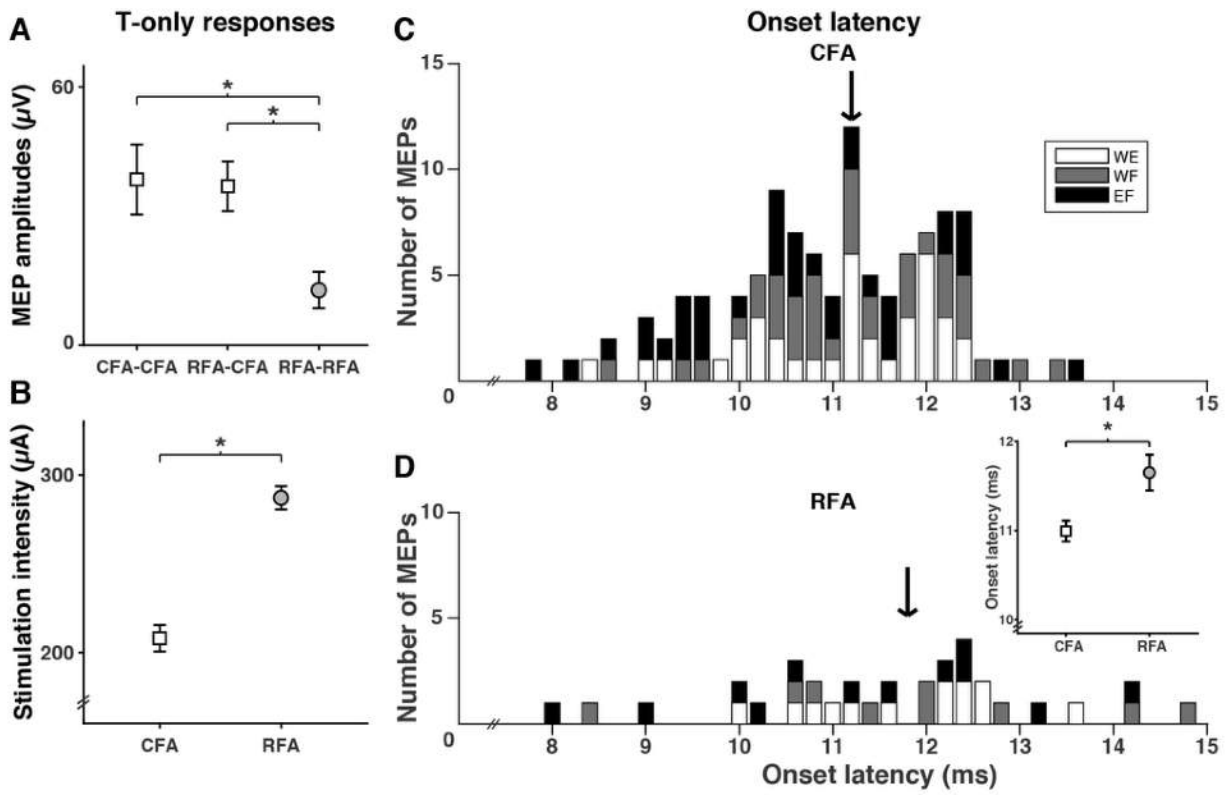

Figure (Ch3)2. Comparison of output latencies from CFA and RFA. A) Mean peak amplitude (±SE) of MEPs in the 3 types of protocols (CFA-CFA; RFA-CFA and RFA-RFA). MEPs from CFA, regardless if they were collected in the CFA-CFA or RFA-CFA protocols, had similar amplitudes. They were however significantly greater than MEPs from RFA. B) Mean threshold stimulation intensity (±SE) necessary to evoke responses from CFA and RFA. Threshold current intensity values were significantly greater in RFA than in CFA. C) MEPs onset latency resulting from T-only stimulation in CFA (n=109) of all 3 muscles (WE: white; WF: gray and EF: black). The histogram shows the count of MEPs with different onset latency values (bins of 0.2ms). Onset latencies of MEPs induced by CFA ranged from 7.8ms to 13.7ms, with a median value of 11.2ms (black arrow). No clear differences of onset latencies were observed between muscles. D) Onset latencies of MEPs resulting from T-only stimulation in RFA (n=34). Onset latencies of

MEPs induced by RFA ranged from 8.0ms to 14.7ms, with a median value of 11.8ms (black arrow). Again, no clear differences for the 3 muscles tested were observed. The inset shows that average (±SE) of onset latencies of MEPs from CFA was shorter than from RFA. * $p<0.05$.

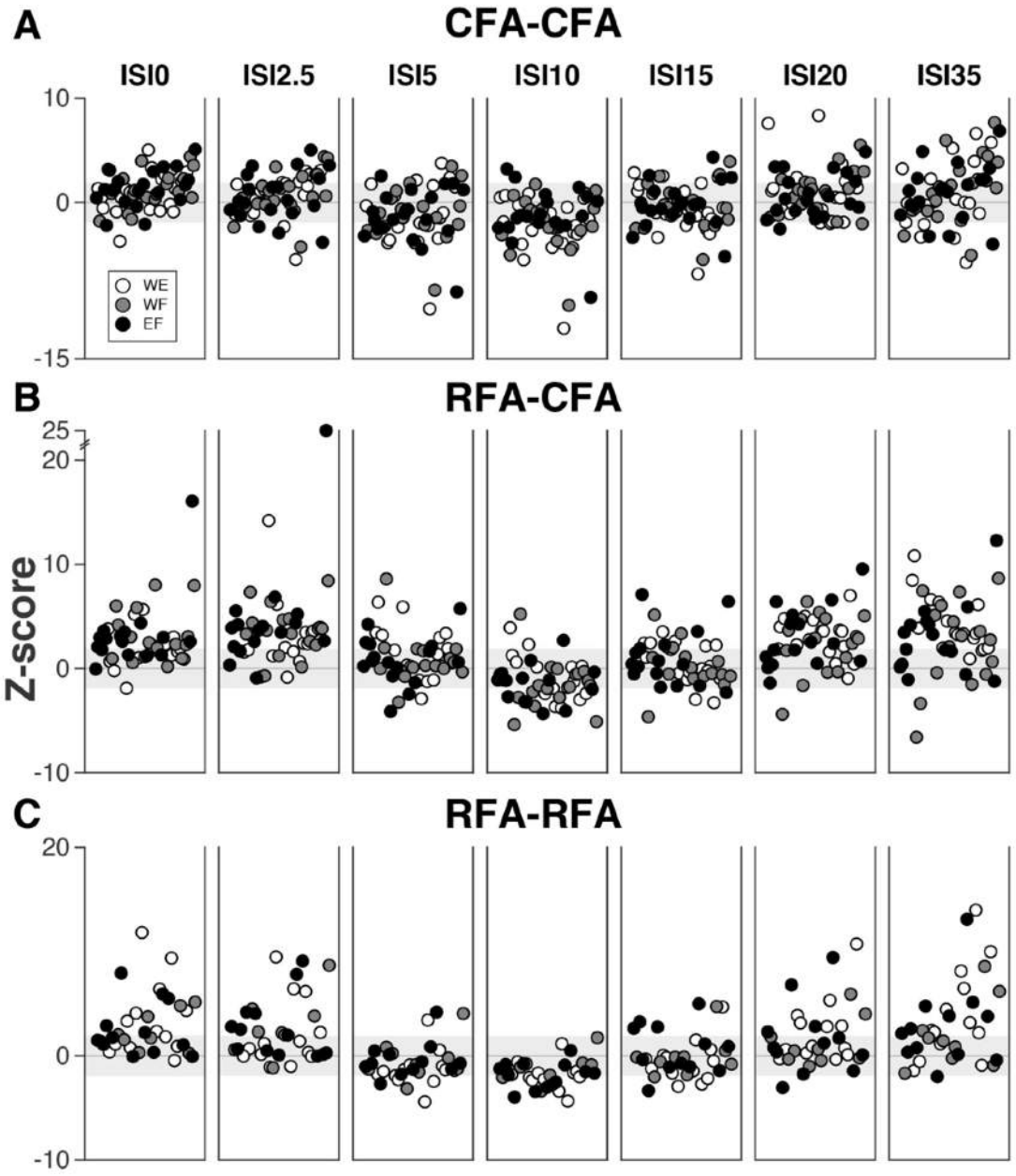

Figure (Ch3)3. Complete data set of modulatory effects from CFA and RFA on outputs from the opposite hemisphere. A) Magnitude of modulatory effects for CFA-CFA protocols. The graph combines data from all rats and all 3 muscles (WE: white; WF: gray and EF: black). Each dot reports the magnitude of the modulation (Z-score) of one MEP by the conditioning stimulation in CFA. Dots are ordered based on the onset latency of the MEP resulting from T-

only stimulation (increasing values from left to right) and the order is kept constant across panels showing modulations with the different ISIs (delays between the C_{stim} and T_{stim}). For this type of protocol, there was 60 significant MEPs (> 1 SD above baseline) with the T-only condition in CFA (i.e. 60 circles plotted per ISI). With ISI0 for example (most left panel), out of these 60 MEPs 47 had larger values (above zero in the plot), and 13 had smaller values (below zero in the plot) with the conditioning stimulation. However, only 21 MEPs were significantly facilitated and 3 significantly inhibited (i.e. outside of the ±1.96 Z-score range; gray background). **B)** Magnitude of modulatory effects for RFA-CFA protocols presented as in (A). In comparison to CFA, RFA appeared to induce more facilitatory effects on the outputs of CFA in the opposite hemisphere. **C)** Magnitude of modulatory effects for RFA-RFA protocols presented as in (A). There was no clear difference in the pattern of modulation between the muscles recorded.

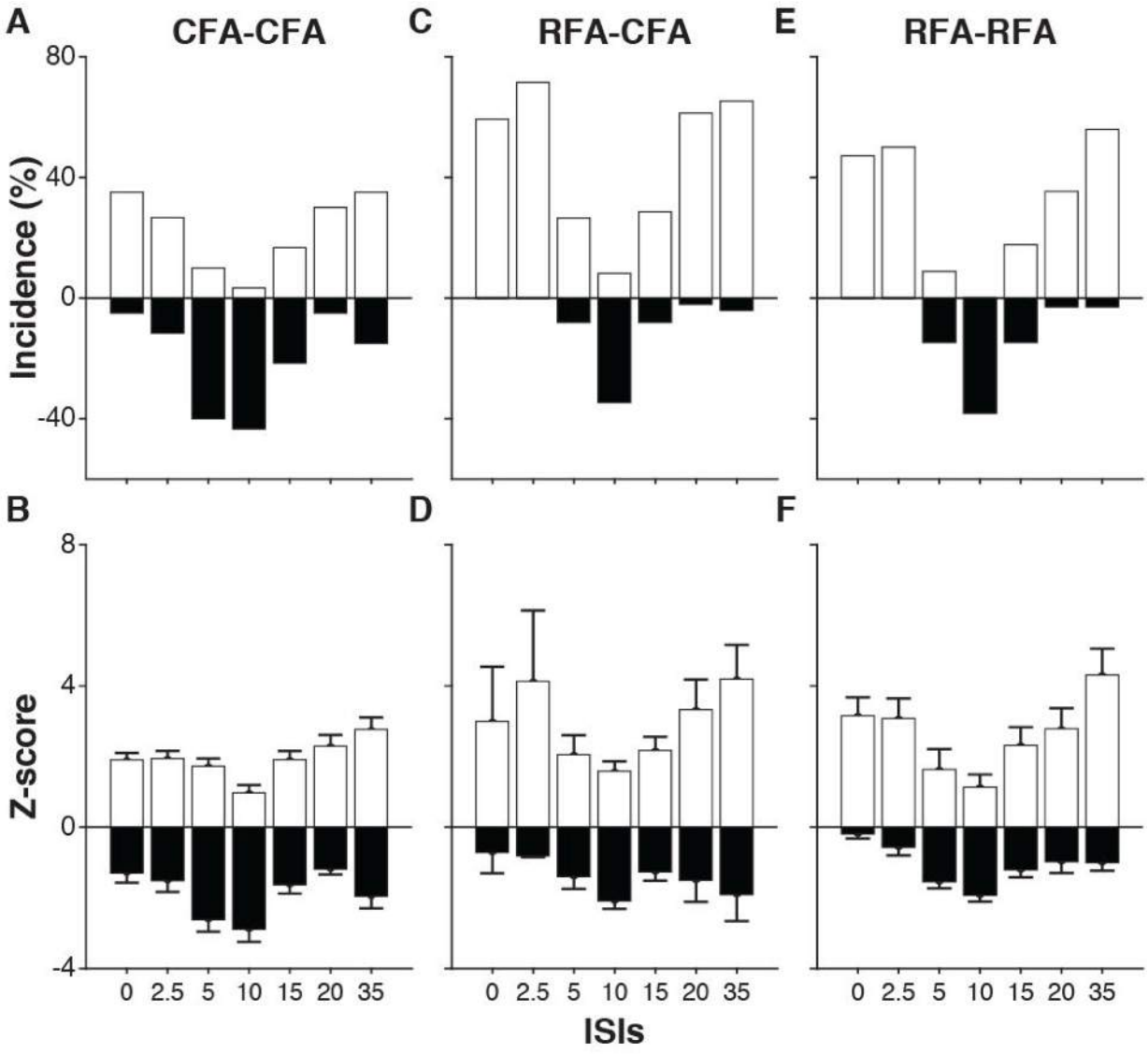

Figure (Ch3)4. Quantification of modulatory effects of CFA and RFA with each ISI tested. **A)** For each ISI, the bars show the incidence (%) of significant modulation from CFA on the outputs of its homolog (CFA-CFA protocols; all 3 muscles combined). For each ISI, we calculated the proportion of significant facilitatory (white bars) and inhibitory (black bars) effects. With ISI0 for example, out of 60 MEPs from CFA, 21 were significantly facilitated (35.0%), and 3 were significantly inhibited (3.5%). **B)** Mean magnitude (Z score ± SE) of

facilitatory and inhibitory modulations from CFA on the outputs of its homolog (all 3 muscles combined). **C)** Incidence of significant modulations from RFA on the outputs of CFA in the opposite hemisphere. Results are presented as in (A). **D)** Mean magnitude (± SE) of facilitatory and inhibitory modulations from RFA on the outputs of CFA in the opposite hemisphere. Results are presented as in (B). **E)** Incidence of significant modulations resulting from RFA on the outputs of its homolog in the opposite hemisphere. Results are presented as in (A). **F)** Mean magnitude (± SE) of facilitatory and inhibitory modulations resulting from RFA on the outputs of its homolog. Results are presented as in (B).

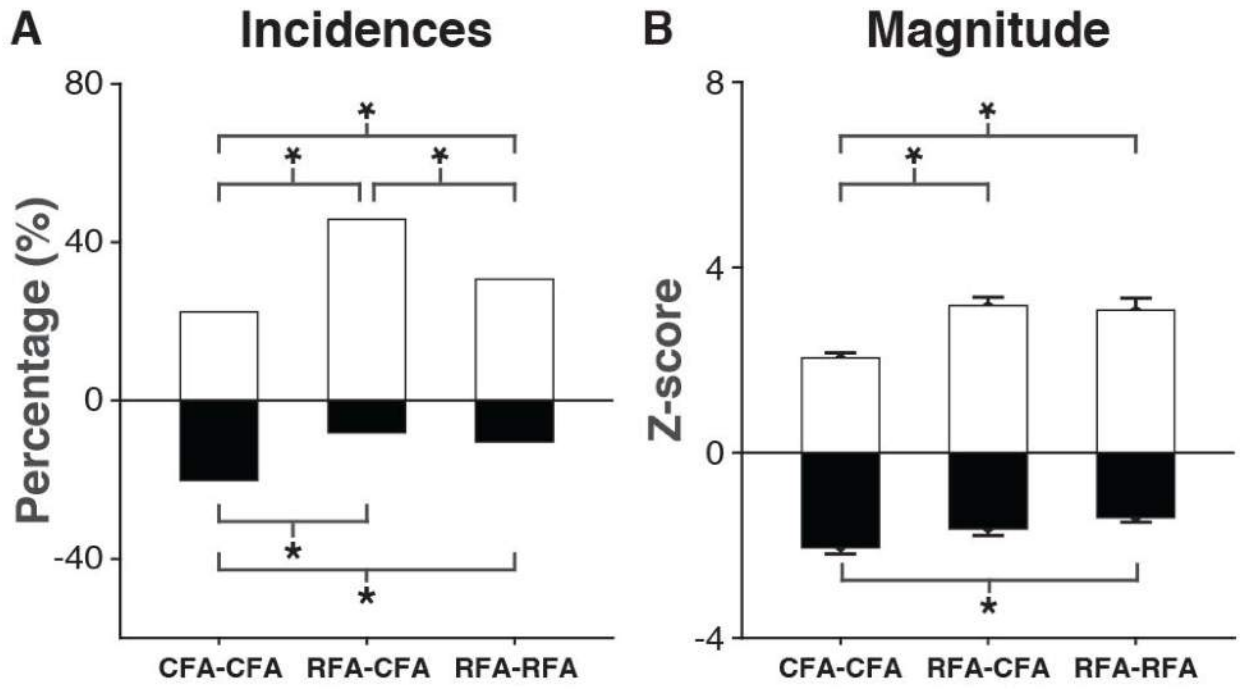

Figure (Ch3)5. Comparison of the modulatory effects of CFA and RFA with all ISIs combined. A) Comparison of the incidence of modulatory effects for CFA-CFA, RFA-CFA, and RFA-RFA protocols with all the ISIs tested combined. We found significantly fewer facilitatory effects and more inhibitory effects for CFA-CFA protocols than for the other two types of protocols. In addition, RFA-CFA induced more facilitatory effects in comparison to RFA-RFA protocols. * $p \leq 0.017$. **B)** Comparison of the magnitude of modulatory effects from all 3 protocols with all the tested ISIs combined. We found that facilitatory effects of CFA-CFA protocols were significantly weaker than for other protocols. Inhibitory effects were significantly more powerful for CFA-CFA than RFA-RFA protocols. * $p \leq 0.05$.

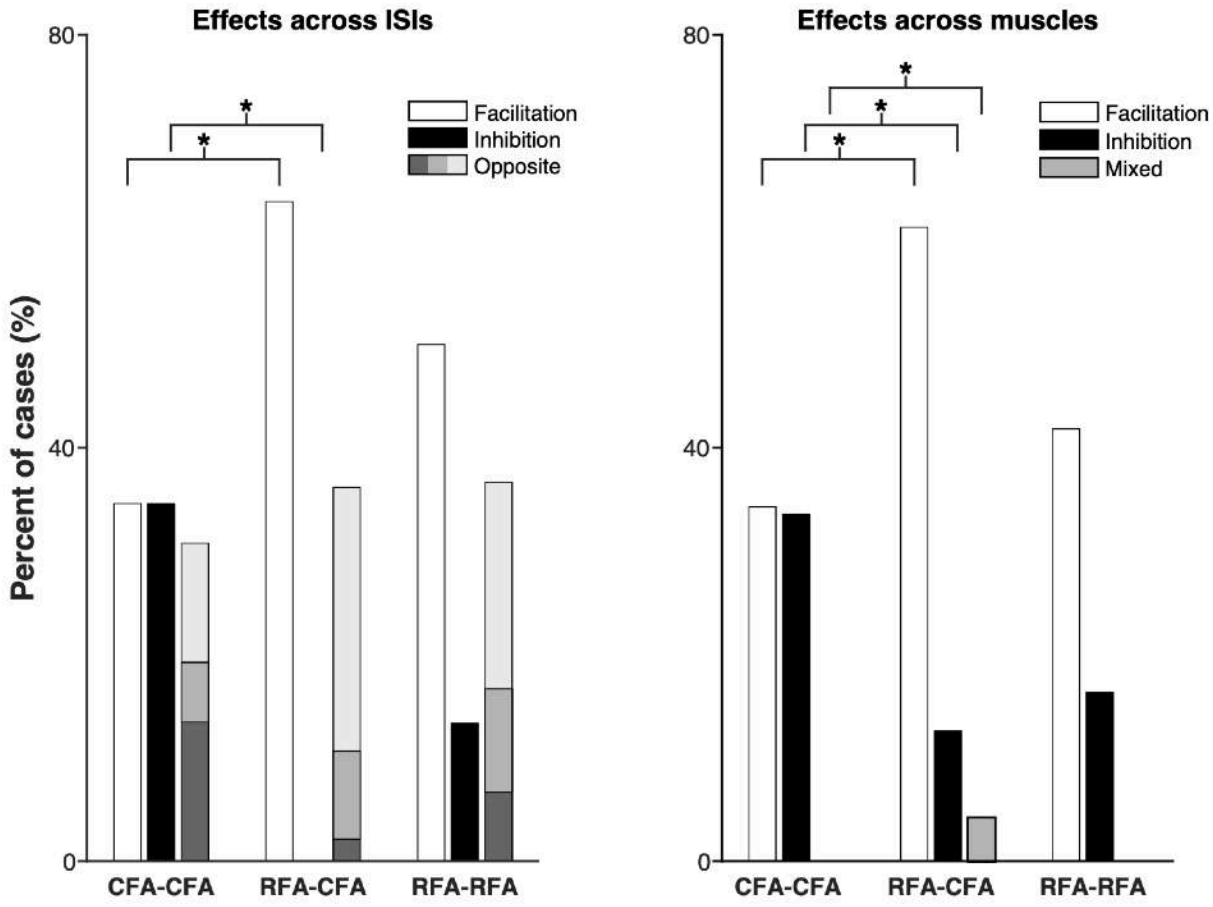

Figure (Ch3)6. Pattern of modulatory effects from CFA and RFA across ISIs and across muscles. A) The bar graph reports the incidence of modulatory effects across ISIs for the 3 types of protocols. For CFA-CFA protocols, we found comparable proportions of pure facilitatory (white bar), pure inhibitory (black bar) and opposite effects (gray bar) across ISIs. Within the population of opposite effects, there were fewer cases with an equal number of facilitation and inhibition across ISIs (mid-tone gray) than cases with a predominance of facilitation (light gray) or a predominance inhibition across ISIs (dark gray). For RFA-CFA protocols, we found more cases of pure facilitation and no cases of pure inhibition. Proportions of pure facilitation and inhibition differed significantly between CFA-CFA and RFA-CFA

protocols. In addition, there were many more cases of opposite effects with a predominance of facilitatory effects across ISIs (light gray). For RFA-RFA protocols, the pattern of modulation across ISIs was somewhat in between the two other types of protocols and there was no difference in the pattern of modulation across ISIs in comparison to the other types of protocols.* $p \leq 0.017$. **B)** Incidence of modulatory effects across muscles for the 3 types of protocols presented as in (A). Proportion of pure facilitation across muscles (white bars), pure inhibition (black bars), and mixed effects across muscles (gray). For CFA-CFA protocols, we found comparable proportion of cases of pure facilitation and pure inhibition, and no cases of mixed effects. In contrast, conditioning stimulation in RFA evoked many more pure facilitation effects across muscles than pure inhibition or mixed effects, and this was true for both the outputs of CFA or RFA in the opposite hemisphere. In all cases of mixed effects in RFA-CFA protocols, there were an equal number of muscles simultaneously facilitated and inhibited (mid-tone gray). When comparing the 3 types of protocols, we found that CFA-CFA protocols evoked fewer pure facilitation and mixed responses than RFA-CFA protocols, and more inhibition than RFA-CFA protocols. There was no difference in the pattern of modulation across muscles from RFA on the outputs of either CFA or RFA in the opposite hemisphere (RFA-CFA versus RFA-RFA). * $p \leq 0.017$.

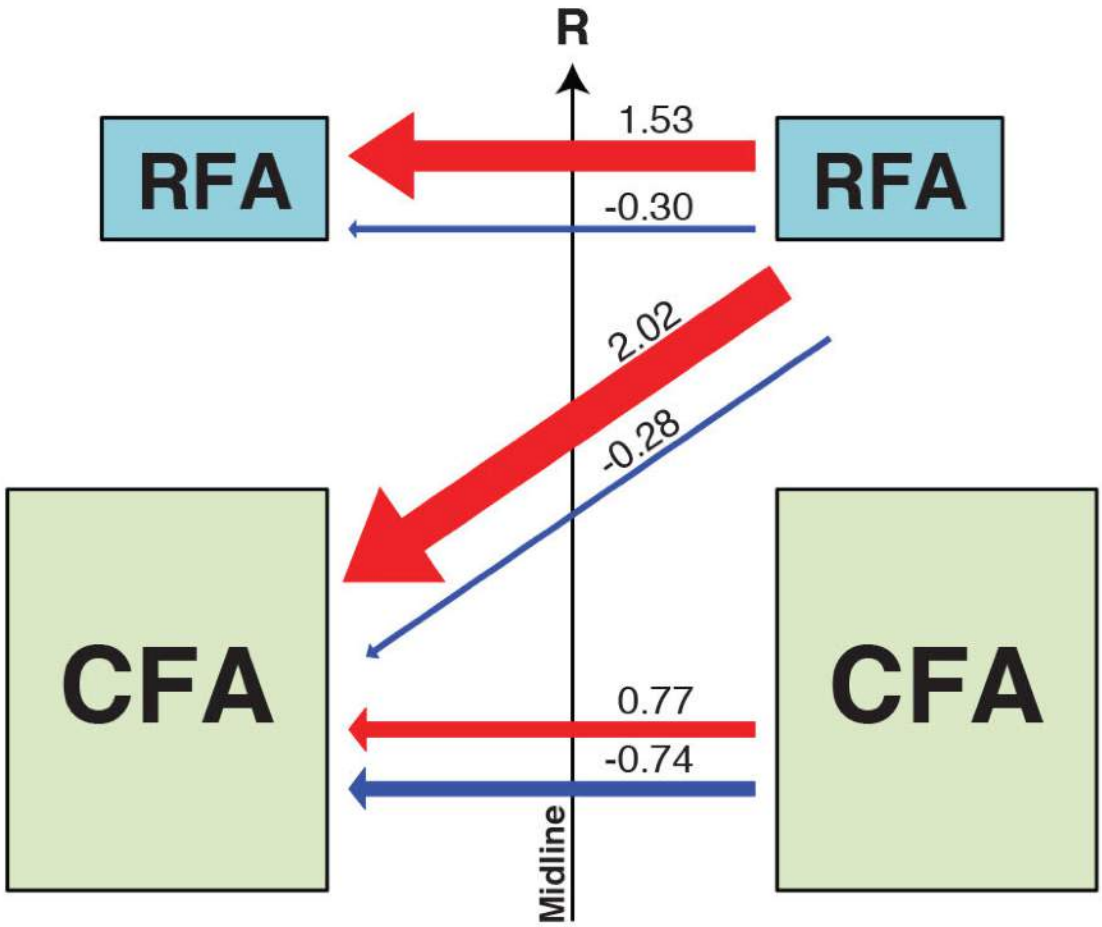

Figure (Ch3)7. Global impact scores of facilitatory and inhibitory effects of CFA and RFA on motor outputs. Box and arrow diagram summarizing the impact scores of CFA and RFA on motor ouputs from the opposite hemisphere. The numbers next to each arrow report the impact score value and the thickness of the arrow is proportional to this value. Impact scores were calculated by multiplying the incidence by the mean of all significant modulations. For example, for all CFA-CFA protocols with all ISIs combined, the ratio of significant facilitatory effects was 0.224 (22.4%) and the average Z-score of these significant effects was 3.42. Therefore, the facilitatory impact factor of CFA on the output of its homolog was 0.77. For CFA-CFA, the impact scores for facilitatory and inhibitory effects were quite similar, suggesting CFA has

comparable capacity to facilitate or inhibit the outputs of its homolog. In contrast for both RFA-CFA and RFA-RFA, the impact scores for facilitatory effects were much greater than for inhibitory effects. This suggests that RFA has a greater potential to facilitate motor outputs from the opposite hemisphere, regardless if the output is originating from CFA or RFA. Overall, the greatest facilitatory impact was from RFA on the outputs of its homolog and the greatest inhibitory impact was from CFA on the outputs of its homolog.

Rat ID	Number of ICMS sites to define border		Number of protocols					
			CFA-CFA		RFA-CFA		RFA-RFA	
	Right	Left	T_{stim} Right	T_{stim} Left	T_{stim} Right	T_{stim} Left	T_{stim} Right	T_{stim} Left
002	5	4	0	0	2	0	0	2
004	5	4	0	0	0	0	2	0
049	6	6	3	0	0	0	0	0
050	4	7	1	0	0	0	0	2
082	3	12	4	0	0	0	2	0
083	3	4	4	0	0	0	3	0
086	3	5	0	2	0	0	0	2
089	7	4	0	5	0	0	0	0
099	37	11	0	0	0	3	0	0
100	11	9	0	1	2	1	0	0
119	25	21	0	0	4	0	0	0
126	5	4	0	0	4	1	0	0
127	17	14	0	0	0	0	1	0

Table (Ch3)1. A summary of the number of ICSM sites required to define the border and the number of protocols collected per animal. Number of ICMS sites report the number of cortical sites that needed to be inspected with ICMS train in order to define the border between CFA and RFA in each hemisphere. Number of protocols report the number of protocols collected for each type of modulatory effect studied (i.e. CFA-CFA; RFA-CFA and RFA-RFA) and in which hemisphere the T_{stim} was located.

Chapter 4.

Reorganization of bilateral interactions and motor output of the ipsilesional forelimb motor cortex following unilateral ischemic stroke in the rat.

Boris Touvykine, Charles Labbé, Stephan Quessy, Numa Dancause

In preparation.

Abstract

Ischemic lesions result in the reorganization of both ipsi- and contra-lesional hemispheres. In the rat, forelimb movements can be evoked from two cortical motor regions the larger caudal and the smaller rostral forelimb areas (CFA and RFA respectively). Ischemic lesions were induced in the CFA to examine the neuroplasticity resulting from stroke. Female Sprague Dawley rats (N=10) received cortical infarcts in the CFA and underwent spontaneous recovery for 5-weeks. Then, the terminal intracortical microstimulation (ICMS) experiment was conducted, with two objectives. First, to examine the reorganization of cortical output to forelimb muscles. Second, paired stimulation was used to quantify the modulation of said output of ipsilesional forelimb cortical motor regions by the contralesional homologues, and to identify the changes compared to healthy animals. For the 1st objective, suprathreshold stimulation was delivered in ether ipsilesional CFA or RFA. Measures of motor evoked potentials (MEPs) latencies evoked from the ipsilesional RFA were greater and more variable, with the further reorganization of amplitudes and latencies of MEPs in different muscles. To achieve the 2nd objective, the suprathreshold test stimulation in the ipsilesional motor regions was paired at different time intervals with a subthreshold stimulus in the contralesional hemisphere to condition the motor output of the ipsilesional motor regions. Comparison of resulting modulation profiles of stroke animals with healthy rats revealed decreased interaction between contralesional and ipsilesional CFA, and a significant increase in magnitude and impact of facilitation from contralesional RFA on its ipsilesional homologue. Our results have identified significant reorganization of motor outputs out of the injured motor cortex, as well as the modulatory drive from the intact on injured hemisphere.

Introduction

Stroke is one of the most prevalent neurological conditions in adults, and every year it leaves millions of people disabled, many severely (Phac, 2011). Damage to the motor cortex is common and results in impairment of motor control (Harrison, 1994). Stroke survivors typically exhibit some recovery of function (Twitchell, 1951), at least in part due to neuroplasticity triggered by the lesions. However, the extent of recovery is highly variable between patients, and functional deficits in the control of distal forelimb are especially persistent, which is highly detrimental to the quality of life of stroke survivors (Kwakkel, Kollen, & Lindeman, 2004). Understanding and eventually being able to harness neuroplasticity to subserve recovery of function is the ultimate goal of studies on recovery after stroke.

The perilesional motor cortex in the lesioned hemisphere is an important site of neuroplasticity and the amount of damage to these ipsilesional regions can predict the extent of functional recovery (Jeffers et al., 2020). Output properties of the surviving motor cortex are known to reorganize after stroke (Traversa, Cicinelli, Bassi, Rossini, & Bernardi, 1997a). Multiple studies have found evidence of remote reorganization in premotor regions following recovery from a lesion in the primary motor cortex (M1). Inactivation or lesion in the ipsilesional supplementary motor area (SMA), dorsal premotor cortex (PMd), ventral premotor cortex (PMv), as well as their putative equivalent in rodents, the rostral forelimb area (RFA), resulted in the reinstatement of deficits (Fridman et al., 2004; Liu & Rouiller, 1999; McNeal et al., 2010; Zeiler et al., 2013).

Reorganization of the central nervous system following stroke is not limited to the ipsilesional cortex. In the contralesional hemisphere, stroke patients often present abnormal activation patterns with the movement of the paretic arm. Higher atypical contralesional activation is associated with greater motor impairments (N. S. Ward, Brown, Thompson, & Frackowiak, 2003; Nick S. Ward & Cohen, 2004). Furthermore, it was shown that inhibition of the contralesional M1 can improve recovery in some patients and animals after stroke (Babak K. Mansoori et al., 2014; Takeuchi, Chuma, Matsuo, Watanabe, & Ikoma, 2005). While these findings suggest that the contralesional motor cortex is detrimental to motor recovery, there is also a body of contradictory results from human and animal studies. Specifically, it was shown that disruption of the contralesional motor cortex in certain patients and animals can lead to the reinstatement of previous deficits (Biernaskie, Szymanska, Windle, & Corbett, 2005; Bradnam, Stinear, Barber, & Byblow, 2012; Mohapatra et al., 2016). Interestingly, it appears that the role the contralesional hemisphere takes in recovery may be affected by the lesion volume and the degree of impairments. While it would either not be involved or play a negative role in less affected individuals, it would support the recovery of the paretic hand in more affected ones.

In a previous study, we found bilateral reorganization following recovery from unilateral stroke in the caudal forelimb area (CFA), the rodent's equivalent of M1. Using intracortical microstimulation (ICMS) mapping, we found evidence of bilateral changes in both ipsi- and contralesional RFA, but not in the contralesional CFA (Touvykine et al., 2016), and these changes were affected by the lesion volume. One way that the contralesional cortex could participate in recovery is by changing its role in the production of motor outputs to the paretic limb. The present set of experiments aims to further define reorganization of output properties

and bilateral interactions of forelimb motor regions of both hemispheres, following recovery from stroke. We set out with two specific goals, the first: to further understand the reorganization of outputs to the paretic forelimb from the ipsilesional motor cortex. The second was to characterize the modulation exerted by the contralesional motor cortex on ipsilesional outputs, following spontaneous recovery from ischemic stroke. To do so, we used a rat model of ischemic strokes and invasive electrophysiological methods. Lesions were induced in the CFA and modulatory effects from the contralesional hemisphere were evaluated using paired-pulse stimulation techniques.

Materials and Methods

Subjects

Our experimental protocol followed the guidelines of the Canadian Council on Animal Care and was approved by the Comité de Déontologie de l'Expérimentation sur les Animaux of the Université de Montréal. Ten individually housed adult female Sprague Dawley rats (Charles River Laboratories, QC, Canada) weighing between 298g and 430g were used in the present experiments. They had water ad libitum and unrestricted access to food for at least 2 hours after the afternoon behavioural testing session (see below). All animals were at least 3 ½ months of age. Females were chosen to keep in line with our previous experiments (Deffeyes, Touvykine, Quessy, & Dancause, 2015; B. K. Mansoori et al., 2014; Touvykine, Elgbeili, Quessy, & Dancause, 2020) (Touvykine et al., 2016). To the best of our knowledge, there are no reported differences between male and female rats regarding the pattern of anatomical projections from either CFA or RFA. We expect our findings are generalizable to both sexes, however, this remains to be experimentally confirmed. Animals were randomly assigned to one of two groups, one received 6 cortical injections of endothelin-1 (ET-1) and the other 9 cortical injections of ET-1. In the animals used in this study, we performed experiments on the modulatory effect of the contralesional CFA on the outputs of ipsilesional CFA (CFA_{lesion}) in 5 rats ($cCFA\text{-}CFA_{lesion}$). Experiments on the modulatory effects of contralesional RFA on the outputs of CFA_{lesion} were collected in 5 rats ($cRFA\text{-}CFA_{lesion}$). Finally, the effects of contralesional RFA on the outputs of ipsilesional RFA ($RFA_{perilesion}$) were studied in 8 rats ($cRFA\text{-}RFA_{perilesion}$). We tried to collect

more than one protocol type from each rat to minimize the number of animals in the study (n=10).

Lesion Induction Surgery

To create cortical lesions of different sizes, we made different numbers of relatively small cortical ET-1 injections in the CFA in different animals (either 6 or 9 injections). Lesion surgeries were done aseptically. Anesthesia was induced with ketamine hydrochloride (80 mg/kg, intraperitoneal) and sustained with ~2% isoflurane. Lesions targeted the CFA based on stereotaxic coordinates. For the animals with 6 ET-1 injections, 6 holes of 0.7 mm in diameter were drilled through the skull (stereotaxic coordinates = +1.5, +0.5, −0.5 mm anteroposterior, +2.5, +3.5 mm mediolateral to bregma). In each hole, a syringe (Hamilton Company, NV) was lowered to a depth of −1.5 mm from the surface of the cortex to inject 330 nL of ET-1 (0.3 μg/μL in saline) at a rate of 3 nL/s with a microinjector. For animals with 9 injections, ET-1 was injected in a similar manner in 9 holes (+2.0, +1.0, 0.0mm anteroposterior, +2.0, +3.0, +4.0mm mediolateral to bregma). After injections, the holes were sealed with bone wax and the skin sutured. At the end of the procedure all animals received dexamethasone (Vetoquinol; 1 mg/kg), enrofloxacin (Baytril; 10 mg/kg), carprofen (Rimadyl; 10 mg/kg), and buprenorphine (Temgesic; 0.005 mg/kg). The recovery of every animal was closely monitored, and the antibiotic and analgesic medication was continued for 2 days following the lesion induction procedures.

Behavioral testing

The motor performance of lesioned animals was quantified with the Montoya Staircase task (Jeffers et al., 2020; Montoya, Campbell-Hope, Pemberton, & Dunnett, 1991). The performance score is based on the number of food pellets animals can successfully retrieve from wells on a staircase. Details of familiarization and behavioral data collection protocols have been previously published (Jeffers et al., 2020; Touvykine et al., 2016). Briefly, rats were food restricted (80% of daily minimum requirement by body weight), then familiarized with the Montoya Staircase reaching task over the next 10 days. A baseline performance score was established at the end of this period. Following the lesion, motor performance was evaluated twice in the first week at 4 and 7 days after the lesion, and then once per week for the following 4 weeks. On any given testing day, the performance score of each arm was the average number of eaten pellets during the two sessions (one in the morning, and one in the afternoon). For each testing session rats had 15 minutes to retrieve up to 21 pellets (3 pellets per well X 7 wells total). To prevent a bias during the familiarization period, we alternated which forelimb was tested in the AM session. Following the lesion, we always tested the paretic hand first to minimize the effect of motivation on the scores obtained with this arm. Behavioral performance was calculated as a percentage of pellets eaten during the testing session normalized to the total number of pellets available (two daily sessions with 21 pellets each = 42 pellets total). Electrophysiological data were collected in a terminal experiment on the 35th day after the lesion.

Terminal Electrophysiological Surgery

All surgical procedures were performed as part of an aseptic, non-sterile, terminal experiment (Deffeyes et al., 2015; Touvykine et al., 2020; Touvykine et al., 2016). Anaesthesia was induced

with a single dose of ketamine hydrochloride via intraperitoneal injection (80mg/kg). The animals were transitioned to ~2% isoflurane general anaesthesia (Furane; Baxter) in 100% oxygen and remained under general anaesthesia for the duration of the surgical procedures. They received a dose of dexamethasone (1mg/kg) intramuscularly and mannitol (~3000mg/kg) intraperitoneally to prevent the inflammation and swelling of the brain, respectively. Subcutaneous injections of physiological saline (2ml) were delivered every 2 hours to prevent dehydration. Body temperature was monitored continuously via an anal probe and kept to ~36.0°C with a homeothermic blanket system (Harvard apparatus, Holliston, Massachusetts, USA).

Multistranded microwires (Cooner Wire, Chatsworth, CA, USA) were implanted intramuscularly to record electromyographic (EMG) signals. In the forearm, we implanted the extensor digitorum communis, a wrist extensor (WE) and the palmaris longus, a wrist flexor (WF). In the arm, we implanted the biceps brachii, an elbow flexor (EF) and the tricep brachii, as well as the spinodeltoid on the back. However, to be able to make meaningful comparisons with previously published data in naïve rats (Touvykine et al., 2020), we focused our analyses on WE, WF and EF muscles. For each muscle, the accurate placement of the EMG wires was confirmed using electrical stimulations through the implanted wires and visual inspection of the evoked movements. To ensure the quality of implantation, movements had to be evoked through the EMG wires with stimulation intensities <300μA. Following the implantation of EMG wires, the animal was positioned in a stereotaxic frame and bilateral craniectomies and durectomies were performed to expose forelimb motor areas of the two cerebral hemispheres. Craniectomies exposed the cortex from approximately 5mm to -1.5mm AP and 1.5mm to 6mm ML in relation

to bregma. Upon completion of the durectomies, the exposed cortex was covered in warm neutral mineral oil to prevent dehydration, which was added as needed until the end of the procedure.

Localization of motor representations

At the end of the surgical procedures, isoflurane was turned off and sedation was maintained with intraperitoneal injections of ketamine hydrochloride (~3-5 mg/kg/10 min) (Touvykine et al., 2020; Touvykine et al., 2016). Prior to collecting electrophysiological data for the paired-pulse experiments, RFA and CFA were located using intracortical microstimulation (ICMS) trains delivered at 1Hz and generated by RZ5 real-time processor (Tucker Davis Technologies (TDT), Alachua, FL, USA). Each train consisted of 13 cathodal 0.2ms duration square pulses with 3.3ms interpulse interval (Touvykine et al., 2016). For each cortical site tested, a glass insulated tungsten microelectrode (~0.5 MΩ impedance; FHC Bowdoin, ME, USA) was lowered 1500-1600µm below the cortical surface with a microdrive (model 2662; David Kopf Instruments, Tujunga, CA) mounted on a micromanipulator (David Kopf Instruments, Tujunga, CA). Trains were delivered with a direct current stimulus isolator (model B51-2; BAK, Mount Airy, MD) and the intensity was gradually increased to a maximum current intensity of 100µA or until a clear movement was evoked. Movements were categorized as forelimb, neck, vibrissae, or mouth (jaw or tongue movements). To delineate RFA from CFA we characterized a strip of cortex between these two areas from which non-forelimb responses (typically neck movements) were evoked (Kleim, Barbay, & Nudo, 1998; Neafsey et al., 1986; Touvykine et al., 2016). To further confirm the extent of RFA, we explored the cortical territory lateral to this representation until mouth motor responses were evoked, as expected (Neafsey et al., 1986). Accordingly,

cortical sites evoking forelimb movements located rostral to the strip of neck responses and medial to the mouth representation were considered to be in RFA. Forelimb responses caudal and typically lateral to the strip of neck motor responses were considered to be in CFA. After establishing the border between CFA and RFA in both hemispheres, no further mapping was done on the experimental animals, and we proceeded to collect paired-pulse stimulation protocols. It should be noted that we managed to find non-forelimb responses delineating RFA and CFA in all experimental rats, which means that cortical strokes did not extend into the ipsilesional RFA.

Paired-pulse stimulations and EMG recording

These experimental procedures were previously described (Touvykine et al., 2020). Briefly, two glass-coated tungsten microelectrodes (~0.5MΩ impedance; FHC Bowdoin, ME, USA) were positioned with two independent micromanipulators for paired-pulse experiments. In different protocols, the conditioning stimulation (C_{stim}) electrode was either positioned in the hemisphere contralateral to the test stimulation in either CFA (cCFA) or RFA (cRFA) and the test stimulation (T_{stim}) electrode was positioned in either CFA_{lesion} or $RFA_{ipsilesional}$. We conducted a total of 51 paired pulse protocols in 10 rats. Protocols were separated into 3 different types. First, the C_{stim} was delivered in cCFA and the T_{stim} in the CFA_{lesion} in order to characterize the modulatory effects from cCFA on motor outputs of its injured homolog (i.e. cCFA-CFA_{lesion} protocols, n = 28). In the second type of protocols (n=16) the C_{stim} was delivered in cRFA and the T_{stim} in CFA_{lesion} to characterize the modulatory effects from cRFA on motor outputs of CFA_{lesion} (i.e. cRFA-CFA_{lesion} protocols). In the third type of protocols (n=19), the C_{stim} was delivered in cRFA

and the T_{stim} in $RFA_{ipsilesional}$ of the opposite hemisphere in order to characterize the modulatory effects from cRFA on motor outputs of its homolog in the ipsilesional hemisphere (i.e. cRFA-$RFA_{ipsilesional}$ protocols). For each cortical site included in these protocols, we first confirmed that it evoked clear forelimb movements in the arm contralateral to the electrodes using ICMS trains, which consisted of 13 monophasic square pulses (0.2 ms duration; 3.3 ms interpulse interval) delivered at 1Hz (Touvykine et al., 2020; Touvykine et al., 2016). Stimulations were then switched to single, 0.2ms cathodal pulses delivered at 2Hz, and current intensity was increased to a maximal intensity of 300µA, while simultaneously looking at the EMG signals of all recorded muscles on a custom-built interface using OpenEx software (TDT, Alachua, FL, USA). Once a motor evoked potential (MEP) was identified in at least one of the muscles in the arm contralateral to the stimulation, the intensity was adjusted to establish the threshold value. This procedure was used for both the electrodes delivering the T_{stim} and C_{stim}. The T_{stim} intensity was then set to 125% of the threshold value and the C_{stim} intensity was set to 75% of threshold. For the T_{stim}, if we found that the MEP was too small with 125% of the threshold value, the intensity was adjusted to produce a clear, but submaximal response. For example, if responses were only visible in 10-15% of trials on the oscilloscope, the intensity was considered “too small” and increased to get responses on ≥40-50% of trials using single pulse stimulation. If no MEPs were evoked with T_{stim} using the maximal stimulation intensity of 300µA, the cortical site was discarded, and the electrode moved to another location. For the C_{stim}, if no response was observed using single pulses with the maximum intensity of 300µA, the stimulation intensity was arbitrarily set to 225µA (i.e. 75% of 300µA). This was the case for 37.3% (n=19) of cortical sites included in the study.

Once the cortical sites were identified and stimulation intensities established, a paired-pulse stimulation protocol was initiated. The protocol included 9 stimulation conditions: the T_{stim} delivered alone (T-only trials), the C_{stim} delivered alone (C-only trials), or both the C_{stim} and the T_{stim} delivered (paired stimulation) with one of 7 different interstimulus intervals (ISIs). In the paired stimulation conditions, the C_{stim} and the T_{stim} were either delivered simultaneously (ISI0) or with the C_{stim} preceding the T_{stim} by 2.5ms (ISI2.5), 5ms (ISI5), 10ms (ISI10), 15ms (ISI15), 20ms (ISI20), and 35ms (ISI35).

During a protocol, the stimulation condition was randomized across trials, until a total of 100 trials were collected for each stimulation condition (total number of trials for each protocol = 900). All cortical sites in an animal were only used once. After data collection for a paired pulse protocol was completed, both electrodes were moved to new cortical locations, and all procedures were repeated. The selection of new sites was random. Data collection was stopped after ~5 hours from the moment the cortex was exposed to ensure stable responsiveness of the preparation and avoid any potential effects of overstimulation. The EMG data were recorded with custom OpenEx software running on an RZ5 real-time processor (TDT, Alachua, FL, USA). Each EMG channel was recorded at 4.9kHz, and raw EMG data were stored for offline analysis.

EMG data analyses

EMG analyses were conducted offline using custom written Matlab (Version R2014a; Natick, MA, USA) code. The continuous EMG data collected during the experiments were separated into individual trials for each condition and aligned to stimulation time stamps. The signal was full wave rectified and smoothed using a five point moving average (window size = 1.02ms), with no

additional filtering. For each condition, the baseline was calculated from a 25ms window before the first stimulus (-26ms to -1ms prior to the first stimulus timestamp). The motor evoked potentials (MEPs) were calculated from a window of 3 to 30ms after the end of the last stimulation timestamp. For each channel of recorded EMG, we first averaged all trials in the T-only condition and compared the average MEP to the average baseline activity for the same trials. MEPs with amplitudes greater than 1 standard deviation (SD) above baseline value were considered large enough to be either facilitated or inhibited by C_{stim} and kept for further analyses. Cases in which the MEP with the T-only condition was smaller than 1 SD above baseline were excluded. Out of the 68 protocols, 2 had no significant MEP (> 1 SD above baseline) in offline analyses and were rejected from further analyses. We also verified that the C-only condition did not evoke MEPs, to validate the assumption of linear summation for the calculation of the predictor (see below) (Baker & Lemon, 1995). Three protocols were removed because of undesirable responses with the C-only condition. A total of 125 significant MEPs from the 63 remaining protocols were greater than 1 SD above the baseline and were included in the study. These MEPs were used to characterize and compare the output properties of CFA_{lesion} and $RFA_{ipsilesional}$ (see below).

To quantify the modulatory effect of the C_{stim} on each of the 125 significant MEPs in paired-pulse conditions, we first calculated a predictor using a modified bootstrapping procedure to generate a population of predicted responses that would be expected to occur if no interaction took place between outputs from Test and Conditioning cortical sites. To this end, we linearly summed all possible combinations of single T-only traces (n=100) with single C-only traces (n=100) to generate a population of 10,000 traces. It should also be noted that since we ensured

that the C_{stim} was subthreshold, any resulting MEPs are largely driven by T-only responses. Next, we randomly drew 100 traces from the population of predicted traces and averaged them to create an average predicted MEP. For each of the average predicted MEPs, we found the peak voltage by taking the maximum value between 8ms and 23ms after the T_{stim} and subtracting the voltage value at peak onset. Peak onset was found by performing a backward march that started at 10% of the peak maximum voltage value. The voltage value of each data point was compared to the one of the previous point, moving back toward the stimulus onset. If the difference between the two points was smaller than 4% of the value of the first point, then that first point was considered as peak onset. Peak amplitude was calculated by subtracting the voltage value at onset from the maximal value. This process was repeated 10,000 times to create a population of predicted amplitudes based on T-only and C-only traces (Quessy, Côté, Hamadjida, Deffeyes, & Dancause, 2016).

The amplitudes of the MEP obtained with paired stimulation conditions were compared to the population of predicted amplitudes. For each of the 7 ISIs, the single trials (n=100) were averaged and the MEP peak amplitude was calculated as described above. The conditioned MEP peak amplitude was compared to the population of predicted amplitudes to establish the direction of modulation (facilitation, inhibition, or no modulation) and the normalized strength of modulation (Z-score) using the following formula:

$$Z - score = \frac{\text{Amplitude with ISI(n)} - \text{mean amplitude of the predicted population}}{\text{SD of the mean amplitude of the predicted population}}$$

Where n is the value of the ISI (e.g. ISI0). A negative Z-score indicates a decrease of the MEP amplitude by the C_{stim} in comparison to the predictor, which we refer to as an 'inhibition'. A

positive Z-score indicates an increase of the MEP amplitudes by the C_{stim} in comparison to the predictor, which refer to as a 'facilitation'. Modulation was considered significant when the Z-score was ≥1.96 (facilitation) or ≤-1.96 (inhibition), and non-significant when the Z-score was >-1.96 and < 1.96.

For each type of protocol (i.e. cCFA-CFA_{lesion}; cRFA-CFA_{lesion} and cRFA-$RFA_{ipsilesional}$), we calculated the proportion of MEPs significantly modulated by the conditioning stimulus (i.e. incidence of significant effects) and the strength of the modulations (average Z-score). In addition, to provide a global measure that reflects the potential impact of CFA and RFA on motor outputs of the opposite hemisphere, we combined the incidence and magnitude values of modulatory effects into a single *Impact score*, calculated for facilitatory or inhibitory effects separately with each ISI separately:

$$Impact\ score\ with\ ISI(m) = \sum_{i=1}^{n} \frac{(\text{incidence of significant modulation with ISI} \times \text{magnitude of modulation of MEPi})}{n}$$

where m stands for one of seven interstimulus intervals, n is the number of significant effects with said ISI (S. L. Côté, Elgbeili, Quessy, & Dancause, 2020; Zaaimi, Edgley, Soteropoulos, & Baker, 2012). For global comparisons between protocol types as well as lesioned and naïve animals impact scores were pooled together.

Statistical analysis

We used paired T-test to compare the baseline behavioral performance of animals with their performance on the final testing day. Then, the output properties of ipsilesional CFA and RFA using the MEPs with the T-only condition were examined. To compare stimulation intensity,

amplitudes of evoked EMG responses, and their onset latencies we used one, two, and three-way ANOVA analysis, followed by Bonferroni corrected post-hoc t-tests when appropriate if the main effect of ANOVA was significant. This was only necessary when we compared three muscles between each other, and the resulting α for post hoc analysis was divided by 3, meaning that the p-value was considered significant if it was ≤ 0.0167. F-test for variance was used to compare the variance of onset latencies of MEPs, resulting from T_{stim} in CFA and RFA, in lesioned and naïve rats.

Second, we examined the modulatory effect of conditioning stimulation. Magnitudes and impact factor comparisons were done separately for facilitatory and inhibitory effects. We were interested in seeing if the magnitude of effects with each ISI differed between lesioned and naïve rats. To this end, we ran a series of Student's T-tests on magnitudes of facilitation and inhibition between the different ISIs. When we were examining the overall magnitude between three protocol types in lesioned animals we used one-way ANOVA, followed by Bonferroni corrected pairwise post hoc comparisons (α = 0.0167), as described previously (Touvykine et al., 2020). Comparison between lesioned and naïve animals was conducted using Student's T-tests between rats with stroke and intact animals. This statistical analysis was repeated to compare the global impact scores between the three protocol types in lesioned versus naïve rats.

Third, we compared incidences of significant facilitation, significant inhibition, and non-significant modulation between three protocol types in stroke rats. This analysis has been used in our previous publication in naïve rats (Touvykine et al., 2020). Incidences for all ISIs were combined by protocol type (cCFA-CFA_{lesion}, cRFA-CFA_{lesion}, and cRFA-$RFA_{ipsilesional}$) and

compared in pairs using Chi-squared test ($\alpha = 0.0167$), followed by a *post hoc* two-proportion *Z* test ($\alpha = 0.05$) (Eisner-Janowicz et al., 2008; Touvykine et al., 2020).

Finally, Chi-squared test was also used to compare incidences of effects between stroke and naive rats. Incidences from all ISIs were combined by protocol type and the frequency of effects was compared for each protocol type. If incidences between stroke and naive rats were significantly different ($P \leq 0.05$), the Chi-squared test was followed by *post hoc* two-proportion *Z* tests ($\alpha = 0.05$). Finally, we wanted to quantify the differences in modulatory profiles with each interstimulus interval. To this end, the Chi-squared test ($\alpha = 0.05$) was used to conduct pair-wise comparisons between stroke and naive rats at each ISI, followed by *post hoc* two-proportion *Z* tests ($\alpha = 0.05$) when appropriate. Unless otherwise specified, results are expressed as mean ± standard error (SE). All statistical analyses were performed using Matlab (Version R2014a).

Histology

On completion of the electrophysiological data collection, animals were killed with a lethal dose of sodium pentobarbital and transcardially perfused. The brain was fixed, cryoprotected, and cut coronally (40 μm thickness) (Dancause et al., 2006). One out of 6 sections was Nissl stained and used to determine the lesion size. Using StereoInvestigator (MicroBrightField, VT) the volume of ipsi and contralesional hemispheres was obtained from the rostral to the caudal extent of the lesion in each animal. Lesion volume was defined as the difference between volumes of contra and ipsilesional hemispheres.

Results

Unilateral ischemic stroke was induced in the CFA of 10 animals. Animals were left to recover for 5 weeks, with behavioral testing on Montoya staircase conducted twice in the first week and then weekly. After the last behavioral session 5 weeks after stroke induction, a terminal paired pulse stimulation experiment was conducted. Animals were perfused at the end of the electrophysiological experiment, their brains were extracted, processed and sliced up on the cryostat, and Nissl stained. The brains were reconstructed using brightfield microscopy and lesion volume was obtained.

Impact of lesion on behavioral performance and quantification of lesion volume

All animals showed decreased performance on the Montoya staircase task, with an average (± SE) decrease of 35.0% ± 4.7 on the fourth day post stroke. While by the end of 5 weeks there was some recovery, it was however incomplete, being still on average 21.4% ± 6.2 smaller than the baseline performance ($T_9 = 3.65$, $p = 0.0053$). Visual inspection of the histological sections confirmed that the ischemic injury destroyed all cortical layers of the sensorimotor cortex (Figure 1A). Similar to our previous publication, lesion induction resulted in a continuum of lesion sizes with the range of lesion volumes from 3.06mm^3 to 22.03mm^3 (mean ± standard deviation: 11.09mm^3 ± 6.55) (Touvykine et al., 2016). We calculated the average lesion volume per-protocol type, they appeared comparable (mean ± SE. cCFA-CFA_{lesion}: 11.96mm^3 ± 0.98; cRFA-CFA_{lesion}: 9.45mm^3 ± 1.44; cRFA-$RFA_{ipsilesional}$: 11.83mm^3 ± 1.37), which we further

confirmed with a one-way ANOVA ($F_{2,60} = 1.16$, $p = 0.32$). Therefore, we analysed 10 rats included in the study as a single lesioned group (Figure 1B).

Overall, the behavioral analysis and histology confirm that our lesions destroyed part of the CFA and resulted in motor deficits in the paretic limb.

Characterization of output properties of ipsilesional CFA and RFA after stroke

When testing the modulatory effects from the contralesional CFA on the motor output of ipsilesional CFA (cCFA-CFA_{lesion} protocols), we obtained 56 significant MEPs (> 1 SD above baseline; see methods) (26 in WE, 9 in WF and 21 in EF) with T-only stimulation. For protocols testing modulatory effects from contralesional RFA on motor outputs of ipsilesional CFA (cRFA-CFA_{lesion} protocols), we found 32 significant MEPs (16 in WE, 3 in WF and 13 in EF) with T-only stimulation. Finally, in protocols that tested the modulatory effects from contralesional RFA on motor outputs of its ipsilesional counterpart (cRFA-$RFA_{ipsilesional}$ protocols) we obtained 37 significant MEPs (16 in WE, 9 in WF and 12 in EF) with T-only stimulation. Our first aim was to characterize the output properties of responses to T_{stim} in the ipsilesional CFA and RFA in the paretic arm and compared these properties to naïve animals (Figure 2). Next, we proceeded to quantify the conditioning effects of C_{stim} in the contralesional forelimb motor areas on the EMG responses evoked out of ipsilesional motor cortex, and compare the conditioning effects to those found in age and sex matched, naïve rats (Touvykine et al., 2020).

We have previously studied the output properties of CFA and RFA in naïve rats (Touvykine et al., 2020). We wanted to see how these outputs changed following recovery from ischemic stroke. In total, 88 MEPs were obtained with T-only stimulation in the ipsilesional CFA

(cCFA-CFA_{lesion} protocols: 56 MEPs; cRFA-CFA_{lesion}: 32 MEPs), and 37 MEPs were obtained from T_{stim} in ipsilesional RFA (cRFA-$RFA_{ipsilesional}$ protocols: 37 MEPs) in lesioned animals. First, we compared the stimulation intensities necessary to evoke significant MEPs (>1 SD of baseline) between CFA and RFA in lesioned and naive animals (Figure 2A). T_{stim} intensities for ipsilesional CFA (mean ± SE: 226.3μA ± 11.0) and naïve CFA (244.3μA ± 12.5) are quite similar, but smaller than ipsilesional (292.1μA ± 7.6) or naïve RFA (287.1μA ± 9.7), which appear comparable between themselves (Figure 2A). This is confirmed by two-way ANOVA, which found no significant effect of lesion (lesioned compared to naïve: $F_{1,105} = 0.15$, $p = 0.7$), whereas there was a significant difference between motor areas (stimulation intensity to evoke MEP was lower in the CFA compared to RFA: $F_{1,104} = 12.9$, $p = 0.0005$), and no significant interaction between the two factors ("lesioned or not" and "motor region": $F_{1,104} = 0.86$, $p =$ 03569).

Next, we checked whether the amplitudes of MEPs were dependent on which motor region T_{stim} was delivered in and whether the animal had a stroke or not. Similar to stimulation intensities, MEP amplitudes appear comparable when evoked from the same motor area whether it was CFA (mean ± SE. ipsilesional: 34.8μV ± 3.8; naïve: 38.2μV ± 5.1) or RFA (ipsilesional: 15.9μV ± 3.0; naïve: 13.6μV ± 4.2), regardless whether the animals were lesioned or naïve (Figure 2B). Statistical analysis confirmed the motor area in which the T_{stim} was delivered significantly affected the MEP amplitudes (responses evoked from CFA were greater than responses from RFA: $F_{1,264} = 14.62$, $p = 0.0002$). However, there were no effect of lesion ($F_{1,264} =$ 0.01, $p = 0.9212$) and no significant interaction between two factors ($F_{1,264} = 0.25$, $p = 0.6204$). In contrast to naïve rats, we found differences in MEP amplitudes between muscles when we

examined responses from ipsilesional CFA ($F_{2,85}$ = 14.99, p = 2.65e-6) and RFA ($F_{2,34}$ = 4.54, p = 0.0178) using one-way ANOVAs (Figure 3A, B). Evoked from the CFA_{lesion} MEP amplitudes of elbow flexor (mean ± SE: 57.07μV ± 7.22) were significantly greater than those evoked in either wrist extensor (23.15μV ± 3.42, Post hoc: p < 0.0001) or wrist flexor (12.66μV ± 3.91; Post hoc: p < 0.0001). When T_{stim} was delivered in the $RFA_{ipsilesional}$, amplitudes of MEPs in elbow flexor (27.41μV ± 7.27) were greater than in wrist flexor (6.30μV ± 2.18; Post hoc: p = 0.0076), but not significantly different from wrist extensor (12.65μV ± 3.14; Post hoc: p = 0.028). Amplitudes of responses in distal muscles were not different from each other whether they were evoked from RFA_{lesion} (Post hoc: p = 0.30) or $RFA_{ipsilesional}$ (Post hoc: p = 0.37). These results are in contrast with naïve animals, where MEP amplitudes did not differ between muscles regardless of which motor area T_{stim} was delivered in (CFA: $F_{2,106}$ = 0.45, p = 0.64; RFA: $F_{2,31}$ = 1.16, p = 0.3275. Figure 3C, D). Furthermore, we used a three-way ANOVA to examine possible interactions between the area of stimulation (CFA compared to RFA), the effect of the stroke (lesioned versus naïve), and muscles (WE, WF, EF). The interactions between the area of stimulation and the effect of lesion ($F_{2,258}$ = 0.65, p = 0.4201), as well as between the area of stimulation and muscles ($F_{2,258}$ = 1.33, p = 0.2656) were not significant. The only significant interaction occurred between muscles and the effect of the lesion ($F_{2,258}$ = 3.49, p = 0.0321), supporting our finding that there is a difference in MEP amplitudes between muscles that is specific to lesioned animals.

We also examined the onset latencies of MEPs from the CFA and the RFA in lesioned animals and compared them to onset latencies obtained in naïve animals. Onset latencies of responses evoked from the CFA were comparable between lesioned (mean ± SE: 11.1ms±0.14) and naïve animals (11.0ms±0.2. Figure 2C). In contrast, onset latencies of MEPs from

ipsilesional RFA (13.4ms±0.4) were greater than those of naïve RFA (11.6ms±0.3. Figure 2C inset) (Touvykine et al., 2020). The difference in MEP latencies evoked from ipsilesional and naïve RFA is further highlighted by their respective medians (13.9ms compared to 11.0ms), and range ($RFA_{ipsilesional}$: range = 10.6ms; $RFA_{naïve}$: range = 6.7ms). In comparison, median values for MEP onsets are comparable between ipsilesional (11.0ms) and naïve (11.2ms) CFA, and the range difference is smaller (ipsilesional: 7.4ms; naïve: 5.9). While long latency responses (>13ms) were more frequent from ipsilesional (10.2%) compared to naïve (2.7%) CFA, the difference was particularly striking for $RFA_{ipsilesional}$ (59.5%) when compared to $RFA_{naïve}$ (14.7%). We did not observe a substantial difference between ipsilesional and naïve CFA (12.5% to 17.3% respectively), nor ipsilesional and naïve RFA (10.8% to 8.8% respectively) for short latency (<10ms) responses. These observations are validated by a two-way ANOVA, which determined that both the motor area (CFA compared to RFA) and lesion (lesioned compared to naïve) had a significant effect on the difference in onset latencies ($F_{1,264} = 45.53$, $p > 0.0001$; $F_{1,264} = 19.28$, $p > 0.0001$). Furthermore, the interaction between motor area and lesion was significant ($F_{1,264} = 13.75$, $p = 0.0003$). Post hoc analysis found that onset latencies of responses evoked from $RFA_{ipsilesional}$ were greater than MEP latencies from ipsilesional CFA_{lesion} ($p > 0.0001$), and $RFA_{naïve}$ ($p > 0.0001$). Overall, these findings highlight that the differences in onset latencies are specific to the cortical motor area (RFA) in lesioned animals.

Next, we verified whether there were differences in MEP onset latencies between different muscles for each motor area. In contrast with naïve animals, there was a significant difference in onset latencies between the three forelimb muscles for MEPs evoked from the ipsilesional CFA ($F_{2,85} = 12.95$, $p = 1.23e\text{-}5$, Figure 4A). Onset latencies of responses in wrist

extensors (mean ± SE: 11.8ms ± 0.19) were longer compared to wrist flexors (mean ± SE: 10.3ms ± 0.35, p = 0.0007), and elbow flexors (mean ± SE: 10.6ms ± 0.19, p = 0.0001), although the flexors did not differ between each other (p = 1.0). No differences in latencies were found between muscles for MEPs produced by T_{stim} in the ipsilesional RFA ($F_{2,34} = 3.09$, p = 0.0584, Figure 4B). As discussed in our previous publication (Touvykine et al., 2020), we did not find any differences in latencies between muscles in naïve animals, whether stimulation was delivered in the CFA, or RFA (Figure 4C-D).

Lastly, we examined variability in onset latencies of responses from both motor areas, in stroke and intact rats (Figure 5). A quick visual examination revealed that responses from ipsilesional RFA were much more variable compared to responses from other motor areas, both between and within individual rats. In fact, Interquartile Range (IQR: 75^{th} percentile – 25^{th} percentile) for CFA_{lesion}, naïve CFA, and naïve RFA (Figure 5A, C-D) are relatively comparable (1.5ms, 1.8ms, and 1.8ms respectively). In contrast, for $RFA_{ipsilesional}$ IQR is more than double (3.9ms) what it is for other areas (Figure 5B). Comparison of variability between lesioned and naïve rats revealed that onset latency variance was comparable for responses evoked from ipsilesional (variance = 1.8) and naïve CFA (variance = 1.4. $F_{87,108} = 1.25$, p = 0.2756). However, responses evoked from ipsilesional RFA (variance = 6.8) were significantly more variable compared to those evoked from naïve RFA (variance = 2.4. $F_{36,38} = 2.81$, p = 0.0035).

In summary, when combining data from all 3 muscles, we found that ischemic stroke did not affect stimulation intensities required to evoke motor outputs and the amplitude of MEPs from the CFA or the RFA. In both controls and animals with stroke, the delivery of smaller stimulation currents in the CFA evoked larger MEPs, whereas in the RFA higher stimulation

intensities evoked smaller motor responses. However, outputs from $RFA_{ipsilesional}$ were slower and more variable after stroke. Stroke also seemed to affect the pattern of outputs to the different muscles. While MEP amplitude and latencies were identical across target muscles in controls, there were significant differences in MEP amplitudes between muscles, for both ipsilesional CFA and RFA in animals that had a stroke.

Modulatory effects with each ISI tested

To explore the modulatory effects of contralesional cortical motor areas on the ipsilesional hemisphere, we compared a population of predicted responses evoked in T-only and C-only trials (see materials and methods) with conditioned MEPs obtained with paired-pulse stimulation conditions for each protocol. Data were separated into one of three types of interaction protocol: conditioning of ipsilesional CFA output by stimulation of contralesional CFA (cCFA-CFA_{lesion}, n = 28); conditioning of ipsilesional CFA by contralesional RFA (cRFA-CFA_{lesion}, n = 16), and finally conditioning of ipsilesional RFA by its contralesional homologue (cRFA-$RFA_{ipsilesional}$, n = 19). We compared the modulation between protocol types in lesioned animals, and to naïve animals (Touvykine et al., 2020).

First, we wanted to know the incidence as well as strength of modulatory effects in lesioned animals at each ISI and how they compared to results in naïve rats. We calculated the proportion of significant facilitatory (Z-score $\geq$ 1.96) and inhibitory (Z-score $\leq$ -1.96) effects caused by conditioning stimulation. Modulation of EMG responses produced by T_{stim} in the ipsilesional CFA by C_{stim} in the contralesional CFA (cCFA-CFA_{lesion} protocols) resulted in 59 (15.0%) significant facilitatory and 35 (8.9%) significantly inhibitory effects out of 392 MEPs

(56 significant responses with T-only, conditioned with 7 different ISIs). The timing of the two stimuli (i.e. ISI) clearly had an effect on the modulation pattern observed in all three protocol types, in both lesioned and naïve animals (Figure 6). In cCFA-CFA$_{lesion}$ protocols, the short duration ISIs (0ms and 2.5ms) as well as long duration ISIs (15ms, 20ms and 35ms) induced more facilitatory than inhibitory effects (Figure 6A top). In contrast, ISIs of intermediate durations (5ms and 10ms) induced more inhibitory effects. We had previously found a similar pattern of effects in naïve rats (Touvykine et al., 2020). Interestingly, the incidence of significant effects, both facilitation and inhibition, was greatly decreased after stroke, with almost all ISIs tested. The decrease of facilitation was significant with ISI0 ($\chi^2 = 6.89$, $p = 0.032$; Post hoc: $p = 0.020$) and decrease of inhibition was significant with ISI15 ($\chi^2 = 8.44$, $p = 0.015$; Post hoc: $p = 0.004$) and ISI35 ($\chi^2 = 8.12$, $p = 0.017$; Post hoc: $p = 0.011$). In lesioned animals, we found more non-significant modulations ($-1.96 >$ Z-score < 1.96) than in controls with all the ISIs we tested (Figure 6B top). These differences were significant with ISI0 ($\chi^2 = 6.89$, $p = 0.032$; Post hoc: $p = 0.0088$), ISI2.5 ($\chi^2 = 7.36$, $p = 0.025$; Post hoc: $p = 0.0073$), ISI5 ($\chi^2 = 8.71$, $p = 0.0128$; Post hoc: $p = 0.0055$), and ISI35 ($\chi^2 = 8.12$, $p = 0.017$; Post hoc: $p = 0.031$). There was an overall tendency to have stronger facilitation with short and long duration ISIs and stronger inhibition with mid duration ISIs for the cCFA-CFA$_{lesion}$ protocols. Next, we examine the strength of modulation, using all MEPs regardless of whether they were significantly modulated or not. Facilitation (Z-score>0) and inhibition (Z-score<0) were examined separately (see methods). Facilitation and inhibition tended to be less powerful in lesioned animals compared to naïve rats, with almost all ISIs (Figure 6C top). These differences were significant for facilitation with ISI2.5 ($T_{62} = 2.16$, $p = 0.035$) and ISI35 ($T_{79} = 2.78$, $p = 0.0068$), and inhibition with ISI0 ($T_{36} =$

-2.29, p = 0.028), ISI5 (T_{88} = -2.86, p = 0.0051), ISI10 (T_{87} = -3.46, p = 0.00084), ISI15 (T_{57} = -2.52, p = 0.014), and ISI35 (T_{33} = -2.44, p = 0.020). In summary, stroke resulted in a reduction of both the incidence and strength of facilitation and inhibition from cCFA on the perilesional tissue in its homolog CFA_{lesion}.

When the motor outputs of ipsilesional CFA were conditioned by stimulation in cRFA (cRFA-CFA_{lesion} protocols), we found 49 (21.9%) significant facilitatory and 18 (8.0%) significant inhibitory effects out of 224 MEPs (32 significant responses with T-only, conditioned with 7 different ISIs). Furthermore, a higher incidence of facilitation was found with short and long duration ISIs and a higher incidence of inhibition with mid duration ISIs (Figure 6A middle). In addition, significant effects tended to be fewer after stroke, but this seemed to mostly affect facilitation (Figure 6B middle). In fact, only decreases of facilitatory effects were significant. They were observed with ISI0 (χ^2 = 10.00, p = 0.0067; Post hoc: p = 0.0025), ISI2.5 (χ^2 = 24.12, p < 0.0001; Post hoc: p < 0.0001), and ISI20 (χ^2 = 8.51, p = 0.0142; Post hoc: p = 0.0036). Once again, there was a general tendency to have more non-significant modulation after stroke with almost all ISI tested, with the exception of ISI10. This increase was significant with ISI0 (Post hoc: p = 0.0062), ISI2.5 (Post hoc: p < 0.0001), ISI20 (Post hoc: p = 0.0048), and ISI35 (χ^2 = 6.013, p = 0.049; Post hoc: p = 0.022). It should be noted that three (ISI0, ISI2.5 and ISI20) out of these four ISIs were the same ones with which we found a significantly smaller incidence of facilitatory effects. Finally, when looking at the strength of effects from cRFA on the perilesional tissue, we found that facilitatory effects with several ISIs (ISI5, ISI10, ISI15 and ISI20) tended to be stronger after stroke, but these changes were only significant with ISI15 (T_{37} = -2.21, p = 0.033). It thus appears that stroke affected the modulatory effects from cCFA and

cRFA on the perilesional cortex differently. It resulted in the loss of both facilitatory and inhibitory effects from cCFA, but it only impacted facilitatory effects from cRFA. Moreover, while the incidence of facilitation was decreased, they tended to be more powerful after stroke.

When C_{stim} delivered in cRFA conditioned EMG responses evoked with T_{stim} in the ipsilesional RFA (cRFA-$RFA_{ipsilesional}$ protocols), we obtained 73 (27.41%) significantly facilitatory effects and 43 (16.60%) significantly inhibitory effects out of the total of 259 MEPs (37 significant responses with T-only, conditioned with 7 different ISIs). Once again, the modulation with the different ISIs followed a similar pattern, with a higher incidence of facilitation with short and long duration ISIs and a higher incidence of inhibition with mid duration ISIs (Figure 6A bottom). In comparison to control animals, animals that had a stroke seemed to have less facilitatory effects with short ISIs and more inhibitory effects with short to intermediate ISIs. However, significant differences were restricted to ISI2.5 ($\chi^2 = 12.68$, $p = 0.0018$). The incidence of facilitatory effects in lesioned animals was significantly smaller (Post hoc: $p = 0.0024$) and the incidence of inhibition was significantly greater (Post hoc: $p = 0.014$) than in intact animals. The incidences of non-significant modulation in the cRFA-$RFA_{ipsilesional}$ protocols also seemed to be much less affected than for the cCFA-iCFA or the cRFA-iCFA protocols (Figure 6B bottom). There were no significant changes for any of the tested ISIs. In fact, the incidence of non-significant effects tended to be reduced with intermediate and long ISIs (ISI5-ISI35). For the strength of modulatory effects, there was a tendency to have more powerful facilitatory effects with longer ISIs (ISI10-ISI35), although these changes were not significant (Figure 6C bottom). Thus, it appears that stroke affected the modulatory effects of cRFA on its

homotopic counterpart quite differently. Perhaps most striking was the preservation of the incidence of significant effects for all tested ISIs.

Comparison of the modulatory effects with all ISIs combined.

To get a better idea of how the incidence and strength of modulation for the 3 types of protocols compared overall, we pooled effects across all ISIs. We first compared the incidence of facilitation, inhibition and non-significant effects on the perilesional cortex when the conditioning stimulation was delivered in the cCFA or in cRFA (i.e. cCFA-CFA_{lesion} versus cRFA-CFA_{lesion} protocols). Although there were slight differences between protocols, they were not significant ($\chi^2 = 4.60$, $p = 0.301$. Figure 7A and B). Second, we compared the incidence of effects when the conditioning stimulation was delivered in cCFA or in cRFA on the outputs of their homolog in the ipsilesional hemisphere (i.e. cCFA-CFA_{lesion} versus cRFA-$RFA_{ipsilesional}$) and found there were significant differences ($\chi^2 = 28.80$, $p < 0.001$). There was significantly less facilitation and inhibition evoked in cCFA-CFA_{lesion} (Post hoc: $p = 0.00013$ and $p = 0.0032$, respectively) in comparison to cRFA-$RFA_{ipsilesional}$ protocols. This was accompanied by a significantly greater proportion of non-significant effects in cCFA-CFA_{lesion} protocols (Post hoc: $p < 0.0001$). Finally, we compared the incidence of effects of cRFA conditioning on the outputs of the perilesional cortex and its homolog (i.e. cRFA-CFA_{lesion} versus cRFA-$RFA_{ipsilesional}$). Once again, the incidence of the various modulation on outputs was significantly different ($\chi^2 = 12.28$, $p = 0.0066$). While the incidence of facilitation was similar, there was significantly less inhibition evoked in cRFA-CFA_{lesion} than cRFA-$RFA_{ipsilesional}$ protocols (Post hoc: $p = 0.0047$)

and this was accompanied by a significantly greater proportion of non-significant effects in cRFA-CFA_{lesion} protocols (Post hoc: $p = 0.0014$).

We performed a similar comparison for the magnitude of facilitatory and inhibitory effects across the types of protocols (Figure 7C). A first ANOVA confirmed that the magnitude of facilitation was different across protocols ($F_{436} = 20.91$, $p < 0.0001$). Facilitatory effects from cCFA on its homolog CFA_{lesion} were weaker than ones from cRFA (Post hoc: $p < 0.0001$) or the ones of cRFA on $RFA_{ipsilesional}$ (Post hoc: $p < 0.0001$). A second ANOVA also confirmed that the magnitude of inhibition was different across protocols ($F_{433} = 8.49$; $p = 0.0002$). Inhibitory effects from cCFA and cRFA on the outputs of CFA_{lesion} were weaker than the ones from cRFA on its homolog (post-hoc: $p = 0.00076$ and $p = 0.00016$, respectively). This pattern was also different from what we found in control animals, in which the strongest facilitatory effects were from RFA on the outputs of CFA and the strongest inhibitory effects were from CFA on the outputs of its homolog.

In summary, facilitatory effects from cCFA on the perilesional cortex in CFA_{lesion} were generally more rarely evoked and weaker than the other interactions we tested. Facilitatory effects from cRFA on CFA_{lesion} were more powerful and from cRFA on $RFA_{ipsilesional}$ both more frequent and more powerful. In contrast, inhibitory effects from cCFA and cRFA on the perilesional cortex were similar but were both less frequent and less powerful than the ones from cRFA on its homolog, $RFA_{ipsilesional}$.

We then compared incidence of modulatory effects and their magnitude between lesioned and naïve animals. The incidence of various modulatory effects from cCFA on the perilesional cortex was affected by the stroke (cCFA-CFA_{lesion} protocols; $\chi^2 = 33.94$, $p < 0.0001$) there was a

decrease of both facilitation ($p = 0.00076$) and inhibition ($p < 0.0001$), and an increase of non-significant effects ($p < 0.0001$. Figure 7A and B). Moreover, both the magnitude of facilitatory and inhibitory effects were decreased after stroke ($T_{414} = 2.40$, $p = 0.017$; and $T_{394} = -5.71$, $p < 0.0001$, respectively. Figure 7C). The incidence of effects from cRFA on the perilesional cortex was also affected by stroke (cRFA-CFA_{lesion} protocols; $\chi^2 = 35.38$, $p < 0.0001$), and there was a decrease of facilitatory effects (Post hoc: $p < 0.0001$) and an increase of non-significant effects ($p < 0.0001$), but no effects on the incidence of inhibitory effects. In contrast, the magnitude of facilitatory effect was not affected ($T_{351} = -0.74$, $p = 0.46$), but the inhibitory effects were weaker after stroke ($T_{212} = -3.84$, $p = 0.00016$). Finally, the incidence of effects from cRFA on its homolog was not affected by stroke (cRFA-$RFA_{ipsilesional}$ protocols; $\chi^2 = 4.00$, $p = 0.1353$). Although there was no effect of stroke on the magnitude of inhibition ($T_{228} = 1.01$, $p = 0.31$), facilitation was significantly more powerful after stroke ($T_{265} = -2.29$, $p = 0.023$).

In summary, it seems interactions between cCFA and the perilesional cortex in its homolog, CFA_{lesion}, were the most disrupted after stroke. Both facilitatory and inhibitory effects were evoked less frequently and they were less powerful than in controls. Although to a lesser extent, interactions between cRFA and the perilesional cortex in CFA_{lesion} also showed signs of being disrupted. Namely, there was a reduction of incidence of facilitation and magnitude of inhibition. Finally, interactions between cRFA and its homolog, $RFA_{ipsilesional}$, seemed much less affected, and facilitatory effects even became more powerful.

Comparison of global impact of cCFA and cRFA on ipsilesional cortical motor outputs

In a last series of analyses, we wanted to provide a "global" measure that reflects the potential impact from cCFA and cRFA on motor outputs of the ipsilesional hemisphere. To do so, we combined the incidence of significant modulations and their magnitude into a single *impact score* (Figure 8). As expected, the greatest impact, for both facilitation and inhibition, was from cRFA on its homolog, $RFA_{ipsilesional}$. This is in contrast with control animals, in which the most impactful facilitation was from cRFA on the outputs of CFA_{naive} and the most impactful inhibition was from cCFA on its homolog (Touvykine et al., 2020). The impact of facilitatory effects across the 3 types of protocols was significantly different ($F_{176} = 17.03$, $p < 0.0001$. Figure 8B). Facilitation from cRFA on $RFA_{ipsilesional}$ was more impactful than both facilitation from cCFA ($p < 0.0001$) or cRFA ($p = 0.002$) on the CFA_{lesion}. The impact of inhibitory effects was also significantly different across protocols ($F_{93} = 5.95$, $p = 0.0037$). Inhibition from cRFA on $RFA_{ipsilesional}$ was more impactful than inhibition from cCFA on the perilesional cortex ($p = 0.0015$).

When comparing to naïve animals, both facilitation and inhibition from cCFA on the perilesional cortex became significantly less impactful after stroke (facilitation: $T_{151} = -2.89$, $p = 0.004$; inhibition: $T_{118} = -3.41$, $p = 0.0009$). While facilitatory effects from cRFA on the perilesional cortex became less impactful ($T_{204} = -2.86$, $p = 0.0046$), conditioning stimulation in cRFA had significantly greater impact on the outputs of $RFA_{ipsilesional}$ after stroke ($T_{142} = 3.70$, $p = 0.00031$).

In summary, the impact of modulations from both cCFA and cRFA on the outputs of the CFA_{lesion} was decreased after stroke. It appears that cCFA was more affected, with a decrease of both

facilitation and inhibition becoming less impactful. In sharp contrast, facilitatory effects from cRFA on its homolog became more impactful after stroke.

Discussion

We induced ischemic stroke in CFA, the putative M1 of rats. Following a recovery period of five weeks, we characterized the properties of outputs from ipsilesional CFA and RFA to forelimb muscles. We then examined how the forelimb motor regions of the contralesional hemisphere, cCFA and cRFA, modulated these outputs from the ipsilesional hemisphere. We found that onset latencies of MEPs from $RFA_{ipsilesional}$ were more variable and longer after stroke. Furthermore, while both MEPs latencies and amplitudes were similar across muscles in controls, there were significant differences after stroke. Namely, stimulation in CFA_{lesion} and $RFA_{ipsilesional}$ evoked larger responses in elbow flexor than in other muscles and MEPs in wrist extensors resulting from stimulation in CFA_{lesion} had longer latencies than MEPs in wrist or elbow flexors. Conditioning of motor outputs of perilesional CFA resulted in decreased significant modulation compared to naïve animals, especially pronounced when CFA_{lesion} was conditioned by its contralesional homologue. The decrease in the incidence of significantly facilitatory effects produced by cRFA conditioning of the perilesional CFA, was accompanied by apparent increases in the power of modulatory effects. Conditioning of $RFA_{ipsilesional}$ produced rates of significant facilitation and inhibition comparable to healthy rats, however we did find an increase in the power of facilitation. Finally, with a new way of calculating impact factor we conducted comparisons, which included both the incidence of significant effects and their magnitudes, to find the impact of facilitation and inhibition for cCFA-CFA_{lesion} protocols was decreased. Furthermore, the impact of facilitation with cRFA-CFA_{lesion} protocols was also decreased. The only instance of strengthening of the impact of modulation was when cRFA conditioned the

output of $RFA_{ipsilesional}$ producing greater facilitation. These results support the idea that significant complex reorganization takes place following unilateral stroke, both in terms of output properties of spared ipsilesional motor cortex, and the interactions that take place between the two hemispheres.

Changes in output properties of ipsilesional motor cortex.

Surprisingly, direct comparison of stimulation intensity necessary to evoke a significant MEP, as well as the magnitudes of resulting MEPs failed to find a difference between ipsilesional motor areas and their counterparts in healthy rats. Furthermore, onset latencies of evoked responses were not different between ipsilesional and naïve CFAs. This was surprising, because stroke leads to hemiparesis and general muscle weakness, and TMS stimulation of perilesional motor cortex in stroke survivors have found both smaller MEP amplitudes and longer onset latencies compared to healthy controls (Traversa, Cicinelli, Bassi, Rossini, & Bernardi, 1997b; Twitchell, 1951). In contrast to the perilesional CFA, onset latencies of MEPs from ipsilesional RFA had increased variance, range, as well as being on average longer compared to both CFA_{lesion} as well as responses in naïve animals. Stimulation intensities necessary to evoke significant MEPs in the $RFA_{ipsilesional}$ were greater, and the amplitudes of said MEPs were smaller compared to perilesional CFA and comparable to those of RFA in healthy animals. These results also contrast findings in human stroke patients, where TMS stimulation of ipsilesional PMd produced MEPs with greater amplitude and shorter onset latencies compared to stimulation of ipsilesional M1 (Fridman et al., 2004). These differences could be due to the differences between the motor systems of the rat and primates.

We also found differences in output properties when we examined output properties by muscle. In stroke animals, MEP amplitudes for elbow flexor were significantly greater compared to the wrist muscles (flexor and extensor), a difference which was absent in naïve animals. We know that stroke patients rely more on the trunk and proximal musculature during reaching movements (Cirstea & Levin, 2000; Jones, 2017). Greater amplitude of elbow flexor evoked from the ipsilesional motor cortex might be indicative of the selective strengthening of proximal musculature in an attempt to compensate for the loss of input from the part of the CFA and its descending projections destroyed by stroke. Another difference between muscles that emerged in lesioned animals was greater onset latencies for wrist extensor muscles compared to the two flexors when evoked from perilesional CFA. Following corticospinal tract lesion in non-human primates, rebalancing of the strength of connections between flexors and extensors takes place, with connections to flexors, but not extensors were strengthened. This effect has been identified in both corticorubralspinal as well as corticoreticularspinal networks, however the exact reasons and functional significance of it are not known (Belhaj-Saïf & Cheney, 2000; Zaaimi et al., 2012). The emerged difference in onset latencies between flexor and extensor muscles might be a sign of similar rebalancing of descending projections from the perilesional CFA in the rat.

The reorganization of output properties following unilateral stroke in rats paints a complex picture, with some results being the opposite of what we expected based on human literature, and others having strong parallels in findings in both human and non-human primates.

Reorganization of the modulatory drive of the contralesional hemisphere.

Following stroke in rats, the first and most obvious change in the modulatory drive of the forelimb motor regions in the intact hemisphere is the increase of non-significant modulation when the motor output of CFA_{lesion} is conditioned (by either cCFA or cRFA). Caused by the stroke in the CFA, there are three principal causes that can explain this phenomenon. One, our lesions often destroyed the dorsal part of the corpus callosum, which would result in decreased interhemispheric communication due to decreased number of fibers in the corpus callosum. Two, lesions in the CFA mean that there is a smaller pool of neurons upon which callosal projections from the contralesional motor cortex can act and modulate. Three, damage to all cortical levels of the CFA means there is a decreased number of outgoing projections, specifically corticorubral, corticoreticular, and corticospinal, resulting in a smaller number of potential sites where converging signals from two hemispheres can interact and produce significant modulation. The first and the second causes can account for the decrease of significant modulation that takes place through the corpus callosum. In our previous study, we discussed that based on the literature callosal interactions likely take place with mid duration ISIs of 5ms and 10ms (Seggie & Berry, 1972). Furthermore, we suggest that while the red nucleus and the spinal cord are possible interaction sites for short duration ISIs (0ms and 2.5ms); based on the literature the number of corticorubral projections from the opposite hemisphere is very small, and considering that corticospinal tract in the rat is very lateralized (~5% of CST is ipsilateral), descending signal from motor cortices in two hemispheres is more likely to converge and interact in the reticular formation (Bernays, Heeb, Cuenod, & Streit, 1988; Brösamle & Schwab, 1997, 2000; Naus, Flumerfelt, & Hrycyshyn, 1985). The corticoreticulospinal pathway appears less lateralized, and the reticular formation receives bihemispheric corticofugal projections from motor cortices of

both hemispheres (Shammah-Lagnado, Negrão, Silva, & Ricardo, 1987; Valverde, 1962). While stroke is known to induce neuroplasticity, no significant increase in corticospinal fibers originating from the uninjured hemisphere has been found in the paretic cervical enlargement (Wahl et al., 2017). Similarly, the number of corticorubral projections from the contralesional hemisphere did not increase significantly following spontaneous recovery (Wenk, Thallmair, Kartje, & Schwab, 1999). Therefore, we believe that the decreased incidence of significant modulation with short duration ISIs (0ms and 2.5ms), when cCFA conditions the output of perilesional CFA, is in large part caused by fewer inputs to the ipsilesional reticular formation from remaining CFA, and the resulting decreased likelihood of descending signals interacting to produce significant modulation. The decrease of significant modulation with ISI5 is likely to be due to the disruption of callosal interactions between ipsilesional and contralesional CFAs. We cannot completely discard the possibility that the damage to the dorsal part of the corpus callosum is the main cause, however it seems more likely that there is simply less ipsilesional CFA remaining to be conditioned by its contralesional homologue. It is next to impossible to narrow down the structures of the central nervous system where interaction with long duration ISIs (15ms, 20ms, and 35ms) take place, therefore we are not going to attempt to do that.

When perilesional CFA was conditioned by cRFA, the decrease in significant modulation with short duration ISIs was even more drastic than compared to cCFA-CFA_{lesion} protocols. The underlying reasons are likely to be similar, with decreased descending input from the ipsilesional CFA, and consequently decreased likelihood of cRFA-CFA_{lesion} interactions at the reticular formation contralateral to CFA_{lesion}. In contrast to cCFA-CFA_{lesion} protocols, the incidences of significant modulation were not decreased with mid duration ISIs when cRFA conditioned output

of CFA_{lesion}. There are abundant projections from RFA to the CFA of the opposite hemisphere, therefore it is likely that the majority of modulations with mid duration ISIs take place through callosal interactions (Rouiller, Moret, & Liang, 1993). The fact that we do not see a difference in the incidence of significant modulation between lesioned and naïve rats suggests that either: callosal projections from the cRFA interact with mostly spared perilesional CFA; or there was reorganization that resulted in increased efficacy of the modulatory effect exerted by cRFA through its callosal projections. It seems more likely that strengthening of the modulatory potential of cRFA through its callosal connections to CFA_{lesion} took place. Nonetheless, we cannot exclude the possibility that the majority of callosal fibers from the cRFA project to the lateral part of the CFA, which was spared by stroke. Similar to cCFA-CFA_{lesion} protocols it is hard to speculate about the precise structures that might be involved in decrease of significant modulation with ISI20 and ISI35 for cRFA-iCFA protocols.

In terms of significant effects there was a decrease in incidences of both facilitatory and inhibitory effects when CFA_{lesion} output was modulated by cCFA, and a decrease of significant facilitation when CFA_{lesion} was modulated by cRFA. Specifically, in cCFA-CFA_{lesion} protocols the incidence of facilitation was smaller with ISI0, and the incidence of inhibition was smaller with ISI15 and ISI35 compared to naïve rats. For cRFA-CFA_{lesion}, the incidence of facilitatory effects was much smaller than in naïve rats with ISIs of 0ms, 2.5ms, and 20ms. We found decreased significant modulation with these ISIs which must be the cause of the observed decrease of significant facilitation. Overall, the decrease in significant modulation for cCFA-CFA_{lesion} protocols happened for both facilitatory and inhibitory effects, whereas for cRFA-CFA_{lesion} the

decrease in significant modulation was due only to the decrease of facilitatory effects, while inhibitory effects stayed comparable to intact rats.

The power of both facilitation and inhibition was smaller for cCFA-CFA_{lesion} protocols mirroring the decreases we found with the incidences of significant facilitation and inhibition. The interactions between cCFA and perilesional CFA appear the most disrupted and changed as a result of a stroke in the CFA. For cRFA-CFA_{lesion} protocols, the facilitatory power was comparable between lesioned and naïve animals, whereas the power of inhibition was significantly smaller compared to naïve rats. This is despite the incidences of significant facilitation for cRFA-CFA_{lesion} being smaller and the incidences of significant inhibition being almost the same compared to naïve rats. It is tempting to suggest that the remaining interaction sites between cRFA and iCFA reorganized to exert stronger facilitation to compensate for the disruption caused by stroke in the CFA, and as a consequence of such reorganization the inhibitory effects became less powerful.

In contrast to the perilesional CFA, conditioning of motor output of ipsilesional RFA was comparable to healthy rats in terms of incidences of significant as well as non-significant effects, although facilitatory effects were more powerful in lesioned animals compared to naïve. This could be a part of ongoing reorganization following stroke, similar to increased magnitude of facilitatory effects between cRFA and CFA_{lesion}, where cRFA-$RFA_{ipsilesional}$ interactions also underwent changes, which resulted in stronger facilitatory effects.

The impact scores give a more complete picture of the reorganization of the modulatory drive of the contralesional hemisphere on the output of the ipsilesional motor cortex. The decrease of modulatory impact (both inhibition and facilitation) of cCFA, as well as decreased

impact of facilitation of cRFA on the perilesional CFA is concurrent with the increased facilitatory impact of the contralesional RFA on the output of its ipsilesional homologue. Considering that we have previously found evidence of bilateral reorganization in ipsi and contralesional RFAs (Touvykine et al., 2016), we think the increase in facilitatory impact is the result of the reorganization of interactions between contralesional and ipsilesional RFA, to compensate for the decreased modulatory impact of perilesional CFA. In the absence of sprouting of new projections without behavioral, stimulatory, or drug manipulations (Ishida et al., 2016; Wahl et al., 2017; Wahl et al., 2014), the rebalancing of existing connections is evidence of reorganization in the motor system to compensate for the damage in the CFA. These changes go beyond the area immediately affected by the lesion and appear to initiate reorganization in interactions between structures not directly impacted by stroke.

Our interpretation of the results presented above is that the system is attempting to reorganize across multiple nodes in the motor axis following a stroke in the CFA. Whereas overall output properties of ipsilesional forelimb motor areas were largely unchanged following stroke, there was a more specific reorganization in terms of output to forelimb muscles. The modulatory drive of the contralesional CFA and RFA on perilesional output is greatly disrupted by stroke. Despite the decreased incidence of modulation, the contralesional RFA appears to strengthen the power of its facilitatory modulation presumably to compensate for the loss of interaction between perilesional CFA and itself. Whereas the overall incidence of modulation of output of ipsilesional RFA was not different from naïve rats, the increased power and impact of facilitation in cRFA-$RFA_{ipsilesional}$ protocols is what we believe to be an attempt by the motor system to return to pre-stroke levels of modulation of the output of the lesioned hemisphere. We

decided to check this and compared impact scores between lesioned and naïve animals. It appears that overall facilitatory impact in lesioned rats (1.91 ± 0.18) does reach levels present in healthy animals (1.89 ± 0.09; T_{501} = -0.1285, p = 0.90). In contrast, inhibitory impact in lesioned animals (-0.74 ± 0.04) does not return to healthy levels (-1.02 ± 0.07; T_{232} = 2.9721, p = 0.0033), largely due to the decrease of inhibitory impact between cCFA-CFA_{lesion}, and no concurrent strengthening with the other two protocols. It is important to note that the animals did not recover to pre-stroke levels of behavioral performance as a result of this reorganization.

Among important questions that remain unanswered is how the ipsilesional RFA modulates the output of ipsilesional CFA following spontaneous recovery from unilateral stroke. Previous publications have shown that stimulation protocols, as well as behavioral interventions, promote sprouting of axons from both ipsilesional and contralesional hemispheres, and result in a level of reorganization absent with spontaneous recovery (Ishida et al., 2016; Ishida et al., 2019; Wahl et al., 2017; Wahl et al., 2014). It would therefore be interesting to study how neuroplasticity resulting from such interventions affects output properties, as well modulatory interactions between forelimb cortical areas of the rat, especially if animals can return to pre-stroke levels of functional performance. Lastly, we found some similarities and some differences in terms of changes of the output of properties of ipsilesional motor cortex between rats and non-human primate studies. Our group has published a series of experiments that examined physiological modulation between ipsilateral and contralateral premotor areas and M1 in healthy non-human primates (S. L. Côté et al., 2020; Sandrine L. Côté, Hamadjida, Quessy, & Dancause, 2017; Quessy et al., 2016). Conducting the next series of experiments in monkeys following recovery from unilateral stroke using the same methodology would allow us to make direct

comparisons to rats and further examine and validate it as the animal model that is suitable to study systemic reorganization following stroke and its relevance to humans.

References

Baker, S. N., & Lemon, R. N. (1995). Non-linear summation of responses in averages of rectified EMG. *Journal of neuroscience methods, 59*(2), 175-181.

Belhaj-Saïf, A., & Cheney, P. D. (2000). Plasticity in the distribution of the red nucleus output to forearm muscles after unilateral lesions of the pyramidal tract. *Journal of Neurophysiology, 83*(5), 3147-3153. Retrieved from http://www.ncbi.nlm.nih.gov/pubmed/10805709

Bernays, R. L., Heeb, L., Cuenod, M., & Streit, P. (1988). Afferents to the rat red nucleus studied by means of D-[3H]aspartate, [3H]choline and non-selective tracers. *Neuroscience, 26*(2), 601-619. Retrieved from http://www.ncbi.nlm.nih.gov/pubmed/3173690

Biernaskie, J., Szymanska, A., Windle, V., & Corbett, D. (2005). Bi-hemispheric contribution to functional motor recovery of the affected forelimb following focal ischemic brain injury in rats. *The European journal of neuroscience, 21*(4), 989-999. doi:10.1111/j.1460-9568.2005.03899.x

Bradnam, L. V., Stinear, C. M., Barber, P. A., & Byblow, W. D. (2012). Contralesional hemisphere control of the proximal paretic upper limb following stroke. *Cerebral Cortex (New York, N.Y.: 1991), 22*(11), 2662-2671. doi:10.1093/cercor/bhr344

Brösamle, C., & Schwab, M. E. (1997). Cells of origin, course, and termination patterns of the ventral, uncrossed component of the mature rat corticospinal tract. *The Journal of comparative neurology, 386*(2), 293-303. doi:10.1002/(sici)1096-9861(19970922)386:2<293::aid-cne9>3.0.co;2-x

Brösamle, C., & Schwab, M. E. (2000). Ipsilateral, ventral corticospinal tract of the adult rat: ultrastructure, myelination and synaptic connections. *Journal of Neurocytology, 29*(7), 499-507. Retrieved from http://www.ncbi.nlm.nih.gov/pubmed/11279365

Cirstea, M. C., & Levin, M. F. (2000). Compensatory strategies for reaching in stroke. *Brain, 123 (Pt 5)*, 940-953. doi:10.1093/brain/123.5.940

Côté, S. L., Elgbeili, G., Quessy, S., & Dancause, N. (2020). Modulatory effects of the supplementary motor area on primary motor cortex outputs. *Journal of Neurophysiology, 123*(1), 407-419. doi:10.1152/jn.00391.2019

Côté, S. L., Hamadjida, A., Quessy, S., & Dancause, N. (2017). Contrasting modulatory effects from the dorsal and ventral premotor cortex on primary motor cortex outputs. *The Journal of Neuroscience: The Official Journal of the Society for Neuroscience*. doi:10.1523/JNEUROSCI.0462-17.2017

Dancause, N., Barbay, S., Frost, S. B., Plautz, E. J., Stowe, A. M., Friel, K. M., & Nudo, R. J. (2006). Ipsilateral connections of the ventral premotor cortex in a New World primate. *The Journal of comparative neurology, 495*(4), 374-390. doi:10.1002/cne.20875

Deffeyes, J. E., Touvykine, B., Quessy, S., & Dancause, N. (2015). Interactions between rostral and caudal cortical motor areas in the rat. *Journal of Neurophysiology*, jn.00760.02014. doi:10.1152/jn.00760.2014

Eisner-Janowicz, I., Barbay, S., Hoover, E., Stowe, A. M., Frost, S. B., Plautz, E. J., & Nudo, R. J. (2008). Early and Late Changes in the Distal Forelimb Representation of the Supplementary Motor Area After Injury to Frontal Motor Areas in the Squirrel Monkey. *Journal of Neurophysiology, 100*(3), 1498-1512. doi:10.1152/jn.90447.2008

Fridman, E. A., Hanakawa, T., Chung, M., Hummel, F., Leiguarda, R. C., & Cohen, L. G. (2004). Reorganization of the human ipsilesional premotor cortex after stroke. *Brain: A Journal of Neurology, 127*(Pt 4), 747-758. doi:10.1093/brain/awh082

Harrison, T. R. (1994). Harrison's principles of internal medicine Vol. 2 Vol. 2. New York [u.a.: McGraw-Hill.

Ishida, A., Isa, K., Umeda, T., Kobayashi, K., Kobayashi, K., Hida, H., & Isa, T. (2016). Causal Link between the Cortico-Rubral Pathway and Functional Recovery through Forced Impaired Limb Use in Rats with Stroke. *The Journal of neuroscience : the official journal of the Society for Neuroscience, 36*(2), 455-467. doi:10.1523/jneurosci.2399-15.2016

Ishida, A., Kobayashi, K., Ueda, Y., Shimizu, T., Tajiri, N., Isa, T., & Hida, H. (2019). Dynamic Interaction between Cortico-Brainstem Pathways during Training-Induced Recovery in Stroke Model Rats. *The Journal of neuroscience : the official journal of the Society for Neuroscience, 39*(37), 7306-7320. doi:10.1523/jneurosci.0649-19.2019

Jeffers, M. S., Touvykine, B., Ripley, A., Lahey, G., Carter, A., Dancause, N., & Corbett, D. (2020). Post-stroke impairment and recovery are predicted by task-specific regionalization of injury. *The Journal of neuroscience : the official journal of the Society for Neuroscience*. doi:10.1523/jneurosci.0057-20.2020

Jones, T. A. (2017). Motor compensation and its effects on neural reorganization after stroke. *Nature Reviews Neuroscience, 18*(5), 267-280. doi:10.1038/nrn.2017.26

Kleim, J. A., Barbay, S., & Nudo, R. J. (1998). Functional Reorganization of the Rat Motor Cortex Following Motor Skill Learning. *Journal of Neurophysiology, 80*(6), 3321-3325. Retrieved from http://jn.physiology.org/content/80/6/3321

files/1022/3321.html

Kwakkel, G., Kollen, B., & Lindeman, E. (2004). Understanding the pattern of functional recovery after stroke: facts and theories. *Restor Neurol Neurosci, 22*(3-5), 281-299.

Liu, Y., & Rouiller, E. M. (1999). Mechanisms of recovery of dexterity following unilateral lesion of the sensorimotor cortex in adult monkeys. *Experimental brain research, 128*(1), 149-159.

Mansoori, B. K., Jean-Charles, L., Touvykine, B., Liu, A., Quessy, S., & Dancause, N. (2014). Acute inactivation of the contralesional hemisphere for longer durations improves recovery after cortical injury. *Exp Neurol, 254*, 18-28. doi:10.1016/j.expneurol.2014.01.010

Mansoori, B. K., Jean-Charles, L., Touvykine, B., Liu, A., Quessy, S., & Dancause, N. (2014). Acute inactivation of the contralesional hemisphere for longer durations improves recovery after cortical injury. *Experimental Neurology, 254*, 18-28. doi:10.1016/j.expneurol.2014.01.010

McNeal, D. W., Darling, W. G., Ge, J., Stilwell-Morecraft, K. S., Solon, K. M., Hynes, S. M., . . . Morecraft, R. J. (2010). Selective long-term reorganization of the corticospinal projection from the supplementary motor cortex following recovery from lateral motor cortex injury. *The Journal of comparative neurology, 518*(5), 586-621. doi:10.1002/cne.22218

Mohapatra, S., Harrington, R., Chan, E., Dromerick, A. W., Breceda, E. Y., & Harris-Love, M. (2016). Role of contralesional hemisphere in paretic arm reaching in patients with severe arm paresis due to stroke: A preliminary report. *Neurosci Lett, 617*, 52-58. doi:10.1016/j.neulet.2016.02.004

Montoya, C. P., Campbell-Hope, L. J., Pemberton, K. D., & Dunnett, S. B. (1991). The "staircase test": a measure of independent forelimb reaching and grasping abilities in rats. *Journal of Neuroscience Methods, 36*(2-3), 219-228. Retrieved from http://www.ncbi.nlm.nih.gov/pubmed/2062117

Naus, C., Flumerfelt, B. A., & Hrycyshyn, A. W. (1985). An anterograde HRP-WGA study of aberrant corticorubral projections following neonatal lesions of the rat sensorimotor cortex. *Experimental Brain Research, 59*(2), 365-371. Retrieved from http://www.ncbi.nlm.nih.gov/pubmed/2411584

Neafsey, E. J., Bold, E. L., Haas, G., Hurley-Gius, K. M., Quirk, G., Sievert, C. F., & Terreberry, R. R. (1986). The organization of the rat motor cortex: a microstimulation mapping study. *Brain Research, 396*(1), 77-96. Retrieved from http://www.ncbi.nlm.nih.gov/pubmed/3708387

Phac. (2011). Tracking Heart Disease and Stroke in Canada - Public Health Agency of Canada. Retrieved from http://www.phac-aspc.gc.ca/cd-mc/cvd-mcv/sh-fs-2011/index-eng.php files/1702/index-eng.html

Quessy, S., Côté, S. L., Hamadjida, A., Deffeyes, J., & Dancause, N. (2016). Modulatory Effects of the Ipsi and Contralateral Ventral Premotor Cortex (PMv) on the Primary Motor Cortex (M1) Outputs to Intrinsic Hand and Forearm Muscles in Cebus apella. *Cerebral Cortex (New York, NY), 26*(10), 3905-3920. doi:10.1093/cercor/bhw186

Rouiller, E. M., Moret, V., & Liang, F. (1993). Comparison of the connectional properties of the two forelimb areas of the rat sensorimotor cortex: support for the presence of a premotor

or supplementary motor cortical area. *Somatosensory & Motor Research, 10*(3), 269-289. Retrieved from http://www.ncbi.nlm.nih.gov/pubmed/8237215

Seggie, J., & Berry, M. (1972). Ontogeny of interhemispheric evoked potentials in the rat: Significance of myelination of the corpus callosum. *Experimental Neurology, 35*(2), 215-232. doi:https://doi.org/10.1016/0014-4886(72)90148-3

Shammah-Lagnado, S. J., Negrão, N., Silva, B. A., & Ricardo, J. A. (1987). Afferent connections of the nuclei reticularis pontis oralis and caudalis: a horseradish peroxidase study in the rat. *Neuroscience, 20*(3), 961-989. Retrieved from http://www.ncbi.nlm.nih.gov/pubmed/2439943

Takeuchi, N., Chuma, T., Matsuo, Y., Watanabe, I., & Ikoma, K. (2005). Repetitive transcranial magnetic stimulation of contralesional primary motor cortex improves hand function after stroke. *Stroke; a journal of cerebral circulation, 36*(12), 2681-2686. doi:10.1161/01.STR.0000189658.51972.34

Touvykine, B., Elgbeili, G., Quessy, S., & Dancause, N. (2020). Interhemispheric modulations of motor outputs by the rostral and caudal forelimb areas in rats. *Journal of Neurophysiology, 123*(4), 1355-1368. doi:10.1152/jn.00591.2019

Touvykine, B., Mansoori, B. K., Jean-Charles, L., Deffeyes, J., Quessy, S., & Dancause, N. (2016). The Effect of Lesion Size on the Organization of the Ipsilesional and Contralesional Motor Cortex. *Neurorehabilitation and Neural Repair, 30*(3), 280-292. doi:10.1177/1545968315585356

Traversa, R., Cicinelli, P., Bassi, A., Rossini, P. M., & Bernardi, G. (1997a). Mapping of motor cortical reorganization after stroke. A brain stimulation study with focal magnetic pulses. *Stroke, 28*(1), 110-117. doi:10.1161/01.str.28.1.110

Traversa, R., Cicinelli, P., Bassi, A., Rossini, P. M., & Bernardi, G. (1997b). Mapping of motor cortical reorganization after stroke. A brain stimulation study with focal magnetic pulses. *Stroke; a journal of cerebral circulation, 28*(1), 110-117. Retrieved from http://www.ncbi.nlm.nih.gov/pubmed/8996498

Twitchell, T. E. (1951). The restoration of motor function following hemiplegia in man. *Brain: A Journal of Neurology, 74*(4), 443-480. Retrieved from http://www.ncbi.nlm.nih.gov/pubmed/14895765

Valverde, F. (1962). Reticular formation of the albino rat's brain stem cytoarchitecture and corticofugal connections. *The Journal of Comparative Neurology, 119*(1), 25-53. doi:10.1002/cne.901190105

Wahl, A. S., Buchler, U., Brandli, A., Brattoli, B., Musall, S., Kasper, H., . . . Schwab, M. E. (2017). Optogenetically stimulating intact rat corticospinal tract post-stroke restores motor control through regionalized functional circuit formation. *Nature Communications, 8*(1), 1187. doi:10.1038/s41467-017-01090-6

Wahl, A. S., Omlor, W., Rubio, J. C., Chen, J. L., Zheng, H., Schröter, A., . . . Schwab, M. E. (2014). Asynchronous therapy restores motor control by rewiring of the rat corticospinal tract after stroke. *Science, 344*(6189), 1250-1255. doi:10.1126/science.1253050

Ward, N. S., Brown, M. M., Thompson, A. J., & Frackowiak, R. S. J. (2003). Neural Correlates of Outcome After Stroke: A Cross-sectional fMRI Study. *Brain, 126*(6), 1430-1448. doi:10.1093/brain/awg145

Ward, N. S., & Cohen, L. G. (2004). Mechanisms underlying recovery of motor function after stroke. *Archives of Neurology, 61*(12), 1844-1848. doi:10.1001/archneur.61.12.1844

Wenk, C. A., Thallmair, M., Kartje, G. L., & Schwab, M. E. (1999). Increased corticofugal plasticity after unilateral cortical lesions combined with neutralization of the IN-1 antigen in adult rats. *The Journal of comparative neurology, 410*(1), 143-157. doi:10.1002/(sici)1096-9861(19990719)410:1<143::aid-cne12>3.0.co;2-#

Zaaimi, B., Edgley, S. A., Soteropoulos, D. S., & Baker, S. N. (2012). Changes in descending motor pathway connectivity after corticospinal tract lesion in macaque monkey. *Brain: A Journal of Neurology, 135*(Pt 7), 2277-2289. doi:10.1093/brain/aws115

Zeiler, S. R., Gibson, E. M., Hoesch, R. E., Li, M. Y., Worley, P. F., O'Brien, R. J., & Krakauer, J. W. (2013). Medial premotor cortex shows a reduction in inhibitory markers and mediates recovery in a mouse model of focal stroke. *Stroke, 44*(2), 483-489. doi:10.1161/strokeaha.112.676940

Figures

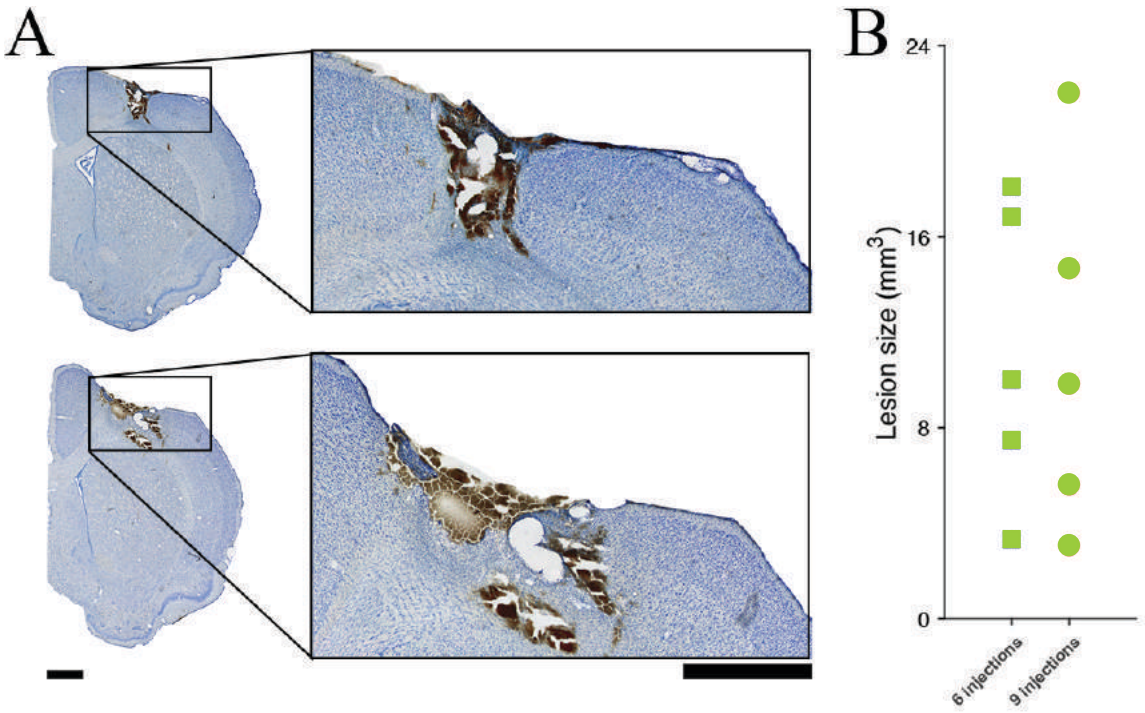

Figure (Ch4)1. Stroke volumes. A. Examples of Nissle stained coronal sections with small (top panel) and large (bottom panel) lesions. The box shows a high-resolution image of the lesion. Lesions affected all cortical layers as well as touched on the dorsal part of the corpus callosum. B. Lesion volumes induced with 6 (squares) or 9 (circles) cortical injections of ET-1. Lesion volumes were obtained by subtracting the volume of the contralesional (intact) hemisphere from ipsilesional (injured) hemispheres and is expressed in mm^3. Lesion protocols have resulted in a wide range of cortical lesion sizes. Black bar = 1mm.

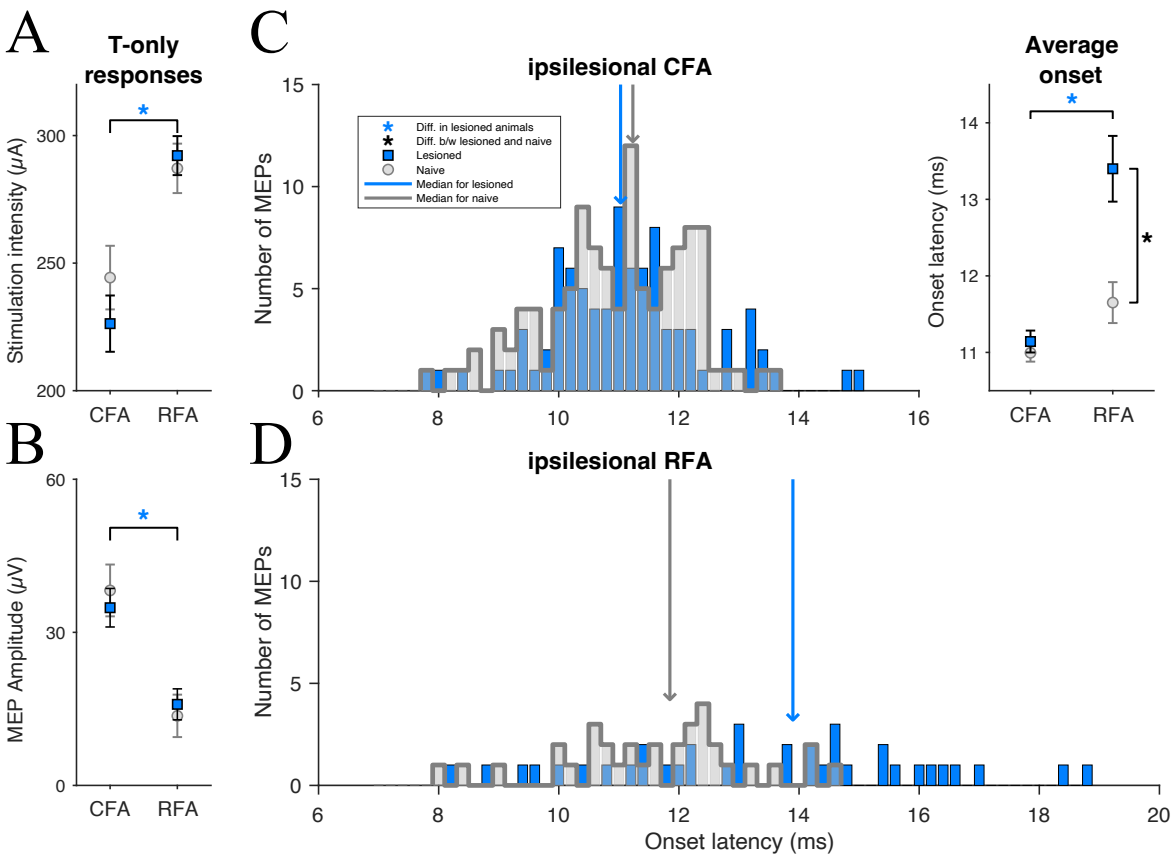

Figure (Ch4)2. Comparison of output properties of ipsilesional motor regions (CFA_{lesion} and $RFA_{ipsilesional}$). A. mean stimulation intensity (±SE) required to produce motor-evoked potentials (MEPs) from CFA_{lesion} and $RFA_{ipsilesional}$ (blue markers). Stimulation intensities to produce MEPs from $RFA_{ipsilesional}$ were significantly greater than CFA_{lesion}, but comparable to their naive counterparts (grey markers). B. mean amplitude of MEPs (±SE) evoked from CFA_{lesion} and $RFA_{ipsilesional}$ with T-only response. MEPs resulting from CFA_{lesion} stimulation were significantly greater than those evoked from $RFA_{ipsilesional}$, but were comparable to the MEP amplitudes evoked from their naive counterparts CFA_{naive} and RFA_{naive}. C. onset latencies of MEPs resulting from T-only stimulation in the CFA_{lesion} (blue, n = 88). The histogram shows the count of MEPs with different onset latency values (bins of 0.2 ms). Onset latencies obtained from CFA_{naive}

(grey) are presented for comparison, along with the median of CFA_{lesion} (blue arrow, 11.2ms) and CFA_{naive} (grey arrow, 11.0ms). D. onset latencies of MEPs resulting from T-only stimulation in the $RFA_{ipsilesional}$ (blue, n = 32). Onset latencies obtained from RFA_{naive} (grey) are presented for comparison, along with the median of RFA_{lesion} (blue arrow, 13.9ms) and CFA_{naive} (grey arrow, 11.0ms). Inset. average (±SE) of onset latencies of MEPs from CFA_{lesion} were comparable to those of CFA_{naive}, but was shorter than those of $RFA_{ipsilesional.}$ Average onset latencies resulting from $RFA_{ipsilesional}$ T-only stimulation were significantly greater than those from RFA_{naive}. *significant difference.

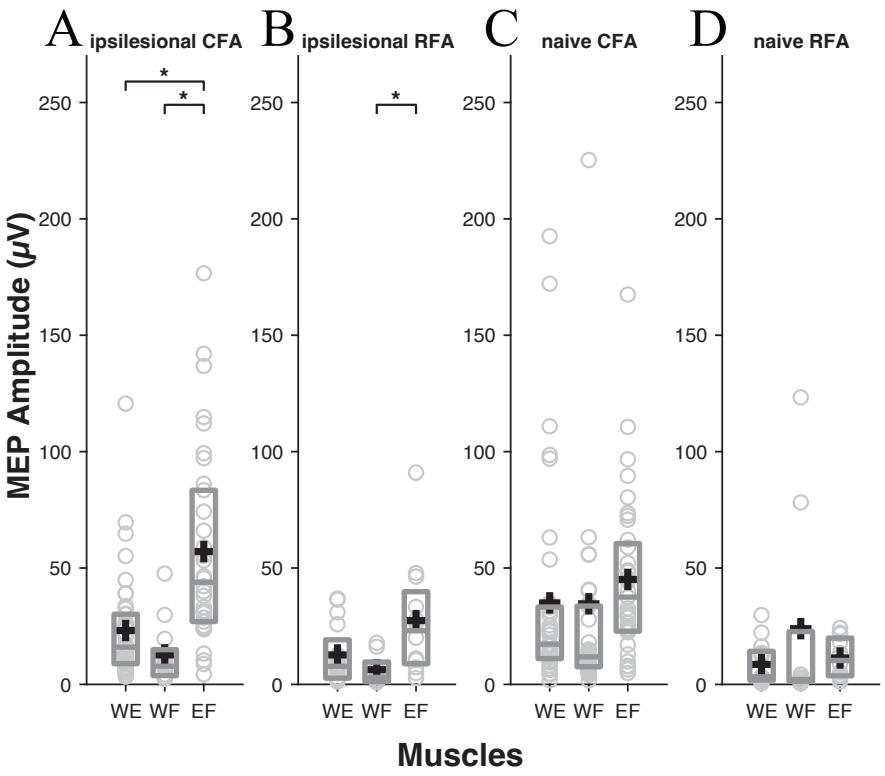

Figure (Ch4)3. All MEPs amplitudes in wrist extension (WE), wrist flexion (WF), and elbow flexion (EF) resulting from T-only stimulation in stroke and naive rats. The Interquartile Range (represented by the lower (25th percentile) and upper (75th percentile) limits of a grey rectangle), the median (grey bar within the grey rectangle), and mean (black cross) values are shown for each muscle. A. amplitudes of MEPs produced by CFA_{lesion} stimulation were significantly greater in EF muscle (mean = 10.6ms, median = 10.5ms) compared to both WE (mean = 11.8ms, median = 11.4ms) and WF (mean = 10.3ms, median = 10.2ms). B. amplitudes of MEPs resulting from $RFA_{ipsilesional}$ stimulation were significantly greater in EF muscle compared to both WF. There were no significant differences in MEP amplitudes evoked from CFA_{naive} (C), nor RFA_{naive}(D). **significant difference.

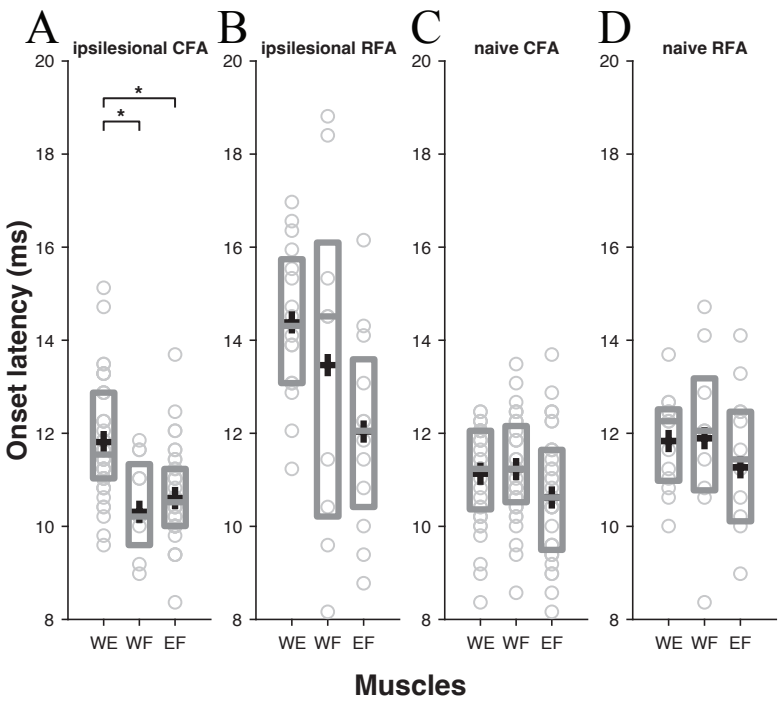

Figure (Ch4)4. All onset latencies of MEPs in wrist extension (WE), wrist flexion (WF), and elbow flexion (EF) resulting from T-only stimulation in stroke and naive rats. The Interquartile Range (represented by the lower (25th percentile) and upper (75th percentile) limits of a grey rectangle), the median (grey bar within the grey rectangle), and mean (black cross) values are shown for each muscle. A. onset latencies of MEPs resulting from CFA_{lesion} stimulation were significantly greater in WE muscle compared to both WF and EF. B. values of MEP onset latencies resulting from of $RFA_{ipsilesional}$ were not significantly different between muscles, but the Interquartile Range representing variance was the largest for responses from $RFA_{ipsilesional}$, specifically for the WF. There were no significant differences between onset latencies resulting from CFA_{naive} (C) and RFA_{naive} (D) stimulation. *significant difference.

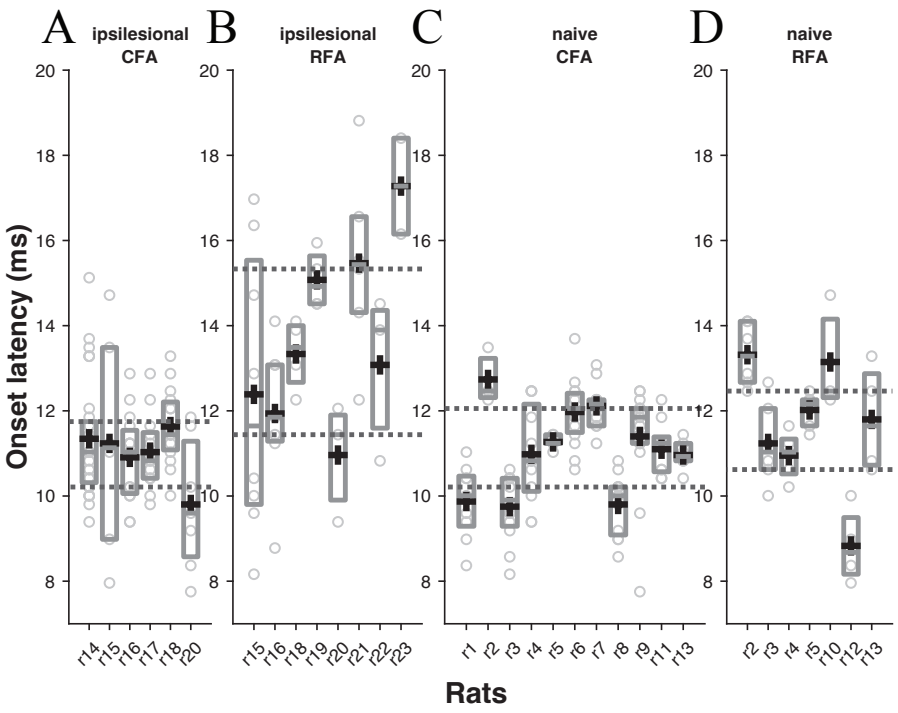

Figure (Ch4)5. All onset latencies of MEPs resulting from T-only stimulation collected in each rat. The Interquartile Range (represented by the lower (25th percentile) and upper (75th percentile) limits of a grey rectangle), the median (grey bar within the grey rectangle), and mean (black cross) values are shown for each rat. A. onset latencies of MEPs obtained from T-only stimulation in CFA_{lesion}, and the upper and lower limits of their interquartile range (dotted lines). B. onset latencies of MEPs obtained from T-only stimulation in $RFA_{ipsilesional}$. The interquartile range (dotted lines) for onset latencies obtained from $RFA_{ipsilesional}$ are larger compared to CFA_{lesion}. Onset values obtained from T-only stimulation in CFA_{naive} (C) and RFA_{naive} (D) had comparable interquartile range.

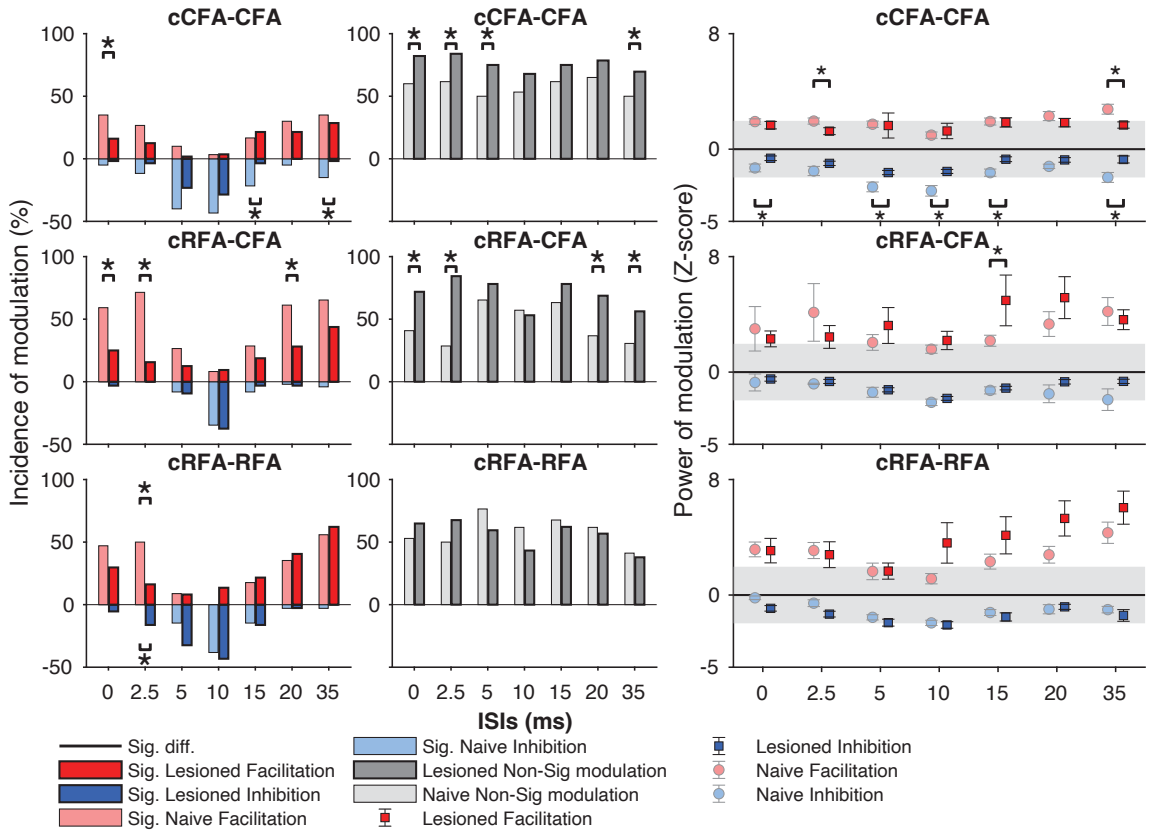

Figure (Ch4)6. Quantification and comparison of modulatory effects with each interstimulus interval between lesioned and naive rats. cCFA-CFA protocols are in the top row, cRFA-CFA protocols are in the middle row, and cRFA-RFA are in the bottom row. A. Each bar represents the incidence (%) of significant faciliation and significant inhibition (stroke animals: red and blue respectively. naive animals: pink and light blue respectively). For example, for cCFA-CFA$_{lesion}$ protocols (top panel) with ISI0, out of 56 motor-evoked potentials (MEPs), 9 were significantly facilitatory (16.1%) and 1 were significantly inhibitory (1.8%). B. For each ISI the bar shows the incidence of non-significant modulation for stroke (dark grey) and naive (light grey) rats. C. Power of modulation with each ISI represented as Z-score (mean±SE) of facilitatory and inhibitory modulations. *significant difference.

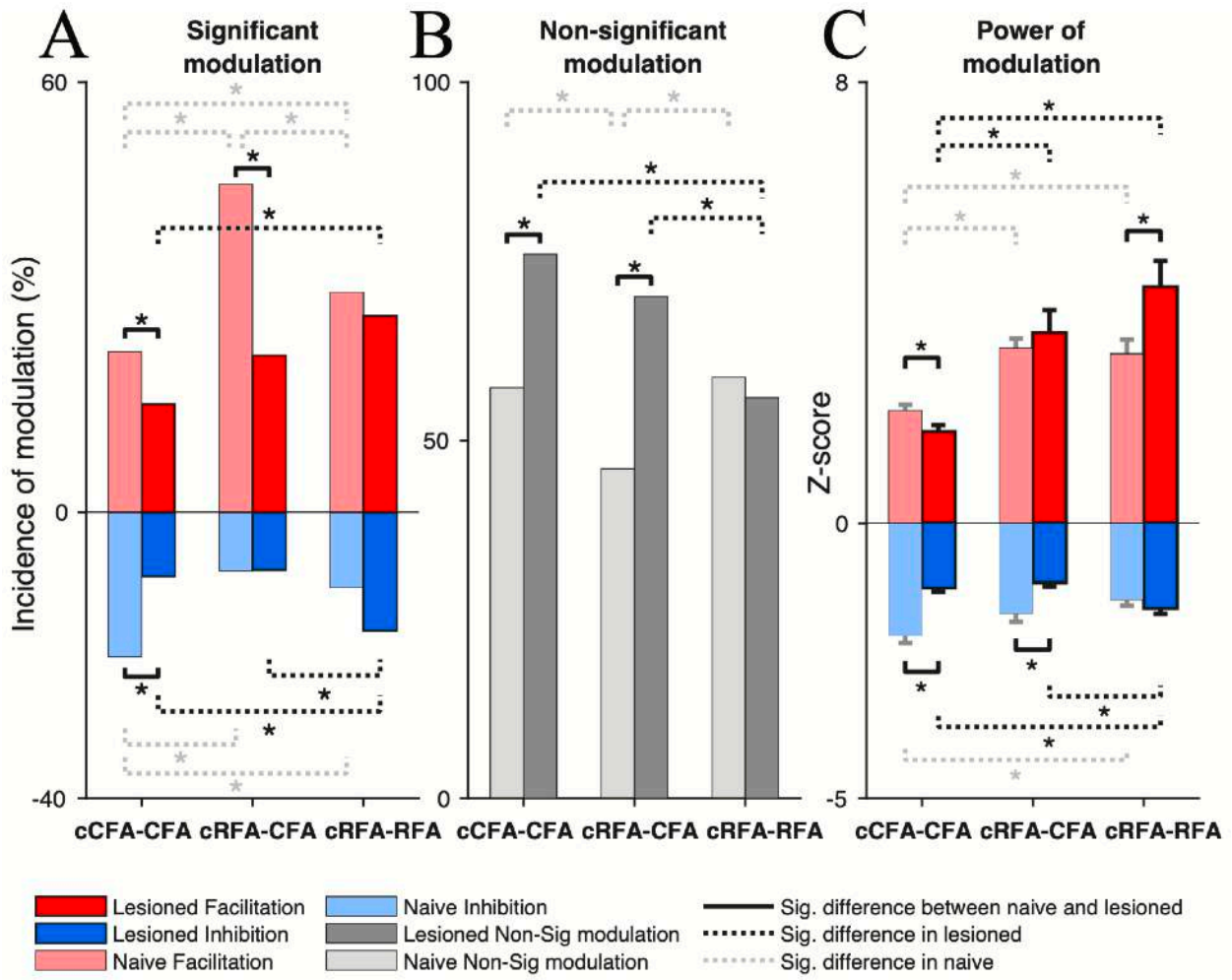

Figure (Ch4)7. Comparison of modulatory effects with all interstimulus intervals (ISIs) combined. In lesioned animals, significant differences between protocol types are denoted with a dashed black line, whereas significant differences between stroke and naive rats are denoted with a solid black line. Differences between protocol types in naive rats are presented as a reminder and denoted by a dashed grey line. A. Comparison of the incidence of significant modulatory effects for cCFA-CFA, cRFA-CFA, and cRFA-RFA protocols in stroke and naive rats. For example, the incidence of significant facilitation for cCFA-CFA_{lesion} (n = 59, 15.0%) is significantly smaller compared to cCFA-CFA_{naive} (n = 94, 22.4%), as well as for cRFA-$RFA_{perilesion}$ (n = 73, 30.7%) B. Comparison of non-significant modulation incidence for cCFA-

CFA, cRFA-CFA, and cRFA-RFA protocols in stroke and naive rats. C. Facilitatory and inhibitory modulation power is expressed as mean magnitude of Z-score (±SE) of facilitatory and inhibitory modulations. *significant difference.

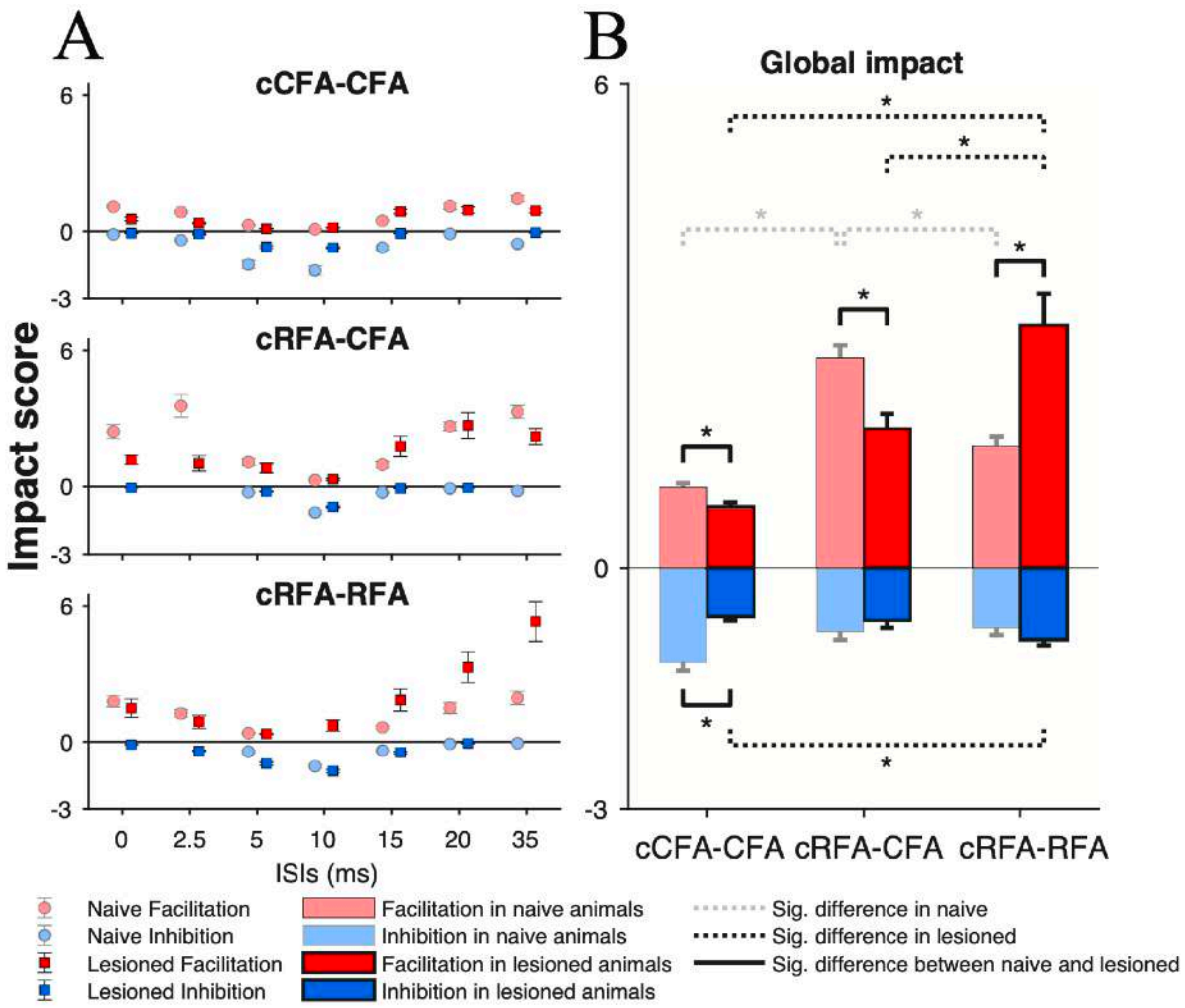

Figure (Ch4)8. Impact of conditioning ipsilesional motor outputs with contralesional conditioning in three protocol types (cCFA-CFA, cRFA-CFA, and cRFA-RFA). A. Impact score of stroke (squares) and naive rats (circles) with each ISI (mean±SE). The top panel shows cCFA-CFA protocols, middle - cRFA-CFA, and the bottom panel shows cRFA-RFA protocols. B. Global impact of each protocol type with all ISIs combined in stroke and naive rats. In stroke animals, comparisons between protocol types are denoted with a dashed black line, comparisons between stroke and naive rats are denoted with a solid black line, and comparisons between protocol types in naive rats are presented with a dashed grey line. For example, the impact score for cCFA-CFA protocols of both facilitation and inhibition was smaller in lesioned (facilitation: 0.76 Z-score; inhibition: 0.60 Z-score) compared to naive rats (facilitation: 1.00 Z-score;

inhibition: -1.170 Z-score. black line). The greatest facilitatory impact in stroke rats was for cRFA-$RFA_{ipsilesional}$ protocols (3.00 Z-score) and was significantly greater than facilitatory impact for cCFA-CFA_{lesion} and cRFA-CFA_{lesion} (dashed black lines). In naive rats, the facilitatory impact scores for cRFA-CFA protocols were greater than for cRFA-CFA_{naive} and cRFA-RFA_{naive} protocols (dashed grey lines). *significant difference.

CHAPTER 5 GENERAL DISCUSSION

The results presented in this thesis demonstrate that recovery from stroke depends on the extent of damage to various cortical regions and will cause substantial changes in output properties of both the spared motor cortex and bilateral interactions between the two hemispheres. Results from Chapter 2 confirmed that the extent of damage to specific cortical motor regions predicts the extent of the initial task-specific deficits. For example, the extent of damage to the forelimb motor cortex predicts the extent of deficits in the single pellet reaching task, whereas damage to the hindlimb motor region predicted the extent of hindlimb deficits on the beam traversal task. Furthermore, we found that the extent of damage to adjacent regions predicted the extent of final recovery on the same modality. Chapter 3 characterized the motor output of cortical forelimb regions and how said motor output is modulated by the activity in the contralateral forelimb motor cortex. The differences in output properties of CFA and RFA were quantified (motor evoked potentials (MEPs) amplitude and onset latency). Furthermore, the modulation of output of cortical forelimb motor regions by their contralateral homologues was systematically characterized in the rat, for the first time. Lastly, in Chapter 4, we quantified the changes in the motor output of the ipsilesional forelimb motor cortex and the modulatory role of the contralesional hemisphere, following spontaneous recovery from stroke. Specifically, muscle responses resulting from the stimulation of the ipsilesional RFA had onset latencies which were longer and more variable compared to healthy rats. Conditioning perilesional CFA by either the intact RFA or CFA resulted almost exclusively in decreases of various parameters we measured, such as decreased frequency of modulatory effects, the strength of modulation, as well as the power of modulation. These results indicated that after stroke the perilesional CFA is less

"connected" to the bilateral motor axis, and the likelihood of contralesional regions modulating motor output is much lower than in healthy animals. The only increases in modulation were found when contralesional RFA conditioned ipsilesional RFA. Specifically, the strength of facilitatory effects as well as the power of facilitation were greater than in healthy rats. The results from Chapter 4 demonstrate that the neuroplasticity in the motor system as a result of stroke is muscle-specific, bihemispheric, and dependent on the motor area.

5.1 RFA and premotor areas in primates.

The potential role of the RFA has been discussed previously, with evidence indicating that the RFA has a separate role from the CFA in the control of the forelimb, and is likely positioned higher in the hierarchy of the motor axis (Brown & Teskey, 2014; Hira et al., 2013a; Rouiller et al., 1993; X. Wang et al., 2017). This raises an important question for translatability of results in rodents to primates. If the CFA is the rat equivalent to the upper limb representation in M1, then what is the closest equivalent of the RFA in primates? In Chapter 3, the output properties of the two forelimb motor cortical regions of the rat were characterized. Stimulation intensities required to evoke motor responses from RFA were higher, the MEP amplitudes smaller, and MEP latency greater compared to CFA. These differences in output properties are in line with the differences between M1 and premotor areas in primates (M.-H. Boudrias, Lee, et al., 2010; M.-H. Boudrias, McPherson, et al., 2010). Considering that rodents are phylogenetically one of the closest clades to primates, it is interesting to ponder what is the closest equivalent to RFA in primates. A hint is provided by a comparative study of 24 animals from clade Eutheria sampled by Nudo and colleagues (1990), which found two separate gross cortical regions of origin for corticospinal

projections in all mammals tested (named A and B). In primates, region A spans S1, M1, PMd, and SMA; whereas region B roughly co-localizes with SII. In rats, region A co-localized with the CFA and hindlimb sensorimotor area, whereas region B roughly co-localized with SII. Interestingly, only rodents, rabbits (Clyde Glires) and primates have a separate third region of origin for descending corticospinal projections. In primates, this additional region (named "regions C") overlaps with the PMv and has been hypothesized to have appeared in response to evolutionary pressures (Wise, 2006). Whereas in rats, this third region dubbed "region C' " by Nudo and colleagues (1990) colocalizes with the RFA. Wise speculates that PMv developed to coordinate unimanual feeding in an arboreal setting when early primates were likely using one forelimb to hang off a branch and the other to grasp food and feed. A PMv feature unique among premotor regions supports this hypothesis. Few corticospinal neurons originating in the PMv descend past upper cervical segments (C2-C4), which isn't the case for other premotor areas (E. Borra, A. Belmalih, M. Gerbella, S. Rozzi, & G. Luppino, 2010; He et al., 1993, 1995). Motoneurons innervating neck and shoulder muscles originate in these segments C2-C4, whereas motoneurons innervating arm and hand muscles originate in segments (C5-T1)(Jenny & Inukai, 1983). Thus corticospinal projections from the PMv do not directly innervate the spinal segments whence motoneurons of the forearm and hand originate, a feature unique among premotor areas. Despite this anatomical arrangement we know that descending projections from the PMv are involved in dexterous motor control of the hand through spinal proprioceptive neurons (Kinoshita et al., 2012). Wise argues that the lack of projections to the lower cervical segments is an artifact of the initial role of PMv, namely coordination of unimanual feeding. Considering that rats and primates are relatively close phylogenetically and had a common ancestor approximately

90–100 million years ago, did RFA and PMv evolve from the same structure in the common mammalian ancestor to both rodents and primates? (Murphy, Pevzner, & O'Brien, 2004; Nei, Xu, & Glazko, 2001) Let's examine what is known. In contrast to PMv, CST neurons originating in RFA send robust projections to the lower cervical segments, the place of origin for motoneurons innervating distal forelimb muscles. For further insight into the likely origin of the RFA let's examine tree shrews. This species (family Tupaiidae) is part of the larger Euarchonta clade, which shared a common ancestor with primates around 70 million years ago, and only have two separate regions of origin of CST projections (A and B) (R. J. Nudo & Masterton, 1990). One explanation of this phenomenon is that a common ancestor to primates, tree shrews, and rodents (Euarchontoglires) acquired an additional region, separate motor region (C) that became RFA in the rodents, PMv in primates, and disappeared from tree shrews. Alternatively, RFA and PMv evolved independently in rodents and primates in response to different environmental pressures; and the fact that they both appear to be segregated from regions A and B is a simple coincidence. In terms of behaviour, neither tree shrews nor rodents eat food by hanging off a branch with one arm and grabbing and eating food with another, typical behavior in arboreal monkeys. Coupled with the aforementioned differences in the projection pattern of CST originating from RFA and PMv, it appears much more likely that the common ancestor (Euarchontoglires) did not possess region C, and it evolved separately in rodents and primates.

Despite likely not sharing evolutionary origin with the PMv, the RFA does act like a premotor area, in terms of its anatomy and hierarchical organization relative to the CFA (Hira et al., 2013a; Rouiller et al., 1993). While it is highly likely that there is no perfect equivalent to RFA in primates, as a secondary motor area it shares a few similarities with the PMd. As was

discussed in Chapter 1, CST from both RFA and PMd projects to lower cervical segments. There are further similarities between these areas in terms of their modulation pattern of both ipsilateral and contralateral CFA. Our group has previously examined the modulatory effect of PMv, PMd, and SMA on motor outputs of M1 in NHP using paired-pulse stimulation (S. L. Côté, Elgbeili, Quessy, & Dancause, 2020; Sandrine L. Côté, Hamadjida, Quessy, & Dancause, 2017; Quessy, Côté, Hamadjida, Deffeyes, & Dancause, 2016). The methodology used was practically the same as in rats, suprathreshold T_{stim} in M1 produced a motor response in forelimb muscles which is modulated by subthreshold C_{stim}. Unfortunately, our first publication to characterize the modulatory effect of ipsilateral RFA on the motor output of ipsilateral CFA used a different analysis to quantify modulation (Deffeyes, Touvykine, Quessy, & Dancause, 2015). While this complicates direct comparison, we can still observe certain similarities in the pattern of modulation across different interstimulus intervals (ISIs). Intrahemispheric modulation of CFA output by conditioning RFA resulted in the strongest and most frequent facilitatory modulation, and complete absence of inhibitory modulation with an interstimulus interval of 0ms. As the ISIs got longer the frequency and strength of facilitatory modulation decreased. The opposite happened with the inhibitory effects, which increased in strength and frequency. In primates, only ipsilateral PMd conditioning of M1 resulted in the pattern of modulation where the most frequent facilitatory effects occur at ISI0 and tend to decrease in frequency as ISIs get longer (Sandrine L. Côté et al., 2017). The greatest incidence of facilitation occurring with ISI0 is a feature shared by RFA and PMd; whereas conditioning by either ipsilateral PMv or SMA produced the greatest incidence of facilitation with ISIs of 1ms and 2ms. In terms of the pattern

of ipsilateral modulation, RFA appears to share more features in common with PMd compared with PMv and SMA.

Comparison of interhemispheric modulatory profiles between RFA and premotor region in primates is more straightforward. The modulatory effects of paired-pulse stimulation have been quantified using the same modified bootstrapping procedure, described in Chapters 3 and 4. Z-score is an excellent measure of modulation and one of the major reasons for its implementation was that it normalized modulatory responses regardless of the amplitude of initial MEPs. This feature of the Z-score accounts for the bigger muscles in primates with motor responses of much greater amplitudes. This allows for meaningful comparison of how the secondary motor area of one hemisphere (RFA in rat and PMv, PMd, and SMA in monkeys) modulates the motor output of a primary motor area (CFA in rats) of the other hemisphere.

The incidence of modulation pooled across ISIs produced by modulation of M1 motor output by contralateral PMv interaction differed greatly from those resulting from RFA-CFA. Whereas RFA-CFA interactions resulted in predominantly facilitatory responses (Facilitation 45.8%, Inhibition 10.5%), cPMv-iM1 interactions resulted in the exact opposite overall modulatory profile (Facilitation: 11.0%, Inhibition: 53.0%). In contrast, PMd-M1 interactions resulted in the majority of modulatory effects being facilitatory (Facilitation: 39.0%) and therefore appeared much closer to those resulting from cRFA-iCFA interactions. Nonetheless, it is worth mentioning that the frequency of inhibitory effects after cPMd modulation (Inhibition: 24.8%) was more than twice that for RFA-CFA interactions (9.2%). Finally, for a more direct comparison between PMv and PMd to RFA, I reanalyzed the data from Quessy et al. (2016) and Côté et al. (2017), as well as Chapter 3 to compare modulatory effects from only the forearm

muscles (Figure D1). The overall proportion of excitatory and inhibitory effects remains more similar between RFA and PMd modulation than between RFA and PMv modulation.

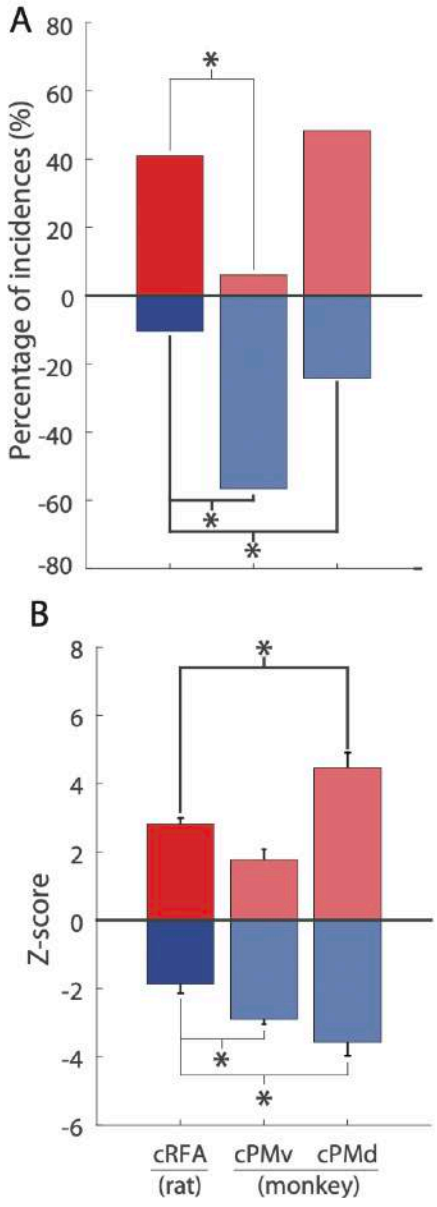

Figure D1. Comparison of the incidence (top panel) and mean (±SE) magnitude (bottom panel) of facilitatory (red) and inhibitory (blue) modulations produced by cRFA, cPMv, and cPMd conditioning in muscles pooled for all tested ISIs. A) Comparison of cPMv and cPMd modulation recorded in four forearm muscles to the modulatory effects produced by cRFA conditioning in two forearm muscles of the rat. In the top left panel, the incidences of significant facilitation by the cRFA in the rat were significantly greater than the instances of significant facilitation by the cPMv (6.00% vs 40.95% respectively; $p<0.001$). The incidences of significant facilitatory effects were comparable after cPMd and cRFA conditioning (48.33% vs 40.95 respectively; $p=0.38$). The instances of significant inhibitory effects were significantly greater for cPMd and cPMv conditioning than for cRFA conditioning (cPMd: 24.17%, cRFA: 10.48%; $p<0.005$ and cPMd: 56.67%, cRFA: 10.48%; $p<0.001$). B) cPMd conditioning in forearm muscles resulted in more powerful mean facilitatory magnitudes compared to mean facilitatory effects produced by cRFA conditioning in forearm muscles (cPMd: 4.47±0.0.44, cPMv: 1.77±0.31, cRFA: 2.81±0.18; ANOVA: $F=13.07$, $p<0.001$). The mean inhibitory effects produced by cPMv and cPMd conditioning resulted in greater inhibitory modulation compared to cRFA conditioning (cPMv: -2.90±0.15, cPMd: -3.58±0.39, cRFA:-1.87±0.20; ANOVA: $F=12.04$, $p<0.001$). Differences in proportion of significant modulatory effects (top row) were tested with Chi-square test with pairwise comparisons with Bonferroni correction. Differences in mean magnitudes of modulatory effects (bottom row) were tested with one-way ANOVA, with subsequent Bonferroni post-hoc. * Significant difference.

Lastly, SMA modulation of M1 motor output has resulted in the following proportion of overall modulatory effects: Facilitation - 16.7%; Inhibition - 31.5%) (S. L. Côté et al., 2020). We can see

that the proportion of overall modulatory effects exerted by RFA on the motor output of CFA is most similar to those resulting from PMd modulation of iM1, which was predominantly facilitatory. In contrast, PMv's and SMA's modulatory profiles are mostly inhibitory and are therefore quite different. These findings further indicated that RFA and PMv likely developed separately in rodents and primates.

No matter how tempting it might be to designate RFA as a PMd precursor or equivalent, the reality is more complicated. Examination of modulatory profiles of secondary motor areas across each ISI between monkey and rat reveals further differences. One of the most surprising findings in the rat was a relatively conserved V-shaped modulatory profile where the greatest incidence of facilitation was with the shortest and longest ISIs for all types of protocols tested (CFA-CFA, RFA-CFA, and RFA-RFA). None of the protocol types tested in the monkeys (PMv-M1, PMd-M1, and SMA-M1) had any sort of "conserved" modulatory profile common to all. This difference could be due to a simpler motor system of the rat, with fewer nodes of interaction, whereas primates have a more complex motor system, and as such it might be less likely to find "conserved" modulation profiles common to interactions between multiple primate cortical motor regions.

Overall, the modulatory drive of RFA on the output of either ipsi or contralateral CFA most closely resembles the effect of PMd on either ipsi or contralateral M1. Despite some gross similarities, the pattern of modulation is different to the point where none of the secondary motor areas in primates contribute to movement generation in the same way as RFA does. To be able to accurately interpret the results of stroke studies in the rat model, it is essential that we improve our understanding of these interspecies differences.

5.2 Importance of lesion size and location.

Previous work in primates and rodents has demonstrated the importance of lesion size or volume (Biernaskie et al., 2005; Dancause et al., 2005; Dancause et al., 2006; Frost, Barbay, Friel, Plautz, & Nudo, 2003; Touvykine et al., 2016). Stroke volume is the volume of dead tissue in the encephalon as a result of the interruption of blood flow. However, to date, no study in human patients has found a clear association between stroke volume and either initial deficits or the extent of motor recovery (Sterr, Dean, Szameitat, Conforto, & Shen, 2014). It is important to discuss the reasons for this discrepancy. In very general terms, stroke or lesion volume has an inverse relationship with the amount of healthy functional neural tissue remaining in the encephalon. The amount of healthy tissue is a useful metric; however, the brain has many different regions and subdivisions that are specialized for different functions. In terms of the sensorimotor function (S1 and M1), the area of cortical tissue dedicated to processing indicates how much of the central nervous system is dedicated to processing information of a particular sensory or motor modality. Penfield theorized as much after discovering that both his sensory and motor homunculi had distorted representations, with thumb, fingers, and lips having a disproportionally large surface area in the S1 and M1 compared to the rest of the body segments (Catani, 2017; Penfield & Boldrey, 1937). The importance of the area of cortical representation is underlined by studies, which found that skilled motor learning results in the increase of the size of relevant modalities (Kleim et al., 1998; R. J. Nudo et al., 1996). Furthermore, loss of one of the digits results in the parts of the M1 formerly dedicated to the control of said lost appendage to reorganize and acquire a new function (Qi, Stepniewska, & Kaas, 2000). Following the said reorganization of the CSN, ICMS stimulation of the M1 representation normally dedicated to lost

digits, now results in movements of remaining digits (Wu & Kaas, 1999). Even more striking, simply restricting the upper limb resulted in the reorganization of the motor cortex (Milliken, Plautz, & Nudo, 2013). Clearly, the size of the surface area and consequently the amount of neural tissue dedicated to a certain modality has an effect on function. Therefore, the most relevant metric to stroke recovery should be how much of each functional region in the brain remains after the injury, which can be estimated by the extent of the damage to said regions. It can be quite easy to obtain these measurements if the volume of a lesion is limited to a specific functional region of the encephalon. Evidently, a cortical M1 lesion with a volume of $10mm^3$ would spare more of M1 than a lesion of $15mm^3$. Therefore, the volume of a lesion limited to a specific region of the brain, such as M1, effectively estimates how much of M1 tissue remains. Unfortunately, outside of controlled scientific experiments, this is seldom the case, and stroke rarely damages just one cortical region. Blockage and damage to the middle cerebral artery or its branches is the most frequent cause of stroke, as it is the biggest blood vessel in the brain and irrigates large parts of the frontal, parietal, and temporal lobes (Nogles & Galuska, 2022). Considering the various brain regions this artery irrigates, lesions resulting from interruption of the blood flow will be highly dependent on the branch of the artery whence the blood flow is interrupted. This leads to situations where patients with lesions of comparable volumes will have varying deficits and will recover to different extents, which in turn results in studies that fail to find any relationship between initial deficits or the extent of final recovery and stroke volume (Sterr et al., 2014).

This is a persistent problem in stroke recovery, as it is difficult for clinicians to give an accurate prognosis of recovery from stroke. Damage to multiple cortical regions, which have

different functions, muddles the relationship between lesion size and the resulting behavioral deficits. For example, Chapters 1 and 3 discussed different output properties of CFA and RFA in the rat, differences in the pattern of anatomical connections, and functional differences. These differences have functional significance for motor control, as the disruption of the RFA function results in different forelimb deficits compared to the disruption of the CFA (Brown & Teskey, 2014). Clinical observations in patients have always been important in instructing the questions to be resolved in animal studies. However, considering the complexity of the human motor system and the variability of lesions and symptoms after stroke, scientists have historically been conducting animal experiments to understand the function of different components of the motor system and deficits associated with damage to said regions. Nonetheless, major technological advances over the last decades have opened new avenues in stroke research.

5.3 Technological advancement and patient observation studies.

In the last few decades, the advent of computers has led to an innovative approach, which was initially adopted in neurosciences and physiology from ecology and epidemiology. The wide availability of computers capable of completing complex calculations within seconds allowed researchers to run more complex statistical analyses. The classic approach to experimental design attempts to evaluate the effect of an independent variable by measuring the change or a difference in a dependent variable. For example, if two groups of subjects are randomized and treatment is introduced (independent variable) to one group; by measuring the differences in an outcome variable (dependent variable) we can evaluate the effect of the treatment. By randomizing the subjects within groups, it is assumed that variability for all variables other than

the independent and dependent variables is equal between groups. Therefore a significant difference in the values of the dependent variable must be due to the introduction of the independent variable. The effect is quantified objectively, by running statistical comparisons between the groups to infer the effect of the independent variable on the measured outcome of the dependant variable. However, in the last few decades, the advent of computers has also popularized a different approach in life sciences. Observational studies were initially utilized in ecology and epidemiology, where a randomizing experimental design was often not feasible and this was the only practical and ethical way to conduct research. In contrast with experimental studies, observational studies do exactly that, they observe the effect of an independent variable on the dependant variables. As the groups are not randomized, in observational studies it becomes important to account for additional variables and their potential effect on the dependent variable. Statistical tests that are capable of doing this tend to be computationally demanding, and while these methods were developed before the advent of personal computers, the convenience of running multiple statistical models within a single day has effectively democratized complex statistical analyses in research.

One such demanding statistical test is the multiple linear regression test, which was used in Chapter 2. It can estimate the relationship between the variability of multiple independent factors and covariates, on a particular dependent variable such as the behavioral score. With this approach, the large variability of lesion volumes, as well as the extent of damage to multiple cortical regions is actually necessary for the analysis to function. Stroke was induced in the experimental group of animals, but contrary to the study in Chapter 4, the purpose was to produce a large variety of lesions, not limited to the CFA. The goal was to model the variability

in stroke sizes and the extent of damage to multiple cortical regions present in human stroke survivors. The results establish a relationship between the extent of damage to different cortical regions and a variety of behavioral outcomes. Based on these results, if we can estimate the extent of damage to various cortical regions, we can now predict the degree of behavioral deficits, and more importantly behavioral recovery on a variety of behavioral tasks with a high degree of confidence.

A similar approach has already been used to perform analysis on populations of stroke survivors and provided interesting findings (Rondina, Park, & Ward, 2017). The researchers combined the Montreal Neurological Institute (MNI) Average Brain MRI atlas and CST tractography obtained from healthy individuals to subdivide the brain into estimated functional regions and approximated stroke damage to each of these functional regions. This approach allowed Rondina and colleagues (2017) to classify stroke survivors into one of two groups: patients who recover well and patients who do not with 90% accuracy. While the results in Chapter 2 are more nuanced, it should be noted that using an established breed of laboratory rodents offers an advantage over both monkeys and humans, in terms of between-subject variability. As was previously discussed, Sprague-Dawley rats are descended from a single pair of rats, and as such are highly inbred, with a significantly lower degree of genetic variability, and consequently lower degree of phenotypic variability between animals. In contrast, humans have a much higher degree of genetic variability between individuals, resulting in greater differences in phenotype. Consequently, any subdivision of the brain into functional regions is likely to be less accurate than in Sprague-Dawley rats, simply due to higher phenotypic variability between individuals. However, using predictive machine learning and even more advanced statistical

analysis, this approach has been shown as promising in recent years. Researchers were able to achieve a high degree of accuracy in predicting whether individual patients will recover well or not by combining two biomarkers obtained from MRI scans. Specifically, the measure of CST integrity obtained with diffusion tensor imaging, an MRI technique, was combined with the extent of damage to functionally define brain regions, based on Automated Anatomical Labeling (AAL) atlas (Tzourio-Mazoyer et al., 2002). The atlas is a parcellation of the brain into functional regions on an fMRI scan and superimposed on the MNI brain atlas obtained from healthy individuals. The algorithm developed by Rondina and colleagues (2017) was able to predict whether a patient will recover well or not with 90% accuracy, based on the two main biomarkers: CST integrity and extent of damage to brain motor regions. Overall, this study demonstrates the value of predictive statistical analysis and large clinical datasets to provide an accurate recovery prognosis for stroke patients.

Another promising technique in prognostic diagnosis after stroke is transcranial magnetic stimulation (TMS). A number of studies have found that if TMS stimulation over the injured hemisphere is capable of evoking EMG responses in the muscles of the paretic limb early after stroke, then it is likely that a patient's recovery will be good, and it is likely to follow the proportional recovery rule (Hendricks, Zwarts, Plat, & van Limbeek, 2002). The presence of MEPs out of the perilesional motor cortex indicates the extent of damage to the CST because enough descending projections remain to permit cortical stimulation to evoke EMG activity (Cathy M. Stinear et al., 2007). Effectively, MEPs in this context signify that sufficient motor circuitry and descending projections remain for the CNS to reorganize and permit proportional recovery. Unfortunately, the situation is more complex when TMS applied over the injured

hemisphere fails to produce MEPs. Some studies have found that patients in whom no motor responses were evoked did not recover well and did not follow proportional recovery (C. M. Stinear et al., 2017b). Others report that a number of such patients don't recover well, whereas others do exhibit proportional recovery (Araç, Sağduyu, Binai, & Ertekin, 1994). Overall, the presence of MEPs after TMS in stroke patients is a very good sign. Unfortunately, utilizing only this biomarker to predict recovery potential leads to the same problem as using exclusively behavioral motor deficit tests such as the Fugl-Meyer Assessment (FMA). The prognosis for patients with severe initial deficits is unreliable. Researchers have also examined the effectiveness of combined biomarkers, such as TMS with clinical motor scores (FMA) and neuroimagery and found the results promising. By combining the two measures, Stinear and colleagues (2012) developed a predicting recovery potential (PREP) algorithm that was able to predict whether the recovery will be good or not with an accuracy of ~75%. Further refinement of this algorithm (PREP2) increased prediction accuracy to 80% (C. M. Stinear et al., 2017a). There are multiple exciting avenues being investigated for prognostic biomarkers, but in terms of predicting recovery potential, combining multiple biomarkers appears to be the most promising avenue for accurate prognosis.

Nonetheless, it is worth remembering that Rondina and colleagues achieved categorization accuracy of 90% using individual sMRI scans of patients. The estimation of damage to motor regions is a novel biomarker, largely underutilized in clinical evaluations, but it should definitely be taken into account when estimating the recovery potential of a patient. If we simplify the motor system to an extreme level, we get the information processing in the brain and the descending wires (axons) through which the descending signal can activate the effectors

(muscles). Most biomarkers examined in humans focus on measuring the integrity of the CST. However, attempts to measure the disruption of motor processing in the brain have largely been overlooked. The Average Brain MRI atlas allows for an approximation of damage to various motor regions of interest and can provide an estimation for the disruption of supraspinal processing. Technological advancement allows us to better estimate the extent of damage to the CNS, and researchers and clinicians should continue to look for more reliable biomarkers able to estimate the disruption of motor processing in the brain and consequently predict the recovery potential.

Estimating the extent of damage to different motor regions to predict recovery should be adapted more universally in the field of stroke recovery. Accurate prediction of the extent of recovery would allow individually tailored treatment programs and better allocation of healthcare resources. In studies that examined the effect of rehabilitation in rodents and humans, researchers have identified subgroups of subjects who do not respond to rehabilitation well (Jeffers, Karthikeyan, & Corbett, 2018; Winters et al., 2015). Being able to identify patients who do not benefit from rehabilitation would allow physiotherapists to concentrate on individuals who are the most likely to benefit from rehabilitation. Moreover, patients who would not respond to rehabilitation would not have to undergo this difficult and ultimately fruitless ordeal, and instead, specialists such as occupational therapists can start training them on how to adapt themselves and their environment to their disability. Considering the high comorbidity of depression with stroke, succeeding at preserving a degree of independence, as well as avoiding failure at a demanding treatment regime would decrease the likelihood of depression, and ensure

that stroke survivors who will live with a permanent disability can have a higher quality of life (Conroy, Brownlowe, & McAllister, 2020).

5.4 The importance of animal models.

A more traditional approach to understanding the role of lesion size and location in predicting the extent of recovery was to use animal models to gain insight into deficits resulting from the loss of various motor structures and the role of remaining motor regions in recovery. Researchers in physiology would experimentally inactivate or destroy particular brain structures and quantify resulting deficits as well as the recovery from said deficits (Brinkman, 1984; Brown & Teskey, 2014; Kurata & Hoffman, 1994; Leyton & Sherrington, 1917; Rizzolatti et al., 1983; M. H. Schieber, 2000; Marc H. Schieber & Poliakov, 1998; Stephan et al., 1999; Travis, 1955). Rodents and non-human primates, capable of such dexterous movements with their forelimb, have been utilized extensively to study stroke and anterior limb deficits resulting from it (Ian Q. Whishaw & Coles, 1996). Monkeys, in particular, offer a great model for such an investigation, as demonstrated by Sherrington, Glees, Travis Nudo, Frost, and Dancause among many others (Dancause et al., 2005; Frost et al., 2003; Glees, Cole, Whitty, & Cairns, 1950; Leyton & Sherrington, 1917; R. J. Nudo & Milliken, 1996; Travis, 1955).

Monkeys offer several advantages over rodents. First and foremost, they are our closest phylogenic relatives with a similarly complex motor system, which makes the interpretation of how the experimental results apply to human beings much easier and more convincing. Furthermore, as non-human primates are larger and more robust than rodents, they can undergo longer surgical interventions and acute experiments, allowing a more thorough scientific

investigation. Researchers can actually perform multiple mapping experiments on the same area in the same animal (Dancause et al., 2005; Dancause et al., 2006; R. J. Nudo & Milliken, 1996; R. J. Nudo et al., 1996). Scientists can use ICMS in the motor cortex to obtain the size of motor representation such as a distal forelimb area in the M1 of non-human primates prior to lesion induction. Then, one can induce a local lesion and remap the region following a period of recovery (Dancause et al., 2006; Frost et al., 2003). Results from such experiments are particularly robust because they are conducted within the same subjects and thus limit the potential number of confounding factors to be considered. By limiting the lesion to a specific location, different lesion volumes result in different behavioral outcomes, because the bigger the stroke, the smaller the remaining M1 area, and consequently the greater the deficits (Dancause et al., 2005; Dancause et al., 2006; Frost et al., 2003; Touvykine et al., 2016). Further understanding of vicarious reorganization can be gleaned from the mapping of premotor areas before the lesion and following a period of recovery. To understand the functional significance of this reorganization scientists can inactivate said premotor regions of interest following recovery and compare the motor deficits to those resulting from inactivation of the same regions in intact monkeys. By comparing the changes in the size of motor representations in premotor regions and correlating them with motor deficits resulting from their inactivation, scientists would establish how neuroplasticity measured with ICMS mapping correlates with motor impairment in recovered stroke monkeys, which improves our understanding of vicarious reorganization in primates. For example, Liu and Rouiller (1999) have demonstrated that reversible inactivation of the ipsilateral premotor cortex after recovery from M1 stroke reintroduces motor deficits, whereas Dancause and colleagues (2006) found a relationship between lesion volume in M1 and

the expansion of distal representation in PMv. Such systematic investigations need to continue by incorporating and investigating other sensorimotor regions. Overall, to study motor control and various conditions affecting it in humans, non-human primates are the most reliable model to do so.

In rats, while it is possible to redo ICMS mapping experiments in the motor cortex of the same animal, it is technically quite demanding. Therefore it is quite difficult to obtain the size of cortical motor regions prior to the stroke. Recent advances in optogenetic motor mapping in mice offer a robust alternative to motor mapping in rats to study motor output properties as well as of connectivity and reorganization of the CNS (Mohajerani et al., 2011). Unfortunately, the smaller size of mice, as well as the higher difficulty of training them on behavioral tasks is its own drawback, limiting the use of these animals in stroke research. Compared to mice, rats, are larger, more robust, and smarter, which assures their continued use in stroke research. Furthermore, rats offer several advantages over primates, in terms of their size, cost, length of the life cycle, and a simpler CNS with fewer variables. The most widely used strains of laboratory rats are at this point very stable with limited phenotype variability because they descend from either one mating pair (Sprague Dawley), or from a few females and a male (Long-Evans). Winstar is the exception, but it is also the first widely used laboratory rat strain, and one thing they all have in common is that they are inbred to limit the natural genetic and phenotypic variability present in wild animals. This is not the case for the majority of NHP used in research today. The greater extent of genetic uniformity within rat strains offers a significant advantage to researchers, as evident from chapter 4, where we used bregma as a reference point to estimate the location of the CFA and induce lesions there. Such an approach in primates would be considered quite risky due

to significantly greater inter-individual variability in the location size of cortical regions. Furthermore, among animal species widely used in biomedical research, rodents are the closest Clyde to primates. Rats, and rodents in general, offer a cheaper, more accessible animal model to study stroke and motor control, but one always has to keep in mind that the interpretation of results and their applicability to humans will be more complicated.

Overall, using animal models is a powerful approach, and has allowed researchers to introduce one independent variable (stroke in a specific region of the motor cortex, i.e. M1 in NHP or CFA in rats), and observe and quantify the resulting changes in one or more dependent variables (e.g. behavioral deficits and recovery, size of cortical motor representations, one or more regions, etc).

5.5 Future avenues.

Understanding the neurobiology of plasticity after the lesion can open new avenues for harnessing plasticity and improving motor recovery. For example, knowing whether contralesional CFA and RFA are supportive or detrimental to motor recovery after stroke, the factors which can affect their role, and the biomarkers associated with it will inform our decision-making on whether or not these regions should be suppressed or facilitated to improve functional recovery. As was discussed above, the motor system in the rat is much simpler than in primates. This is a drawback in terms of the interpretability of results and their applicability to humans. Nonetheless, the rat is a very useful animal model to investigate the motor system and neuroplasticity at the system level in a mammal capable of prehension and relatively close evolutionarily to primates. Our findings in Chapters 3 and 4 raised questions, answering which

will further our understanding of the rat motor system both before and after stroke and whether this understanding can be leveraged to improve recovery.

1) In which CNS structures do the signals from opposing motor cortices interact with different ISIs? (Understanding this in rats can lead to an investigation in humans in hope of finding biomarkers etc?)

2) What is the role of the contralesional pathways in supporting recovery from strokes of different sizes?

3) Answers to these questions can inform which structures to target and in which animals to improve motor recovery after stroke.

1) In which CNS structures do the signals from opposing motor cortices interact with different ISIs?

The experiments in Chapter 3 have characterized how the motor output of CFA and RFA of the rat is modulated by conditioning their homologues in the contralateral hemisphere. The observed differences in the frequency of facilitatory and inhibitory effects with different ISIs were discussed in terms of known anatomical connections between cortical motor areas of both hemispheres and their projection pattern. In Chapter 4, we quantified changes in frequency and magnitude of facilitatory and inhibitory effects with various ISIs after recovery from stroke and inferred the possible role of these changes. However, the exact pathways involved, and the functional significance of these changes for motor recovery are not known and remain to be elicited. A number of follow-up experiments involving new techniques can provide answers to these questions.

One of the complications of using electrical stimulation to activate neurons is the lack of specificity. For example, a test stimulus delivered in the CFA will activate pyramidal neurons which form the corticospinal tract, as well as descending cortical projections to the red nucleus and the reticular formation, whence rubrospinal and reticulospinal tract originate. As CFA is heavily interconnected with numerous cortical and subcortical areas, a test stimulus will also activate projections to the putamen, as well as other sensorimotor areas both ipsi and contralateral. Novel molecular techniques, such as targeted viral transfections and optogenetics allow for dissection of these neural circuits. Optogenetics is a technique that allows one to control the behaviour of modified neurons with exposure to light. Double viral transfection of neurons is a molecular technique, which allows researchers to target specific projections, e.g. corticorubral projections from the CFA (Akintunde & Buxton, 1992). The technique consists of two different viral vectors each carrying a specific DNA (or RNA) sequence necessary to express proteins of interest in the targeted neural population. One viral vector is engineered to transfect neuronal cell bodies in the area of injection, in our case - the CFA. The second viral vector is engineered to transfect axonal terminals and is injected into the ipsilateral red nucleus. Each carries a nucleotide sequence essential to express the protein of interest, and only neurons that have been transfected by both viral vectors will be capable of expressing it, in this case, neurons projecting from the CFA to the ipsilateral red nucleus. This technique will allow researchers to manipulate a specific population of neurons, in this example corticorubral projections. Depending on the parameters of the experiment a variety of proteins can be expressed in double transfected neurons. For example, Channelrhodopsin-2 is a non-specific cation channel, which will open when exposed to light with a wavelength of around 480 nm, and allow sodium ions to

pass, producing local depolarization (Bamann, Kirsch, Nagel, & Bamberg, 2008). If enough Channelrhodopsin-2 channels open, and the depolarization reaches the axon hillock, it will cause an action potential to travel down the axon. Opposite results can be accomplished by using halorhodopsin instead of Channelrhodopsin-2 (Engelhard, Chizhov, Siebert, & Engelhard, 2018). When activated halorhodopsin transports chloride ions to cross the cell membrane of a neuron, resulting in local hyperpolarization, and effectively inhibiting the neuron from firing. However, what we can "package" in viral vectors is not limited to optogenetic content. One particularly impressive recent innovation consists of packaging conditionally expressed inhibitor agents in the double transfected neurons (Kinoshita et al., 2012; Sooksawate et al., 2013). This design consists of a modified tetanus toxin, only expressed in double transfected neurons when a specific condition is met, such as the presence of a non-endogenous molecule, such as the antibiotic tetracycline. In this setup tetracycline can be administered systemically, resulting in translation of tetanus toxin sequence in double and only double transfected cells. The toxin will bind to synaptobrevin, preventing exocytosis and neurotransmitter release at the axonal terminals, and effectively silencing the double transfected neurons. The advantage of this technique consists of being able to inhibit the target neurons for long periods of time with daily peritoneal injections of a widely available antibiotic - tetracycline. These advances in molecular biology allow us to manipulate specific pathways, which was previously only possible in genetically modified mice. The techniques described in this paragraph permit for previously impossible dissection of circuitry in the CNS.

By selectively transfecting neural pathways originating in the hemisphere where conditioning stimulation will be administered, we can deduce which pathways are responsible

for modulatory effect at specific interstimulus intervals. Transfecting one pathway per group of animals will result in 4 experimental groups, one per pathway: corticospinal, corticorubral, corticoreticular, and callosal projections originating in the hemisphere in which conditioning stimulation will be delivered. Double transfected neurons will express channelrhodopsin-2. Then, we simply have to repeat the experiments in chapter 3, but instead of delivering conditioning stimulation by injecting current through an electrode, the conditioning stimulation will shine a light of a wavelength of ~480nm, to activate channelrhodopsin-2 in the pathway transfected in this specific group of animals. Test stimulation will remain the same as in chapter 3 and will consist of injecting suprathreshold electrical current through the electrode lowered to layer V of the cortex. Comparing each of the 4 proposed experimental groups with results from chapter 3 and identifying differences in modulation with different ISIs will inform us with which ISIs the descending signals from the forelimb motor cortex of both hemispheres interact in the spinal cord, the red nucleus, and the reticular formation.

2) What is the role of the contralesional pathways in supporting recovery from strokes of different sizes?

The next step would be to investigate the involvement of these four pathways in recovery from strokes of different sizes. Rats will once again be randomly assigned into 4 groups based on the pathway which will be manipulated (corticospinal, corticorubral, corticoreticular, and callosal). Instead of channelrhodopsin-2, neurons will be double transfected with the tetracycline-dependent tetanus toxin expression machinery described above. The transfected pathways will originate in the forelimb motor cortex contralesional to stroke. After transfection, but prior to

lesion induction, baseline performance will be obtained in the battery of behavioral tests from Chapter 2. The goal is to produce lesions of various sizes to evaluate the effect of lesion size on the reorganization of specific pathways. Following a period of recovery of 5 weeks, when stroke rats are in the chronic stage of recovery, group-specific transfected pathways will be inactivated with systemic tetracycline injections, and any return of deficits will be evaluated on the aforementioned battery of behavioral tests from Chapter 2. Once the behavioral data has been obtained, terminal paired-pulse experiments will be conducted, with the same methodology as in Chapters 3 and 4. Return of deficits due to inhibition of specific pathways should highlight the importance of each pathway in supporting functional recovery and help us identify future therapeutic targets. Lesion size is expected to be a factor in which pathways would support functional reorganization and reinstatement of motor control. Results of paired-pulse stimulation will be examined to see if there is an interplay between specific ISIs, lesion size, and the extent of final recovery, in an effort to identify potential biomarkers predictive of the extent of recovery.

3) Answers to these questions can inform which structures to target and in which animals to improve motor recovery after stroke.

The goal of this study would be to manipulate pathways or pathways previously identified in the proposed study (#2), by either inhibiting or exciting these pathways periodically to improve spontaneous recovery of motor function. The methodology will consist of the techniques described above. Pathways of interest can be either inhibited or excited in an effort to improve functional recovery. Important factors to investigate in this study would be the timing and duration of intervention, and of course, lesion size is always a consideration!

These experiments would identify possible therapeutic targets in rats. The next step would be to manipulate these structures in primates to verify how well findings in rats translate to non-human primates, with their significantly more complex motor system.

5.6 Conclusion.

Experimental results presented in this thesis shed further light on the cortical motor system and neuroplasticity taking place after stroke. A lot of work remains to be done to improve clinical outcomes for stroke patients, and it should proceed in two parallel directions, clinical and mechanistic, that is to say basic science research. The clinical side should take advantage of big data when available (data collection should be kept in a uniform format between different Canadian hospital centers, anonymized, and made accessible for research purposes), more complex statistical analysis techniques and machine learning should help us in solving or managing the most immediate problems in stroke recovery. Specifically, finding ways to predict the extent of recovery accurately using currently available technology such as TMS and MRI scans will improve clinical outcomes and efficiency of treatment for stroke survivors. If a patient is accurately categorized as being likely to recover some degree of motor function following stroke, then appropriate resources such as physiotherapists should be allocated, whereas if a patient will not undergo any significant recovery of motor function, then instead of wasting time and valuable recourses with a physiotherapist, such patient should be taught adaptive movement strategies and trained in the use of specialized equipment by an occupational therapist (ergothérapeute). However, such analysis only identifies the targets, such as CNS structures implicated in recovery, but not the neurobiological mechanisms responsible for functional

outcomes. Therefore, basic and translational research should advance in parallel to improve our understanding of neuroplasticity and reorganization in the motor system. A better understanding of these processes and factors that influence them gives us more targets to investigate in hopes of finding therapeutic interventions and treatment options. Such studies must involve animal models, as we simply cannot conduct such invasive experiments in humans. Rats are important animal models in such studies, but prior to moving to test clinical interventions on patients, NHPs should be an essential preliminary step, which has often been overlooked in pre-clinical and clinical stroke trials. The results presented in this thesis are important steps on our journey to understand neuroplasticity and reorganization after stroke, but the journey is far from complete and many more such steps will need to be taken before we are able to create treatments capable of completely restoring motor functionality after stroke.

GENERAL REFERENCES

Akintunde, A., & Buxton, D. F. (1992). Origins and collateralization of corticospinal, corticopontine, corticorubral and corticostriatal tracts: a multiple retrograde fluorescent tracing study. *Brain Research, 586*(2), 208-218. Retrieved from http://www.ncbi.nlm.nih.gov/pubmed/1381650

Allred, R. P., & Jones, T. A. (2008). Maladaptive effects of learning with the less-affected forelimb after focal cortical infarcts in rats. *Experimental neurology, 210*(1), 172-181. doi:10.1016/j.expneurol.2007.10.010

Andersen, K. K., Olsen, T. S., Dehlendorff, C., & Kammersgaard, L. P. (2009). Hemorrhagic and ischemic strokes compared: stroke severity, mortality, and risk factors. *Stroke, 40*(6), 2068-2072. doi:10.1161/strokeaha.108.540112

Angulo-Kinzler, R. M., Mynark, R. G., & Koceja, D. M. (1998). Soleus H-reflex gain in elderly and young adults: modulation due to body position. *J Gerontol A Biol Sci Med Sci, 53*(2), M120-125. doi:10.1093/gerona/53a.2.m120

Araç, N., Sağduyu, A., Binai, S., & Ertekin, C. (1994). Prognostic value of transcranial magnetic stimulation in acute stroke. *Stroke, 25*(11), 2183-2186. doi:10.1161/01.str.25.11.2183

Asanuma, H. (1975). Recent developments in the study of the columnar arrangement of neurons within the motor cortex. *Physiological reviews, 55*(2), 143-156. Retrieved from http://www.ncbi.nlm.nih.gov/pubmed/806927

Asanuma, H., & Rosén, I. (1972). Topographical organization of cortical efferent zones projecting to distal forelimb muscles in the monkey. *Experimental Brain Research, 14*(3), 243-256. doi:10.1007/BF00816161

Asanuma, H., & Sakata, H. (1967). Functional Organization of a Cortical Efferent System Examined with Focal Depth Stimulation in Cats | Journal of Neurophysiology. *Journal of Neurophysiology, 30*(1), 35-54. doi:10.1152/jn.00348.2014

Ashe, J., & Georgopoulos, A. P. (1994). Movement parameters and neural activity in motor cortex and area 5. *Cerebral Cortex (New York, NY), 4*(6), 590-600. doi:10.1093/cercor/4.6.590

Badoud, S., Borgognon, S., Cottet, J., Chatagny, P., Moret, V., Fregosi, M., . . . Rouiller, E. M. (2017). Effects of dorsolateral prefrontal cortex lesion on motor habit and performance assessed with manual grasping and control of force in macaque monkeys. *Brain Struct Funct, 222*(3), 1193-1206. doi:10.1007/s00429-016-1268-z

Bamann, C., Kirsch, T., Nagel, G., & Bamberg, E. (2008). Spectral characteristics of the photocycle of channelrhodopsin-2 and its implication for channel function. *J Mol Biol, 375*(3), 686-694. doi:10.1016/j.jmb.2007.10.072

Barbas, H., & Pandya, D. N. (1987). Architecture and frontal cortical connections of the premotor cortex (area 6) in the rhesus monkey. *The Journal of comparative neurology, 256*(2), 211-228. doi:10.1002/cne.902560203

Bernhardt, J., Dewey, H., Thrift, A., & Donnan, G. (2004). Inactive and alone: physical activity within the first 14 days of acute stroke unit care. *Stroke, 35*(4), 1005-1009. doi:10.1161/01.Str.0000120727.40792.40

Biernaskie, J., Szymanska, A., Windle, V., & Corbett, D. (2005). Bi-hemispheric contribution to functional motor recovery of the affected forelimb following focal ischemic brain injury in rats. *The European journal of neuroscience, 21*(4), 989-999. doi:10.1111/j.1460-9568.2005.03899.x

Borra, E., Belmalih, A., Gerbella, M., Rozzi, S., & Luppino, G. (2010). Projections of the hand field of the macaque ventral premotor area F5 to the brainstem and spinal cord. *The Journal of comparative neurology, 518*(13), 2570-2591. doi:10.1002/cne.22353

Borra, E., Belmalih, A., Gerbella, M., Rozzi, S., & Luppino, G. (2010). Projections of the hand field of the macaque ventral premotor area F5 to the brainstem and spinal cord. *The Journal of Comparative Neurology, 518*(13), 2570-2591. doi:10.1002/cne.22353

Bortoff, G. A., & Strick, P. L. (1993). Corticospinal terminations in two new-world primates: further evidence that corticomotoneuronal connections provide part of the neural substrate for manual dexterity. *The Journal of neuroscience : the official journal of the Society for Neuroscience, 13*(12), 5105-5118. doi:10.1523/jneurosci.13-12-05105.1993

Boudrias, M.-H., Lee, S.-P., Svojanovsky, S., & Cheney, P. D. (2010). Forelimb Muscle Representations and Output Properties of Motor Areas in the Mesial Wall of Rhesus Macaques. *Cerebral Cortex (New York, NY), 20*(3), 704-719. doi:10.1093/cercor/bhp136

Boudrias, M.-H., McPherson, R. L., Frost, S. B., & Cheney, P. D. (2010). Output Properties and Organization of the Forelimb Representation of Motor Areas on the Lateral Aspect of the Hemisphere in Rhesus Macaques. *Cerebral Cortex (New York, NY), 20*(1), 169-186. doi:10.1093/cercor/bhp084

Boudrias, M. H., Belhaj-Saïf, A., Park, M. C., & Cheney, P. D. (2006). Contrasting properties of motor output from the supplementary motor area and primary motor cortex in rhesus macaques. *Cerebral Cortex (New York, NY), 16*(5), 632-638. doi:10.1093/cercor/bhj009

Bradnam, L. V., Stinear, C. M., Barber, P. A., & Byblow, W. D. (2012). Contralesional hemisphere control of the proximal paretic upper limb following stroke. *Cerebral Cortex (New York, N.Y.: 1991), 22*(11), 2662-2671. doi:10.1093/cercor/bhr344

Brinkman, C. (1984). Supplementary motor area of the monkey's cerebral cortex: short- and long-term deficits after unilateral ablation and the effects of subsequent callosal section. *The Journal of Neuroscience: The Official Journal of the Society for Neuroscience, 4*(4), 918-929. Retrieved from http://www.ncbi.nlm.nih.gov/pubmed/6716131

Brodmann, K. (1999). Brodmann's localisation in the cerebral cortex [Vergleichende Lokalisationslehre der Grosshirnrinde in ihren Orinzipien dargestellt auf Grund des Zellenbaus]. In: London: Imperial College Press.

Brösamle, C., & Schwab, M. E. (1997). Cells of origin, course, and termination patterns of the ventral, uncrossed component of the mature rat corticospinal tract. *The Journal of comparative*

neurology, 386(2), 293-303. doi:10.1002/(sici)1096-9861(19970922)386:2<293::aid-cne9>3.0.co;2-x

Brösamle, C., & Schwab, M. E. (2000). Ipsilateral, ventral corticospinal tract of the adult rat: ultrastructure, myelination and synaptic connections. *Journal of Neurocytology, 29*(7), 499-507. Retrieved from http://www.ncbi.nlm.nih.gov/pubmed/11279365

Brown, A. R., & Teskey, G. C. (2014). Motor Cortex Is Functionally Organized as a Set of Spatially Distinct Representations for Complex Movements. *Journal of Neuroscience, 34*(41), 13574-13585. doi:10.1523/JNEUROSCI.2500-14.2014

Calautti, C., Leroy, F., Guincestre, J. Y., Marié, R. M., & Baron, J. C. (2001). Sequential activation brain mapping after subcortical stroke: changes in hemispheric balance and recovery. *Neuroreport, 12*(18), 3883-3886. Retrieved from http://www.ncbi.nlm.nih.gov/pubmed/11742203

Catani, M. (2017). A little man of some importance. *Brain, 140*(11), 3055-3061. doi:10.1093/brain/awx270

Chen, S. X., Kim, A. N., Peters, A. J., & Komiyama, T. (2015). Subtype-specific plasticity of inhibitory circuits in motor cortex during motor learning. *Nat Neurosci, 18*(8), 1109-1115. doi:10.1038/nn.4049

Chen, X. Y., Chen, L., Chen, Y., & Wolpaw, J. R. (2006). Operant conditioning of reciprocal inhibition in rat soleus muscle. *Journal of Neurophysiology, 96*(4), 2144-2150. doi:10.1152/jn.00253.2006

Cheney, P. D., & Fetz, E. E. (1985). Comparable patterns of muscle facilitation evoked by individual corticomotoneuronal (CM) cells and by single intracortical microstimuli in primates: evidence for functional groups of CM cells. *Journal of Neurophysiology, 53*(3), 786-804. Retrieved from http://www.ncbi.nlm.nih.gov/pubmed/2984354

Churchland, M. M., Santhanam, G., & Shenoy, K. V. (2006). Preparatory activity in premotor and motor cortex reflects the speed of the upcoming reach. *Journal of Neurophysiology, 96*(6), 3130-3146. doi:10.1152/jn.00307.2006

Churchland, M. M., & Shenoy, K. V. (2007). Delay of movement caused by disruption of cortical preparatory activity. *Journal of Neurophysiology, 97*(1), 348-359. doi:10.1152/jn.00808.2006

Cisek, P., Crammond, D. J., & Kalaska, J. F. (2003). Neural activity in primary motor and dorsal premotor cortex in reaching tasks with the contralateral versus ipsilateral arm. *Journal of Neurophysiology, 89*(2), 922-942. doi:10.1152/jn.00607.2002

Clarey, J. C., Tweedale, R., & Calford, M. B. (1996). Interhemispheric modulation of somatosensory receptive fields: evidence for plasticity in primary somatosensory cortex. *Cerebral Cortex (New York, N.Y.: 1991), 6*(2), 196-206. Retrieved from http://www.ncbi.nlm.nih.gov/pubmed/8670650

Classen, J., Liepert, J., Wise, S. P., Hallett, M., & Cohen, L. G. (1998). Rapid plasticity of human cortical movement representation induced by practice. *Journal of Neurophysiology, 79*(2), 1117-1123. Retrieved from http://www.ncbi.nlm.nih.gov/pubmed/9463469

Conroy, S. K., Brownlowe, K. B., & McAllister, T. W. (2020). Depression Comorbid With Stroke, Traumatic Brain Injury, Parkinson's Disease, and Multiple Sclerosis: Diagnosis and Treatment. *Focus (Am Psychiatr Publ), 18*(2), 150-161. doi:10.1176/appi.focus.20200004

Côté, S. L., Elgbeili, G., Quessy, S., & Dancause, N. (2020). Modulatory effects of the supplementary motor area on primary motor cortex outputs. *Journal of Neurophysiology, 123*(1), 407-419. doi:10.1152/jn.00391.2019

Côté, S. L., Hamadjida, A., Quessy, S., & Dancause, N. (2017). Contrasting modulatory effects from the dorsal and ventral premotor cortex on primary motor cortex outputs. *The Journal of Neuroscience: The Official Journal of the Society for Neuroscience*. doi:10.1523/JNEUROSCI.0462-17.2017

Cramer, S. C. (2008). Repairing the human brain after stroke. II. Restorative therapies. *Ann Neurol, 63*(5), 549-560. doi:10.1002/ana.21412

Dancause, N. (2006). Vicarious Function of Remote Cortex Following Stroke: Recent Evidence from Human and Animal Studies. *The Neuroscientist, 12*(6), 489-499. doi:10.1177/1073858406292782

Dancause, N., Barbay, S., Frost, S. B., Plautz, E. J., Chen, D., Zoubina, E. V., . . . Nudo, R. J. (2005). Extensive Cortical Rewiring After Brain Injury. *The Journal of Neuroscience, 25*(44), 10167-10179. doi:10.1523/JNEUROSCI.3256-05.2005

Dancause, N., Barbay, S., Frost, S. B., Zoubina, E. V., Plautz, E. J., Mahnken, J. D., & Nudo, R. J. (2006). Effects of Small Ischemic Lesions in the Primary Motor Cortex on Neurophysiological Organization in Ventral Premotor Cortex. *Journal of Neurophysiology, 96*(6), 3506-3511. doi:10.1152/jn.00792.2006

Dancause, N., Touvykine, B., & Mansoori, B. K. (2015). Inhibition of the contralesional hemisphere after stroke: reviewing a few of the building blocks with a focus on animal models. *Progress in Brain Research, 218*, 361-387. doi:10.1016/bs.pbr.2015.01.002

Davare, M., Andres, M., Cosnard, G., Thonnard, J.-L., & Olivier, E. (2006). Dissociating the Role of Ventral and Dorsal Premotor Cortex in Precision Grasping. *The Journal of Neuroscience, 26*(8), 2260-2268. doi:10.1523/JNEUROSCI.3386-05.2006

Dayan, E., & Cohen, L. G. (2011). Neuroplasticity subserving motor skill learning. *Neuron, 72*(3), 443-454. doi:10.1016/j.neuron.2011.10.008

Dea, M., Hamadjida, A., Elgbeili, G., Quessy, S., & Dancause, N. (2016). Different Patterns of Cortical Inputs to Subregions of the Primary Motor Cortex Hand Representation in Cebus apella. *Cerebral Cortex (New York, N.Y.: 1991), 26*(4), 1747-1761. doi:10.1093/cercor/bhv324

Deffeyes, J. E., Touvykine, B., Quessy, S., & Dancause, N. (2015). Interactions between rostral and caudal cortical motor areas in the rat. *Journal of Neurophysiology*, jn.00760.02014. doi:10.1152/jn.00760.2014

di Pellegrino, G., & Wise, S. P. (1993). Visuospatial versus visuomotor activity in the premotor and prefrontal cortex of a primate. *The Journal of neuroscience : the official journal of the Society for Neuroscience, 13*(3), 1227-1243. doi:10.1523/jneurosci.13-03-01227.1993

Drew, T., Jiang, W., Kably, B., & Lavoie, S. (1996). Role of the motor cortex in the control of visually triggered gait modifications. *Canadian Journal of Physiology and Pharmacology, 74*(4), 426-442. Retrieved from http://www.ncbi.nlm.nih.gov/pubmed/8828889

Dum, R. P., & Strick, P. L. (1991). The Origin of Corticospinal Projections from the Premotor Areas in the Frontal Lobe. *The Journal of Neuroscience, 11*(3), 667-689. Retrieved from http://www.jneurosci.org/content/11/3/667

http://www.jneurosci.org/content/11/3/667.long

Dum, R. P., & Strick, P. L. (1996). Spinal cord terminations of the medial wall motor areas in macaque monkeys. *The Journal of neuroscience : the official journal of the Society for Neuroscience, 16*(20), 6513-6525. doi:10.1523/jneurosci.16-20-06513.1996

Dum, R. P., & Strick, P. L. (2002). Motor areas in the frontal lobe of the primate. *Physiol Behav, 77*(4-5), 677-682.

Duncan, P. W., Goldstein, L. B., Matchar, D., Divine, G. W., & Feussner, J. (1992). Measurement of motor recovery after stroke. Outcome assessment and sample size requirements. *Stroke, 23*(8), 1084-1089. doi:10.1161/01.str.23.8.1084

Engelhard, C., Chizhov, I., Siebert, F., & Engelhard, M. (2018). Microbial Halorhodopsins: Light-Driven Chloride Pumps. *Chem Rev, 118*(21), 10629-10645. doi:10.1021/acs.chemrev.7b00715

Ferrier, D. (1874). The localization of function in the brain. *Proc. R. Soc. Lond., 22*, 228-232. doi:https://doi.org/10.1098/rspl.1873.0032

Ferrier, D. (1883). The Effects of Lesions of Different Regions of the Cerebral Hemispheres. *Proceedings of the Royal Society of London., 36*, 222-224.

Fogassi, L., Gallese, V., Buccino, G., Craighero, L., Fadiga, L., & Rizzolatti, G. (2001). Cortical mechanism for the visual guidance of hand grasping movements in the monkey: A reversible inactivation study. *Brain, 124*(Pt 3), 571-586. doi:10.1093/brain/124.3.571

Frost, S. B., Barbay, S., Friel, K. M., Plautz, E. J., & Nudo, R. J. (2003). Reorganization of remote cortical regions after ischemic brain injury: a potential substrate for stroke recovery. *Journal of Neurophysiology, 89*(6), 3205-3214. doi:10.1152/jn.01143.2002

Fu, Q. G., Flament, D., Coltz, J. D., & Ebner, T. J. (1995). Temporal encoding of movement kinematics in the discharge of primate primary motor and premotor neurons. *Journal of Neurophysiology, 73*(2), 836-854. doi:10.1152/jn.1995.73.2.836

Fujii, Y., & Nakada, T. (2003). Cortical reorganization in patients with subcortical hemiparesis: neural mechanisms of functional recovery and prognostic implication. *Journal of neurosurgery, 98*(1), 64-73. doi:10.3171/jns.2003.98.1.0064

Fulton, J. F. (1935). A Note on the Definition of the "motor" and "premotor" Areas. *Brain, 58*(2), 311-316. doi:10.1093/brain/58.2.311

Georgopoulos, A. P. (1986). On reaching. *Annu Rev Neurosci, 9*, 147-170. doi:10.1146/annurev.ne.09.030186.001051

Georgopoulos, A. P., Kalaska, J. F., Caminiti, R., & Massey, J. T. (1982). On the relations between the direction of two-dimensional arm movements and cell discharge in primate motor cortex. *The Journal of neuroscience : the official journal of the Society for Neuroscience, 2*(11), 1527-1537. doi:10.1523/jneurosci.02-11-01527.1982

Georgopoulos, A. P., Schwartz, A. B., & Kettner, R. E. (1986). Neuronal population coding of movement direction. *Science, 233*(4771), 1416-1419. doi:10.1126/science.3749885

Glees, P., Cole, J., Whitty, C. W., & Cairns, H. (1950). The effects of lesions in the cingular gyrus and adjacent areas in monkeys. *Journal of Neurology, Neurosurgery, and Psychiatry, 13*(3), 178-190. doi:10.1136/jnnp.13.3.178

Godschalk, M., Mitz, A. R., van Duin, B., & van der Burg, H. (1995). Somatotopy of monkey premotor cortex examined with microstimulation. *Neurosci Res, 23*(3), 269-279. doi:10.1016/0168-0102(95)00950-7

Grillner, S. (1985). Neurobiological bases of rhythmic motor acts in vertebrates. *Science, 228*(4696), 143-149. doi:10.1126/science.3975635

Gross, C. G. (2007). The discovery of motor cortex and its background. *J Hist Neurosci, 16*(3), 320-331. doi:10.1080/09647040600630160

Hakim, A. M., Silver, F., & Hodgson, C. (1998). Organized stroke care: A new era in stroke prevention and treatment. *CMAJ: Canadian Medical Association Journal, 159*(6), S1. Retrieved from http://www.ncbi.nlm.nih.gov/pmc/articles/PMC1255890/

Halley, A. C., Baldwin, M. K. L., Cooke, D. F., Englund, M., & Krubitzer, L. (2020). Distributed Motor Control of Limb Movements in Rat Motor and Somatosensory Cortex: The Sensorimotor Amalgam Revisited. *Cerebral Cortex (New York, NY)*. doi:10.1093/cercor/bhaa186

Hamadjida, A., Dea, M., Deffeyes, J., Quessy, S., & Dancause, N. (2016). Parallel Cortical Networks Formed by Modular Organization of Primary Motor Cortex Outputs. *Current biology: CB, 26*(13), 1737-1743. doi:10.1016/j.cub.2016.04.068

Harel, N. Y., & Strittmatter, S. M. (2006). Can regenerating axons recapitulate developmental guidance during recovery from spinal cord injury? *Nature Reviews Neuroscience, 7*(8), 603-616. doi:10.1038/nrn1957

Harrison, T. R. (1994). Harrison's principles of internal medicine Vol. 2 Vol. 2. New York [u.a.: McGraw-Hill.

Hawe, R. L., Scott, S. H., & Dukelow, S. P. (2018). Taking Proportional Out of Stroke Recovery. *Stroke*, Strokeaha118023006. doi:10.1161/strokeaha.118.023006

He, S. Q., Dum, R. P., & Strick, P. L. (1993). Topographic organization of corticospinal projections from the frontal lobe: motor areas on the lateral surface of the hemisphere. *The Journal of neuroscience : the official journal of the Society for Neuroscience, 13*(3), 952-980. doi:10.1523/jneurosci.13-03-00952.1993

He, S. Q., Dum, R. P., & Strick, P. L. (1995). Topographic organization of corticospinal projections from the frontal lobe: motor areas on the medial surface of the hemisphere. *The Journal of neuroscience : the official journal of the Society for Neuroscience, 15*(5 Pt 1), 3284-3306. doi:10.1523/jneurosci.15-05-03284.1995

Hendricks, H. T., Zwarts, M. J., Plat, E. F., & van Limbeek, J. (2002). Systematic review for the early prediction of motor and functional outcome after stroke by using motor-evoked potentials. *Archives of Physical Medicine and Rehabilitation, 83*(9), 1303-1308. doi:10.1053/apmr.2002.34284

Hermer-Vazquez, L., Hermer-Vazquez, R., Moxon, K. A., Kuo, K. H., Viau, V., Zhan, Y., & Chapin, J. K. (2004). Distinct temporal activity patterns in the rat M1 and red nucleus during skilled versus unskilled limb movement. *Behavioural Brain Research, 150*(1–2), 93-107. doi:10.1016/S0166-4328(03)00226-2

Hess, G. (2004). Synaptic plasticity of local connections in rat motor cortex. *Acta Neurobiologiae Experimentalis, 64*(2), 271-276. Retrieved from http://www.ncbi.nlm.nih.gov/pubmed/15366258

Hira, R., Ohkubo, F., Tanaka, Y. R., Masamizu, Y., Augustine, G. J., Kasai, H., & Matsuzaki, M. (2013a). In vivo optogenetic tracing of functional corticocortical connections between motor forelimb areas. *Frontiers in neural circuits, 7*, 55. doi:10.3389/fncir.2013.00055

Hira, R., Ohkubo, F., Tanaka, Y. R., Masamizu, Y., Augustine, G. J., Kasai, H., & Matsuzaki, M. (2013b). In vivo optogenetic tracing of functional corticocortical connections between motor forelimb areas. *Frontiers in Neural Circuits, 7*. doi:10.3389/fncir.2013.00055

Hoshi, E., & Tanji, J. (2007). Distinctions between dorsal and ventral premotor areas: anatomical connectivity and functional properties. *Current Opinion in Neurobiology, 17*(2), 234-242. doi:10.1016/j.conb.2007.02.003

Ince, L. P. (1980). Behavioral Psychology in Rehabilitation Medicine: Clinical Applications: Williams & Wilkins Company.

Jackson, J. H. (1870). A Study of Convulsions. Transactions of St. Andrews Medical Graduates' Association, 3, 162-204.

Jacobs, K. M., & Donoghue, J. P. (1991). Reshaping the cortical motor map by unmasking latent intracortical connections. *Science (New York, N.Y.), 251*(4996), 944-947. Retrieved from http://www.ncbi.nlm.nih.gov/pubmed/2000496

Jaillard, A., Martin, C. D., Garambois, K., Lebas, J. F., & Hommel, M. (2005). Vicarious function within the human primary motor cortex? A longitudinal fMRI stroke study. *Brain, 128*(Pt 5), 1122-1138. doi:10.1093/brain/awh456

Jeffers, M. S., Karthikeyan, S., & Corbett, D. (2018). Does Stroke Rehabilitation Really Matter? Part A: Proportional Stroke Recovery in the Rat. *Neurorehabilitation and Neural Repair, 32*(1), 3-6. doi:10.1177/1545968317751210

Jenny, A. B., & Inukai, J. (1983). Principles of motor organization of the monkey cervical spinal cord. *The Journal of neuroscience : the official journal of the Society for Neuroscience, 3*(3), 567-575. doi:10.1523/jneurosci.03-03-00567.1983

Jurgens, U. (1984). The efferent and afferent connections of the supplementary motor area. *Brain Res, 300*(1), 63-81.

Kakei, S., Hoffman, D. S., & Strick, P. L. (2001). Direction of action is represented in the ventral premotor cortex. *Nat Neurosci, 4*(10), 1020-1025. doi:10.1038/nn726

Kawai, R., Markman, T., Poddar, R., Ko, R., Fantana, Antoniu L., Dhawale, Ashesh K., . . . Ölveczky, Bence P. Motor Cortex Is Required for Learning but Not for Executing a Motor Skill. *Neuron*. doi:10.1016/j.neuron.2015.03.024

Kermadi, I., Liu, Y., & Rouiller, E. M. (2000). Do bimanual motor actions involve the dorsal premotor (PMd), cingulate (CMA) and posterior parietal (PPC) cortices? Comparison with

primary and supplementary motor cortical areas. *Somatosensory & Motor Research, 17*(3), 255-271.

Kermadi, I., Liu, Y., Tempini, A., Calciati, E., & Rouiller, E. M. (1998). Neuronal activity in the primate supplementary motor area and the primary motor cortex in relation to spatio-temporal bimanual coordination. *Somatosensory & Motor Research, 15*(4), 287-308.

Kerr, A. L., Wolke, M. L., Bell, J. A., & Jones, T. A. (2013). Post-stroke protection from maladaptive effects of learning with the non-paretic forelimb by bimanual home cage experience in C57BL/6 mice. *Behav Brain Res, 252*, 180-187. doi:10.1016/j.bbr.2013.05.062

Kim, S., Stephenson, M. C., Morris, P. G., & Jackson, S. R. (2014). tDCS-induced alterations in GABA concentration within primary motor cortex predict motor learning and motor memory: a 7 T magnetic resonance spectroscopy study. *NeuroImage, 99*, 237-243. doi:10.1016/j.neuroimage.2014.05.070

Kim, Y.-H., Park, J.-W., Ko, M.-H., Jang, S. H., & Lee, P. K. W. (2004). Facilitative effect of high frequency subthreshold repetitive transcranial magnetic stimulation on complex sequential motor learning in humans. *Neuroscience Letters, 367*(2), 181-185. doi:10.1016/j.neulet.2004.05.113

Kinoshita, M., Matsui, R., Kato, S., Hasegawa, T., Kasahara, H., Isa, K., . . . Isa, T. (2012). Genetic dissection of the circuit for hand dexterity in primates. *Nature, 487*(7406), 235-238. doi:10.1038/nature11206

Kitago, T., Liang, J., Huang, V. S., Hayes, S., Simon, P., Tenteromano, L., . . . Krakauer, J. W. (2013). Improvement after constraint-induced movement therapy: recovery of normal motor control or task-specific compensation? *Neurorehabilitation and Neural Repair, 27*(2), 99-109. doi:10.1177/1545968312452631

Kleim, J. A., Barbay, S., & Nudo, R. J. (1998). Functional Reorganization of the Rat Motor Cortex Following Motor Skill Learning. *Journal of Neurophysiology, 80*(6), 3321-3325. Retrieved from http://jn.physiology.org/content/80/6/3321

files/1022/3321.html

Kosinski, R. J., Neafsey, E. J., & Castro, A. J. (1986). A comparative topographical analysis of dorsal column nuclear and cerebral cortical projections to the basilar pontine gray in rats. *The Journal of comparative neurology, 244*(2), 163-173. doi:10.1002/cne.902440204

Künzle, H. (1975). Bilateral projections from precentral motor cortex to the putamen and other parts of the basal ganglia. An autoradiographic study in Macaca fascicularis. *Brain Res, 88*(2), 195-209. doi:10.1016/0006-8993(75)90384-4

Künzle, H. (1978). An autoradiographic analysis of the efferent connections from premotor and adjacent prefrontal regions (areas 6 and 9) in macaca fascicularis. *Brain Behav Evol, 15*(3), 185-234. doi:10.1159/000123779

Kurata, K. (1993). Premotor cortex of monkeys: set- and movement-related activity reflecting amplitude and direction of wrist movements. *Journal of Neurophysiology, 69*(1), 187-200. doi:10.1152/jn.1993.69.1.187

Kurata, K., & Hoffman, D. S. (1994). Differential effects of muscimol microinjection into dorsal and ventral aspects of the premotor cortex of monkeys. *Journal of Neurophysiology, 71*(3), 1151-1164. doi:10.1152/jn.1994.71.3.1151

Kurata, K., & Hoshi, E. (1999). Reacquisition deficits in prism adaptation after muscimol microinjection into the ventral premotor cortex of monkeys. *Journal of Neurophysiology, 81*(4), 1927-1938. doi:10.1152/jn.1999.81.4.1927

Kurata, K., & Hoshi, E. (2002). Movement-related neuronal activity reflecting the transformation of coordinates in the ventral premotor cortex of monkeys. *Journal of Neurophysiology, 88*(6), 3118-3132. doi:10.1152/jn.00070.2002

Kurata, K., & Tanji, J. (1985). Contrasting neuronal activity in supplementary and precentral motor cortex of monkeys. II. Responses to movement triggering vs. nontriggering sensory signals. *Journal of Neurophysiology, 53*(1), 142-152. doi:10.1152/jn.1985.53.1.142

Kwakkel, G. (2006). Impact of intensity of practice after stroke: issues for consideration. *Disabil Rehabil, 28*(13-14), 823-830. doi:10.1080/09638280500534861

Kwakkel, G., Veerbeek, J. M., van Wegen, E. E., & Wolf, S. L. (2015). Constraint-induced movement therapy after stroke. *Lancet Neurol, 14*(2), 224-234. doi:10.1016/s1474-4422(14)70160-7

Lang, C. E., Macdonald, J. R., Reisman, D. S., Boyd, L., Jacobson Kimberley, T., Schindler-Ivens, S. M., . . . Scheets, P. L. (2009). Observation of amounts of movement practice provided during stroke rehabilitation. *Archives of Physical Medicine and Rehabilitation, 90*(10), 1692-1698. doi:10.1016/j.apmr.2009.04.005

Leyton, A. S. F., & Sherrington, C. S. (1917). Observations on the Excitable Cortex of the Chimpanzee, Orang-utan, and Gorilla: Griffin.

Li, X. G., Florence, S. L., & Kaas, J. H. (1990). Areal distributions of cortical neurons projecting to different levels of the caudal brain stem and spinal cord in rats. *Somatosensory & Motor Research, 7*(3), 315-335. Retrieved from http://www.ncbi.nlm.nih.gov/pubmed/2248004

Liu, Y., & Rouiller, E. M. (1999). Mechanisms of recovery of dexterity following unilateral lesion of the sensorimotor cortex in adult monkeys. *Experimental brain research, 128*(1), 149-159.

Lukashin, A. V., & Georgopoulos, A. P. (1993). A dynamical neural network model for motor cortical activity during movement: population coding of movement trajectories. *Biol Cybern, 69*(5-6), 517-524.

Luke, L. M., Allred, R. P., & Jones, T. A. (2004). Unilateral ischemic sensorimotor cortical damage induces contralesional synaptogenesis and enhances skilled reaching with the ipsilateral forelimb in adult male rats. *Synapse (New York, N.Y.), 54*(4), 187-199. doi:10.1002/syn.20080

Luppino, G., Matelli, M., Camarda, R., & Rizzolatti, G. (1993). Corticocortical connections of area F3 (SMA-proper) and area F6 (pre-SMA) in the macaque monkey. *The Journal of comparative neurology, 338*(1), 114-140. doi:10.1002/cne.903380109

M. Rouiller, E. (2003). The dual pattern of corticothalamic projection of the premotor cortex in macaque monkeys (Vol. 2).

McCabe, J., Monkiewicz, M., Holcomb, J., Pundik, S., & Daly, J. J. (2015). Comparison of robotics, functional electrical stimulation, and motor learning methods for treatment of persistent upper extremity dysfunction after stroke: a randomized controlled trial. *Archives of Physical Medicine and Rehabilitation, 96*(6), 981-990. doi:10.1016/j.apmr.2014.10.022

Messier, J., & Kalaska, J. F. (2000). Covariation of primate dorsal premotor cell activity with direction and amplitude during a memorized-delay reaching task. *Journal of Neurophysiology, 84*(1), 152-165. doi:10.1152/jn.2000.84.1.152

Milliken, G. W., Plautz, E. J., & Nudo, R. J. (2013). Distal forelimb representations in primary motor cortex are redistributed after forelimb restriction: a longitudinal study in adult squirrel monkeys. *Journal of Neurophysiology, 109*(5), 1268-1282. doi:10.1152/jn.00044.2012

Mitz, A. R., & Wise, S. P. (1987). The somatotopic organization of the supplementary motor area: intracortical microstimulation mapping. *The Journal of neuroscience : the official journal of the Society for Neuroscience, 7*(4), 1010-1021. doi:10.1523/jneurosci.07-04-01010.1987

Mohajerani, M. H., Aminoltejari, K., & Murphy, T. H. (2011). Targeted mini-strokes produce changes in interhemispheric sensory signal processing that are indicative of disinhibition within minutes. *Proceedings of the National Academy of Sciences of the United States of America, 108*(22), E183-191. doi:10.1073/pnas.1101914108

Molina-Luna, K., Hertler, B., Buitrago, M. M., & Luft, A. R. (2008). Motor learning transiently changes cortical somatotopy. *NeuroImage, 40*(4), 1748-1754. doi:10.1016/j.neuroimage.2007.11.018

Moreau-Debord, I., Serrano, É., Quessy, S., & Dancause, N. (2021). Rapid and Bihemispheric Reorganization of Neuronal Activity in Premotor Cortex after Brain Injury. *The Journal of neuroscience : the official journal of the Society for Neuroscience, 41*(44), 9112-9128. doi:10.1523/jneurosci.0196-21.2021

Muakkassa, K. F., & Strick, P. L. (1979). Frontal lobe inputs to primate motor cortex: evidence for four somatotopically organized 'premotor' areas. *Brain Res, 177*(1), 176-182. doi:10.1016/0006-8993(79)90928-4

Murphy, W. J., Pevzner, P. A., & O'Brien, S. J. (2004). Mammalian phylogenomics comes of age. *Trends Genet, 20*(12), 631-639. doi:10.1016/j.tig.2004.09.005

Neafsey, E. J., Bold, E. L., Haas, G., Hurley-Gius, K. M., Quirk, G., Sievert, C. F., & Terreberry, R. R. (1986). The organization of the rat motor cortex: a microstimulation mapping study. *Brain Research, 396*(1), 77-96. Retrieved from http://www.ncbi.nlm.nih.gov/pubmed/3708387

Neafsey, E. J., & Sievert, C. (1982). A second forelimb motor area exists in rat frontal cortex. *Brain Research, 232*(1), 151-156. doi:10.1016/0006-8993(82)90617-5

Nei, M., Xu, P., & Glazko, G. (2001). Estimation of divergence times from multiprotein sequences for a few mammalian species and several distantly related organisms. *Proceedings of the National Academy of Sciences of the United States of America, 98*(5), 2497-2502. doi:10.1073/pnas.051611498

Nielsen, J., Crone, C., & Hultborn, H. (1993). H-reflexes are smaller in dancers from The Royal Danish Ballet than in well-trained athletes. *European Journal of Applied Physiology and Occupational Physiology, 66*(2), 116-121. Retrieved from http://www.ncbi.nlm.nih.gov/pubmed/8472692

Nieuwenhuys, R. (2013). The myeloarchitectonic studies on the human cerebral cortex of the Vogt-Vogt school, and their significance for the interpretation of functional neuroimaging data. *Brain Struct Funct, 218*(2), 303-352. doi:10.1007/s00429-012-0460-z

Nogles, T. E., & Galuska, M. A. (2022). Middle Cerebral Artery Stroke. In *StatPearls*. Treasure Island (FL): StatPearls Publishing Copyright © 2022, StatPearls Publishing LLC.

Nudo, R. J., & Frost, S. B. (2007). The Evolution of Motor Cortex and Motor Systems. *Evolution of Nervous Systems, 3*, 373-395.

Nudo, R. J., & Masterton, R. B. (1990). Descending pathways to the spinal cord, III: Sites of origin of the corticospinal tract. *The Journal of comparative neurology, 296*(4), 559-583. doi:10.1002/cne.902960405

Nudo, R. J., & Milliken, G. W. (1996). Reorganization of movement representations in primary motor cortex following focal ischemic infarcts in adult squirrel monkeys. *Journal of Neurophysiology, 75*(5), 2144-2149. Retrieved from http://www.ncbi.nlm.nih.gov/pubmed/8734610

Nudo, R. J., Milliken, G. W., Jenkins, W. M., & Merzenich, M. M. (1996). Use-Dependent Alterations of Movement Representations in Primary Motor Cortex of Adult Squirrel Monkeys. *The Journal of Neuroscience, 16*(2), 785-807. Retrieved from http://www.jneurosci.org/content/16/2/785

files/1699/Nudo et al. - 1996 - Use-Dependent Alterations of Movement Representati.html

Ochiai, T., Mushiake, H., & Tanji, J. (2005). Involvement of the ventral premotor cortex in controlling image motion of the hand during performance of a target-capturing task. *Cerebral Cortex (New York, NY), 15*(7), 929-937. doi:10.1093/cercor/bhh193

Osu, R., Franklin, D. W., Kato, H., Gomi, H., Domen, K., Yoshioka, T., & Kawato, M. (2002). Short- and long-term changes in joint co-contraction associated with motor learning as revealed

from surface EMG. *Journal of Neurophysiology, 88*(2), 991-1004. Retrieved from http://www.ncbi.nlm.nih.gov/pubmed/12163548

Park, M. C., Belhaj-Saïf, A., & Cheney, P. D. (2004). Properties of primary motor cortex output to forelimb muscles in rhesus macaques. *Journal of Neurophysiology, 92*(5), 2968-2984. doi:10.1152/jn.00649.2003

Penfield, W., & Boldrey, E. (1937). Somatic motor and sensory representation in the cerebral cortex of man as studied by electrical stimulation. *Brain, 60*(4), 389-443. doi:10.1093/brain/60.4.389

Pesaran, B., Nelson, M. J., & Andersen, R. A. (2006). Dorsal premotor neurons encode the relative position of the hand, eye, and goal during reach planning. *Neuron, 51*(1), 125-134. doi:10.1016/j.neuron.2006.05.025

Peters, A. J., Lee, J., Hedrick, N. G., O'Neil, K., & Komiyama, T. (2017). Reorganization of corticospinal output during motor learning. *Nat Neurosci, 20*(8), 1133-1141. doi:10.1038/nn.4596

Phac. (2011). Tracking Heart Disease and Stroke in Canada - Public Health Agency of Canada. Retrieved from http://www.phac-aspc.gc.ca/cd-mc/cvd-mcv/sh-fs-2011/index-eng.php

files/1702/index-eng.html

Picard, N., & Strick, P. L. (1996). Motor Areas of the Medial Wall: A Review of Their Location and Functional Activation. *Cerebral Cortex, 6*(3), 342-353. doi:10.1093/cercor/6.3.342

Platz, T., Adler-Wiebe, M., Roschka, S., & Lotze, M. (2018). Enhancement of motor learning by focal intermittent theta burst stimulation (iTBS) of either the primary motor (M1) or somatosensory area (S1) in healthy human subjects. *Restorative Neurology and Neuroscience, 36*, 117-130. doi:10.3233/RNN-170774

Platz, T., Roschka, S., Christel, M. I., Duecker, F., Rothwell, J. C., & Sack, A. T. (2012). Early stages of motor skill learning and the specific relevance of the cortical motor system--a combined behavioural training and θ burst TMS study. *Restor Neurol Neurosci, 30*(3), 199-211. doi:10.3233/rnn-2012-110204

Prabhakaran, S., Zarahn, E., Riley, C., Speizer, A., Chong, J. Y., Lazar, R. M., . . . Krakauer, J. W. (2008). Inter-individual variability in the capacity for motor recovery after ischemic stroke. *Neurorehabilitation and Neural Repair, 22*(1), 64-71. doi:10.1177/1545968307305302

Qi, H. X., Stepniewska, I., & Kaas, J. H. (2000). Reorganization of primary motor cortex in adult macaque monkeys with long-standing amputations. *Journal of Neurophysiology, 84*(4), 2133-2147. doi:10.1152/jn.2000.84.4.2133

Qü, M., Buchkremer-Ratzmann, I., Schiene, K., Schroeter, M., Witte, O. W., & Zilles, K. (1998). Bihemispheric reduction of GABAA receptor binding following focal cortical photothrombotic

lesions in the rat brain. *Brain Research, 813*(2), 374-380. Retrieved from http://www.ncbi.nlm.nih.gov/pubmed/9838197

Quessy, S., Côté, S. L., Hamadjida, A., Deffeyes, J., & Dancause, N. (2016). Modulatory Effects of the Ipsi and Contralateral Ventral Premotor Cortex (PMv) on the Primary Motor Cortex (M1) Outputs to Intrinsic Hand and Forearm Muscles in Cebus apella. *Cerebral Cortex (New York, NY), 26*(10), 3905-3920. doi:10.1093/cercor/bhw186

Rahman, A. A., Amruta, N., Pinteaux, E., & Bix, G. J. (2021). Neurogenesis After Stroke: A Therapeutic Perspective. *Transl Stroke Res, 12*(1), 1-14. doi:10.1007/s12975-020-00841-w

Rehme, A. K., Eickhoff, S. B., Rottschy, C., Fink, G. R., & Grefkes, C. (2012). Activation likelihood estimation meta-analysis of motor-related neural activity after stroke. *NeuroImage, 59*(3), 2771-2782. doi:10.1016/j.neuroimage.2011.10.023

Rioult-Pedotti, M. S., Friedman, D., Hess, G., & Donoghue, J. P. (1998). Strengthening of horizontal cortical connections following skill learning. *Nature Neuroscience, 1*(3), 230-234. doi:10.1038/678

Rizzolatti, G., Matelli, M., & Pavesi, G. (1983). Deficits in attention and movement following the removal of postarcuate (area 6) and prearcuate (area 8) cortex in macaque monkeys. *Brain, 106 (Pt 3)*, 655-673. doi:10.1093/brain/106.3.655

Rondina, J. M., Park, C.-h., & Ward, N. S. (2017). Brain regions important for recovery after severe post-stroke upper limb paresis. *Journal of Neurology, Neurosurgery, and Psychiatry, 88*(9), 737-743. doi:10.1136/jnnp-2016-315030

Rouiller, E. M., Babalian, A., Kazennikov, O., Moret, V., Yu, X. H., & Wiesendanger, M. (1994). Transcallosal connections of the distal forelimb representations of the primary and supplementary motor cortical areas in macaque monkeys. *Exp Brain Res, 102*(2), 227-243.

Rouiller, E. M., Moret, V., & Liang, F. (1993). Comparison of the connectional properties of the two forelimb areas of the rat sensorimotor cortex: support for the presence of a premotor or supplementary motor cortical area. *Somatosensory & Motor Research, 10*(3), 269-289. Retrieved from http://www.ncbi.nlm.nih.gov/pubmed/8237215

Rouiller, E. M., Tanné, J., Moret, V., Kermadi, I., Boussaoud, D., & Welker, E. (1998). Dual morphology and topography of the corticothalamic terminals originating from the primary, supplementary motor, and dorsal premotor cortical areas in macaque monkeys. *The Journal of Comparative Neurology, 396*(2), 169-185. Retrieved from http://www.ncbi.nlm.nih.gov/pubmed/9634140

Sacrey, L. A., Alaverdashvili, M., & Whishaw, I. Q. (2009). Similar hand shaping in reaching-for-food (skilled reaching) in rats and humans provides evidence of homology in release, collection, and manipulation movements. *Behav Brain Res, 204*(1), 153-161. doi:10.1016/j.bbr.2009.05.035

Saunders, D. H., Greig, C. A., & Mead, G. E. (2014). Physical activity and exercise after stroke: review of multiple meaningful benefits. *Stroke, 45*(12), 3742-3747. doi:10.1161/strokeaha.114.004311

Schaar, K. L., Brenneman, M. M., & Savitz, S. I. (2010). Functional assessments in the rodent stroke model. *Exp Transl Stroke Med, 2*(1), 13. doi:10.1186/2040-7378-2-13

Schallert, T., Fleming, S. M., Leasure, J. L., Tillerson, J. L., & Bland, S. T. (2000). CNS plasticity and assessment of forelimb sensorimotor outcome in unilateral rat models of stroke, cortical ablation, parkinsonism and spinal cord injury. *Neuropharmacology, 39*(5), 777-787. doi:10.1016/s0028-3908(00)00005-8

Schieber, M. H. (2000). Inactivation of the ventral premotor cortex biases the laterality of motoric choices. *Exp Brain Res, 130*(4), 497-507. doi:10.1007/s002219900270

Schieber, M. H., & Hibbard, L. S. (1993). How somatotopic is the motor cortex hand area? *Science (New York, N.Y.), 261*(5120), 489-492. Retrieved from http://www.ncbi.nlm.nih.gov/pubmed/8332915

Schieber, M. H., & Poliakov, A. V. (1998). Partial Inactivation of the Primary Motor Cortex Hand Area: Effects on Individuated Finger Movements. *The Journal of Neuroscience, 18*(21), 9038-9054. Retrieved from http://www.jneurosci.org/content/18/21/9038

http://www.jneurosci.org/content/18/21/9038.long

Schiene, K., Bruehl, C., Zilles, K., Qü, M., Hagemann, G., Kraemer, M., & Witte, O. W. (1996). Neuronal hyperexcitability and reduction of GABAA-receptor expression in the surround of cerebral photothrombosis. *Journal of cerebral blood flow and metabolism: official journal of the International Society of Cerebral Blood Flow and Metabolism, 16*(5), 906-914. doi:10.1097/00004647-199609000-00014

Schmidlin, E., Brochier, T., Maier, M. A., Kirkwood, P. A., & Lemon, R. N. (2008). Pronounced Reduction of Digit Motor Responses Evoked from Macaque Ventral Premotor Cortex after Reversible Inactivation of the Primary Motor Cortex Hand Area. *The Journal of Neuroscience, 28*(22), 5772-5783. doi:10.1523/JNEUROSCI.0944-08.2008

Schwartz, A. B., Moran, D. W., & Reina, G. A. (2004). Differential representation of perception and action in the frontal cortex. *Science, 303*(5656), 380-383. doi:10.1126/science.1087788

Scott, S. H., Sergio, L. E., & Kalaska, J. F. (1997). Reaching movements with similar hand paths but different arm orientations. II. Activity of individual cells in dorsal premotor cortex and parietal area 5. *Journal of Neurophysiology, 78*(5), 2413-2426. doi:10.1152/jn.1997.78.5.2413

Shima, K., & Tanji, J. (1998a). Both supplementary and presupplementary motor areas are crucial for the temporal organization of multiple movements. *Journal of Neurophysiology, 80*(6), 3247-3260. doi:10.1152/jn.1998.80.6.3247

Shima, K., & Tanji, J. (1998b). Role for cingulate motor area cells in voluntary movement selection based on reward. *Science (New York, N.Y.), 282*(5392), 1335-1338. Retrieved from http://www.ncbi.nlm.nih.gov/pubmed/9812901

Shima, K., & Tanji, J. (2000). Neuronal activity in the supplementary and presupplementary motor areas for temporal organization of multiple movements. *Journal of Neurophysiology, 84*(4), 2148-2160. doi:10.1152/jn.2000.84.4.2148

Shinoda, Y., Yokota, J., & Futami, T. (1981). Divergent projection of individual corticospinal axons to motoneurons of multiple muscles in the monkey. *Neuroscience Letters, 23*(1), 7-12. Retrieved from http://www.ncbi.nlm.nih.gov/pubmed/6164967

Sooksawate, T., Isa, K., Matsui, R., Kato, S., Kinoshita, M., Kobayashi, K., . . . Isa, T. (2013). Viral vector-mediated selective and reversible blockade of the pathway for visual orienting in mice. *Frontiers in Neural Circuits, 7*. doi:10.3389/fncir.2013.00162

Starkey, M. L., Bleul, C., Zörner, B., Lindau, N. T., Mueggler, T., Rudin, M., & Schwab, M. E. (2012a). Back seat driving: hindlimb corticospinal neurons assume forelimb control following ischaemic stroke. *Brain: A Journal of Neurology, 135*(Pt 11), 3265-3281. doi:10.1093/brain/aws270

Starkey, M. L., Bleul, C., Zörner, B., Lindau, N. T., Mueggler, T., Rudin, M., & Schwab, M. E. (2012b). Back seat driving: hindlimb corticospinal neurons assume forelimb control following ischaemic stroke. *Brain, 135*(11), 3265-3281. doi:10.1093/brain/aws270

Stephan, K. M., Binkofski, F., Halsband, U., Dohle, C., Wunderlich, G., Schnitzler, A., . . . Freund, H. J. (1999). The role of ventral medial wall motor areas in bimanual co-ordination. A combined lesion and activation study. *Brain, 122 (Pt 2)*, 351-368. doi:10.1093/brain/122.2.351

Stepniewska, I., Preuss, T. M., & Kaas, J. H. (2006). Ipsilateral cortical connections of dorsal and ventral premotor areas in New World owl monkeys. *The Journal of comparative neurology, 495*(6), 691-708. doi:10.1002/cne.20906

Sterr, A., Dean, P. J., Szameitat, A. J., Conforto, A. B., & Shen, S. (2014). Corticospinal tract integrity and lesion volume play different roles in chronic hemiparesis and its improvement through motor practice. *Neurorehabilitation and Neural Repair, 28*(4), 335-343. doi:10.1177/1545968313510972

Stinear, C. M., Barber, P. A., Smale, P. R., Coxon, J. P., Fleming, M. K., & Byblow, W. D. (2007). Functional potential in chronic stroke patients depends on corticospinal tract integrity. *Brain: A Journal of Neurology, 130*(Pt 1), 170-180. doi:10.1093/brain/awl333

Stinear, C. M., Byblow, W. D., Ackerley, S. J., Smith, M. C., Borges, V. M., & Barber, P. A. (2017a). PREP2: A biomarker-based algorithm for predicting upper limb function after stroke. *Ann Clin Transl Neurol, 4*(11), 811-820. doi:10.1002/acn3.488

Stinear, C. M., Byblow, W. D., Ackerley, S. J., Smith, M. C., Borges, V. M., & Barber, P. A. (2017b). Proportional Motor Recovery After Stroke: Implications for Trial Design. *Stroke, 48*(3), 795-798. doi:10.1161/strokeaha.116.016020

Stoney, S. D., Thompson, W. D., & Asanuma, H. (1968). Excitation of pyramidal tract cells by intracortical microstimulation: effective extent of stimulating current. *Journal of Neurophysiology, 31*(5), 659-669. Retrieved from http://www.ncbi.nlm.nih.gov/pubmed/5711137

Takada, M., Tokuno, H., Nambu, A., & Inase, M. (1998). Corticostriatal projections from the somatic motor areas of the frontal cortex in the macaque monkey: segregation versus overlap of input zones from the primary motor cortex, the supplementary motor area, and the premotor cortex. *Exp Brain Res, 120*(1), 114-128. doi:10.1007/s002210050384

Tanji, J. (1985). Comparison of neuronal activities in the monkey supplementary and precentral motor areas. *Behav Brain Res, 18*(2), 137-142. doi:10.1016/0166-4328(85)90069-5

Tanji, J., & Kurata, K. (1985). Contrasting neuronal activity in supplementary and precentral motor cortex of monkeys. I. Responses to instructions determining motor responses to forthcoming signals of different modalities. *Journal of Neurophysiology, 53*(1), 129-141. doi:10.1152/jn.1985.53.1.129

Taub, E. (1976). Movement in nonhuman primates deprived of somatosensory feedback. *Exercise and Sport Sciences Reviews, 4*, 335-374.

Touvykine, B., Mansoori, B. K., Jean-Charles, L., Deffeyes, J., Quessy, S., & Dancause, N. (2016). The Effect of Lesion Size on the Organization of the Ipsilesional and Contralesional Motor Cortex. *Neurorehabilitation and Neural Repair, 30*(3), 280-292. doi:10.1177/1545968315585356

Travis, A. M. (1955). Neurological deficiencies after ablation of the precentral motor area in Macaca mulatta. *Brain, 78*(2), 155-173. doi:10.1093/brain/78.2.155

Tzourio-Mazoyer, N., Landeau, B., Papathanassiou, D., Crivello, F., Etard, O., Delcroix, N., . . . Joliot, M. (2002). Automated anatomical labeling of activations in SPM using a macroscopic anatomical parcellation of the MNI MRI single-subject brain. *NeuroImage, 15*(1), 273-289. doi:10.1006/nimg.2001.0978

Wahl, A. S., Buchler, U., Brandli, A., Brattoli, B., Musall, S., Kasper, H., . . . Schwab, M. E. (2017). Optogenetically stimulating intact rat corticospinal tract post-stroke restores motor control through regionalized functional circuit formation. *Nature Communications, 8*(1), 1187. doi:10.1038/s41467-017-01090-6

Wahl, A. S., Omlor, W., Rubio, J. C., Chen, J. L., Zheng, H., Schröter, A., . . . Schwab, M. E. (2014). Asynchronous therapy restores motor control by rewiring of the rat corticospinal tract after stroke. *Science, 344*(6189), 1250-1255. doi:10.1126/science.1253050

Wang, X., Liu, Y., Li, X., Zhang, Z., Yang, H., Zhang, Y., . . . He, Z. (2017). Deconstruction of Corticospinal Circuits for Goal-Directed Motor Skills. *Cell, 171*(2), 440-455.e414. doi:10.1016/j.cell.2017.08.014

Wang, Y., Pillai, S., Wolpaw, J. R., & Chen, X. Y. (2006). Motor learning changes GABAergic terminals on spinal motoneurons in normal rats. *The European Journal of Neuroscience, 23*(1), 141-150. doi:10.1111/j.1460-9568.2005.04547.x

Ward, N. S., Brown, M. M., Thompson, A. J., & Frackowiak, R. S. (2003). Neural correlates of outcome after stroke: a cross-sectional fMRI study. *Brain, 126*(Pt 6), 1430-1448. doi:10.1093/brain/awg145

Whishaw, I. Q., & Coles, B. L. K. (1996). Varieties of paw and digit movement during spontaneous food handling in rats: Postures, bimanual coordination, preferences, and the effect of forelimb cortex lesions. *Behavioural Brain Research, 77*(1), 135-148. doi:10.1016/0166-4328(95)00209-X

Whishaw, I. Q., Pellis, S. M., Gorny, B. P., & Pellis, V. C. (1991). The impairments in reaching and the movements of compensation in rats with motor cortex lesions: an endpoint, videorecording, and movement notation analysis. *Behavioural Brain Research, 42*(1), 77-91. Retrieved from http://www.ncbi.nlm.nih.gov/pubmed/2029348

Winters, C., van Wegen, E. E. H., Daffertshofer, A., & Kwakkel, G. (2015). Generalizability of the Proportional Recovery Model for the Upper Extremity After an Ischemic Stroke. *Neurorehabilitation and Neural Repair, 29*(7), 614-622. doi:10.1177/1545968314562115

Wise, S. P. (2006). The ventral premotor cortex, corticospinal region C, and the origin of primates. *Cortex; a Journal Devoted to the Study of the Nervous System and Behavior, 42*(4), 521-524.

Wolf, S. L., Thompson, P. A., Winstein, C. J., Miller, J. P., Blanton, S. R., Nichols-Larsen, D. S., . . . Sawaki, L. (2010). The EXCITE Stroke Trial. *Stroke, 41*(10), 2309-2315. doi:doi:10.1161/STROKEAHA.110.588723

Wolpaw, J. R. (2007). Spinal cord plasticity in acquisition and maintenance of motor skills. *Acta Physiologica (Oxford, England), 189*(2), 155-169. doi:10.1111/j.1748-1716.2006.01656.x

Woolsey, C. N., Settlage, P. H., Meyer, D. R., Sencer, W., Pinto Hamuy, T., & Travis, A. M. (1952). Patterns of localization in precentral and "supplementary" motor areas and their relation to the concept of a premotor area. *Res Publ Assoc Res Nerv Ment Dis, 30*, 238-264.

Wu, C. W., Bichot, N. P., & Kaas, J. H. (2000). Converging evidence from microstimulation, architecture, and connections for multiple motor areas in the frontal and cingulate cortex of prosimian primates. *The Journal of comparative neurology, 423*(1), 140-177. doi:10.1002/1096-9861(20000717)423:1<140::aid-cne12>3.0.co;2-3

Wu, C. W., & Kaas, J. H. (1999). Reorganization in primary motor cortex of primates with long-standing therapeutic amputations. *The Journal of neuroscience : the official journal of the Society for Neuroscience, 19*(17), 7679-7697. doi:10.1523/jneurosci.19-17-07679.1999

Yiu, G., & He, Z. (2006). Glial inhibition of CNS axon regeneration. *Nature Reviews Neuroscience, 7*(8), 617-627. doi:10.1038/nrn1956

Zeiler, S. R., Gibson, E. M., Hoesch, R. E., Li, M. Y., Worley, P. F., O'Brien, R. J., & Krakauer, J. W. (2013). Medial premotor cortex shows a reduction in inhibitory markers and mediates

recovery in a mouse model of focal stroke. *Stroke, 44*(2), 483-489. doi:10.1161/strokeaha.112.676940